

**THE DEVELOPMENT AND APPLICATION OF A 3D
GEOTECHNICAL MODEL FOR MINING OPTIMISATION
SANDSLOOT OPEN PIT PLATINUM MINE
SOUTH AFRICA**

Alan Russell Bye

Submitted in Fulfilment of the Academic Requirements for the Degree of
Doctor of Philosophy in Engineering Geology in the
School of Geological and Computer Sciences,
University of Natal
Durban

December 2003

ABSTRACT

Detailed geological knowledge is often a major unknown factor in open pit mining and design, and therefore poses a significant risk in the mining venture. As the knowledge of the geology improves so the risk of unforeseen conditions reduces and therefore safety and productivity can be increased. Historically, geotechnical methods and information have predominantly been used exclusively for pit slope optimisation. This research documents the procedures and developments undertaken to compile a comprehensive geotechnical database, and the application of the geotechnical data to open pit mining, beneficiation and planning. The utilisation of the geotechnical information has been enhanced through the novel development and application of a computerised, 3D geotechnical model.

Sandsloot open pit was developed to extract the Platreef pyroxenite orebody, which is hosted within the Northern Limb of the Bushveld Complex. Sandsloot is currently the world's largest open pit exploiting Platinum Group Metals. Interaction of the basic magma with the footwall sediments of the Transvaal Supergroup and varying degrees of assimilation has resulted in a unique suite of hybrid rock types. These various rock types provide significant engineering geological challenges.

Geology and the detailed understanding of its properties are fundamental to the optimal design and successful operation of any mine. Extensive fieldwork was conducted to collect geotechnical information, both from exploration boreholes and in-pit mining faces. Over a 5-year period, geotechnical data were collected from 29,213 m of exploration core and 6,873 m of exposed mining faces. Extensive field and laboratory testing was undertaken in order to define the complete set of geotechnical properties for each rock type in the Sandsloot mining area.

The geotechnical information relating to each borehole and facemap was stored in the Datamine® software package. The information was collected in the form of rock mass rating (RMR), uniaxial compressive strength (UCS), fracture frequency (FF/m) and rock quality designation (RQD). The architecture of the database was developed along the principals used for generating an ore reserve model.

One of the novel applications was the development of a computerized 3D, geotechnical model in Datamine®. The geotechnical parameters, namely RMR, UCS, FF/m and RQD, were modelled for each rock type, using geostatistics, to generate a 3D model. The data were interpolated between exploration boreholes and exposed mining faces and the modelling was constrained using wireframes separated by rock type. The result is a 3D model containing 15 m³ model blocks populated with interpolated geotechnical information. The dimensions of the model blocks are linked to the mining bench height of 15 m. The model can be queried to give predictions on rock mass conditions for any planned mining area, as is the case with the ore reserve model, which provides predictions on platinum grades.

The crux of the innovative research is the practical application of the 3D geotechnical model. This was achieved through the development of both a fragmentation and a slope design model, which read the interpolated geotechnical information. These models provided an engineering tool to

optimise mining and milling performance.

Rather than viewing the drill and blast department as an isolated cost centre and focussing on minimising drill and blast costs, the application of the model concentrated on the fragmentation requirements of the milling and mining business areas. Two hundred and thirty-eight blasts were assessed to determine the optimum fragmentation requirements for ore and waste. Based on the study a mean fragmentation target of 150 mm was set for delivery to the crushing circuit and a mean fragmentation of 230 mm was set for waste loading from the pit.

The mine operates autogenous mills, which are sensitive to the fragmentation profile delivered. The harder zones occurring in the ore zone have a major impact on the plant's performance. The geotechnical parameters in the model were related to Lilly's Blastability Index, and in turn to required explosive volumes and the associated drill and blast costs. Having defined the fragmentation targets, the Kuz-Ram equation was used in the fragmentation model to predict the explosive volumes required to ensure consistent mining and milling performance. The geotechnical model is used to predict changes in geotechnical conditions and therefore the blasting parameters can be adjusted in advance to ensure the milling and mining fragmentation requirements are met. Through the application of the fragmentation model over an eighteen-month period the loading and milling efficiencies improved by 8.5% and 8.8% respectively, resulting in additional revenue of R29 million for PPL.

Based on the mining rock mass rating (MRMR) values within the geotechnical model a stable slope design model was created in order to calculate optimum inter-ramp angles. From a slope design perspective the model was used to target data-deficient zones and highlight potentially weak rock mass areas. As this can be viewed in 3D, the open pit slopes were designed to accommodate the poor quality areas before they are excavated. It also follows that competent geotechnical zones can be readily identified and the slope optimised accordingly.

Due to the detailed geotechnical information being available in three dimensions, the open pit slopes were designed based on a risk versus reward profile. As a significant geotechnical database was available, more accurate and reliable designs were generated resulting in the overall slope angle increasing by 3 degrees. This optimisation process will result in a revenue gain of R900 million over the life of the mine. The revenue and safety benefits associated with this design methodology are substantial and have potential application to all open pit mining operations.

The research has enabled detailed geotechnical information to be available in three dimensions. This information can be readily accessed and interpreted, thus providing a powerful planning and financial tool from which production optimisations, feasibility studies and planning initiatives can be implemented. The development and application of a 3D geotechnical model has added a new dimension to the constant strive for business improvement and reflects a novel and successful approach towards the application of engineering geology at the Sandsloot mining operation.



PREFACE

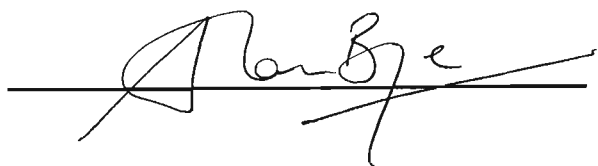
The experimental work described in this thesis was carried out on site at Sandsloot open pit, Potgietersrust Platinums Limited, from February 1997 to September 2003. Over that period the research was supervised by Professor Bell and Professor Jermy from the School of Geological and Computer Sciences, University of Natal, Durban. After Professor Bell retired in 2000, Professor Stacey from WITS University, Department of Mining Engineering, undertook supervision of the research work in conjunction with Professor Jermy.

These studies represent original work by the author and have not otherwise been submitted in any form for any degree or diploma to any tertiary institution. Where use has been made of work of others it is duly acknowledged in the text.

Date

8-12-03.

Signature of candidate

A handwritten signature in black ink, appearing to read 'Alan Bye', is written over a horizontal line.

Alan Russell Bye

ACKNOWLEDGEMENTS

I would like to express my gratitude to my supervisors Professor C. A. Jermy, Professor F.G. Bell and Professor T. R. Stacey for their advice and guidance during the preparation of the thesis.

I would also like to acknowledge the contribution of the following:

- Thanks are accorded to the management of Anglo Platinum for the funding and permission to publish the research.
- A specific note must be made to the management of Potgietersrust Platinums Limited (PPL) for allowing me the latitude to experiment and trial new technology and initiatives in an active mining environment.
- The PPL Geology Department is gratefully acknowledged for their contribution towards the thesis.
- The valuable advice of Mr P. Terbrugge of Steffen, Robertson and Kirsten Consulting Engineers is most appreciated.
- Lance Reynolds for training on Datamine and assisting with valuable advice throughout the thesis.
- Megan Little for her critical review and assistance during the compilation of the thesis.

Finally, to my family and friends for their unfailing support throughout the preparation of the thesis.

CONTENTS

	Page
ABSTRACT	ii
PREFACE	iv
ACKNOWLEDGEMENTS	v
CONTENTS	vi
LIST OF TABLES	x
LIST OF FIGURES	xii
GLOSSARY OF TERMS	xvi
1 INTRODUCTION	1
1.1 Objectives of the Research	1
1.2 Format of the Thesis	2
1.3 Sandsloot Description	4
1.4 Collection of Data	6
1.5 3D Models	6
1.6 Geostatistics	6
1.7 Engineering Application of the Geotechnical Model	7
1.7.1 Fragmentation Model	8
1.7.2 Slope Stability Model	8
1.8 Summary	9
2 OPEN PIT MINING	10
2.1 Introduction	10
2.2 History	10
2.3 Mining Overview	11
2.4 Summary and Conclusions	15
3 GEOLOGY	16
3.1 General Geology	16
3.1.1 Genesis and Crustal Emplacement of the Bushveld Complex	20
3.2 Local Geology	22
3.2.1 PGE Mineralisation	24
3.3 Structural Geology	26
3.3.1 Tectonic Evolution	29
3.3.2 Jointing	31

3.4	Geohydrology	34
3.5	Summary and Conclusions	37
4	GEOTECHNICAL INFORMATION	38
4.1	Introduction	38
4.2	Rock Mass Classification	42
4.3	Face Mapping	45
4.4	Borehole Logging	51
4.5	Rock Strength Testing	57
4.6	Kinematic Failure Analysis	67
4.6.1	Zone A (wedge failure)	69
4.6.2	Zone B (planar failure)	70
4.6.3	Zone C (circular failure)	74
4.6.4	Zone D (nose zone)	76
4.6.5	Zone E (planar and toppling failure)	78
4.7	Summary and Conclusions	79
5	DEVELOPMENT OF THE 3D GEOTECHNICAL MODEL	80
5.1	Introduction	80
5.2	Geostatistics and Geotechnical Engineering	81
5.2.1	Geostatistics	82
5.2.2	Optimisation of Site Investigation Locations	84
5.2.3	Simulation and Numerical Modelling	84
5.2.4	Successful Application of Geostatistics to the Channel Tunnel Project	85
5.2.5	Integration of Geostatistics	86
5.3	Ore Reserve Modelling Process	87
5.4	Geotechnical Model Development	90
5.4.1	Data Input	90
5.4.2	Block Model	93
5.4.3	Geostatistical Interpolation	96
5.5	Summary and Conclusions	104
6.	DEFINITION OF CUSTOMER RELATIONSHIPS AND TARGETS	106
6.1	Introduction	106
6.2	Processing Plant	109

6.2.1	Digital Fragmentation Analysis	115
6.3	Load and Haul	119
6.3.1	Instantaneous Loading Rates	121
6.4	Summary and Conclusions	128
7	FRAGMENTATION MODEL	130
7.1	Introduction	130
7.2	Blastability Index	132
7.2.1	Joint Plane Spacing	133
7.2.2	Rock Mass Description	133
7.2.3	Joint Plane Orientation	134
7.2.4	Rock Density Influence	134
7.2.5	Rock Hardness	134
7.3	Calculation of the Blastability Index from the Geotechnical Model	136
7.4	Fragmentation Model	140
7.5	Drill and Blast Costing Model	142
7.6	Model Query and Planning Functionality	145
7.7	Summary and Conclusions	151
8	APPLICATION OF THE FRAGMENTATION MODEL	153
8.1	Introduction	153
8.2	Mine to Mill Optimisation	156
8.3	Production Loading Optimisation	164
8.4	Summary and Conclusions	168
9	SLOPE DESIGN MODEL	170
9.1	Introduction	170
9.2	Development and Application of the Slope Design Model	172
9.3	Numerical Modelling and Design of Final Slope	177
9.4	Risk and Reward Design Application	181
9.5	Summary and Conclusions	184
10	CONCLUSIONS	185
10.1	Geotechnical Information	186
10.2	Model Development	186
10.3	Customer Requirements	187
10.4	Fragmentation Model	188

10.5	Customer Performance	189
10.6	Slope Optimisation	190
10.7	Suggestions for Further Research	192
10.7.1	Geostatistics	192
10.7.2	Economic Pit Design	192
10.7.3	Feasibility Projects	193
11	REFERENCES	195

APPENDICES

(All Appendix Data is Stored Digitally in the Attached Compact Disk)

APPENDIX 1	FULL GEOTECHNICAL DATABASE USED IN DATAMINE®
APPENDIX 2	GEOTECHNICAL BOREHOLE LOGS
APPENDIX 3	FACE MAPPING DATA BY BENCH
APPENDIX 4	LABORATORY TESTING – FULL RESULTS
APPENDIX 4.1	MiningTek Reports
APPENDIX 4.2	Natural Joint Shear Tests
APPENDIX 5	FRAGMENTATION GRAPHS
APPENDIX 6	INSTANTANEOUS LOADING RATES
APPENDIX 7	SOFTWARE AND PRESENTATION
APPENDIX 7.1	PowerPoint Presentation (3D Model)
APPENDIX 7.2	Datamine® Visualiser Software and Model Viewing File
APPENDIX 8	DATAMINE BROCHURE

TABLES

Table 3.1	Joint set information collected at Sandsloot open pit.
Table 4.1	The calculated mining adjustments for Sandsloot open pit.
Table 4.2	Geotechnical properties of the dominant rock types present at Sandsloot.
Table 4.3	Summation and statistical analysis of all the geotechnical data collected from both exploration boreholes and in-pit face maps.
Table 4.4	Detail of the testing programme undertaken, including numbers of test samples per rock type.
Table 4.5	Comprehensive summary of the lab testing results.
Table 4.6	Natural joint shear test results.
Table 4.7	Summary of rock drillability tests.
Table 4.8	Comparison of the Bushveld Complex rock properties.
Table 4.9	Data relating to the critical joint sets (JS) causing wedge failure on the footwall ramps.
Table 4.10	Data relating to planar failure diagram, Figure 4.14.
Table 5.1	Example tabulation of all the geotechnical data stored in the Datamine® database. (Full table in Appendix 1).
Table 6.1	Adjustments made to ore blast designs during 1997 and 1998.
Table 6.2	Summary of the digital fragmentation analysis for ore and waste blasts.
Table 6.3	Comparison of powder factors and loading rates in ore and waste.
Table 6.4	Comparison of explosive formulation performance.
Table 6.5	Data relating to the 69 ore blasts analysed.
Table 6.6a	Data relating to the 169 waste blasts analysed.
Table 6.6b	Data relating to the 169 waste blasts analysed.
Table 6.7	Summary of the base data used to define the customer targets.
Table 6.8	Benchmark design information for the drill and blast department's customers.
Table 7.1	Joint Plane Spacing (JPS).
Table 7.2	Rock Mass Description (RMD).
Table 7.3	Joint Plane Orientation (JPO).
Table 7.4	Table relating FF/m to JPS developed to apply more accurate JPS ratings to the detailed jointing information in the geotechnical model.
Table 7.5	Information relating rock type information in the model to density, JPO and RMD.

Table 7.6	Information used to calculate the relationship between cost and energy.
Table 7.7	Summary table of information derived from the geotechnical model query function “evaluate mining blocks”.
Table 8.1	Impact of primary crusher feed size on energy consumption and crushing costs.
Table 8.2	Analysis of the instantaneous loading rates from 2001 to 2003.
Table 9.1	Mining adjustments, for the slope design model applied to the rock types present at Sandsloot.
Table 9.2	Rock mass input parameters for the FLAC ubiquitous joint model.
Table 9.3	Summary of risk-reward design information plotted in Figure 9.8.

FIGURES

- Figure 1.1 Engineering design process used for the research.
- Figure 1.2 Map of the Bushveld Complex including insets of the mine area and location within South Africa.
- Figure 1.3 Local geology and Potgietersrust Platinums Limited lease area.
- Figure 2.1 Photographs illustrating the Sandsloot open pit and the phases 2-4 cutback, which is the area of focus of this geotechnical study.
- Figure 2.2 Sandsloot open pit cut back phases.
- Figure 3.1 Stratigraphic column comparing the western Bushveld stratigraphy to the Platreef.
- Figure 3.2 (Top map) Illustration of the Bushveld Complex emphasizing the RLS and showing the location of the northern limb. (Main map) Simplified geological map of the northern Bushveld limb showing the location of the Sandsloot pit after Armitage *et al.* (2002).
- Figure 3.3 Proposed Bushveld Complex intrusion mechanism utilising the Thabazimbi-Murchison Lineament, allowing ascent along a deep-seated lithospheric shear zone (i.e. Thabazimbi-Murchison and Barberton-Magaliesberg lineaments), acting as a conduit. At a critical level in the crust, the magmatic pressure equalled the lithostatic pressure which allowed the massive “sill-like” intrusion of the Bushveld Complex to occur, after Good (1999).
- Figure 3.4. Stratigraphic column of the dominant rock types occurring at Sandsloot.
- Figure 3.5 Major structural plan of the Platreef mining area, after Friese (2002).
- Figure 3.6 Stereonet depicting the joint set families present at Sandsloot.
- Figure 3.7 The effect of dry vs. wet conditions on the factor of safety of the design slopes (SRK, 1991).
- Figure 3.8 View of the open pit highwalls showing no obvious water seepage.
- Figure 4.1 Geotechnical plan of Sandsloot open pit.
- Figure 4.2 Geotechnical cross-section of Sandsloot open pit.
- Figure 4.3 Flow diagram illustrating Laubscher’s (1990) MRMR system.
- Figure 4.4 Geotechnical and structural face mapping sheet for MRMR evaluation.
- Figure 4.5 Geological face map including geotechnical and structural information.
- Figure 4.6 AutoCAD data capture and MRMR analysis screens.
- Figure 4.7 Plan view of bench 14 geological and geotechnical face maps.
- Figure 4.8 Geotechnical borehole logging sheet, after Dempers (1996).
- Figure 4.9 MRMR geomechanics spread sheet.

- Figure 4.10 Location of exploration boreholes that were logged geotechnically.
- Figure 4.11 Graphs relating tangent modulus to UCS for all Sandsloot rock types.
- Figure 4.12 Diagrammatic illustration of identified failure mechanisms at Sandsloot
- Figure 4.13 Photograph of a planar failure occurring on the western highwall.
- Figure 4.14 Stereonet depicting the planar failure mechanism on the hangingwall.
- Figure 4.15 Damage to an operational shovel as a result of a planar failure.
- Figure 4.16 Planar failure sensitivity analysis (relationship between FOS, cohesion, joint angle and rock mass saturation).
- Figure 4.17 Photograph illustrating the Satellite pit eastern highwall.
- Figure 4.18 Photograph illustrating the problematic nose area.
- Figure 4.19 Graph illustrating the influence of slope curvature on slope stability (SRK, 1991).
- Figure 4.20 Toppling failure mechanism, after Hoek and Bray (1981).
- Figure 5.1 A histogram plot of the frequency of geotechnical publications on geostatistics over the last 33 years, after Rocscience (2003).
- Figure 5.2 Geological cross-section through the seafloor of the Channel Tunnel from Rocscience (2003) and after Chiles *et al.* (1999).
- Figure 5.3 Ore reserve data flow diagram (Reynolds and Millan, 1997).
- Figure 5.4 Three-dimensional view of Sandsloot open pit, exploration boreholes and the orebody. The open pit is approximately 2 km in length and 0.8 km wide.
- Figure 5.5 The process followed in the development of the geotechnical model.
- Figure 5.6 Oblique view illustrating the boreholes and facemaps as presented in Datamine®.
- Figure 5.7 Development of wireframes from the drillhole lithology contacts.
- Figure 5.8 Datamine® visualisation illustrating the extents of the block model.
- Figure 5.9 Section through the block model illustrating a vertical slice through the three wireframe-constrained, lithology models (blue = norite, red = pyroxenite and magenta = parapyroxenite).
- Figure 5.10 RMR histograms for all the rock types occurring in the pit.
- Figure 5.11 FF/m histograms for all the rock types occurring in the pit.
- Figure 5.12 RQD histograms for all the rock types occurring in the pit.
- Figure 5.13 UCS histograms for all the rock types occurring in the pit.
- Figure 5.14 Datamine® visualisation of final interpolated block model with boreholes.
- Figure 5.15 Datamine® screen illustrating the resultant model cell data from a query process.
- Figure 6.1 Diagram illustrating the ore material flow from the pit to the plant.
- Figure 6.2 Illustrates the impact the mill feed gradings have on the AG mill production.
- Figure 6.3 Schematic flow diagram of the PPL concentrator plant after the 1998 expansion.

- Figure 6.4 An example of a drill and blast plan illustrating the geotechnical information provided manually to the drill and blast department between 1998 and 2001.
- Figure 6.5 Autogenous milling performance for 2001.
- Figure 6.6 Slide illustrating the digital fragmentation analysis process.
- Figure 6.7 Photograph illustrating the loading conditions at Sandsloot.
- Figure 6.8 Illustrating the transfer of truck and shovel time and motion information.
- Figure 6.8 Average instantaneous loading rates from 1999 to 2001.
- Figure 6.9 Illustrates graphically the loading rates per shift achieved over a one year period. 1,069 loading shifts were assessed and yielded an average loading rate of 3,249 t/hr.
- Figure 7.1 Flow diagram illustrating how the geotechnical model is used to calculate the Blastability Index, required energy factor and subsequent optimisations.
- Figure 7.2 Graph depicting a poor correlation of JPS to FF/m for a single equation.
- Figure 7.3 Graph illustrating the correlation for JPS and FF/m greater than 1.
- Figure 7.4 Graph depicting a better correlation for JPS and FF/m less than 1.
- Figure 7.5 Relationship between energy factor and cost per m³, for Sandsloot open pit.
- Figure 7.6 Illustrates graphically the effect of Blastability Index on the required energy factor and the associated drill and blasts costs for set fragmentation targets.
- Figure 7.7 Computer front end developed for the interface with the 3D geotechnical model.
- Figure 7.8 Screen view of the model query for blast outline 123–056, filtered on energy factor (Ef). Note: 123-056 \equiv (1 = pit one (Sandsloot); 23 = bench 23; 056 = the 56th blast on bench 23).
- Figure 7.9 Plan view of slice through the fragmentation model on elevation 1,005 m, including future mining blocks to be queried for blast design. The filters illustrate the information associated with each colour-coded block.
- Figure 8.1 Section through the model illustrating the information available in each model cell. The information listed on the left is related to the cell with the white cross.
- Figure 8.2 Graph illustrating the impact feed size has on mill throughput and revenue.
- Figure 8.3 Actual AG milling rate comparison for 2001 and 2002.
- Figure 8.4 Blast design powder factors and AG mill performance for 2003.
- Figure 8.5 Mill feed fragmentation profiles obtained from belt cut samples for March and May 2003.
- Figure 8.6 Comparison of blast powder factor and primary crushing costs for 2003.
- Figure 8.7 Loading rates showing the impact of the fragmentation model for blast design.
- Figure 8.8 Instantaneous loading rates recorded by shift for 2001.

- Figure 8.9 Instantaneous loading rates recorded by shift for 2002.
- Figure 8.10 Graph illustrating the performance of the drill and blast department in terms of costs and instantaneous loading rates, related to powder factor.
- Figure 8.11 Loading and milling performance from 2001 to 2003.
- Figure 8.12 Graph illustrating the performance of the drill and blast departments two customers during 2003. The loading rates include ore and waste and the milling rates include both the AG and ball mills.
- Figure 9.1 Flow diagram illustrating the process used for slope optimisation.
- Figure 9.2 Design chart for the determination of stable slope angles from MRMR classification data, after Haines and Terbrugge (1991).
- Figure 9.3 Slope design charts for Sandsloot rock types based on MRMR and FLAC modelling.
- Figure 9.4 Stable slope design chart for 100m stacks, incorporated in the 3D geotechnical model.
- Figure 9.5 Section through the slope design model, colour filtered on the 100m stable slope angle.
- Figure 9.6 Wireframe sliced through the 3D slope stability model illustrating the appropriate stack design angle for the various areas of the pit.
- Figure 9.7 Stability envelope of the norite hangingwall developed from the series of FLAC analyses.
- Figure 9.8 Risk-reward slope design chart developed for Sandsloot open pit.

GLOSSARY OF TERMS

Bench:	Standard height of a mining block.
Boulders:	Oversize rocks produced from a production blast. Boulders are a good indication that the drill and blast design is not effective or has not been implemented to specifications.
Burden:	Distance between blast hole rows parallel to the free face.
Catchment Berm:	Step-off at the base of a stack, designed to catch rockfall from the slope above.
Compressive stress:	Normal stress tending to shorten a body in the direction in which it acts.
Crest:	The top of a mining bench.
Deformation:	A change in shape or size of a solid body.
Dip:	Angle at which a stratum or other planar feature is inclined from the horizontal.
Discontinuity surface:	Any surface across which some property of a rock mass is discontinuous (e.g. bedding planes, fractures)
Dump:	Area where waste rock from the pit is dumped permanently or where ore is stockpiled for crushing.
Elasticity:	Property of a material whereby it returns to its original form or condition after an applied force is removed.
Footwall:	Mass of rock beneath a discontinuity surface. (In tabular mining, the rock below the bottom contact of the reef.)
Geotechnical area/zone:	A portion of the mine where similar geological conditions exist, which give rise to a unique set of identifiable rock-related hazards for which a common set of strategies can be employed to minimise the risk resulting from mining.
Hangingwall:	Mass of rock above a discontinuity surface (in tabular mining, the rock above the reef plane).
Hard toe:	Solid area at the base of a presplit face that has not achieved the planned limit. Hard toes commonly occur from vertical presplits, inadequately charged presplits or a buffer step off that is too large.

High bottom:	Area on a ramp or at the floor of a bench that is above the planned mining elevation. These areas usually occur due to poor drilling and blasting, insufficient subdrill or harder zones within the rock mass.
Highwall:	Term used to describe the open pit slopes above the active mining benches.
Limit blasting:	All forms of blasting designed to preserve the integrity of the remaining rock mass (e.g. smooth blasting, presplitting, post-splitting, buffer blasting).
Mining slot/block:	Area on a bench that is planned to be drilled and blasted. At Sandsloot the dimensions are usually 100 m x 50 m x 15 m.
Muckpile:	Term referring to the fragmented rock mass after a production blast.
Normal force:	Force directed normal (perpendicular) to the surface element across which it acts.
Normal stress:	Component of stress normal to the plane on which it acts.
Overbreak:	The quantity of rock that is removed beyond the planned perimeter of the final excavation.
Plasticity:	State in which material continues to deform indefinitely whilst sustaining a constant stress.
Poisson's ratio:	Ratio of shortening in the transverse direction to elongation in the direction of an applied force in a body under tension below the proportional limit.
Presplit:	Presplit blasting or pre-shearing uses a row of small diameter, closely spaced holes drilled along the line of the final face. The row is fired before the main charge and the reinforcing effect of the closely spaced holes together with the very large burden results in the formation of a clean fracture running from one hole to the next. This is done to create a final excavation perimeter that is stable and safe.
Ramp:	Inclined haul road designed into the pit highwalls so that material can be transported out of the pit. Ramps are usually designed at an angle of 10% or 5.6°.

Reef/Orebody:	A vein, bed or deposit (other than a surface alluvial deposit) that contains economically exploitable minerals.
Rockfall (fall of ground):	Fall of a rock fragment without the simultaneous occurrence of a seismic event.
Rock mass:	Rock as it occurs <i>in-situ</i> , including its discontinuities.
Rock mass instability:	A softening within a critical volume of rock indicated by accelerating deformation and a drop in stress.
Stack :	Slope configuration used between major catchment berms or ramps. Usually two to three benches inclined at 70 degrees.
Stockpile:	Reserve of blasted ore that is accumulated prior to crushing & processing.
Strike:	Direction of the azimuth of a horizontal line in the plane of an inclined stratum (or other planar feature) within a rock-mass.
Toe:	The base of a mining bench.
Young's Modulus:	The relationship between tension, or compression, and deformation in terms of change in length.

1 INTRODUCTION

Detailed geological knowledge is often a major unknown factor in open pit mining and design, and therefore poses a significant risk in the mining venture. As the knowledge of the geology improves so the risk of unforeseen conditions reduces and therefore safety and productivity can be increased. Historically, geotechnical methods and information have predominantly been used exclusively for pit slope optimisation. This research documents the procedures and developments undertaken to compile a comprehensive geotechnical database, and the application of the geotechnical data to open pit mining, beneficiation and planning. The utilisation of the geotechnical information has been enhanced through the novel development and application of a computerised 3D geotechnical model.

1.1 Objectives of the Research

The objective of the research was to develop an engineering solution, based on a significant geotechnical database, which was automated, sustainable and aligned with the company's business objectives. The innovative application of a 3D geotechnical model, developed from geostatistical techniques, for the optimisation of blast fragmentation and the significant impact on mine profitability is presented. This was achieved in the following manner:

- i). Collect a significant database of geotechnical information from exploration boreholes, in-pit face mapping and rock strength testing.
- ii). Develop an interpolated 3D geotechnical model from the data.
- iii). Verify the representivity of the model to field conditions.
- iv). Use the model to develop engineering design tools for mine optimisation, namely fragmentation and slope design models.
- v). Calibrate, test and evolve the model through rigorous field testing.
- vi). Develop a simple user-interface (front-end) to the model to enable mine planners and engineers to use the model.
- vii). Apply the model over a significant period of time and assess the benefits to the mine.

The design process is illustrated in Figure 1.1. The engineering models developed are site specific to the Sandsloot operation due to the data set collected and the targets used. The design methodology and engineering process can, however, be applied to other mining operations.

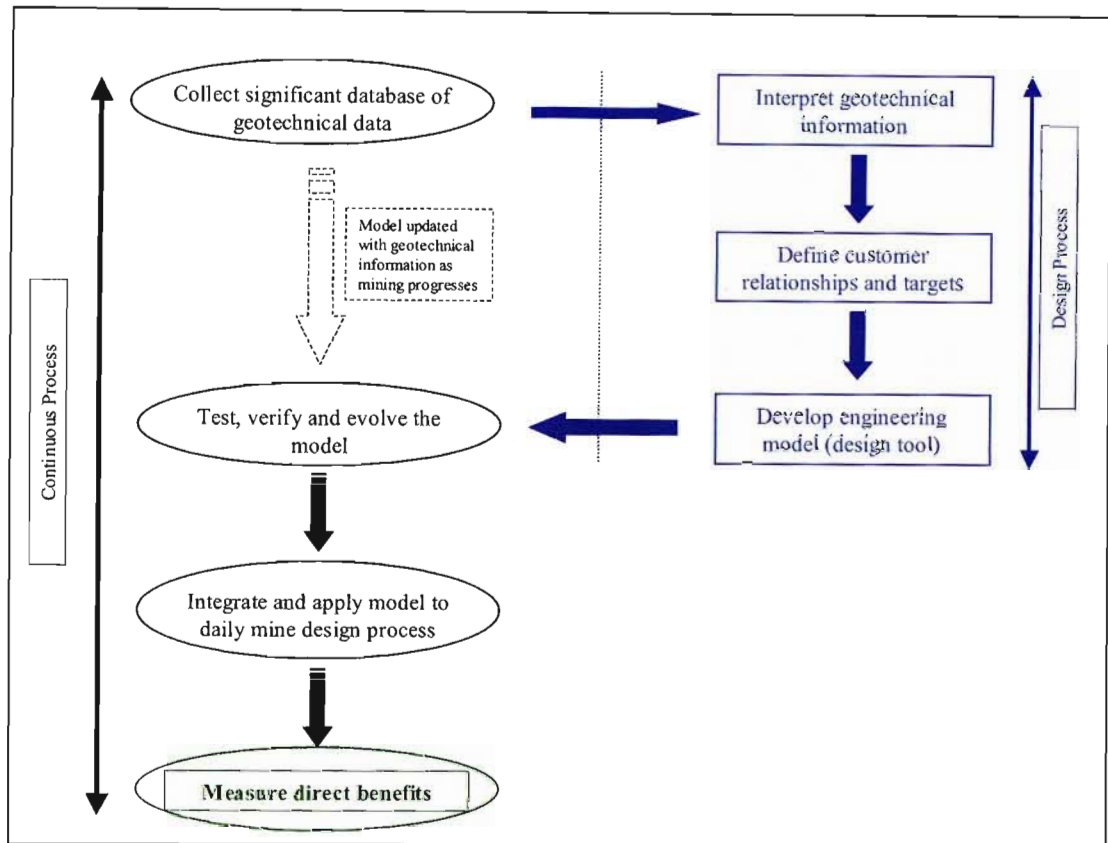


Figure 1.1 Engineering design process used for the research.

1.2 Format of the Thesis

Rather than dedicate a chapter specifically to literature review, the thesis reviews the relevant references at the appropriate descriptive sections. Although over 90 references are cited, the thesis represents novel research and as such very few directly relevant papers were discovered. Only one paper, by Syrjänen and Lovén (1998), could be located on the development of a geotechnical model and none on the engineering application to mining.

During the five years of research a significant data set was collected in order to produce this thesis. The printing of these data sets as appendices would yield an unmanageable appendix volume. In order to resolve this issue, the full appendices are recorded digitally and attached to the thesis in the form of a compact disk. The reader is given an appreciation of all the data collected through the use of relevant examples presented throughout the text. The data sets are recorded for the most part in either Microsoft Word or Excel. A Microsoft PowerPoint presentation illustrating the functionality of the 3D geotechnical model is stored in Appendix 7.1. Additionally, a copy of the Datamine® visualisation software for viewing the 3D model

files is attached, should the reader wish to install and view the files.

In Chapter 2 a description of the history of Potgietersrust Platinums Limited (PPL) is presented as well as the open pit mining practices, as applied to Sandsloot open pit. This was written to give the reader an appreciation of the site and the conditions the research was applied to.

Mine design is based on the *in-situ* geotechnical conditions and as such an overview of the geological and structural setting within the research area is discussed in Chapter 3. This chapter develops an understanding of the geotechnical conditions and the impact it has on mine productivity.

The relevant data and sampling methods are introduced in Chapter 4. The interpretation of this data into useful engineering numbers is discussed as well as the methods used to ensure consistent, quality data capture. Kinematic failure analysis and rock strength testing data is also presented as it is used as a basis for slope design.

An overview of geostatistics and geotechnical engineering in general are laid out in Chapter 5. Geostatistical analysis and methods as applied to the model are discussed as well as the specific processes used for the development of the Sandsloot 3D geotechnical model.

The crux of the thesis focuses on the application of the geotechnical model to consistently achieve the mine's production targets. Chapter 6 examines the relationships between the drill and blast department and the downstream customers, namely the load and haul department and the processing plant. Through analysis of significant data sets, design targets are prescribed for these customers and the model is configured to achieve these targets.

Chapter 7 discusses the development of the fragmentation model and the application of the model as an engineering tool, which is designed to achieve the customer targets. Chapter 8 and 9 demonstrate the significant benefits achieved through the application of the fragmentation and slope design models over an eighteen-month period.

1.3 Sandsloot Description

Sandsloot open pit was developed to extract the platinum-bearing, Platreef orebody, which is hosted within the Northern Limb of the Bushveld Complex, some 250 km north-east of Johannesburg (Figure 1.2). It is the first of six potential open pits to be mined by Potgietersrust Platinums Limited (PPL), a subsidiary of Anglo Platinum. Figure 1.3 illustrates the current mining lease area. Sandsloot is currently the world's largest open pit exploiting platinum group metals (PGMs). In a single month the mine processes 400,000 tonnes of ore and excavates 40 million tonnes of material annually. The current pit has an economic depth of 320 m, after which underground mining will commence. Interaction of the basic magma with the footwall sediments of the Transvaal Supergroup exhibiting varying degrees of assimilation has resulted in a unique suite of hybrid rock types. These various rock types provide significant engineering geological challenges.

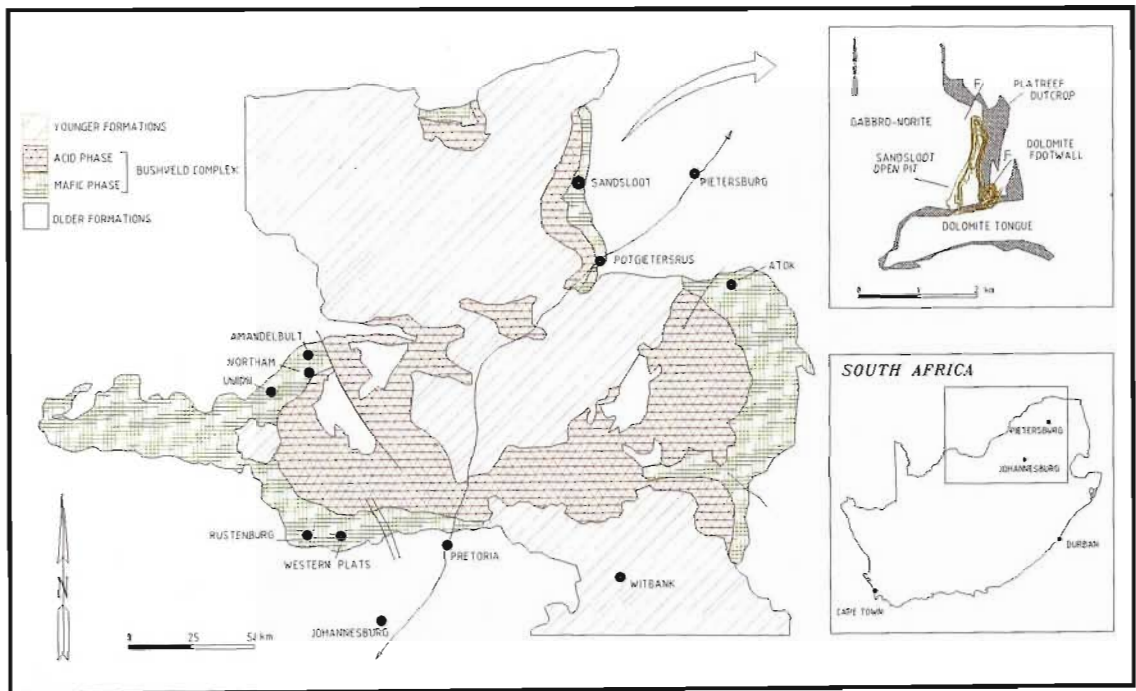


Figure 1.2 Map of the Bushveld Complex including insets of the mine area and location within South Africa.

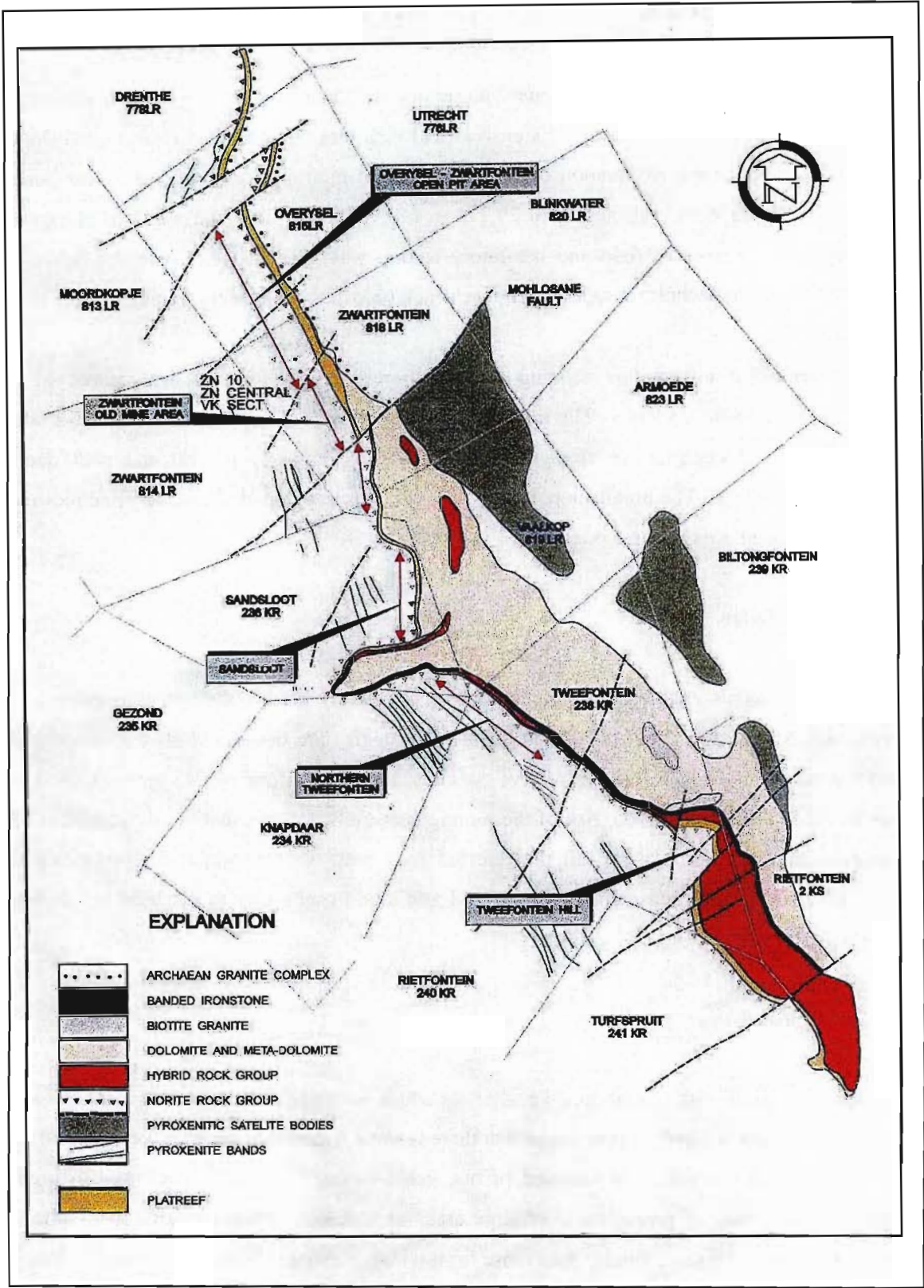


Figure 1.3 Local geology and Potgietersrust Platinums Limited lease area.

1.4 Collection of Data

The detailed understanding of geological properties is fundamental to the optimal design and successful operation of any mine. Extensive fieldwork was conducted to collect geotechnical information, both from exploration boreholes and in-pit mining faces. Over a 5-year period, geotechnical data were collected from 29,213 m of exploration core and 6,873 m of exposed mining faces. Extensive field and laboratory testing was undertaken in order to define the complete set of geotechnical properties for each rock type in the Sandsloot mining area.

The geotechnical information relating to each borehole and facemap was stored in the Datamine® software package. The information was collected in the form of rock mass rating (RMR), uniaxial compressive strength (UCS), fracture frequency (FF/m) and rock quality designation (RQD). The architecture of the database was developed along the principles used for generating an ore reserve model.

1.5 3D Models

Ore reserve models enable mining operations to effectively predict the potential value of an economic deposit and all planning and business strategies are dependant on that model. The more detailed information the ore reserve contains, the more informed management decisions can be made thus lowering the risk of the mining venture. It follows that the development of a geotechnical model, containing all the relevant rock mass information and representing the variability in the rock mass conditions, would add significant value to the business decision process.

1.6 Geostatistics

Geostatistics deals with spatial data, i.e. data for which each value is associated with a location in space. In such analysis, it is assumed that there is some connection between location and data value. From known values at sampled points, geostatistical analysis can be used to predict spatial distributions of properties over large areas or volumes. Measurements from adjacent boreholes tend to be more similar than those from widely separated boreholes. This observation forms the basis of the assumption in geostatistics that location has a relationship to measured properties. Geostatistical analysis interprets statistical distributions of data and also examines spatial relationships. Ultimately it produces predictions of the probable distribution of properties

in space and facilitates the accurate interpretation of ground conditions based on the sparse input information characteristic of geotechnical engineering (Rocscience, 2003).

One of the novel applications was the development of a computerized 3D, geotechnical model in Datamine®. The geotechnical parameters, namely RMR, UCS, FF/m and RQD, were modelled for each rock type, using geostatistics to generate a 3D model. The data were interpolated, using the inverse distance geostatistical technique, between exploration boreholes and exposed mining faces. The modelling process was constrained using wireframes separated by rock type, i.e. only rock mass data for that specific rock type was used to interpolate information for the same rock type within the model. The result is a 3D model containing 15 m³ model blocks populated with interpolated geotechnical information. The dimensions of the model blocks are linked to the mining bench height of 15 m. The model can be queried to give predictions on rock mass conditions for any planned mining area, as is the case with the ore reserve model, which provides predictions on platinum grades.

The geotechnical model provides geotechnical information well in advance of the mining face. Using the model, mining slots can be evaluated not only for grade and tonnage predictions but also for predictions of rock mass quality. Potential milling and penetration rates, powder factors, blast designs, as well as equipment and explosives requirements can be derived from the rock mass quality predictions. This information can be used for overall mine planning and evaluation, costing, production optimisation and slope design.

1.7 Engineering Application of the Geotechnical Model

The crux of the innovative research is the practical application of the 3D geotechnical model. This was achieved through the development of both a fragmentation and a slope design model, which read the interpolated geotechnical information. These models provided an engineering tool to optimise mining and milling performance.

1.7.1 Fragmentation Model

Rather than viewing the drill and blast department as an isolated cost centre and focussing on minimising drill and blast costs, the application of the model concentrated on the fragmentation requirements of the milling and mining business areas. Two hundred and thirty eight blasts were assessed to determine the optimum fragmentation requirements for ore and waste. The fragmentation model was therefore calibrated with real information collected over a two year period. Based on the study, a mean fragmentation target of 150 mm was set for delivery to the crushing circuit and a mean fragmentation of 230 mm was set for waste loading from the pit.

The mine operates autogenous mills, which are sensitive to the fragmentation profile delivered. The harder zones occurring in the ore zone have a major impact on the plant's performance. The geotechnical parameters in the model were related to Lilly's Blastability Index (Lilly, 1986), and in turn to required explosive volumes and the associated drill and blast costs. Having defined the fragmentation targets, the Kuz-Ram equation developed by Cunningham (1986) was used in the fragmentation model to predict the explosive volumes required to ensure consistent mining and milling performance. The geotechnical model is used to predict changes in geotechnical conditions thus the blasting parameters can be adjusted in advance to ensure the milling and mining fragmentation requirements are met.

1.7.2 Slope Stability Model

Based on the mining rock mass rating (MRMR) values within the geotechnical model a stable slope design model was created in order to calculate optimum inter-ramp angles. From a slope design perspective, the model was used to target data-deficient zones and highlight potentially weak rock mass areas. As this can be viewed in 3D, the open pit slopes were designed to accommodate the poor-quality areas before they are excavated. It also follows that competent geotechnical zones can be readily identified and the slope angle optimised accordingly.

Due to the detailed geotechnical information being available in three dimensions, the open pit slopes were designed based on a risk versus reward profile. As a significant geotechnical database was available, more accurate and reliable designs were generated resulting in the overall slope angle increasing by 3 degrees. This optimisation process will result in a revenue gain of R 900 million over the life of the mine. The revenue and safety benefits associated with

this design methodology are substantial and have potential application to all open pit mining operations.

1.8 Summary

The research has enabled detailed geotechnical information to be available in three dimensions. This information can be readily accessed and interpreted, thus providing a powerful planning and financial tool, from which production optimisations, feasibility studies and planning initiatives can be implemented. The ore reserve model has gained widespread acceptance as an invaluable tool to a mining operation. Certainly most financial organisations will not invest in a mining project that does not have an ore reserve model. There is the potential that geotechnical models will become as vital to the mining process. The development and application of a 3D geotechnical model has added a new dimension to the constant strive for business improvement and reflects a novel and successful approach towards the application of engineering geology at the Sandsloot mining operation.

2 OPEN PIT MINING

2.1 Introduction

This chapter is dedicated to giving the reader an appreciation of the site and the conditions the research was applied to. The history of Potgietersrust Platinums Limited (PPL) is presented as well as the open pit mining practices, as applied to Sandsloot open pit. The chapter lays the foundation for understanding how important detailed geotechnical information is for an integrated approach to mine design.

2.2 History

In 1924, Dr Hans Merensky located platinum-bearing reef in both the Rustenburg and the Potgietersrus areas (Allen, 1996). This subsequently resulted in a “platinum rush” and a scramble for mineral prospecting options in both regions. In 1925, over fifty companies had been floated to exploit the deposits of the Bushveld Complex. One of the more prominent was Potgietersrust Platinums Limited (PPL).

By the end of 1925, some eight shallow trenches had exposed the pyroxenite orebody (now known as the Platreef) on the farm Sandsloot, 27 km north north-west of Potgietersrus. A shaft was sunk to a depth of 11 m and exploratory cross-cuts and reef drives were developed. A vertical shaft and a 62° winze were subsequently sunk to examine the ore deposit to a depth of 30 m. On the farms Vaalkop and Zwartfontein, two shafts were also sunk in the latter part of 1925.

PPL established a treatment plant in September 1926 and by late 1928 it had produced 1,122 tonnes of concentrate. It is estimated that during the life of the mine some 110,000 tonnes of ore were extracted and treated. The financial depression of the 1930's, however, resulted in the closure of mining operations at Potgietersrust Platinums.

From 1966 onwards, Johannesburg Consolidated Investments (JCI) again focussed on the Platreef and various exploration programmes were conducted. Drilling was largely concentrated around the area of the old mine workings on Zwartfontein, Vaalkop and Sandsloot, and several boreholes reported good mineralisation. More detailed information was obtained from two exploratory winzes, which were sunk in late 1968. Bulk samples were

extracted for metallurgical testing and for extensive mineralogical investigations. A compilation of all the information was then undertaken and various feasibility studies were conducted.

In March 1967, a systematic regional exploration programme was initiated and in 1979/80 an exploration shaft was sunk on Overysel to a depth of 50 m (Figure 1.3). This study represented the most detailed and systematic examination undertaken on the Platreef and permitted the recognition of a broad-based stratigraphy for the Platreef.

In September 1987, Rustenburg Platinum Mines concluded an agreement with the Lebowa Government to exploit the reserves of the Bushveld Complex within Lebowa and, in September 1990, the decision was made to go ahead with a new platinum mine on the Platreef. The proposed venture would mine 200,000 tonnes of ore per month.

In October 1990, various estimates of the new mine were made public and it was stated that open pit mining methods would initially be employed. On the 10th January 1992, waste stripping commenced and, on the 12th February 1992, the first blast in the Sandsloot open pit area took place. The official mine opening was on the 3rd September 1993 and the first dividend declared on the 31st December 1993. As of 2003, over 300 million tonnes of rock have been excavated from the pit. The current Sandsloot pit is two thirds of its final size and is the first of six sequential pits scheduled for mining along the outcrop of the Platreef.

2.3 Mining

Stewart and Kennedy (1971) showed that the steepness of the ultimate slopes in an open pit mine was not the only factor that had an influence upon the overall profitability of an operation. They contended that on the basis of cash flow calculations there is frequently considerable economic advantage to be gained from using steep slopes during the initial stripping programme. This is particularly the case at Sandsloot where the stripping ratio plays a large role in profitability.

In order to reduce to a minimum the amount of waste rock that has to be removed to expose an orebody, the ultimate slopes of an open pit mine are generally cut to the steepest possible angle. Since the economic benefits gained in this way can be negated by a major slope failure, continual evaluation of the stability of the ultimate slopes is a vital part of open pit planning.

As rock slope failures, or the remedial measures necessary to prevent them, cost money, Hoek and Bray (1981) therefore suggested that a sum of 1% of the total mining cost was a reasonable amount to spend on slope design and correction costs.

The Platreef orebody at Sandsloot is tabular in geometry, dips at 45° and is approximately 50 m in width. These properties allow the orebody to be excavated by open pit mining methods, which is considerably cheaper than conventional underground mining. Due to the 45° dip of the orebody the stripping ratio is relatively high at 6.2:1, when compared with most open pits, for example Phalaborwa open pit, which has stripping ratio of 1.5:1. The stripping ratio is the ratio between the waste and ore mined or the amount of waste that has to be removed in order to access the ore.

During the 1970's and 1980's Steffen, Robertson and Kirsten (SRK) Consulting Engineers were commissioned to conduct the open pit feasibility study, which addressed the mining geotechnics and stable slope designs. The recommendations from the study are documented in SRK (1980). This was followed by a subsequent study and report by SRK (1991). These geotechnical reports formed the basis for the Sandsloot open pit slope designs.

Sandsloot open pit is the largest open pit platinum mine in the world. In a single month the mine crushes over 400,000 tonnes of ore and excavates 40 million tonnes of ore and waste annually. The mine is highly mechanised with 37,000 tonnes mined annually per employee. The open pit is in the process of a fourth cutback, which has a final depth of 200 m below surface while later cutbacks will extend this to a maximum of 320 m. The benches are 15 m in height and mining blocks are usually 100 m x 50 m. The ramps are 35 m wide and have a gradient of 10%. The pit is scheduled to expand in a series of phased cutbacks as shown in Figures 2.1 and 2.2. The last bench, bench 65, will be completed during 2010 when mining will cease in Sandsloot open pit.

Once a mining block has been scheduled, it must be reduced to mineable proportions by drilling and blasting. Each blast hole is 18 m in depth and there are, on average, 400 holes per blast (100 m by 50 m area). It follows that a reduction in the number of blast holes per blast and the rate at which those holes are drilled will have a considerable affect on mining cost. Include then the amount and type of explosives per hole, as well as the life of the drilling consumables and an idea of the number of parameters that can be adjusted to improve mining efficiencies is obtained.

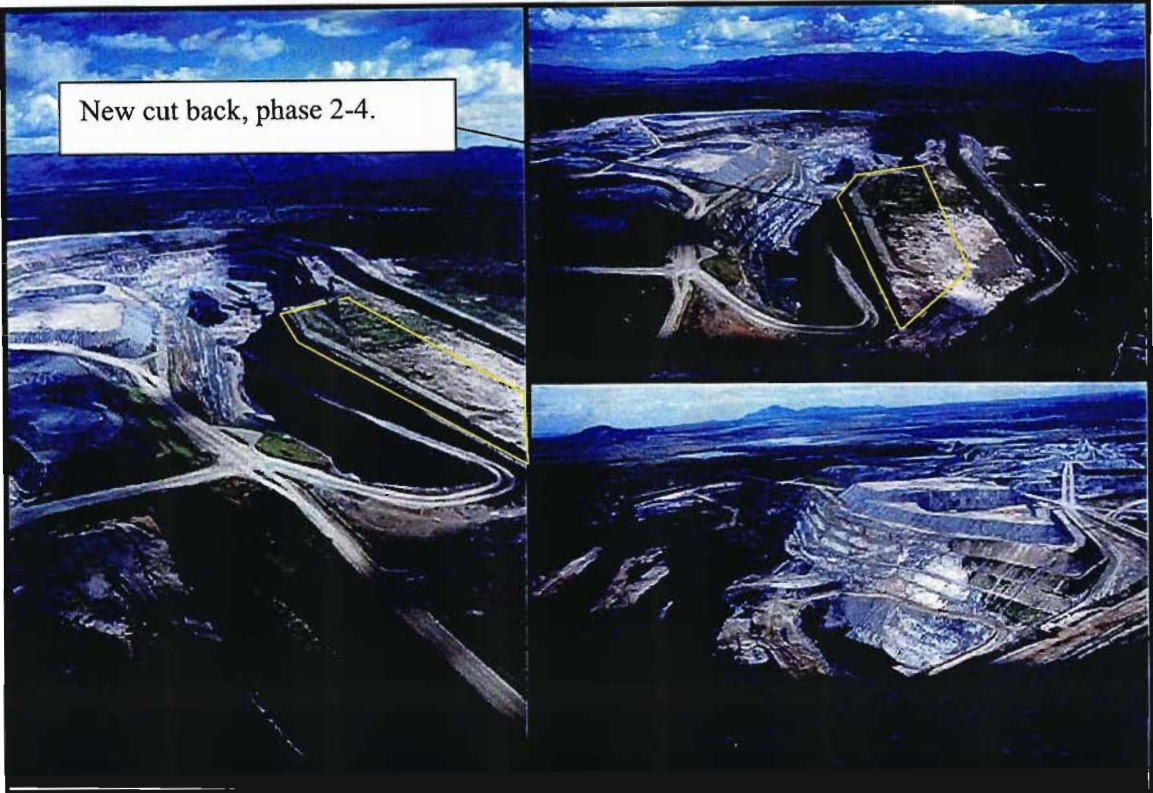


Figure 2.1 Photographs illustrating the Sandsloot open pit and the phases 2-4 cutbacks, which is the area of focus of this geotechnical study.

Potgietersrust Platinums Limited currently operates four Orenstein and Koppel (O & K) RH 200 hydraulic face shovels and a fleet of twenty-four CAT 785B dump trucks. The dump trucks have a capacity of 130 tonnes while the face shovels can accommodate 45 tonnes of material in a single pass. The productivity of this equipment depends largely on the blast fragmentation size. An economic balance has to be found between the very high loading rates produced from a highly fragmented rock mass, and the drill and blast costs associated with producing such a fragmented rock mass. Introduce the crushing and milling benefits associated with very fine blasting of the ore and it can be seen that achieving a minimum mining cost is not as simple as optimizing isolated cost centres such as explosive quantities used. The process can be optimised by having detailed geotechnical, geomechanical and mineralogical information of the rock mass. From this information, mining blocks can be assigned optimum drill and blast configurations that not only improve comminution and loading rates but also the ore concentration process. It follows that an integrated approach to mining that involves all cost centres is needed to successfully reduce overall mining costs and improve productivity.

2.4 Summary and Conclusions

In order for a mining company to stay competitive in the modern economy, it is essential that it operates at the lowest possible cost. Mining companies are therefore constantly striving to reduce the operating costs of the mining equipment by improving its performance. By providing comprehensive geotechnical information, equipment requirements can be accurately defined and therefore performance and mining efficiencies can be optimised.

Mine design is based on the *in-situ* geotechnical conditions and as such an overview of the geological and structural setting within the research area is discussed in Chapter 3. This chapter develops an understanding of the geotechnical conditions and the impact it has on mine productivity.

3 GEOLOGY

3.1 General Geology

The Bushveld Complex (BC) represents the largest intrusive body in the world and has a surface extent of 65,000 km² (Figure 1.2). Rock types related to this complex extend from near Zeerust in the west to Burgersfort in the east (± 500 km) and from Pretoria in the south to 100 km north of Potgietersrus (now Mokopane). The age of the Bushveld Complex has been estimated by Walraven *et al.* (1990) at approximately 2,060 million years, and emplacement of the BC probably extended over a period of at least 500 million years. The sequence of events commenced with the surface extrusion of large volumes of basaltic lava and acidic volcanics (White, 1992), which are the Rooiberg rhyolites, and granophyres, comprising the roof rocks. Subsequently, the intrusion was emplaced by repeated injections of magma in the form of sills, which may, in themselves, exceed 2,000 m in thickness (Cawthorn, 1996).

The Bushveld Complex intruded the Transvaal Supergroup, which consists of basal quartzite, followed by a dolomite and banded ironstone sequence, an alternating quartzite shale package, and an upper basaltic and acid volcanic phase (Button, 1976). The age of the Transvaal Supergroup is approximately 2,500 million years (Walraven *et al.*, 1990). In the Northern Limb of the BC, the intrusion occurred at the level of the Magaliesberg Quartzite in the south, but transgressed downwards to the north, until the mafic rocks abut Archaean Hout River gneisses, Turfloop and Utrecht granites (van der Merwe, 1976, Cawthorn *et al.*, 1985).

The layered mafic component of the Bushveld Complex outcrops in four discrete compartments. Each compartment possesses at least one supposed feeder, however Sharpe *et al.* (1981) have identified seven main feeders from gravity data. A feeder pipe close to Potgietersrus is thought to have resulted in the Potgietersrus or Northern Limb. The main period of igneous activity resulted in the emplacement of a mafic phase - the Rustenburg Layered Suite, and an acid phase - the Bushveld Granophyre and the Lebowa Granite Suite Complex (Figure 3.1).

The first phase of the mafic component of the Bushveld Complex, the Rustenburg Layered Suite (RLS) has been sub-divided into five zones, namely the Marginal, Lower, Critical, Main and Upper Zones, and comprises a stratigraphical sequence in excess of 9,000 m in thickness (Figure 3.1). Cawthorn (1996) documents in detail the various zones of the Rustenburg Layered Suite.

The Bushveld Complex is an important repository for a wide variety of economic deposits, ranging from dimension stone quarries to tin mines, with important copper, vanadium and magnetite deposits. The most economically important metalliferous deposits are, however, the platinum group element mineralised zones, which are concentrated in the Merensky Reef, the UG-2 chromitite layer and the Platreef. The Merensky and UG-2 reefs are found on the western and eastern limbs of the complex while the Platreef is located on the Northern Limb as seen in Figures 1.2 and 3.1. It has been estimated that up to 85% of the total known platinum reserves in the world are contained within these three horizons in the Bushveld Complex (Buchanan, 1988).

The Northern Limb occupies a buffalo-horn-shaped area of roughly 2,000 km² and constitutes one of the compartments of the Bushveld Complex. The stratigraphy and thickness of the sequence differs from that of the rest of the Bushveld Complex and therefore appears to be a separate compartment. Van der Merwe (1976) contended that the magma chamber from which the limb originated had at least four major influxes of fresh, undifferentiated magma. The exposed limb of the complex has a length of 110 km and strikes north north-west of Potgietersrus and it attains a maximum width of 15 km (Figure 1.2).

A platiniferous horizon in the Northern Limb (the Platreef) forms the base of the Main Zone and it is believed to be the local equivalent of the Merensky reef portion of the uppermost part of the Critical Zone of the Bushveld Complex. It hosts economic platinum group element (PGE) mineralisation within a sulphide-bearing pyroxenite body. The Marginal and Lower Zones of the Rustenburg Layered Suite are only sporadically present when compared to the stratigraphy of the western Bushveld as seen in Figure 3.1. The Platreef is also significantly different in genesis and mineralisation from the western part of the Bushveld Complex.

The entire Platreef pinches and swells in thickness and exhibits a slightly rolling hangingwall contact and an irregular footwall contact (White, 1992). The basal contact of the Platreef has a transgressive relationship with the underlying sediments of the Transvaal Supergroup in the south and Archaean granites to the north (Ainsworth, 1994). The transgressive basal contact is of primary importance as the degree of metamorphism, metasomatism and assimilation of the floor rock is directly related to the nature of the original sedimentary units. The contamination of the Bushveld rocks and the style and distribution of the mineralisation within the igneous units are thus directly related to the footwall rock types (Figure 3.2). In addition, the interaction of the Platreef pyroxenitic unit with different sedimentary sequences has resulted in a highly complex and unique suite of rock types (Buchanan, 1988).

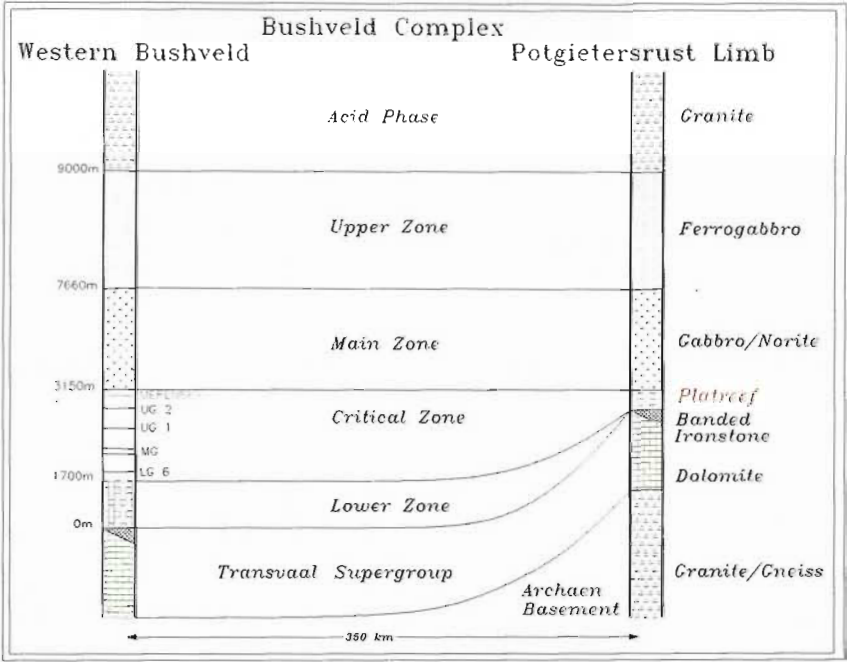


Figure 3.1 Stratigraphic column comparing the western Bushveld stratigraphy to the Platreef.

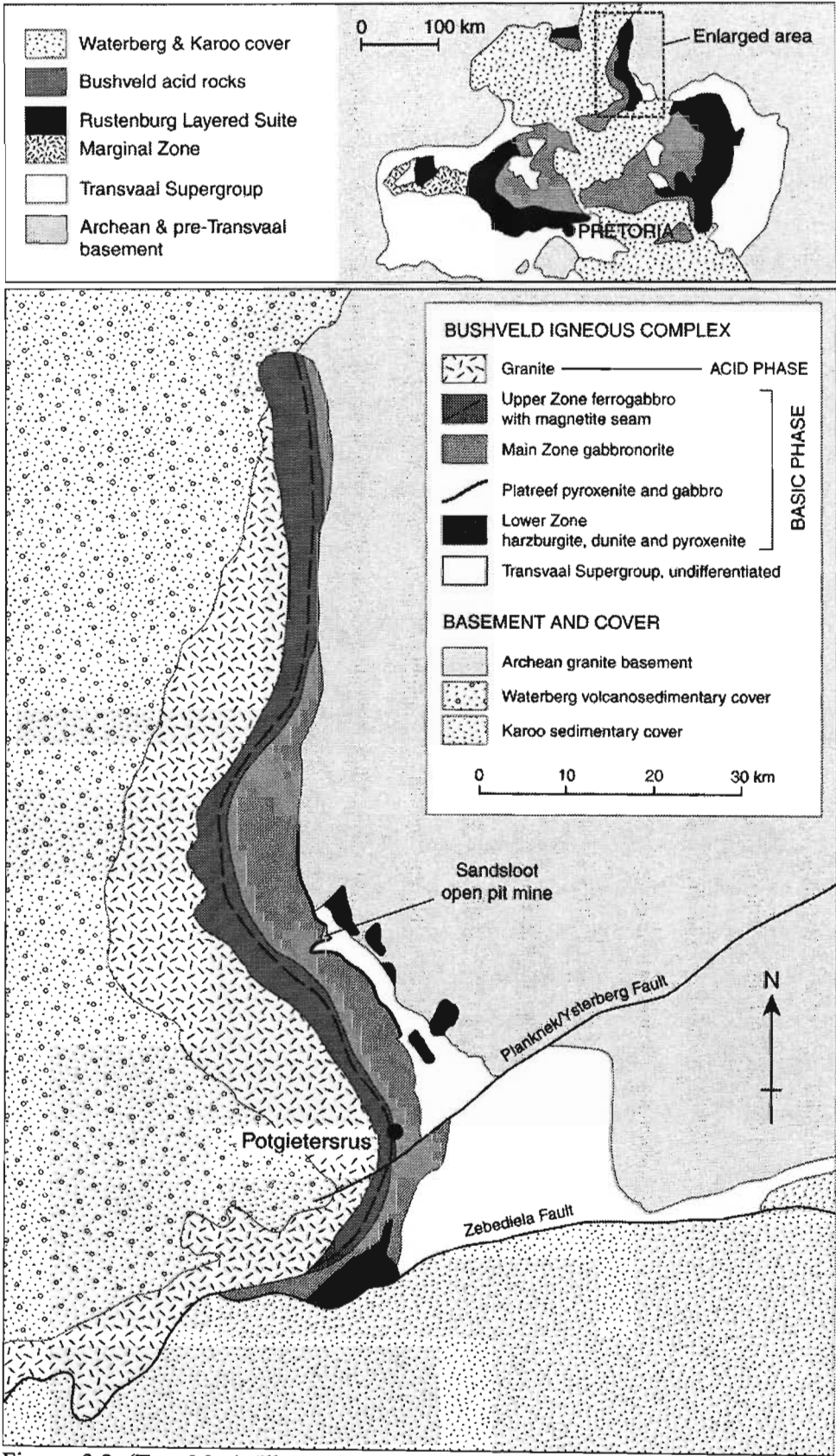


Figure 3.2 (Top Map) Illustration of the Bushveld Complex, emphasizing the RLS and showing the location of the northern limb. (Main map) Simplified geological map of the Northern Limb showing the location of the Sandsloot open pit, after Armitage *et al.* (2002).

3.1.1 Genesis and Crustal Emplacement of the Bushveld Complex

Friese (2002) has proposed a structurally controlled model for the emplacement of the BC. Continent-continent collision and accretional processes along the north-western margin of the Kaapvaal Craton induced NW-SE compressive far field stress into the lithosphere of the northern Kaapvaal Craton. This took place during the Palaeoproterozoic Ubendian (Magondi-Kheis) Orogeny at 2.06 - 1.8 Ga. In response to these compressional far field stress conditions, Archaean (>2.97 Ga) translithospheric suture zones (Figure 3.3) and Neoarchaean (2.81-2.64 Ga) Limpopo Orogeny-related shear zones within the northern Kaapvaal Craton, experienced reactivation. This was initially dextral strike-slip and later progressively more dextral oblique reverse-slip. Examples are the Pietersburg, Thabazimbi-Murchison and Magaliesberg-Barberton suture zones.

The initial trans-tensional reactivation of Archaean suture zones in combination with the trans-tensional rejuvenation of the Pongola Rift Basin resulted in decompressional melting of the sub-lithospheric, upper mantle and the formation of mafic-ultramafic magmas. This took place within the northern Kaapvaal Craton, during the early stages of the Ubendian Orogeny, at 2.05 - 1.93 Ga. The magma ascent through the continental crust was facilitated primarily along the deep-seated, trans-lithospheric suture zones and partly along extensional faults of the Pongola Rift Basin. The mechanical reactivation of these suture zones was accompanied and accelerated by thermal softening due to a higher geothermal gradient, caused by the intra-plating of these magmas (Figure 3.3). At a critical level in the crust, when the magmatic pressure was equalising and exceeding the overburden pressure, the mantle-derived magmas were emplaced as sills within sedimentary deposits of the Transvaal Supergroup, between major suture zones, at 2.06 - 2.054 Ga, to form the BC.

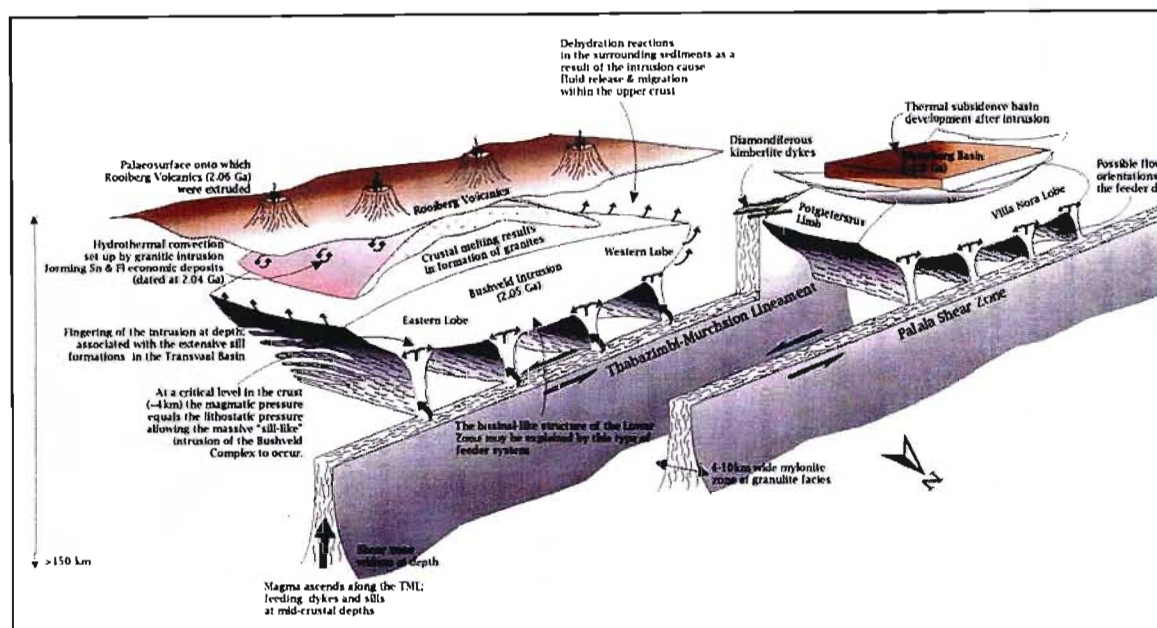


Figure 3.3 Proposed Bushveld Complex intrusion mechanism utilising the Thabazimbi-Murchison Lineament, allowing ascent along a deep-seated lithospheric shear zone (i.e. Thabazimbi-Murchison and Barberton-Magaliesberg lineaments), acting as a conduit. At a critical level in the crust, the magmatic pressure equalled the lithostatic pressure, which allowed the massive "sill-like" intrusion of the Bushveld Complex to occur, after Good (1999).

3.2 Local Geology

The origin of the Platreef succession has been the subject of some debate. Buchanan (1988) concluded that the Platreef crystallised from a Merensky reef-type magma, but that salic contamination from the footwall caused changes in the silicate chemistry towards the base of the unit (Vermaak, 1976). Armitage *et al.* (2002) has proposed a dominant hydrothermal control on the Platreef mineralisation.

In the Sandsloot area significant PGE mineralisation has been recorded to a current exploration depth of 800 m and in excess of 70 m in width. There is considerable variation in thickness of the Platreef at Sandsloot, ranging between 15 m and 100 m. A contaminated, serpentinised pyroxenitic sequence hosts the mineralisation, which is normally located close to the hangingwall gabbronorites (White, 1992). Gold occurs as electrum and in places ranges from 5 - 11 volume % of the total PGMs, significantly higher than in the Merensky reef. The PGMs are associated with base metal sulphides, and a higher proportion is encapsulated within silicates. According to Buchanan (1988) the variability of the mineral composition and the textural relationship along strike appears to be related to floor rock lithology.

The outcrop of the Platreef exhibits a slightly sinuous pattern with local changes in strike and dip, while the contact zone is disturbed and interrupted by the “dolomite tongue” at Sandsloot (Figure 1.3). The dolomite tongue is thought to represent a truncated diapir of footwall material.

The Platreef has an economic strike length of 40 km which contains platinum group elements, as well as copper, gold and nickel concentrations. The Platreef is capped by a sparsely mineralised hangingwall sequence of RLS Main Zone gabbronorites. This in turn is overlain by Upper Zone sequences of ferrogabbros (Ainsworth, 1994). Figure 3.4 illustrates stratigraphically the sequence of rock types occurring at Sandsloot. The mineralisation is hosted predominantly within pyroxenite and metamorphosed pyroxenite, locally known as parapyroxenite.

The pyroxenitic unit varies from coarse crystalline to fine crystalline feldspathic pyroxenite with phlogopite and sulphide mineralisation generally visible. The hangingwall contact is distinct and the overlying gabbronorites become more melanocratic near the contact.

The parapyroxenites hug the Transvaal Supergroup on the footwall and are essentially contaminated, metamorphosed pyroxenite formed between the cold dolomitic country rock and the Platreef intrusive phase. The footwall to the Platreef in the Sandsloot open pit is metadolomite known generically as “calc-silicate”. The metadolomites are generally yellow to brown in colour and are very fine grained. Remnant bedding is found in the calc-silicates with which a number of bedding faults are associated. The footwall contact with the calc-silicate is gradational and complicated with lenses of hybrid and pyroxenite rocks (SRK, 1980).

Interaction of the basic magma with the footwall sediments of the Transvaal Supergroup and the varying degrees of assimilation has resulted in a unique suite of hybrid rock types. These various rock types provide a host of engineering geological challenges.

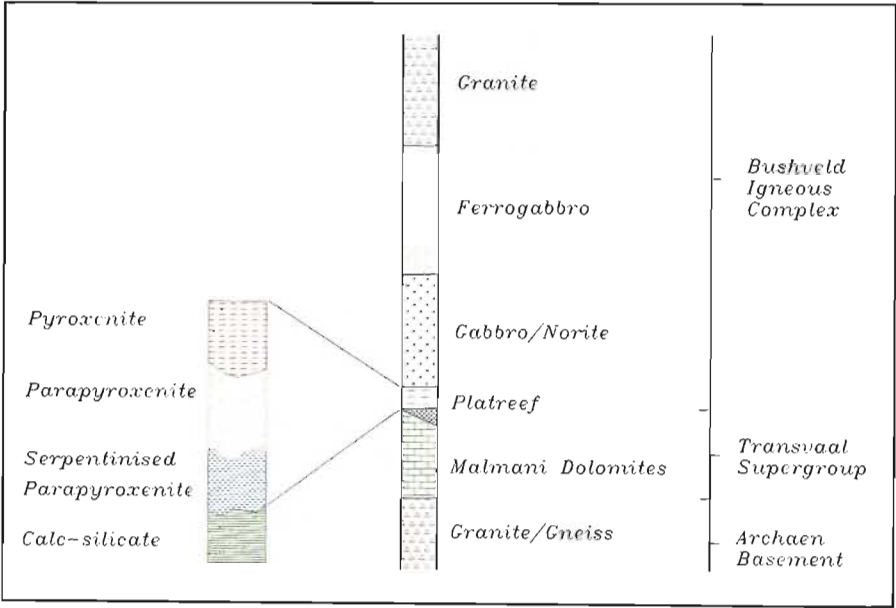


Figure 3.4 Stratigraphic column of the dominant rock types occurring at Sandsloot.

3.2.1 PGE Mineralisation

According to Armitage *et al.* (2002), at the Sandsloot open pit mine, the Platreef consists of coarse to pegmatoidal pyroxenites and gabbro-norites with accessory phlogopite, base-metal sulphides and oxides. Thermal metamorphism of siliceous dolomites that comprise the footwall has produced clinopyroxenites and calc-silicate hornfelses with a variety of skarn assemblages. These were subjected to later hydrothermal alteration and serpentinisation that also affected parts of the Platreef. The link between sulphides and PGEs in the Platreef has led previous authors to consider the mineralisation as an orthomagmatic sulphide deposit where sulphide separation collected PGEs from a large volume of melt. In the reef and footwall, however, the extensive alteration zones and high concentrations of PGEs and semi-metal (Te, Sb, Se, Bi and Ge) -bearing PGMs, typical of many low-temperature PGE deposits, suggest syn- to post-magmatic crystallisation or redistribution of PGE by hydrothermal fluids. Results of this study to date suggest that the Platreef at Sandsloot is a complex PGE deposit that has been subjected to a number of different processes during its development.

Comparison of the PGE ratios of the Platreef and footwall lithologies with the Merensky Reef and UG-2 chromitite reveals some interesting features. The pyroxenites and footwall are richer in Pt, Pd and Au relative to Ir than the Merensky or UG-2 reefs, producing more fractionated PGE patterns. Pt/Pd and Pt/Au ratios in the Platreef and footwall are lower than those in the Merensky or UG-2 reefs, indicating that the Platreef is richer in Pd and Au relative to Pt than the Merensky or UG-2 reefs. PGE-rich footwall samples and pegmatoidal aplites have lower Pt/Pd (consistently <1.0) than gabbro-norites or pyroxenites (≥ 1.0). This would appear to indicate some fractionation of Pd over Pt into late-stage fluids in the reef and footwall, a feature noted by Wagner (1929) and Ainsworth (1998). Rh/Ir in the Platreef is comparable with the Merensky Reef, but lower than the UG-2.

The pyroxenite and the PGE-rich footwall lithologies show a remarkably close similarity in terms of PGE ratios and normalised patterns. This type of footwall mineralisation is a general feature of the Platreef and it is present across the Sandsloot pit as well as along strike at Tweefontein Hill to the south and Zwartfontein to the north (Wagner, 1929). Armitage *et al.* (2002) suggest that any comprehensive genetic model for the Platreef must take into account hydrothermal fluid activity as a mineralisation process.

The PGM distribution in the Platreef is very different from all of the varieties of Merensky Reef described by Kinloch and Peyerl (1990) with the exception of some pothole reef and reef affected by late-stage dunite pegmatoids. The associations of Pt-Fe alloys, at the core of pegmatoid potholes, and telluride-rich mineralisation around the rim have both been attributed to the effects of fluids (Kinloch and Peyerl, 1990). Given the strong evidence for fluid activity in the Platreef and the footwall, it is likely that fluids have influenced the development of PGMs in the Platreef in a similar manner to volatile-rich portions of Merensky Reef.

Wagner (1929) recognised the division between the pyroxenite reef and the underlying footwall assemblages and ascribed the formation of these units to magmatic and metamorphic / metasomatic processes, respectively. Two of the most significant results to come out of the Armitage *et al.* (2002) study are the complete absence of PGE sulphides, particularly laurite (RuS₂), and the abundance of alloys and semi-metallides in the Platreef. This trend acquires greater significance when compared to other Bushveld PGE reefs (Kinloch and Peyerl, 1990) and PGE-bearing sulphide deposits in other mafic intrusions such as the Great Dyke and the Munni Munni complex. In these deposits PGE sulphides comprise anywhere between 10 % - 60 % of the PGM assemblage. The PGM assemblage in the Platreef at Sandsloot is distinctly different from any of these deposits.

On the basis of stable isotope data, Harris and Chaumba (2001) concluded that the Platreef fluid was a mixture of predominantly magmatic water with a minor component derived from the footwall. Armitage *et al.* (2002) propose that the metre-scale variability in PGE concentration, coupled with the absence of any PGE sulphides and the abundance of low-temperature PGMs, cannot be linked to any orthomagmatic model and is best explained by the action of fluids. These played the dominant role in mobilising and homogenising PGEs within the Platreef and carrying them into the footwall, where they formed irregular zones containing high PGE concentrations. The PGM assemblage crystallised under hydrothermal conditions in a fluid envelope that affected both the reef and the footwall.

3.3 Structural Geology

There are two principal fault sets observable in regional maps and orthophoto images affecting the Platreef mining area (Figure 3.5). The regional geological pattern is disturbed by these NE trending faults. Both sets of structures influence the Transvaal Group sedimentary rocks and predate the intrusion of the Bushveld Complex. The basic fault architecture was in place when the Bushveld Complex was intruded. Additionally, both sets have been active since the intrusive event and have controlled much of the first order fracture pattern in the pit and environs (Etheridge, 2001). A series of strike faults, which trend NNW, is also evident in the area (yellow lines in Figure 3.5), one of which marks the basal contact between the Bushveld Complex and the Transvaal Supergroup over certain sections of the Northern Limb (White, 1992).

Fault Set One

Fault set one strikes ENE and has strike lengths in excess of 100 km. These faults control the distribution of most of the large scale folds in the Transvaal sediments and generally have the character of thrust or reverse faults. They commonly form straight river segments and cause small offsets in the N-S trending Northern Limb.

In order to place these fault zones into their regional context, one has to look at the structural framework of the northern Kaapvaal Craton. The NE-SW striking Ysterberg Fault to the south of the Sandsloot pit represents a segment of the Mesoarchaeon Pietersburg terrane boundary, from which most of the major, NE-SW striking shear zones splay. These strike-slip shear zones formed due to the transpressional reactivation of the palaeo-suture zone during oblique continental collision of the Limpopo Central Zone Terrane and the Kaapvaal Craton. The continental collision took place along the Palala suture zone during the Limpopo Orogenic Cycle at 2.81-2.64 Ga (Friese, 2002).

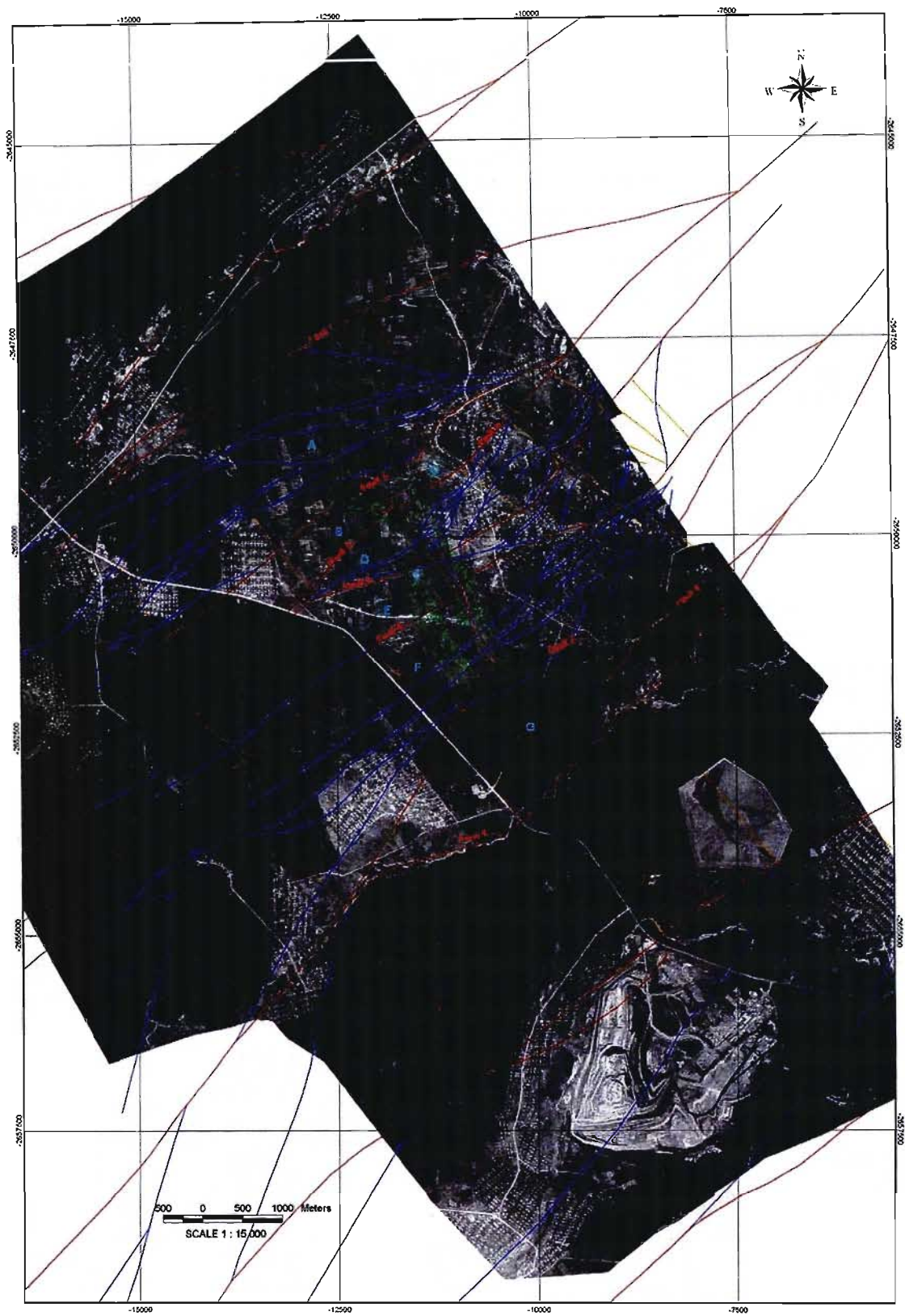


Figure 3.5 Major structural plan of the Platreef mining area, after Friese (2002).

A pre-BC age for these shear zones was also envisaged by Etheridge (2001), who proposed that the distribution of PGE and Ni-Cu mineralisation along the Northern Limb appears to be influenced significantly by such shear zones. An example would be the Ni-Cu mineralisation on the Tweefontein farm, which is situated in an embayment in the BC-Transvaal Supergroup contact. The mineralisation occurs at the contact intersection with numerous NE-SW striking shear zones (Figure 1.3). Furthermore, the thickness and facies of lithologies of the Transvaal Supergroup appear to have been influenced by these shear zones, which also certainly exerted the primary control on fold/thrust patterns in the Transvaal Supergroup that at least partly predate the intrusion of the BC (Etheridge, 2001).

The Sandsloot open pit is disturbed by three major north-east trending faults (Figure 3.5). There are two normal faults in the north pit, which form a graben structure with a 30 m downthrow. The major oblique-sinistral “Satellite pit fault” which has displaced the Sandsloot orebody to the south east by approximately 400 m is the third major fault. This fault has caused extensive alteration and deformation in the surrounding rock types. Other notable structures include a highly sheared zone of pyroxenite up to 5 m in width and dipping at 45° to the west, which separates the barren hangingwall gabbro-norites from the pyroxenite orebody.

Fault Set Two

Fault set two strikes N to NE and these faults have strike lengths in excess of 100 km. These faults partition and offset the fault set one thrusts, and have the character of steeply dipping transfer or relay faults. Fault set two constitutes the principal geotechnical risk throughout much of the pit. This is due to the large scale planar failures created where the fault set two intersects the western highwall. The faults occur as clusters of joint and fault planes 1 m - 2 m in width throughout the pit (Etheridge, 2001).

Based on a structural interpretation of remote sensing data sets over the Platreef prospect area (Friese, 2002), in combination with existing published and unpublished geotechnical information, the main observations can be summarized as follows: most of the structural discontinuities identified in the prospect area can be grouped into three main classes of structures:

1. Reverse to strike-slip shear zones:
 - In general NE-SW striking, steep (70-85°) south-east dipping
2. Normal to oblique-slip fault zones:

-In general NW-SE striking, moderate to shallow (60-40°) south-west dipping

3. Thrust to reverse fault zones:

-In general NE-SW striking, moderate to shallow (60-40°) north-west dipping

The majority of the fault and shear zones cross-cutting and off-setting lithologies of the BC within the prospect area, are pre-BC in age (Neoarchaeon). These zones experienced tectonic reactivation as a result of NW-SE compressive far field stress conditions induced in the northern Kaapvaal Craton during the Ubendian Orogenic Cycle at 2.05 - 1.8 Ga.

3.3.1 Tectonic Evolution

The following tectonic history for the Platreef prospect area was proposed by Friese (2002):

Limpopo Orogenic Cycle 2.81 - 2.64 Ga.

- NW-SE striking extensional faults of the Neoarchaeon (2.97 - 2.95 Ga) Pongola impactogenel rift basin underwent trans-tensional reactivation during the Limpopo Orogenic Cycle.
- Developments of first-order NE-SW striking and second-order E-W striking, strike-slip shear zones along the Palala suture zone. This was as a result of NE-SW compressive stress induced into the lithosphere of the northern Kaapvaal Craton during continent-continent collision with the Limpopo Central Zone Terrane.

Ubendian Orogeny 2.05-1.93 Ga

- The transtensional reactivation of Archaean terrane boundaries, in combination with the rejuvenation of the Pongola rift basin within the northern Kaapvaal Craton, resulted in decompressional melting of the sublithospheric, upper mantle and the formation of mafic-ultramafic magmas to form the BC and related satellite intrusions.
- Major NE-SW striking shear zones splay from the tectonically reactivated Pietersburg suture zone, thereby forming a tessellated array with second-order shear zones. This resulted in a shear zone geometry dominated by strike to reverse-slip duplexes on a regional to small scale.
- Continent-continent collision and accretional processes along the north-western margin of the Kaapvaal Craton induced NW-SE compressive stress into the lithosphere of the northern

Kaapvaal Craton. In response to these compressional conditions, Archaean translithospheric suture zones (e.g. Pietersburg, Thabazimbi-Murchison and Magaliesberg-Barberton suture zones) and the Neoarchaeal, Limpopo Orogeny-related shear zones within the northern Kaapvaal Craton, experienced reactivation.

Suturing stages of the Ubendian Orogeny 1.93 - 1.8 Ga

- After the emplacement of the BC, NW-SE orientated compressive stress conditions prevailed and peaked at 1.93 - 1.8 Ga. This occurred during the main and final continental collision and suturing stages of the Ubendian Orogeny. This event caused the folding, thrusting and transpressional reactivation of the shear zones within the northern Kaapvaal Craton. Shearing along the N-S trending Platreef ore contact, which dips at 45-65° to the west, is expected to have occurred during NW-SE compressive tectonics within the northern Kaapvaal Craton in the form of strike to reverse-slip movements. The presence of this contact shear zone is also expected within the Overysel-Zwartfontein North prospect area.

Kibaran Orogenic Cycle 1.45 - 1.0 Ga

- Intracratonic transtensional tectonism formed N-S striking extensional fractures zones, which were later reactivated along the NW-SSE trending Pongola rift faults (1.2-1.0 Ga). Minor extensional reactivation of the Pongola rift faults and possibly some of the Archaean shear zones occurred in response to NW-SE extensional stress conditions generated during the Namaqualand-Natal Orogeny at 1.2-1.0 Ga, representing the culmination and closing stage of the Kibaran Orogenic Cycle (1.45-1.0 Ga).

Dispersal of the Gondwana Supercontinent 210 Ma – to present

- Minor extensional reactivation of all the pre-existing structural discontinuities throughout the entire Kaapvaal Craton occurred. In addition, the formation of new, approximately NE-SW striking, fracture zones occurred in response to intra-cratonic extensional tectonics during the fragmentation and dispersal of the Gondwana supercontinent from 210 Ma until present time. Predominantly doleritic and subordinately kimberlitic magmatism accompanied the extensional tectonics within the Kaapvaal Craton, leading to the intrusion of these magmas as dykes along reactivated pre-existing structures and the newly formed fracture zones.

3.3.2 Jointing

The characteristic fracture and joint patterns at Sandsloot are associated with, and have formed in response to, movements along shears and faults. In addition to being potential failure zones in their own right, the identified fault and shear zones control much of the distribution, orientation and density of smaller scale fracture/joint sets. That is, they form the boundaries of geotechnical rock mass domains.

Discontinuities occur in the form of fissures, bedding planes, joints or faults within any rock mass. Their presence strongly affects the mechanical and hydrogeological properties of the rock mass in terms of its strength, deformability, stability, porosity, water storage capacity and transmissivity. These properties play a major role in the design and maintenance of open pits (Sen and Kazi, 1984).

There are four major joint sets influencing the Sandsloot area. The remaining minor joints are thought to have formed by randomised contraction jointing on cooling of the Bushveld intrusive phase. Figure 3.6 and Table 3.1 detail the joint data collected at Sandsloot open pit. The most prominent joint set (JS1) strikes north-west, has pronounced slickensides and is associated with felsite veining. This major joint set causes significant planar failures on the western highwall. A critical joint phenomenon is identified within the set (Bye, 1996). The critical joints represent those joints that are open and weak and therefore prone to failure. It was identified that these joints occur at a regular spacing. These large foliation planes (critical joints) dip steeply, and are both laterally and vertically continuous over hundreds of metres. They not only pose slope stability problems but affect drilling and blasting. Due to the size of the critical joints, blast energy is vented up them and drill steels tend to deflect along their planes.

The Sandsloot area has been intruded by late phase quartzo-feldspathic veins, which are associated with critical jointing of joint set one. These felsite veins cross-cut the open pit causing drill and blast problems due to their high strength (320 MPa) and related sympathetic jointing, which provide a vent for blast energy and result in a high percentage of re-drills. They also provide weak release surfaces for kinematic failures.

Joint sets two and three do not result in significant stability problems due to the near vertical dip and sealed nature of the joints. Joint set four is related to the calc-silicate bedding and is therefore only present on the footwall. The low angle dip and rough nature of the bedding joints

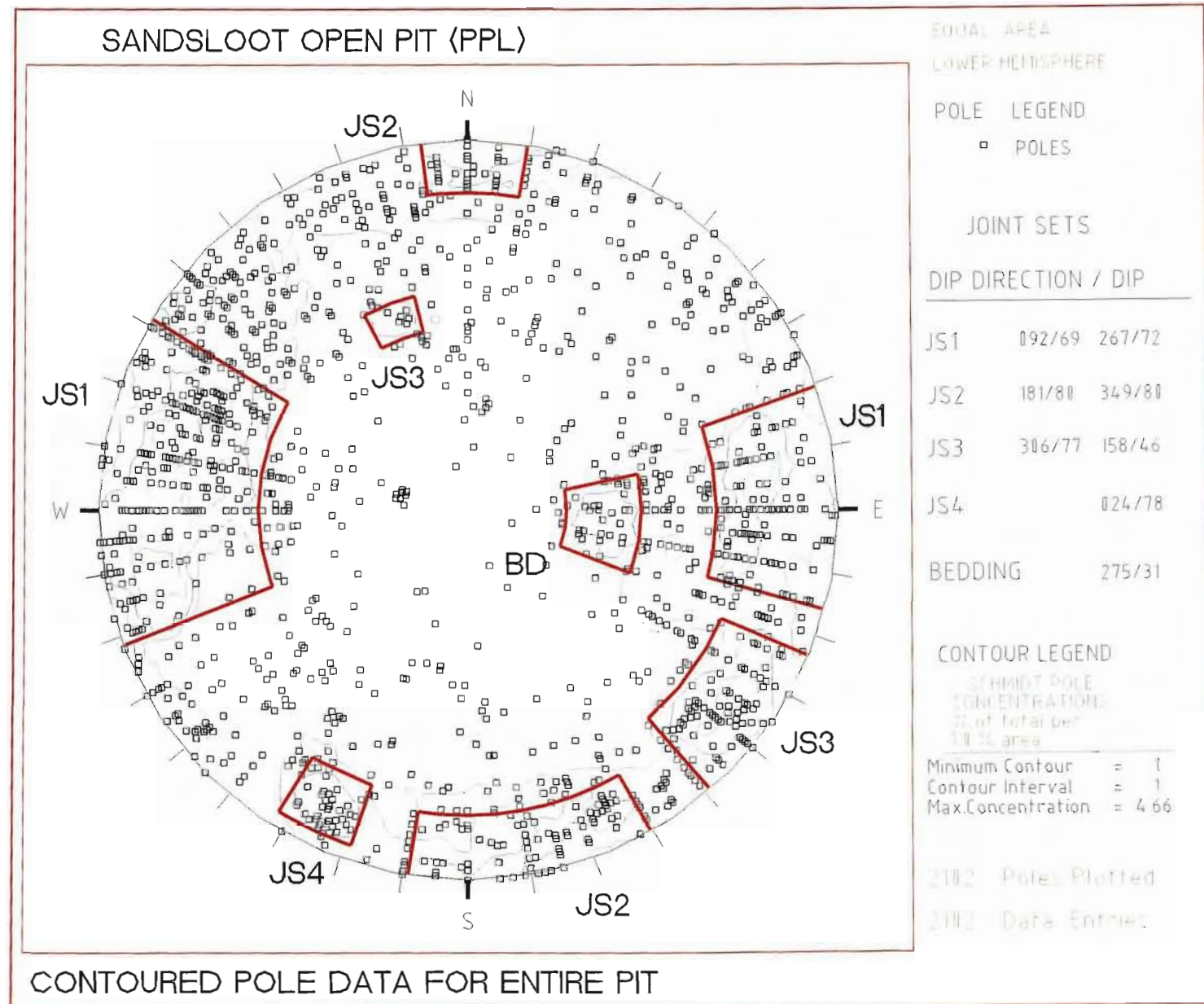
result in few failures. A detailed study on kinematic failure mechanisms related to the discontinuities encountered in the pit is discussed in Chapter 4.6. A kinematic failure plan (Figure 4.1) has been generated which depicts the various modes and locations of failures within the pit.

SRK (1980) contended that the nature of the major discontinuities at Sandsloot reflect their tectonic environment with three major lineaments controlling the emplacement of the Northern Limb of the Bushveld Complex. Thus, the major features at Sandsloot result mainly from the intrusive and cooling history and the tectonics of the Bushveld Complex. The major joint sets are continuous throughout the pit and all the main rock types, which indicates that the major joint sets have a regional structural control.

Table 3.1 Joint set information collected at Sandsloot open pit.

	DIP	DIP DIRECTION	JOINT ROUGHNESS	JOINT FILLING	JOINT SPACING
JS1	72	088	(IV) Rough Irregular	Calcite	0.5 m
	73	263	Undulating	Serpentine	(0.2-2.0m)
JS2	78	357	(II) Smooth Stepped	Calcite	0.4 m
	82	183			(0.2-1.0m)
JS3	70	310	(V) Smooth Undulating	Serpentine	0.3 m
	62	125			(0.1-5.0m)
JS4	72	237	(VII) Rough/Irregular	Calcite	0.15 m
	63	065	Planar		(0.05-0.40m)

Figure 3.6 Stereonet depicting the joint set families present at Sandsloot.



3.4 Geohydrology

The topography of the lease area consists of flat flood plains separated by high granite koppies and ridges. The mine is situated on the eastern side of the shallow valley of the Groot Sandsloot River, which is within the Mogalakwena River catchment. The Groot Sandsloot River has a mean annual runoff of $1.731 \times 10^6 \text{ m}^3$ and contributes 5% of the surface runoff into the Mogalakwena River. The recorded average annual rainfall generally varies from 380 mm to just over 700 mm. Precipitation occurs mainly in the form of thunder storms during the summer months with the peak of the rainy season in January.

Extensive borehole investigations in the lease area and the surrounding catchments have indicated that the main groundwater bearing zones lie at the base of the weathering profile at depths of between 2 m and 43 m. The mine is heavily dependent on its well fields for a large portion of the approximately $5.0 \times 10^6 \text{ m}^3$ of water it requires per annum for its processes. The annual groundwater recharge rate is approximately $1.86 \times 10^6 \text{ m}^3/\text{a}$ (+/- 3% of MAP). The mine has three wellfields, which are hosted within two main aquifer types.

The area surrounding PPL contains few primary aquifers and is therefore a groundwater poor area. Owing to the igneous intrusion and subsequent metamorphism of the surrounding geology, the local rock types form a fractured rock aquifer where water is stored in discontinuities and pores along the fractures. Fractured rock aquifers have low storage potential and because their response to pumping is controlled by the extent and interconnection of fractures, are usually unpredictable in behaviour.

The three PPL wellfields take the form of a series of elongated troughs approximately parallel to the strike of the Bushveld rocks. Fracturing has enhanced the water bearing capacity of these deeply weathered basins and most high-yielding boreholes are associated with them. The fracturing is generally perpendicular to the strike of the Bushveld Complex and is well developed at Zwartfontein and Overysel. In these aquifers the overlying weathered horizon supplies most of the storage with the underlying fracture zone forming a highly transmissive zone. The highest yielding wells are located within weathered troughs in pyroxenite, as the permeability is higher and varies less than in other weathered rock types. Campbell (1994) concluded that the aquifer had a transmissivity value of $60 \text{ m}^2/\text{day}$, storativity of 4×10^{-3} and a hydraulic conductivity 10^{-3} cm/sec .

A study conducted by SRK (1991) estimated that the open pit at Sandsloot has an influence on the surrounding ground water systems only within a radius of 400 m because of the low

permeability and consequently slow movement of water through the rock mass. There are no groundwater users within this radius. The SRK (1991) investigation on dewatering of Sandsloot open pit concluded that the total groundwater flow into the pit would be 112 m³/hour. Of this approximately 22 m³/hour would enter via the footwall and approximately 90 m³/hour would enter via the hangingwall.

Although localized high water pressures in fractured zones may cause slope stability problems, there has been no evidence of this occurring within the highwalls. Figure 3.7 illustrates graphically the effect of dry vs wet conditions on the factor of safety of the design slopes (SRK, 1991). In general, groundwater inflow into the open pit is not a major problem for the mine and conventional dewatering by pumping from sumps is adequate to control the situation. Figure 3.8 illustrates the lack of groundwater ingress into the pit via the highwalls.

Pit dewatering is an essential component to an open pit operation, not only for slope stability but also for in-pit productivity. In-pit water causes a high percentage of blast holes to be redrilled owing to their collapse under saturated conditions. Charging of saturated blast holes is difficult and requires more costly explosives to be used. Wet loading areas cause extensive damage to the rubber tyres of the haul trucks (wet rubber is more susceptible to wear and cuts than dry rubber) and it is dangerous to operate electrical equipment in wet areas. These factors can have a cumulative cost effect on the mining process and it is therefore essential to implement a comprehensive dewatering programme.

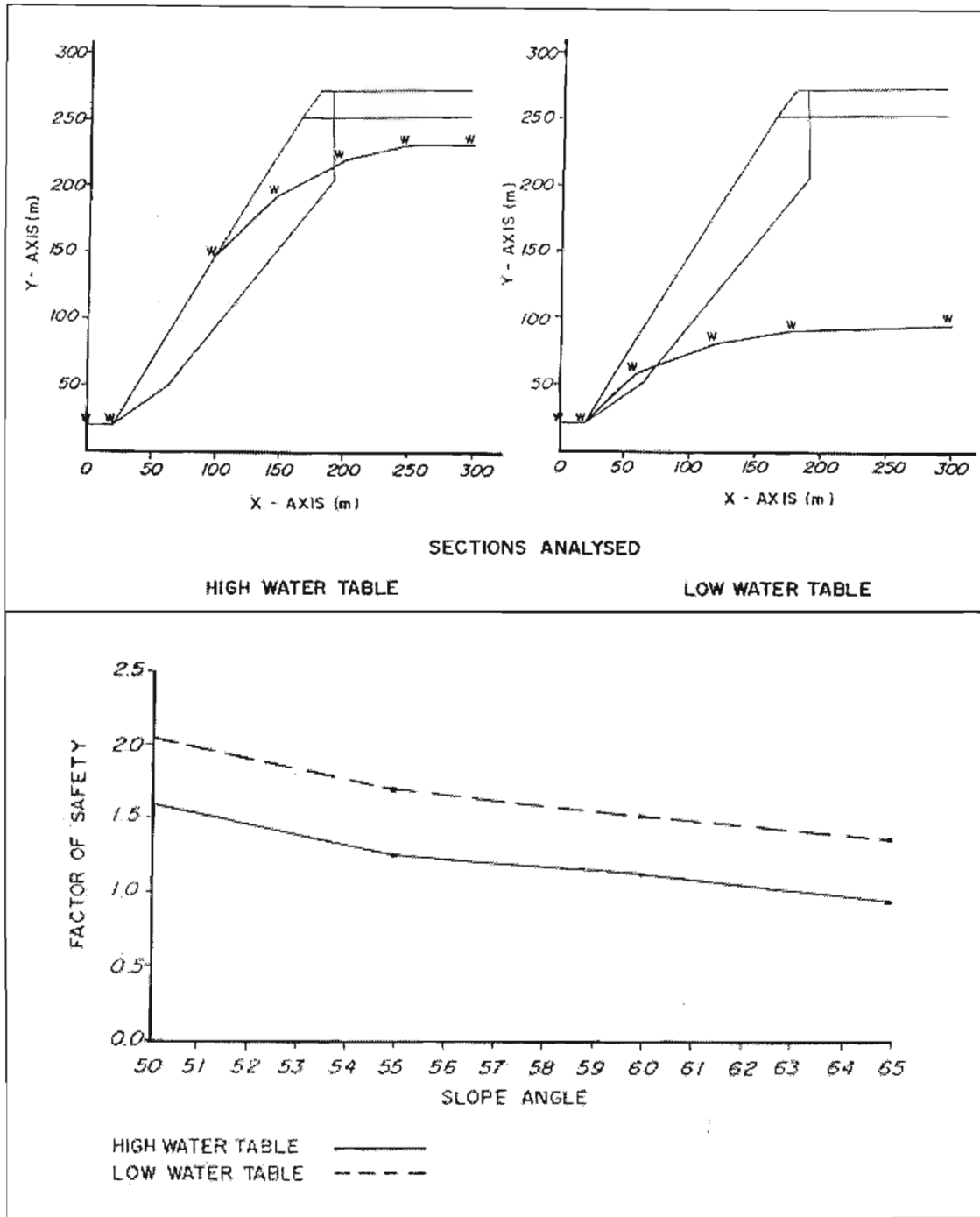


Figure 3.7 The effect of dry vs wet conditions on the factor of safety of the design slopes (SRK, 1991).



Figure 3.8 View of the open pit highwalls showing no obvious groundwater seepage.

3.5 Summary and Conclusions

An overview of the general and local geological setting including theories on the genesis and crustal emplacement of the Bushveld Complex was given. The possible mineralisation processes of the Platreef were also reviewed and the major structures, jointing, geohydrology and proposed tectonic evolution within the research area were discussed. This chapter developed an understanding of the geological and structural conditions present at Sandsloot.

The relevant geotechnical data and sampling methods are introduced in Chapter 4. The interpretation of this data into useful engineering numbers will be discussed, as well as the methods used to ensure consistent, quality data capture. Kinematic failure analysis and rock strength testing data is also presented as it is used as a basis for slope design.

4 GEOTECHNICAL INFORMATION

4.1 Introduction

A geotechnical design zone represents a portion of the mine where unique geological, structural and geotechnical conditions exist. These conditions give rise to a particular set of identifiable rock related properties or hazards, which can be quantified and for which a common set of strategies and mining methods can be employed to optimise productivity and minimise the risk resulting from mining.

The collection of geotechnical data at Sandsloot was based upon extensive field mapping using line surveys as well as geotechnical face mapping and logging of exploration boreholes. Over a five-year period, geotechnical data were collected from 29,213 m of exploration core and 6,873 m of exposed mining faces (Appendix 1). Extensive field and laboratory testing was also undertaken in order to define the complete set of geotechnical properties for each rock type in the Sandsloot mining area. The PPL geology department is gratefully acknowledged for their contribution in collecting the geotechnical data.

Geotechnical mapping involved the visual separation of a mining face into similar geotechnical zones based on rock type and structure. Each zone was then mapped individually and the following data collected:

- All the data required to rate the zone using Laubscher's (1990) mining rock mass rating system (described in Section 4.2).
- Line survey joint and major structural information such as joint orientation, roughness and continuity as well as Schmidt hammer readings for calculation of intact rock strength.
- Geological mapping defining rock contacts, mineralogy and rock descriptions.

The diamond drill exploration boreholes are logged for the same information as described above before being dispatched for assaying. There was then a common set of data between the open pit faces and the exploration boreholes from which interpolation and predictions were made.

The data collected were evaluated using a number of recognized software packages as well as specialized software developed in-house, as described in Section 4.2. Unique geotechnical zones based on mining rock mass rating (MRMR), rock quality designation (RQD), intact rock strength (IRS) and kinematic failure mechanisms were initially developed. This geotechnical zoning was used to optimise production, reduce slope hazards and improve mine planning decisions.

The historical way of representing this information is on comprehensive plans and sections as illustrated in Figures 4.1 and 4.2. The development of a geotechnical plan, representing all the structural (major joints and faults), geological (rock types and descriptions) and geotechnical data (MRMR, IRS and RQD) collected can be used for detailed mine planning, scheduling and slope design. As the plan is developed and extrapolated to tie in with geological and structural data, so the risks associated with structural features will be reduced. This creates a safer mining environment and increased productivity.

The plans and sections (Figure 4.1 and 4.2) concisely illustrate all the geotechnical data, which enables planning and production decisions to be made. The plans were used as a basis for interaction with drilling and blasting engineers so they can develop empirical drilling and blasting parameters for each geotechnical zone.

Sections were used to make more reliable assessments of the potential stability of successive slope cutbacks as well as highlighting failure modes and their extent. They are also used to assess the planned versus actual slope profiles, which enable evaluation of the limit blasting programme. The geotechnical plans and sections enable prediction of geotechnical conditions in two dimensions and as such were important tools during the initial phases of the research.

The geotechnical programme was, however, taken to another level by the development of the three-dimensional (3D) model. Two-dimensional (2D) plans, while being informative (Figure 4.1), become rapidly outdated as mining progresses and are onerous to update. It is here that the 3D geotechnical model becomes a powerful tool, replacing the 2D plans. The geotechnical focus shifts from extrapolating information as the mining faces advance to updating a predictive model. The model becomes progressively more accurate as the information is updated in three dimensions when the mining faces advance, whereas the 2D plans are dependent on extrapolation of the previous mining face.

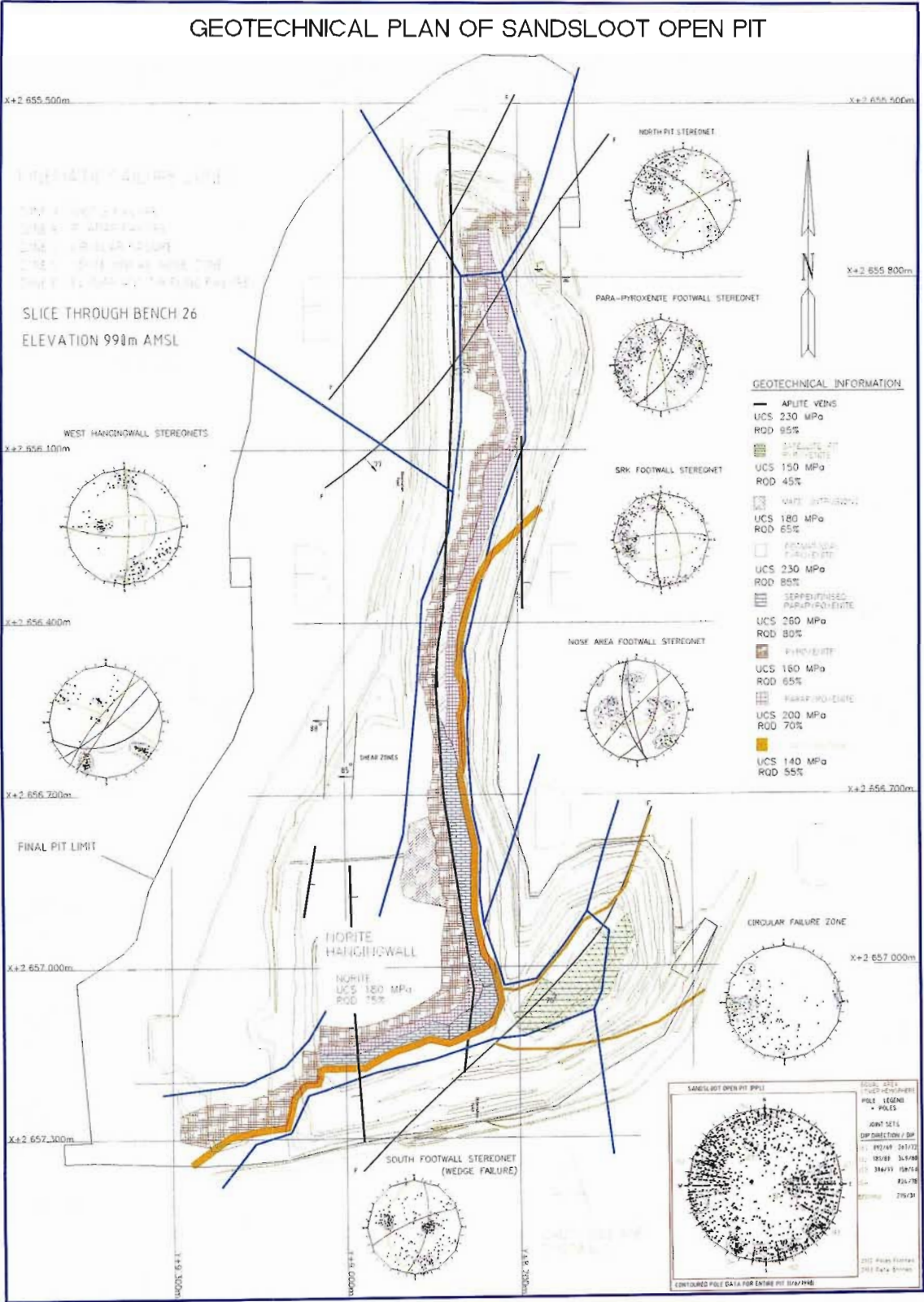


Figure 4.1 Geotechnical plan of Sandsloot open pit.

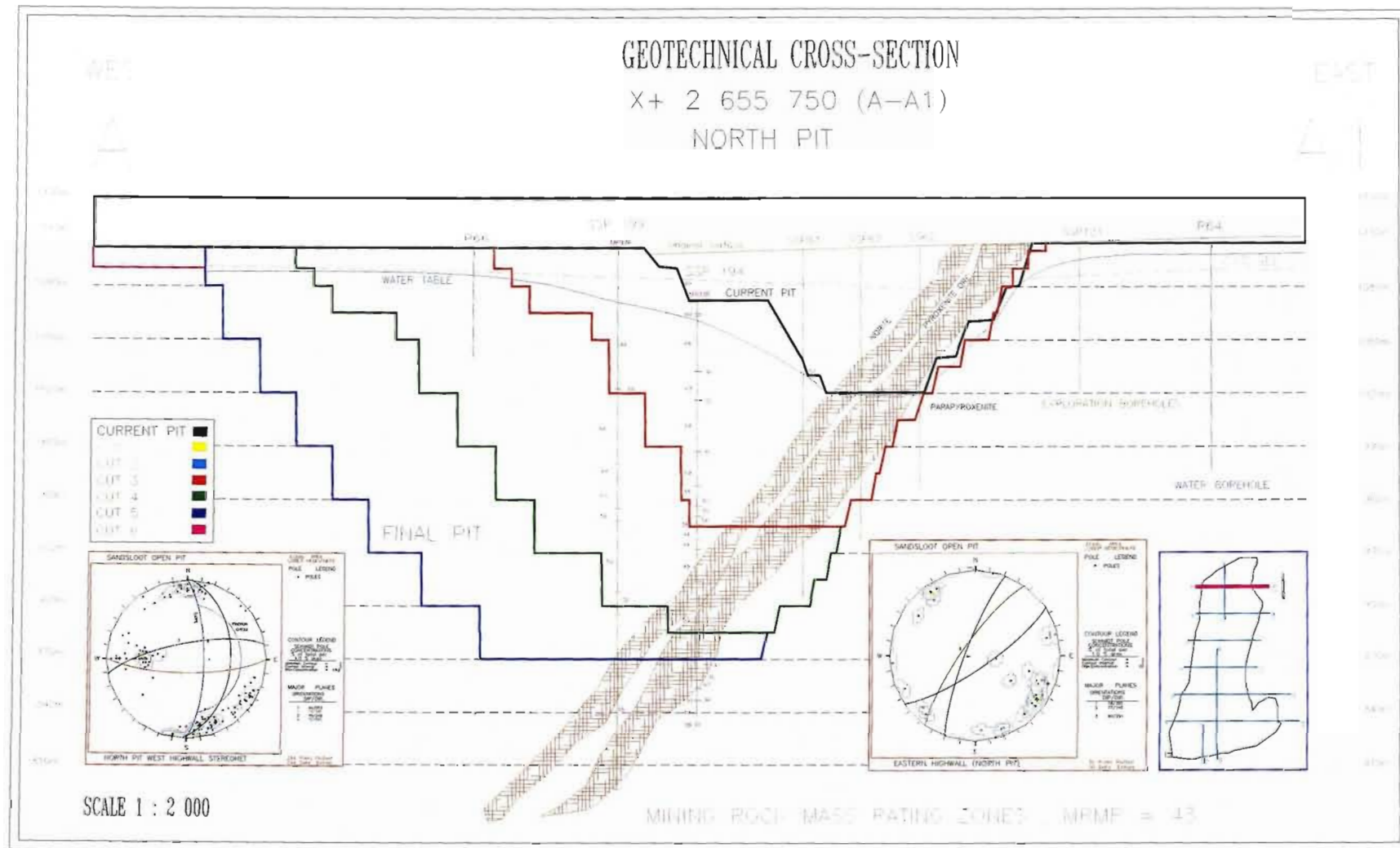


Figure 4.2 Geotechnical cross-section of Sandsloot open pit.

4.2 Rock Mass Classification

The mining rock mass rating system (MRMR) of Laubscher (1990) was developed for rock mass quality assessment. However, more important than the choice of method is consistency in the quality and method of data collection. After comparison with the rock mass rating (RMR) system of Bieniawski (1973) and the Barton *et al.* (1974) Q-System, it was found that the results were very similar. The MRMR system, however, yielded more conservative results than the other two systems, mainly due to the mining adjustments, and was therefore more suitable. As stated by Laubscher (1990) his system is suitable for both face mapping and borehole logging and ensures consistency in data capture. Additionally, all the initial evaluation work undertaken by SRK Consulting Engineers utilised the MRMR system. For these reasons the decision was made to build on this database rather than introduce a new system. With any interpretation of scientific data, account must be taken of the variability of the measured parameters. Sensitivity analyses were therefore undertaken on the data, as discussed in Chapter 5.

The MRMR system involves the assignment to the rock mass of an *in-situ* rating based on measurable geological and geotechnical parameters. These rock mass parameters include discontinuity spacing, joint condition and intact rock strength. Each parameter is weighted according to its importance and, if assigned a maximum rating, gives a total of 100 for all the parameters. The rating is then adjusted for mining conditions such as stress, joint orientation, weathering and blasting. The flow diagram in Figure 4.3 illustrates the MRMR system and the weighting of each factor. The range of 0-100 is used to cover all variations in jointed rock masses with the classes ranging from very poor to very good. For a detailed description of how to use the MRMR system see Laubscher (1990).

A Schmidt hammer was used to give a rough estimate of the intact rock strength (IRS) for all rock types and structural zones within the pit (Table 4.2). The Schmidt hammer is simply a spring-loaded instrument measuring rebound strength off a rock unit. It was originally designed to test the hardness of concrete. Using the Deere and Miller (1966) conversion graph and the rock unit weight, the Schmidt hammer readings are converted to intact rock strength (IRS) values. Once calibrated with the uniaxial compressive strength (UCS) laboratory testing results, the Schmidt hammer values were used for RMR calculation and the delineation of “hard zones”.

One of the strongest points of the MRMR system is the ability to assign adjustment factors to suit unique mining situations. In assessing the behaviour of the rock mass in the mining environment the ratings are adjusted for weathering, mining induced stresses or change in stress field, joint

orientation and blasting effects. The site-specific mining adjustments for Sandsloot are represented in Table 4.1.

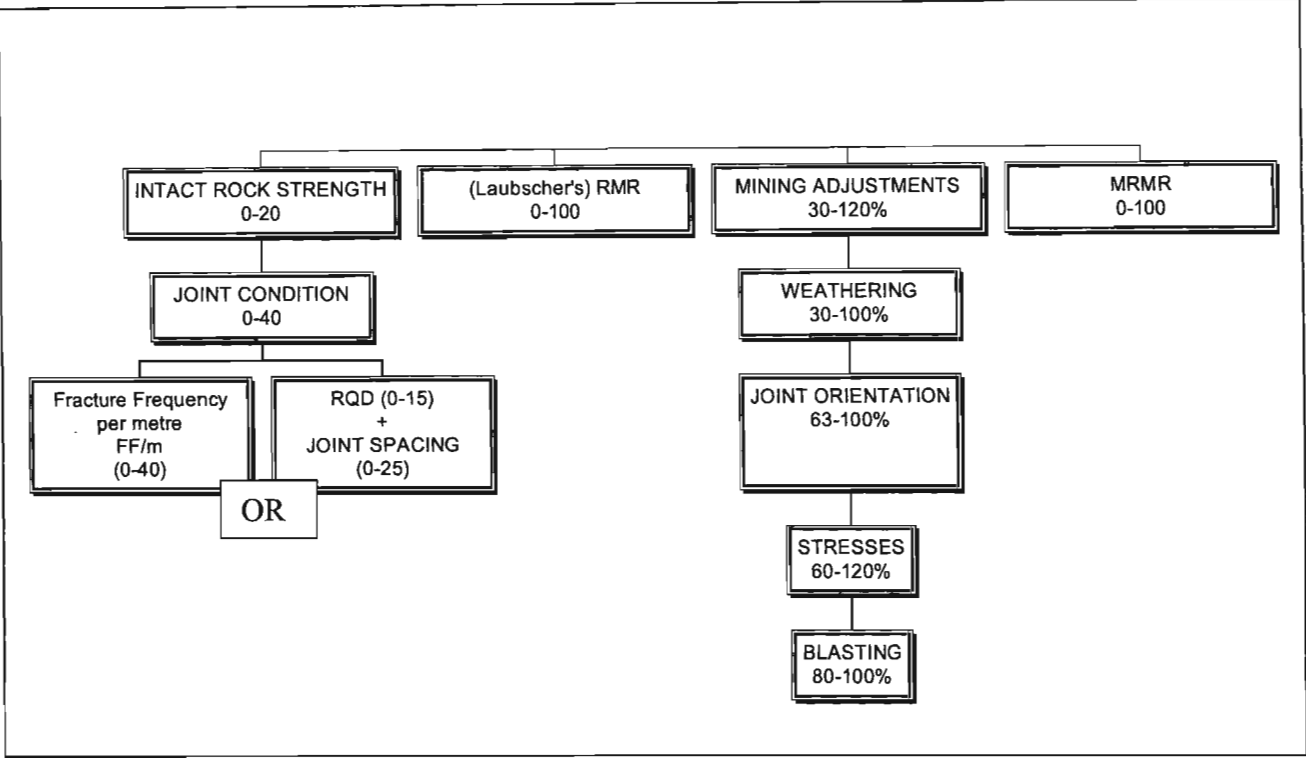


Figure 4.3 Flow diagram illustrating Laubscher's (1990) MRMR system.

Table 4.1 The calculated mining adjustments for Sandsloot open pit.

SANDSLOOT MRMR MINING ADJUSTMENTS		
Weathering	100 %	All rock types have UCS > 140 MPa and do not weather significantly within a 5-year period.
Joint Orientation	95%	One unfavourably orientated joint set (JS1).
Stresses	96%	Accounts for relaxation and destressing of the open pit slopes.
Blasting	95%	Accounts for smooth wall blasting and high blast activity in narrow pit.
Total Adjustment	87%	The total adjustment is large to ensure a conservative rating.

Table 4.2 Geotechnical properties of the dominant rock types present at Sandsloot.

	HANGING WALL	ORE ZONE			FOOT WALL
	NORITE	PYROXENITE	PARA PYROXENITE	SERPENTINISED PARAPYROXENITE	CALC-SILICATE
IRS (MPa) Schmidt Hammer	175 (150-210)	160 (120-180)	200 (180-250)	270 (200-310)	140 (100-180)
RQD %	80 (40-100)	65 (25-100)	75 (55-100)	70 (50-100)	55 (20-80)
FF/m	9 (20-3)	13 (29-3)	10 (15-3)	11 (16-3)	16 (32-9)
MRMR	53 (48-60)	48 (35-52)	56 (50-61)	61 (51-70)	42 (32-50)
MRMR CLASS	(III A) Fair	(III B) Fair	(III A) Fair	(II B) Good	(III B) Fair
Unit weight (kN/m ³)	2.9	3.2	3.3	3.2	2.9
Deformation modulus (GPa)	81.0	73.52	133.67	107.88	49.77
Poisson's ratio (μ)	0.235	0.187	0.218	0.254	0.291
Tensile strength (MPa)	9.5 (7.5-10.5)	8.0 (6-9)	10.0 (9-12.5)	13.5 (10-15.5)	7.0 (5-9)
ϕ_p (°)	57-64	40-58	55	-	50
ϕ_b (°)	38-48	29-37	34-36	-	32
JRC	6-10	2-12	8-10	8-12	8-10
JCS (MPa)	87-100	62-100	75	100-150	50
Slope angles (°)	56-59	48-50	51-59	56-59	51

 ϕ_p ° -Peak friction angle

JRC -Joint roughness coefficient

 ϕ_b ° -Base friction angle

FF/m -Fracture frequency per metre

JCS -Joint wall compressive strength

IRS -Intact rock strength (MPa)

RQD -Rock quality designation

MRMR-Mining Rock Mass Rating

4.3 Face Mapping

During open pit mining operations the mining blocks or benches are sequentially drilled, blasted and excavated. There is a short period between loading a blast muck pile and blasting a subsequent mining block when a bench face is available for mapping. These benches usually provide a 15 m high by 50 m wide section through the orebody. The bench face is then mapped as described below and provides valuable structural, lithological and geotechnical information.

Due to the need for real time information in a rapidly developing open pit, standardised field mapping sheets for capturing rock mass rating, geological and structural data were developed. Real time refers to a sufficiently short turn around time from data capture to interpretation and recommendation so that maximum benefit can be derived from the resultant recommendations. This is particularly important at Sandsloot where large tonnages are moved within a narrow pit and therefore exposed faces are only available for data collection for a short period. To make maximum use of the geotechnical data, the resultant recommendations must be available before the next mining slot is developed.

The sheets (Figure 4.4) contain lookups derived from the Laubscher (1990) rock mass classification system and standardized input columns which considerably improve mapping time, to the extent that a 50 m face can be mapped and classified within an hour. The lookups include discontinuity type, continuity and filling, as well as weathering grades and joint condition assessments. Schmidt hammer readings are also captured on the data sheet.

In the field the face to be mapped was visually divided into zones based on a change in rock type or major structural features. Any structural zones wider than 1 m are classified separately. Each individual zone was then mapped using a separate mapping sheet to which all the relevant information is captured. Schmidt hammer readings were taken for each identified zone so that the IRS can be calculated for the MRMR classification.

The mapping includes an abbreviated line survey. The four dominant joint families are identified within the face and line survey information on joint roughness, continuity, joint condition, spacing and orientation are collected as depicted in part 6 of the mapping sheet (Figure 4.4). As a maximum of three joints define the blocks within a rock mass only the three most prominent/closely spaced joint sets are mapped for rock mass rating purposes (Laubscher, 1990).

The data collected in the field is then transferred to computer for digital storage. AutoCAD is a

draughting software package that is used extensively in the mining industry. Through consultation with CGGS (1998) the standard AutoCAD functions have been customised at PPL to aid storage and interpretation of geological and geotechnical information.

The customised AutoCAD systems enable diagrammatic storage of geological and geotechnical data as illustrated in Figure 4.4, 4.5 and 4.6. Figure 4.4 is a diagrammatic illustration of a typical mapped face with the collected field information transferred into AutoCAD, where a 3D image is created. The face map has known reference co-ordinates, which are collected by accurate surveying in the field. All structural, geological and geotechnical information is therefore located and given true spatial co-ordinates.

Different structural features and geotechnical zones were tagged (Figure 4.5) on the face map and all relevant structural and geotechnical information was attached thereto. Once the Mining Rock Mass Rating (MRMR) data was captured (Figure 4.6), automatic calculation of MRMR was done within AutoCAD (Figure 4.6). This considerably improved data capture and manipulation time as well as reducing user errors. All relevant information was stored digitally. The data collected from the 6,800 m of face mapping is detailed in Appendix 3. Table 4.3 summarises all the geotechnical data collected per rock type.

Structural features, lithologies and RMR zones were automatically exported to a structural and a geotechnical plan which incorporates all relevant information for that bench. Therefore a structural, lithological and geotechnical plan is available for every bench. From these plans, geotechnically similar zones were delineated and major structural features noted. This information was used to create a geotechnical plan containing predictions for all the areas to be mined in the next month. The plan forms the basis for liaison with the drilling, blasting and planning engineers in order to develop optimised designs per zone, as well as forming the basis for geotechnical recommendations for blast design, crushing and milling rates, drilling performance, limit blasting and slope design.

Routines developed within the AutoCAD software allow exporting of relevant geotechnical and structural information in ASCII format. This geotechnical information includes the X, Y and Z co-ordinates for each mapped zone with the MRMR, UCS, RQD, FF/m and rock type for that zone. This information was then imported into the Datamine® modelling package and combined with geotechnically logged borehole information to produce the geotechnical model.

Figure 4.4 An example of a geotechnical face mapping sheet for MRMR evaluation.

DATE: 28/07/1997 RECORDED BY: ALAN BYE	PIT: SWE FACE ORIENTATION: STRIKE 180	BENCH/BLAST: 17/008 FACE: EAST FACE	ZONE : 1 OF 4 GEO POINT: 17GP-004
---	--	--	--

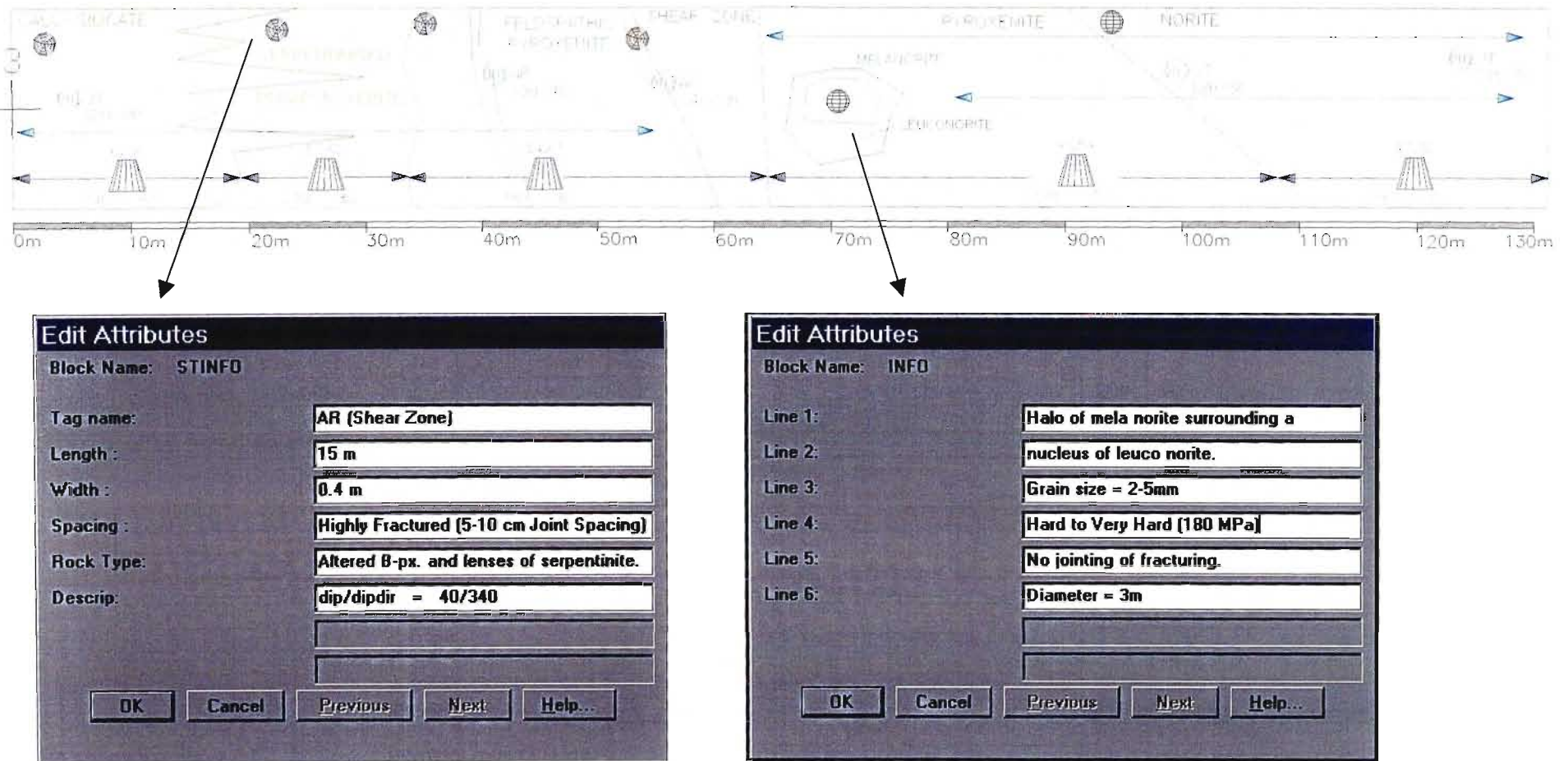
1. INTACT MATERIAL STRENGTH: <div style="display: flex; justify-content: space-between;"> <div style="width:45%;"> SCHMIDT REBOUND READINGS (R) <table border="1" style="width:100%; text-align: center;"> <tr><td>1</td><td>50</td><td>6</td><td>50</td></tr> <tr><td>2</td><td>52</td><td>7</td><td>52</td></tr> <tr><td>3</td><td>48</td><td>8</td><td>49</td></tr> <tr><td>4</td><td>54</td><td>9</td><td></td></tr> <tr><td>5</td><td>46</td><td>10</td><td></td></tr> </table> <table border="1" style="width:100%; text-align: center;"> <tr><th colspan="2">Mean</th><th>High</th></tr> <tr><td>R</td><td>50</td><td>54</td></tr> <tr><td>MPa</td><td>195</td><td>250</td></tr> </table> </div> <div style="width:45%;"> HAMMER ORIENTATION: Horizontal Up: <input type="text"/> Horizontal Down: <input type="text"/> 45 Up: <input type="text"/> 45 Down: <input type="text"/> Vertical: <input type="text" value="*"/> </div> </div> <div style="display: flex; justify-content: space-between; margin-top: 10px;"> <div style="width:45%;"> SPECIMEN TYPE: IN-SITU: <input type="text" value="*"/> BLASTED ROCK: <input type="text"/> </div> </div>	1	50	6	50	2	52	7	52	3	48	8	49	4	54	9		5	46	10		Mean		High	R	50	54	MPa	195	250	2. ROCK TYPE PARA-PYROXENITE 3. JOINT WIDTH 10 m 4. BLASTING EFFECTS JOINTS EXTENSIVELY OPENED BY BLASTING 5. RQD FOR ZONE 80% 6A. JOINT TYPE 1 JOINT 3 FAULT ZONE 5 FAULT 2 BEDDING 4 CRITICAL JOINT
1	50	6	50																											
2	52	7	52																											
3	48	8	49																											
4	54	9																												
5	46	10																												
Mean		High																												
R	50	54																												
MPa	195	250																												

6B. JOINT FILLING A NO SOFTENING & SHEARED MATERIAL (e.g. Quartz) 1. COARSE 2. MED 3. FINE B SOFTENED MATERIAL (e.g. Clay) 1. COARSE 2. MED 3. FINE 6C. DEGREE OF WEATHERING 1 FRESH 4 HIGH 2 SLIGHT 5 COMPLETE 3 MODERATE 6 RESIDUAL SOIL 6D. JOINT CONTINUITY (ENDS) 1 BOTH JOINT ENDS EXTEND OUT OF THE FACE 2 BOTH JOINT ENDS END IN THE FACE 3 ONE JOINT END ENDS IN THE FACE	6E. WATER 1 DRY 2 MOIST 3 WET 4 DRIPPING 5 FLOWING
--	--

6. ROCK MASS DISCONTINUITIES																		
JOINT SET	JOINT TYPE (6A)	ORIENTATION		JOINT CONDITION					WEATHERING (6C)		JOINT SPACING			JOINT CONTINUITY (6D)				WATER (6E)
		DIP DIR	DIP	JOINT FILLING TYPE	ROUGHNESS		JOINT WALL ALTERATION	JOINT SURFACE	ROCK SURFACE	Ave m	CJS m	FF/m	Dip Length m	End 1-3	Strike Length m	End 1-3		
					SMALL	LARGE												
1	4	090	72	Ca & Sep	A 2	0.95	0.80	-	3	1	0.4 m	1.5 m		15 m	1	40 m	1	DRY
	1	085	78	Calcte	A 2	0.90	0.90		2	1	0.3 m			15 m	1	5 m	1	
	1	100	65	Sep	B 3													
2	1	350	85	Calcte	A 3	0.90	0.95	-	1	1	0.2 m	3 m		10 m	1	1 m	1	MOIST
	1	005	83	Chy	B 2													
	1	355	80	-														
3	1	040	45	-		0.70	0.80	-	2	1	0.6 m	-		8 m	3	3 m	2	DRY
4	2	250	30	Chy	B 3	0.75	0.75	-	2	1	0.1 m	-		20 m	1	0.5 m	1	DRY
	2	220	35	-														
FAULT	3	300	75	Qts	A 1	0.80	0.60	YES	2	4	0.4 m	-		15 m	1	0.2 m	1	DRIPPING

(PPL Geology Dept.- Alan Bye)

Figure 4.5 An example of a geotechnical face map in AutoCAD format.



PPL: GeoTech information: 123F-003

Joint details
Set No: 1
Type: Joint
Dip direction: 125
Dip: 078

Joint Condition
Fill type: Calcite
No: A Fine
Rough L: 0.8
Rough S: 0.85
Alteration: 1.0

Surface Weathering
Joint: Fresh
Rock: Fresh
Joint Spacing
Ave (m): 0.4
CJS (m): 3
FF/m: 2.5

Joint Continuity
Dip length: 15m
Strike length: 5m
IRS (MPa): 270
RQD (%): 80
Water: Dry
Ends: Both beyond face
Ends: Both beyond face

Accept Set
RMR
Place
Update
OK
Cancel

PPL: Mining factors
Weathering: 1.00
Joint Orient: 0.95
Stress: 0.96
Blasting: 0.95
OK
Cancel

PPL: Mining Rock Mass Rating evaluation: 123F-003

	Reading	Adjustment	Contribution	Rating
IRS (MPa):	270		20.0	20.00
RQD (%):	80		15.0	12.00
Spacing Set 1:	0.4	0.68		
Spacing Set 2:	0.5	0.67	25.0	11.39
Spacing Set 3:				
SS Roughness:	0.85			
LS Roughness:	0.80	0.58	40.0	23.12
Alteration:	1.00			
Filling:	0.85			
Rock Mass Rating prior to Mining Adjustments:			66.51	
Mining Rock Mass Rating:			57.62	
Slope Angle:	100m Slope		64 Degree	
Mining Adjustments ...			OK	Evaluate

Figure 4.6 An example of AutoCAD data capture and MRMR analysis screens.

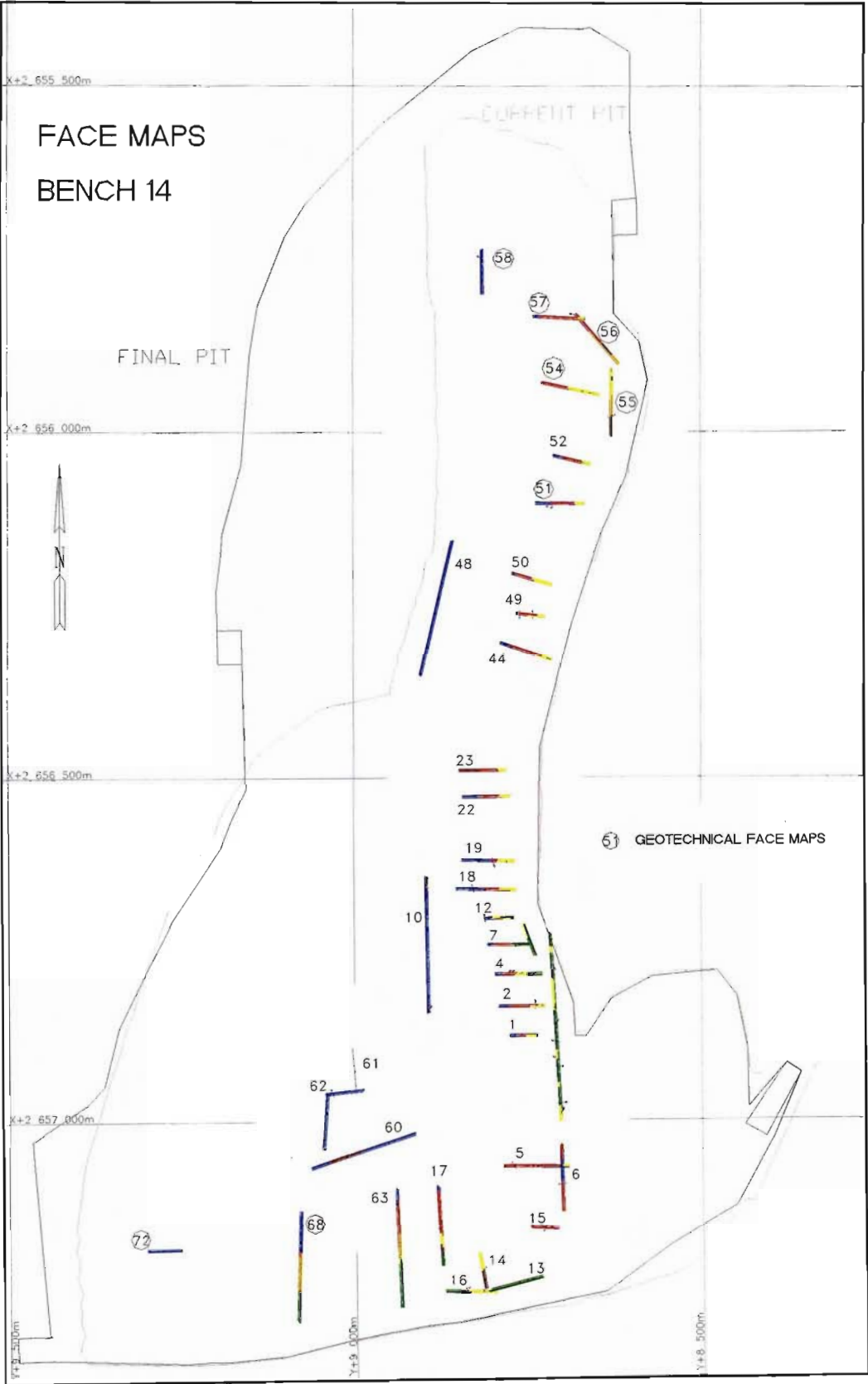


Figure 4.7 Plan view of bench 14 geological and geotechnical face maps.

4.4 Borehole Logging

Dempers (1996) has customised the MRMR system into a borehole logging procedure, which allows optimal utilisation of large volumes of borehole core available on mine feasibility and exploration programmes. The procedure is straightforward and practical and allows rapid assessment of core for geotechnical evaluation. The logging method reduces the time taken to evaluate core and therefore more borehole data can be collected. In conjunction with the logging technique, a spreadsheet has been specifically designed whereby the relevant parameters required for input into the MRMR classification system can be analysed and interpreted. The results can be used to produce final MRMR ratings and preliminary slope angles, from the charts developed by Haines and Terbrugge (1991), for each geotechnical zone or design region. The logging spreadsheet is shown in Figure 4.8 and the MRMR geomechanics sheet is shown in Figure 4.9. An important aspect of the rapid assessment procedure is that it can be applied at the feasibility or execution stages of a mining project.

The principal of the new core logging technique differs from conventional logging where each core run drilled is individually assessed for each geotechnical parameter required for engineering classification systems (Dempers, 1996). Essentially the MRMR method of rock classification is used to evaluate the core exploration diamond drill boreholes. The borehole is, however, visually separated into similar geotechnical zones or design regions based primarily on rock type and then any major structural features wider than one metre, as is the case with face mapping procedures described in Section 4.3. After the borehole has been grouped into geotechnical zones each relevant parameter required for geotechnical evaluation is determined within a particular geotechnical zone. Again, standardised mapping sheets and lookups are used based on the MRMR data requirements. All data necessary for RMR calculation, as described by Laubscher (1990), are collected as well as structural and lithological information.

In assessment of the RQD for exploration core it is important to realise that small diameter core is more sensitive to drilling and handling conditions than larger diameter core. The threshold value used in an evaluation of RQD should reflect this increased sensitivity. The original concept of RQD was based on NQ size core, and is defined as the percentage of intact core greater than a threshold value of 100 mm. Nickson *et al.* (1996) suggested the use of a threshold value that is based on twice the core diameter, hence a threshold value of 75 mm should be used for BQ size core and 50 mm for AQ size core. Mechanical breaks due to the drilling and handling process should not be included in the RQD evaluation. Nickson *et al.* (1996)

concluded that fracture frequency can be a more sensitive measure of rock mass structure than RQD, which is relatively insensitive in good quality rock.

Seventy-four boreholes comprising over 29,000 m of core were logged geotechnically. The geotechnical logs are represented in Appendix 2 and the locations of the boreholes are illustrated in Figure 4.10. As the exploration core is evaluated with the same RMR procedure as face mapping, the data correlation is very good. Table 4.3 summarises all the face mapping and core logging information per rock type.

The logged data is then captured to a geomechanics mining rock mass rating (GMRMR) spreadsheet, specifically designed to interpret the data required for input into the MRMR system and expanded by Haines and Terbrugge (1991) for rock slopes. A spreadsheet program is easily developed to automatically calculate final MRMR values. Relevant geotechnical information was subsequently exported directly to Datamine® for interpretation. The interpreted data was used to estimate stable slope configurations and predict rock mass conditions.

As seen in the cross-section depicted in Figure 4.2, the MRMR logging data can be correlated with face mapping and used for prediction and modelling of geotechnical zones. The logged geotechnical data was imported into the Datamine® modelling program where it was used to create a geotechnical model between face map data and exploration holes, therefore geotechnical information was available in advance of the mining face. The interpolated geotechnical information was then used for rock quality prediction, production optimisation, slope evaluation and design, as well as planning and costing.

Table 4.3 Summation and statistical analysis of all the geotechnical data collected from both exploration boreholes and in-pit face maps.

ROCK TYPE	NORITE				PYROXENITE				A-REEF				PARA-PYROXENITE				SERPENTINISED PARA-PYROXENITE				CALC-SILICATE			
PROPERTY	RMR	UCS (MPa)	RQD (%)	FF/m	RMR	UCS (MPa)	RQD (%)	FF/m	RMR	UCS (MPa)	RQD (%)	FF/m	RMR	UCS (MPa)	RQD (%)	FF/m	RMR	UCS (MPa)	RQD (%)	FF/m	RMR	UCS (MPa)	RQD (%)	FF/m
NO. OF RECORDS	1041	1041	1041	1041	1041	1041	1041	1041	1041	1041	1041	1041	1041	1041	1041	1041	1041	1041	1041	1041	1041	1041	1041	1041
NO. OF SAMPLES	464	464	464	464	185	185	185	185	43	43	43	43	136	136	136	136	108	108	108	108	92	92	92	92
MINIMUM VALUE	0	0	0	0	33.42	16	0	0.66	43	180	63.47	0.85	42.80	20	0	0.95	46	106	50	1	38	28	0	0.64
MAXIMUM VALUE	85	298	100	98	77	281	100	50	79.40	250	98.75	12.34	76.40	270	100	36.36	80.01	280.00	97.83	16.41	68.34	250.00	126.91	17.14
RANGE	85	298	100	98	43.58	265	100	49.34	36.40	70	35.28	11.49	33.60	250	100	35.41	34.01	174.00	47.83	15.41	30.34	222.00	126.91	16.3
MEAN	58.85	182.85	80.75	7.54	54.30	184.56	73.28	8.58	56.96	228.12	89.78	3.55	59.19	209.08	77.21	7.71	60.82	242.95	78.85	7.59	52.20	140.59	82.45	6.12
VARIANCE	89.08	959.08	461.80	144.24	46.35	607.96	370.25	34.55	49.04	423.45	77.50	8.25	39.96	1,606.03	358.69	24.07	42.83	1,797.21	252.22	24.00	43.77	655.25	353.20	21.91
STANDARD DEVIATION	9.44	30.97	21.49	12.01	6.81	24.66	19.24	5.88	7.00	20.58	8.80	2.87	6.32	40.08	18.94	4.91	6.54	42.39	15.88	4.90	6.62	25.60	18.79	4.68
STANDARD ERROR	0.44	1.44	1.00	0.56	0.50	1.81	1.41	0.43	1.07	3.14	1.34	0.44	0.54	3.44	1.62	0.42	0.63	4.08	1.53	0.47	0.69	2.67	1.96	0.49
SKEWNESS	-1.46	-3.58	-1.73	5.40	0.53	0.39	-0.85	1.88	0.86	-0.67	-1.52	1.45	-0.14	-1.88	-2.15	2.04	0.42	-1.28	-0.79	0.61	0.48	0.17	-1.67	0.87
KURTOSIS	9.67	20.51	3.07	33.69	0.57	13.80	1.09	11.51	1.34	-0.86	2.08	1.63	0.37	8.85	5.63	9.38	0.40	0.48	-0.68	-0.77	-0.01	10.93	4.17	-0.65
GEOMETIC MEAN	58.64	180.10	77.98	4.26	53.88	161.96	70.59	6.41	56.55	227.14	89.29	2.66	58.84	200.80	75.19	6.13	60.47	238.44	77.01	5.93	51.79	137.47	80.98	4.50
MEAN LOG	4.07	5.19	4.36	1.45	3.99	5.09	4.26	1.86	4.04	5.43	4.49	0.98	4.07	5.30	4.32	1.81	4.10	5.47	4.34	1.78	3.95	4.92	4.39	1.51
LOG VARARIENCE	0.02	0.08	0.16	1.14	0.02	0.05	0.10	0.72	0.01	0.01	0.01	0.56	0.01	0.14	0.12	0.57	0.01	0.04	0.05	0.56	0.02	0.06	0.07	0.65
LOG ESTIMATE MEAN	59.27	187.59	84.40	7.52	54.30	165.66	74.33	9.19	56.95	228.14	89.81	3.52	59.20	214.98	79.82	8.13	60.82	243.48	79.01	7.86	52.20	141.50	84.01	6.23
	21,184 m of logging/mapping				4,841 m of logging/mapping				1,667 m of logging/mapping				2,965 m of logging/mapping				3,160 m of logging/mapping				2,175 m of logging/mapping			

4.5 Rock Strength Testing

Laboratory and field tests provide information on the physical properties and mechanical reactions of intact rock. They assist in classifying the rock, thereby allowing relevant engineering design and construction within the rock mass. A detailed rock testing programme was implemented in order to further define the distribution of the rock mass characteristics for not only Sandsloot but also the subsequent open pits that will be mined by PPL.

With the rock strength database, empirical relationships were defined and information carried over to future pits. The data was used in the model for operational designs, such as drilling and blasting equipment selection and crushing and milling requirements. Additionally, the data collected was used for better definition of the variables controlling slope stability, which subsequently improved stability modelling results and final wall angles. An outline of the rock testing programme for Sandsloot open pit is given in Table 4.4 and the full laboratory testing results are presented in Appendix 4. Brown (1981) gives a detailed description of the range of laboratory testing methods available for rock characterisation.

The main objective of this testing programme was to characterise the rock properties of all the rock types occurring at Sandsloot open pit. The tests yielded the following properties; uniaxial compressive strength, deformation modulus, Poisson's ratio, Mohr-Coulomb parameters of intact rock, the strain softening parameters, base friction angles and the slake durability index. The rock properties were obtained from the following type of tests; uniaxial compressive strength tests with strain gauge measurements up to the point of failure, triaxial compressive strength tests with deformability and post failure measurements, shear tests on artificial saw-cut joints and slake durability index tests. Additionally, a suite of drillability tests were undertaken to characterise the rock types at Sandsloot so that optimum blast design, drill bit selection and milling requirements could be determined. All tests were done in accordance with the relevant suggested methods of the International Society for Rock Mechanics, Commission on Standardisation of Laboratory and Field Tests.

Field Tests

Field testing is a rapid means of obtaining indicative rock property information. A combination of field and laboratory testing was undertaken so that the field testing could be validated with more accurate laboratory testing. The following field tests were used at Sandsloot:

- The point load test is portable and is used to test exploration core. The test generates tensile stress, normal to the axis of loading, on the specimen (Norbury, 1986). It enables the indirect tensile strength to be determined, which can then be related to the uniaxial compressive strength of the rock sample.
- Tilt tests are conducted between two blocks of loose rock or three pieces of exploration core that are of similar rock type. The samples are placed on top of one another and tilted until the upper block slides off. The resultant angle (which is the base friction angle) is then measured with a protractor or clino-rule.
- The Schmidt hammer is a portable device that expends a definite amount of stored energy from a spring and indicates the degree of rebound of a hammer mass within the instrument following impact. The hammer is held vertically at right angles to the specimen and the plunger is pushed against the specimen (Hucka, 1965). It has a button, which when pressed in locks the reading in place. At least twenty tests must be done on each specimen to obtain an average Schmidt hardness (R) value. Using the chart developed by Deere and Miller (1966) the uniaxial compressive strength can be estimated from the rebound value (R). The Schmidt hammer is used in the field on borehole core and rock specimens. It must be noted that Schmidt hammer results should only be used as a guide until results from laboratory testing can be obtained for verification.

Laboratory Tests

Six rock types were supplied, in the form of blocks, to the CSIR MiningTek testing laboratory. At the laboratory, core samples with a diameter of ± 42 mm were drilled from the bulk rock samples. The determination of the following parameters were obtained; uniaxial compressive strength, deformation modulus, Poisson's ratio, Mohr-Coulomb parameters of intact rock, the strain softening parameters, the base friction properties, drillability parameters and the slake durability index. Summaries of the results are given in Tables 4.5, 4.6 and 4.7. Detailed tables, graphs and summary sheets are given in Appendix 4.

Uniaxial Compressive Strength Tests

Uniaxial compressive strength (UCS) is the highest stress that a rock specimen can carry when a unidirectional stress is applied, normally in an axial direction, to the ends of a cylindrical specimen (ISRM, 1979). In other words, the UCS represents the maximum load supported by the specimen during the test, divided by the cross-sectional area of the specimen.

Uniaxial compressive strength testing with axial and lateral deformation measurements (UCM), by means of strain gauges up to the point of failure, provides data to determine the elastic constants. The value of Young's modulus (E) and Poisson's ratio (ν) can therefore be determined from this test. Young's modulus is defined as the relationship between tension, or compression and deformation in terms of change in length. Poisson's ratio (ν) is defined as the ratio of shortening in the transverse direction to elongation in the direction of an applied force in a body under tension, within the proportional limit (Bell, 1992).

Uniaxial Compressive Strength tests with deformability measurements were done on all the rock types. The test results of the UCM tests are summarised in Tables 4.5. The respective relationships between the uniaxial compressive strength and the tangent modulus are shown in Figure 4.11.

Generally the modulus ratio (tangent modulus divided by the UCS) values tend to range between 200:1 and 500:1 for intact specimen failures. Although most of the specimens tested showed intact failure modes, the modulus ratio values are in many cases higher than 500:1.

Triaxial Compressive Strength Tests

Triaxial compressive strength (TCM) is a more complete test than the UCS test. A constant hydraulic pressure is applied to the cylindrical surface of the specimen, whilst applying an axial load to the ends of the sample (ISRM, 1983). The axial load is increased until the specimen fails (Vogler and Kovari, 1978). A number of tests like this are done at various hydraulic pressures to calculate the angle of friction and cohesion value of the specimen. The test results can then be used in the Hoek and Brown criteria (1997) for design purposes.

Triaxial compressive strength tests with pre- and post-failure deformation measurements were done on three of the six rock types (norite, parapyroxenite and calc-silicate). The TCM results, including the strain-softening and Mohr-Coulomb parameters, are summarised in Table 4.5. For all three types of rock tested in triaxial compression, the Mohr-Coulomb parameters were determined when the triaxial test results were evaluated. The post failure deformation measurements were used to determine the strain-softening parameters.

Shear Tests on Artificial Saw-Cut Joints

During base friction shear tests the rock specimen is cut in half and the shear surfaces polished. The base friction angle (ϕ_b) can be derived from shearing of the two surfaces using a shear box (ISRM, 1974). Shear tests on artificial saw-cut joints were done on three of the six rock types that will support final pit slopes, namely norite, parapyroxenite and calc-silicate. The shear test results are summarised in Table 4.5. The comprehensive tables and graphs are presented in Appendix 4.

Natural Joint Shear Testing

Natural joint shear tests were undertaken for the dominant rock types occurring in the pit slopes. Thirteen shear tests were undertaken in order to obtain a complete assessment of the critical joints in terms of slope stability for the hangingwall and footwall rock types. No critical joints were evident in the parapyroxenite therefore only norite and calc-silicate samples were tested.

During shear testing of actual joints a constant normal force is applied to the rock specimen (which is an intact rock with a joint plane), which is then sheared along the discontinuity surface (Bell, 1992). After incremental loading a stress-strain curve is produced. A number of tests each at a higher normal stress are undertaken so that the shear strength (τ) versus normal stress (σ_n) graph can be drawn. The values of cohesion (c) and peak friction angle (ϕ_p) are then derived from this graph (Table 4.6). A value of residual strength was obtained by repeating the test on the same specimen.

Slake Durability Index Tests

Slake durability tests (ISRM, 1979) were completed only on the calc-silicate rock type as it is the weakest material occurring in the open pit slopes. The slake durability tests involves mechanically stressing the sample by rotating a finite volume of material through a sieve and measuring the reduction in sample volume as a percentage. The calc-silicate sample retained 99.3% of the sample mass after 4 cycles. This classifies a slake durability index for the calc-silicate as “very high” and indicates that the rock material was more durable than expected and therefore testing of the other harder rock types was not justified.

Rock Drillability Tests

A number of indicative drillability tests were undertaken on all the rock types occurring at Sandsloot in order to determine their drillability and abrasive indices. The results and descriptions of the test results are detailed in Table 4.7. In summary, all the rock types had medium to low drillability classification while norite, A-reef pyroxenite and serpentinitised parapyroxenite had high abrasive indices. This information is used for the optimum selection of drill bits and mill linings.

Comparison of Northern, Eastern and Western Limb Rock Properties

Table 4.8 details a comparison of the Platreef versus the typical eastern and western limb rock properties. UCS, Poisson's ratio and the deformation modulus values were compared. The tabulated results clearly show the harder and more elastic nature of the Platreef material properties. The UCS, and in particular the deformation modulus values, are considerably higher for the Platreef ore types. The interaction of the Bushveld magma with the Transvaal sediments is thought to have resulted in the increased strength of the Platreef rock types.

Table 4.4 Detail of the testing programme undertaken, including numbers of test samples per rock type.

ROCK TYPE	NUMBER OF TESTS				
	Uniaxial Compressive Strength Test with Strain Gauge Measurements.	Triaxial Compressive Strength Test with Deformability Measurements	Slake Durability Index Test	Shear Test on Artificial Saw-cut joints	Shear Test On Natural Joint
	UCM	TCM	SDI	SHS	SHJ
Norite	3	3	0	6	11
B-Pyroxenite	6	0	0	0	0
A-Pyroxenite	6	0	0	0	0
Parapyroxenite	6	3	0	6	0
Serpentinised Parapyroxenite	12	0	0	0	0
Calc-silicate	3	3	1	6	2
Total	36	9	1	18	13

Table 4.5 Comprehensive summary of the lab testing results.

ROCK CHARACTERIZATION INFORMATION					SLOPE DESIGN INFORMATION (Only for rock types intersecting the final pit walls)					
ROCK TYPE	Uniaxial Compressive Strength Test with Strain Gauge Measurements (UCM).				Triaxial Compressive Strength Test with Deformability Measurements (TCM).				Shear Test on Artificial Saw-cut Joints (SHS)	
	Strength (UCS - MPa)	Tangent @ 50% UCS		Modulus Ratio	Strain Softening Parameters		Mohr-Coulomb Parameters		Base Friction Angle (Degrees)	
		Poisson's Ratio	Deformation Modulus (GPa)		Shear Modulus (GPa)	Bulk Modulus (GPa)	Phi (Degrees)	C (MPa)		
NORITE	162.4	0.254	82.3	507	32.7	57.2	54	28.7	32.9	32.7
	178.9	0.232	82.4	461					33.1	33.5
	185.5	0.220	78.3	422					32.3	33.8
	AVERAGE	175.60	0.235	81.00					463.33	33.05
PYROXENITE	184.6	0.228	88.2	478						
	151.6	0.149	69.4	458						
	171.0	0.178	75.0	439						
	150.1	0.181	72.7	484						
	151.6	0.270	78.2	516						
	144.4	0.113	57.6	399						
AVERAGE	158.88	0.187	73.52	462.33						
A-PYROXENITE (FELDSPATHIC)	240.7	0.237	140.0	582						
	361.3	0.244	134.0	371						
	352.7	0.254	115.0	326						
	160.2	0.264	161.0	1005						
	152.3	0.279	93.5	614						
	148.7	0.245	98.4	662						
AVERAGE	235.98	0.254	123.65	593.33						
PARA-PYROXENITE	172.4	0.269	157.0	911	38.36	63.9	51.3	34	33.1	
	158.8	0.206	120.0	756					31.9	
	152.3	0.148	101.0	663					32.4	
	191.8	0.242	139.0	725					33.9	
	164.5	0.208	148.0	900					33.2	
	126.9	0.236	137.0	1079					34.3	
AVERAGE	161.12	0.218	133.67	839.00					33.13	
SERP. PARA-PYROXENITE	274.6	0.293	108.0	393						
	265.6	0.255	106.0	399						
	262.6	0.366	107.0	407						
	173.3	0.265	92.8	535						
	273.0	0.278	106.0	388						
	204.0	0.205	95.4	468						
	247.8	0.241	123.0	496						
	209.9	0.270	136.0	648						
	196.1	0.248	116.0	591						
	195.4	0.234	124.0	635						
	216.2	0.251	85.8	397						
	104.7	0.147	94.5	903						
AVERAGE	218.60	0.254	107.88	521.67						
CALC-SILICATE	128.7	0.276	51.9	403	17.5	42.8	40.5	26.3	21.5	19.4
	123.6	0.308	50.9	412					19.1	19.1
	137.9	0.288	46.5	337					20.3	20.9
	AVERAGE	130.07	0.291	49.77					384.00	20.05

Table 4.6 Natural joint shear test results.

SHEAR TEST NUMBER	ROCK TYPE	PEAK FRICTION ANGLE	RESIDUAL FRICTION ANGLE	RESIDUAL COHESION @ RESIDUAL FRICTION ANGLE	PEAK COHESION @ PEAK FRICTION ANGLE (MPa)	PEAK COHESION @ RESIDUAL FRICTION ANGLE (MPa)
2141-SHJ-71	NORITE	N/A	25.3	0	N/A	0.22
2141-SHJ-72	NORITE	N/A	21.8	0	N/A	0.05
2141-SHJ-73	NORITE	30	27.6	0	0.80	0.16
2141-SHJ-74	NORITE	22.9	22.3	0	0.11	0.13
2141-SHJ-75	NORITE	33.5	33.4	0	0.15	0.18
2141-SHJ-76	NORITE	27.4	27.4	0	0.10	0.10
2141-SHJ-77	NORITE	N/A	28.4	0	N/A	0.05
2141-SHJ-78	NORITE	28.9	30.3	0	0.02	0.02
2141-SHJ-81	NORITE	29.6	29.4	0	0.05	0.06
2141-SHJ-69	NORITE	N/A	33.6	0	N/A	N/A
2141-SHJ-70	NORITE	36.3	33.6	0	0.30	0.38
		29.80	28.46	0.00	0.22	0.14
2141-SHJ-55	CALC-SILICATE	28.1	23.1	0	0.29	0.42
2141-SHJ-56	CALC-SILICATE	27.6	25	0	0.25	0.34
		27.85	24.05	0	0.27	0.38

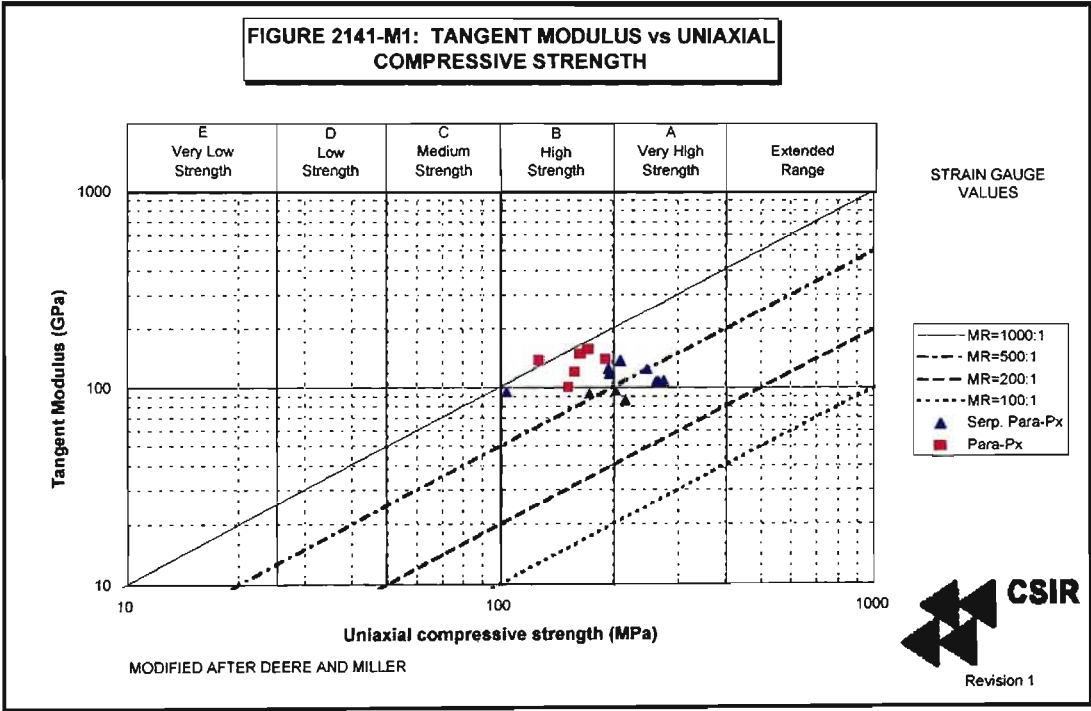
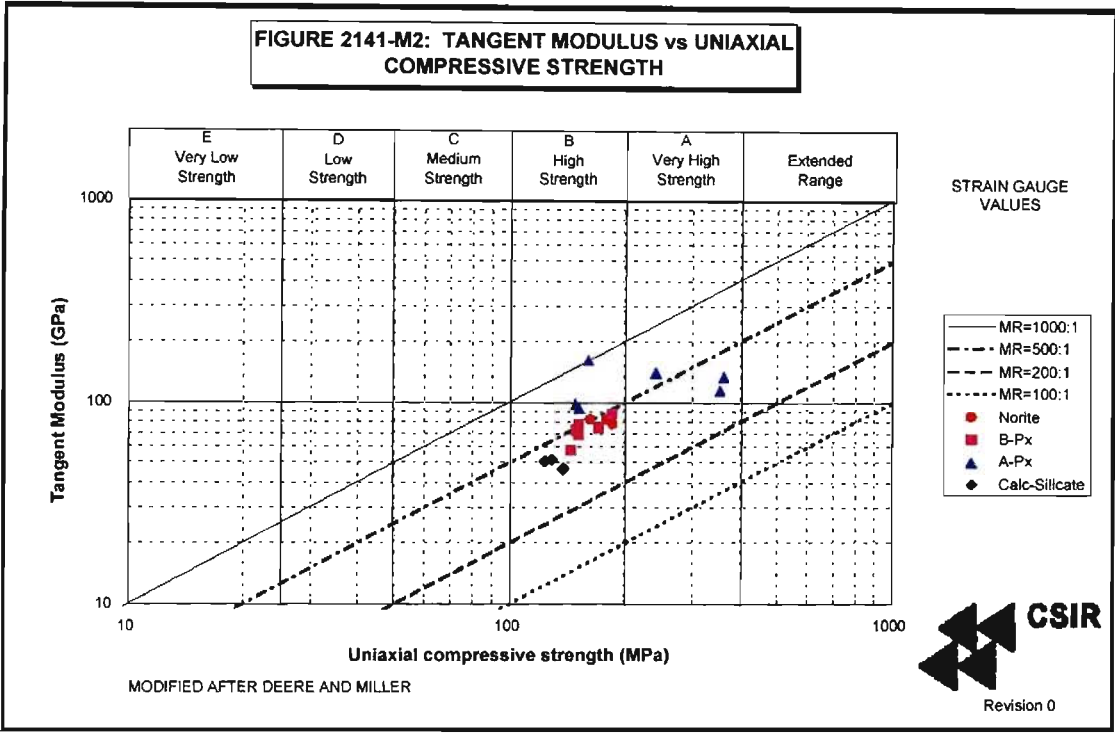


Figure 4.11 Graphs relating tangent modulus to UCS for all Sandsloot rock types.

Table 4.7 Summary of rock drillability tests.

SUMMARY OF ROCK DRILLABILITY TESTS

Potgietersrust Platinum Ltd. SANDSLOOT OPEN PIT MININGTEK

SPECIMEN PARTICULARS		SPECIMEN TEST RESULTS									
CSIR	Rock	Aver.	Brittleness	SJ	Abrasion	Abrasion	Drilling	Drillability	Bit	Cutter	Abrasive
Specimen		UCS	Value	Value	Value	Value	Rate		Wear	Life	
No	Type					Steel	Index	Class	Index	Index	Class
2135		MPa	S20	SJ	AV	AVS	DRI		BWI	CLI	
01	Norite	180.0	41.6	7.7	2.9	13.9	39	Low	34	11.0	Medium-High
02	B-Px	160.0	33.7	26.6	1.5	3.3	38	Low	26	30.9	Low
03	A_px	270.0	38.4	2.0	2.5	5.0	31	Very low	41	9.7	High
04	Para-Px	220.0	36.5	76.9	2.1	3.7	46	Medium	25	44.5	Low-medium
05	Serp.Para-Px	240.0	33.3	23.1	2.2	9.2	37	Low	36	19.7	Medium-High
06	Calc-Silicate	130.0	38.4	99.8	1.1	2.6	52	Medium-High	17	56.3	Very low

Note: Drilling Rate and Rock Abrasiveness Classification Table			
Drilling Rate Index (DRI)		Bit Wear Index (BWI)	
Extremely low	21	Extremely high	63
Very low	28	Very high	53
Low	37	High	43
Medium	49	Medium	33
High	65	Low	23
Very high	86	Very low	13
Extremely high	115	Extremely low	3

NOTES:
AV : Test pieces are Tungsten Carbide
AVS: Tests pieces are disc steel from Tunnel Boring Machine cutters.
SJ : J-factor is the measured drilling depth in millimetre multiplied by 10.
S20: Brittleness value equals the percentage of material which passes the 11.2 mm mesh after the aggregate has been crushed in the mortar.

Table 4.8 Comparison of the Bushveld Complex rock properties.

ROCK TYPE	UCS		POISSON'S RATIO		DEFORMATION MODULUS
	MPa				GPa
	RANGE	AVERAGE	RANGE	AVERAGE	AVERAGE
ANORTHOSITE	-	190	-	0.30	60
PYROXENITE	-	130	-	0.22	98
NORITE	-	170	-	0.36	70
MERENSKY	80-140	110	0.20-0.25	0.22	88
UG2	80-160	105	0.20-0.25	0.22	85
PLATREEF	170-270	220	0.20-0.30	0.25	105

4.6 Kinematic Failure Analysis

Rock slopes generally fail along existing geological defects. It is only in very high slopes and/or weak rocks that failure in intact material becomes significant. Most rock-slope problems therefore require consideration of the geometrical relationships between discontinuity planes, the slope and force vectors involved (Bell, 1992).

Discontinuities occur in the form of fissures, bedding planes, joints or faults within any rock mass. Their presence strongly affects the mechanical and hydrological properties of a rock mass in terms of its strength, deformability, stability, porosity, water storage capacity and transmissivity. These properties play a major role in the design and maintenance of open pits (Sen and Kazi, 1984).

In order to assess the stability of individual benches, so as to aid stack and overall slope design, a detailed kinematic failure analysis was undertaken. Kinematic failure zones, representing a dominant or critical failure mechanism, were delineated from multiple line surveys and detailed face mapping. The zones which represent the geotechnically similar portions of the pit and modes of failure are predominantly structurally controlled rather than by rock type. The exception is Zone C where instability is due to the *in-situ* rock-soil material (Figure 4.12).

Based on the geotechnical and structural data collected, the pit has been divided into kinematic failure zones. Each zone was studied individually to gain a better knowledge of any potential problems. Five kinematic failure zones have been identified, namely wedge, planar, toppling and circular failure zones, which represented classical failure conditions as well as a geotechnical “nose” zone. A nose zone is a portion of the pit that has a prominent convex geometry (Figure 4.12). Although the major modes of failure have been identified it is often unexpected random structures that are the root cause of major failures. To this end it is vital that all structures are identified and captured to a major feature plan. The defined kinematic failure zones are represented in Figure 4.12.

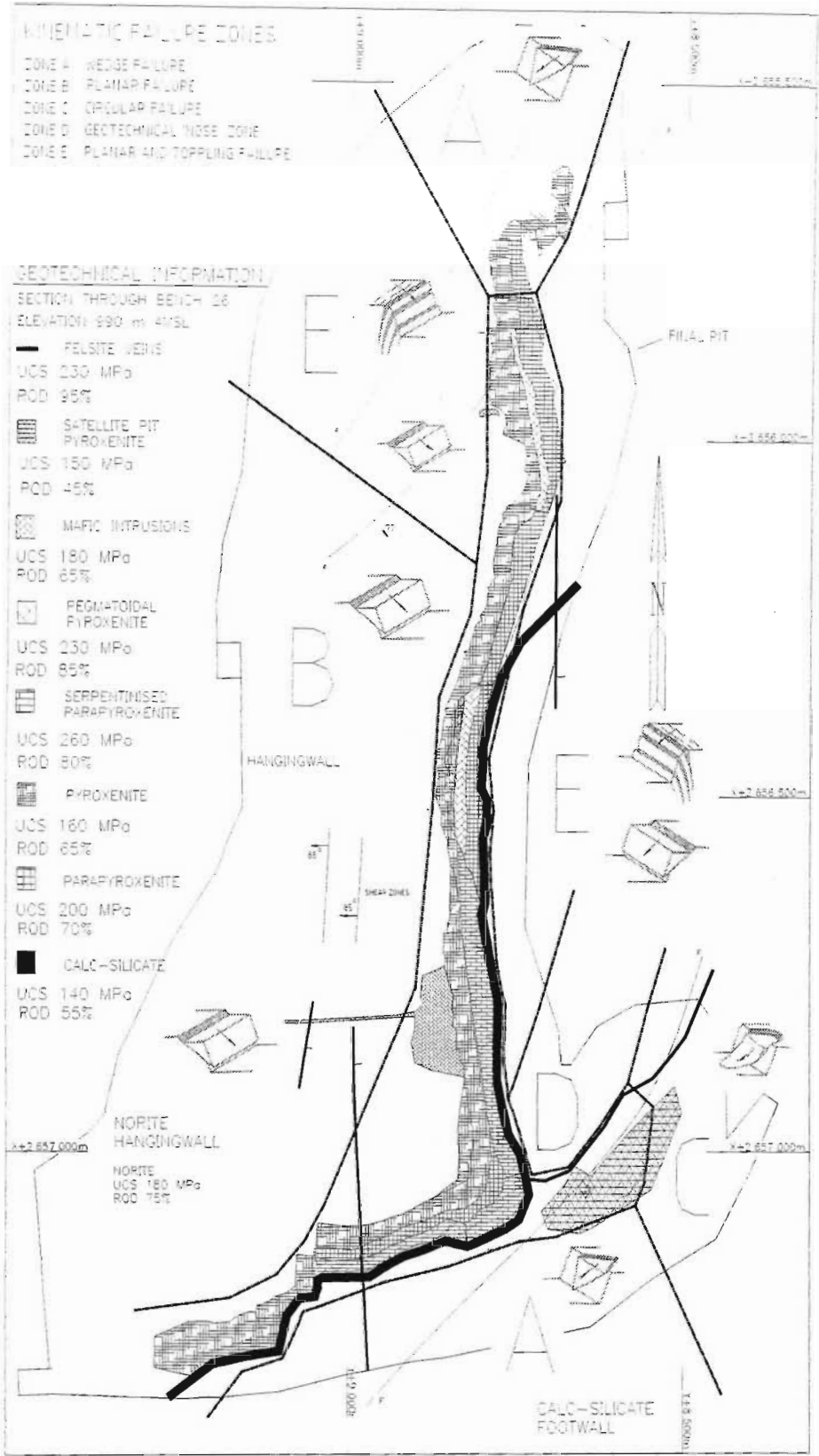


Figure 4.12 Diagrammatic illustration of identified failure mechanisms at Sandsloot.

4.6.1 Zone A (wedge failure)

Potential wedge failures are formed by the intersection of two discontinuities, which dip out of a slope face (Table 4.9). The condition for movement to occur is that the line of intersection of the wedge daylights in the slope face and is steeper than the friction angle of the joint surfaces. Sliding can occur along the line of intersection or, depending on the critical joint orientations, along either major joint, or along both planes.

There are two distinct zones within the pit where wedge failure is evident. In the north pit the wedge failures are formed due to the intersection of the hangingwall contact fault and joint set one. In the south pit the wedges are formed due to the intersection of the sympathetic jointing related to the Satellite pit fault and the relict bedding within the calc-silicate. A concern is that footwall ramp systems fall within both wedge failure zones. However, the observed wedge failures generally occur in association with a nearby production blast and are smaller than 100 tonnes. The risk they pose to ramps and production operations is therefore small.

The calculations indicate that small-scale wedge failures are inevitable even in small benches and under dry conditions. The solution, therefore, is to design regular catchment berms to accommodate the small failures rather than going to the expense of a rock bolting programme.

Table 4.9 Data relating to the critical joint sets (JS) causing wedge failure on the footwall ramps.

	JS 1	JS 2	JS 3
DIP (°)	85 (80-90) 75 (60-90)	86 (81-90) 79 (68-90)	61 (42-80)
DIP DIRECTION (°)	087 (075-098) 253 (233-272)	014 (355-032) 196 (177-215)	124 (098-149)
CONTINUITY (m)	1-10	2-10	1-10
JOINT FILLING	Calcite	Serpentinite, Calcite	Calcite
JOINT SPACING (m)	0.40	0.50	0.30
JOINT THICKNESS (mm)	2-20	2-20	2-20
JOINT ROUGHNESS (After Barton, 1978)	IV Undulating rough	VII Planar rough	V Undulating smooth

4.6.2 Zone B (planar failure)

Planar failures are translational failures and occur by sliding along a single plane, which daylights in the slope face. According to Hoek and Bray (1981) the planar failure depicted in Figure 4.13 is a comparatively rare sight in rock slopes because it is only occasionally that all the geometrical conditions required to produce such a failure occur in an actual slope.

All these geometrical conditions are satisfied by the major joint sets on the western highwall. Joint set one (JS1) strikes at 352° and dips at 50° while the slope strikes 355° and dips at 75°. It also daylights in the slope and the failure plane dips more steeply than the friction angle of 32°. Additionally, joint sets two and three provide release surfaces for failure to occur. The major joint set data, relating to the planar failure stereonet in Figure 4.14, are presented in Table 4.10.

A prominent joint set, sub-parallel to the western highwall, is causing multiple planar failure along a critical joint spacing. Even though this is not a permanent highwall it is vital to characterise the joint properties in order to design a safe final wall that will accommodate the failure mechanism. The three critically aligned joint sets are presented in the stereonet of Figure 4.14 with joint set one falling within the friction circle and within 20 degrees of the slope orientation.

Table 4.10 Data relating to planar failure diagram, Figure 4.14.

JOINT SET	DIP (°)	DIP DIRECTION (°)	CRITICAL JOINT SPACING (M)	SPACING (M)	VARIATION (°)		CONTINUITY (M)	JOINT FILLING	JOINT WIDTH (mm)	ROUGHNESS (After Barton, 1978)
					DIP	DIP DIRECTION				
JS 1	48	093	1.5	0.2	17-55	073-114	1 - 70	Thick calcite, serpentinite, some inactive clay	2 - 60	Planar rough (VII)
JS 2	71 73	354 180	4	0.3	65-90 66-90	329-018 163-199	4- 10	Calcite, serpentinite, inactive clay	2 -20	Planar rough (VII)
JS 3	80	303	3	0.4	70-90	291-315	4 - 50	Calcite, serpentinite	2 - 20	Planar rough (VII)

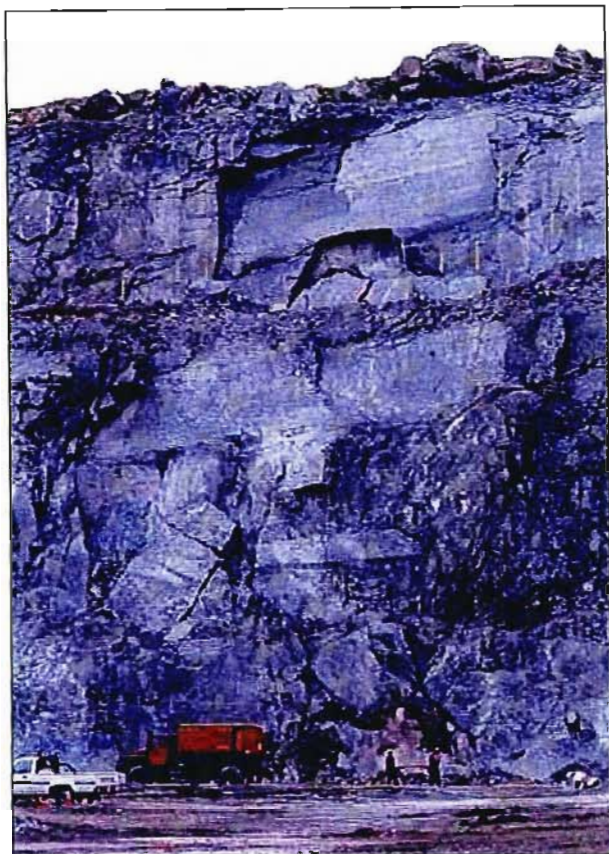


Figure 4.13 Photograph of a planar failure occurring on the western highwall.

The critical joints have shown significant water flow after heavy rainfall, which drastically reduces the slope stability. The reduction in stability is evident from the sensitivity analyses, which show a reduction in factor of safety from 1.38 to 0.80 under saturated conditions. The stability analysis data correlate well with field observations as a planar failure occurred during the pit mapping exercise after a period of heavy rainfall, as illustrated in Figure 4.15. Figure 4.16 illustrates graphically the back analysis undertaken on the planar failure that damaged the shovel in Figure 4.15.

Figure 4.16 illustrates the sensitivity of the planar failures, at Sandsloot, to rock mass saturation. For example, a planar failure analysis with cohesion of 150 kPa and joint dip of 50° will fail once joint saturation reaches 70%. The back analysis of the actual failure illustrated in Figure 4.15 indicated that the joint cohesion was 125 kPa and the saturation level equivalent to 70%.

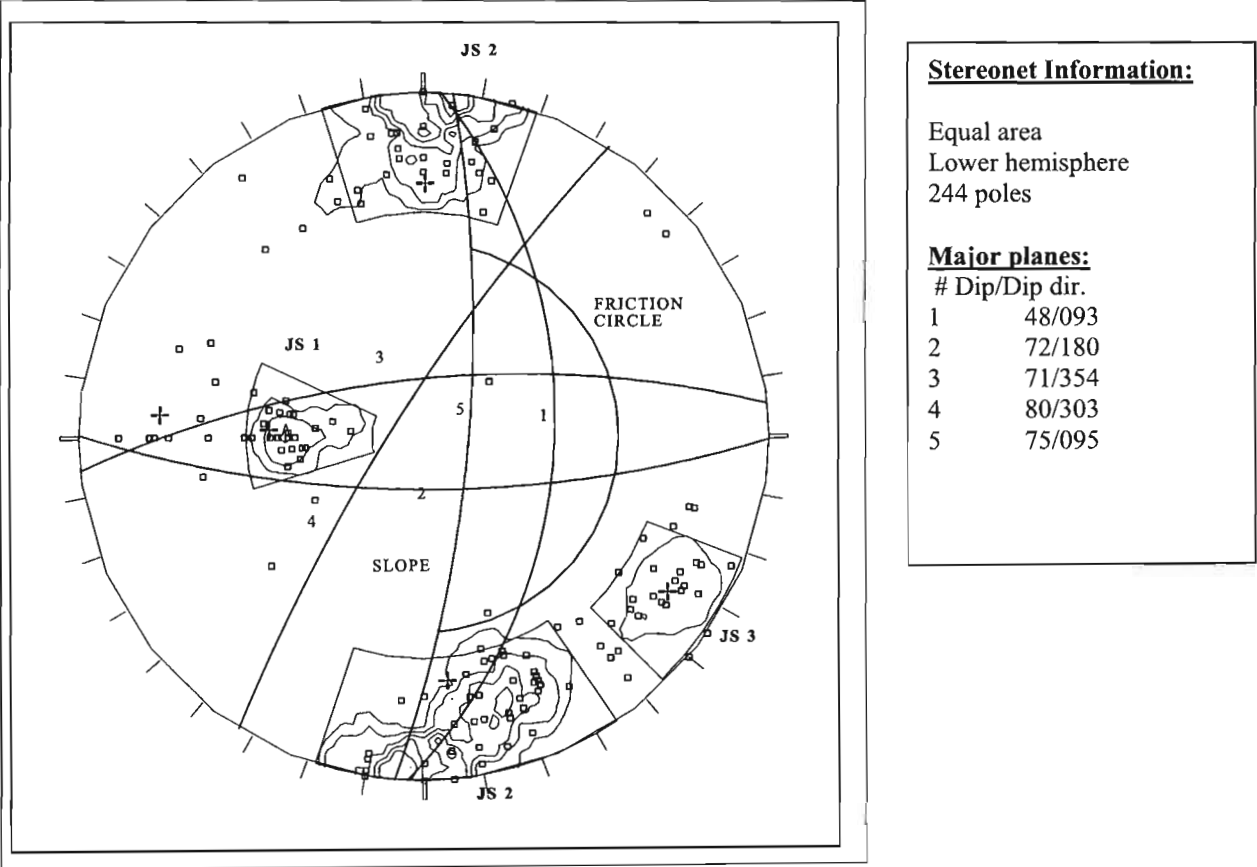


Figure 4.14 Stereonet depicting the planar failure mechanism on the hangingwall.



Figure 4.15 Damage to an operational shovel as a result of a planar failure.

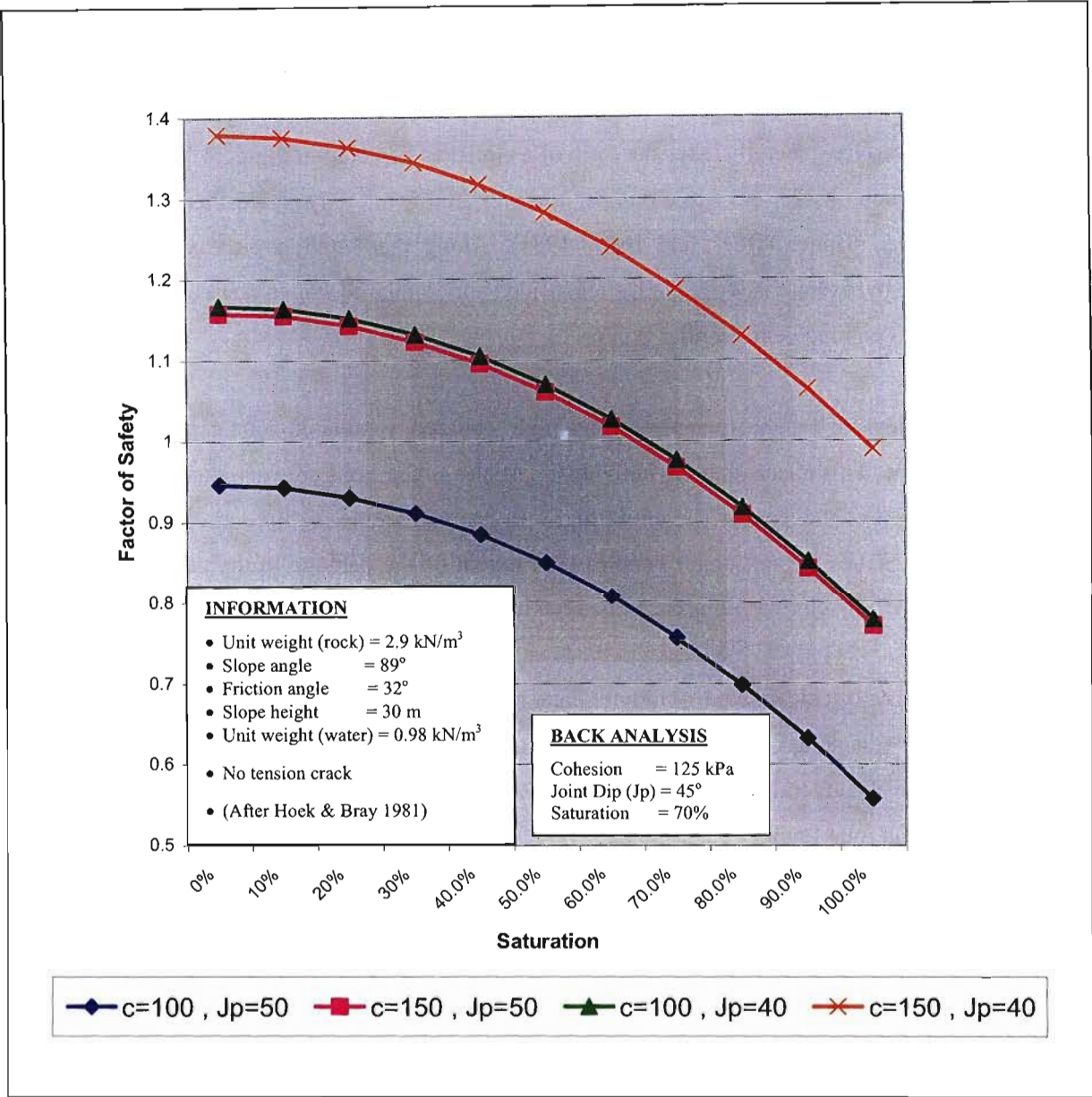


Figure 4.16 Planar failure sensitivity analysis (relationship between FOS, cohesion, joint angle and rock mass saturation).

4.6.3 Zone C (circular failure)

Circular failures may occur in rock masses that are so intensely fractured in relation to the scale of the slope they may be considered as randomly jointed and isotropic. Unlike wedge and planar failures in competent rock, which are controlled by geological features, circular failure is not defined by a structural pattern and the failure surface is free to find the line of least resistance. This failure surface generally takes the form of a circle, as depicted in Figure 4.17. Circular failure is more common in soils and waste dumps, however, highly altered and weathered rocks also tend to fail in this manner (Hoek and Bray, 1981). Along the Satellite pit eastern highwall the serpentinised pyroxenite is weathered, slickensided and jointed to such a degree that it approaches the conditions conducive to circular failure.

For the purposes of a stability analyses, this highly altered, weathered zone can be classified as a rock-soil slope. This means that the individual particles in the mass are very small when compared with the height of the slope. The entire highwall has undergone multiple circular failures to the extent that benches are no longer visible. The extent of the damage to the permanent highwall benches, caused by circular failure, can be seen in Figure 4.17.

Zone C consists of calc-silicate, parapyroxenite and serpentinised pyroxenite (Figure 4.12). In the stronger calc-silicate small scale wedges and planar failures were mapped which are insignificant in relation to the overall slope stability. In the serpentinised pyroxenite along the south east highwall, numerous small circular failures were mapped which reduced the safety in that area.

The ore body within the Satellite pit has now been mined out (June 1998) and back-filled with waste to surface elevation. The hazards presented by the highwall are therefore resolved. From an overall slope design point of view the slope was very successful. Knowing that the slope would only have a 3-year life span, it was designed to its upper stability limit. Slope instability was evident over the last year of mining, but the slope did not fail. Considerable waste stripping savings were accrued due the aggressive design.

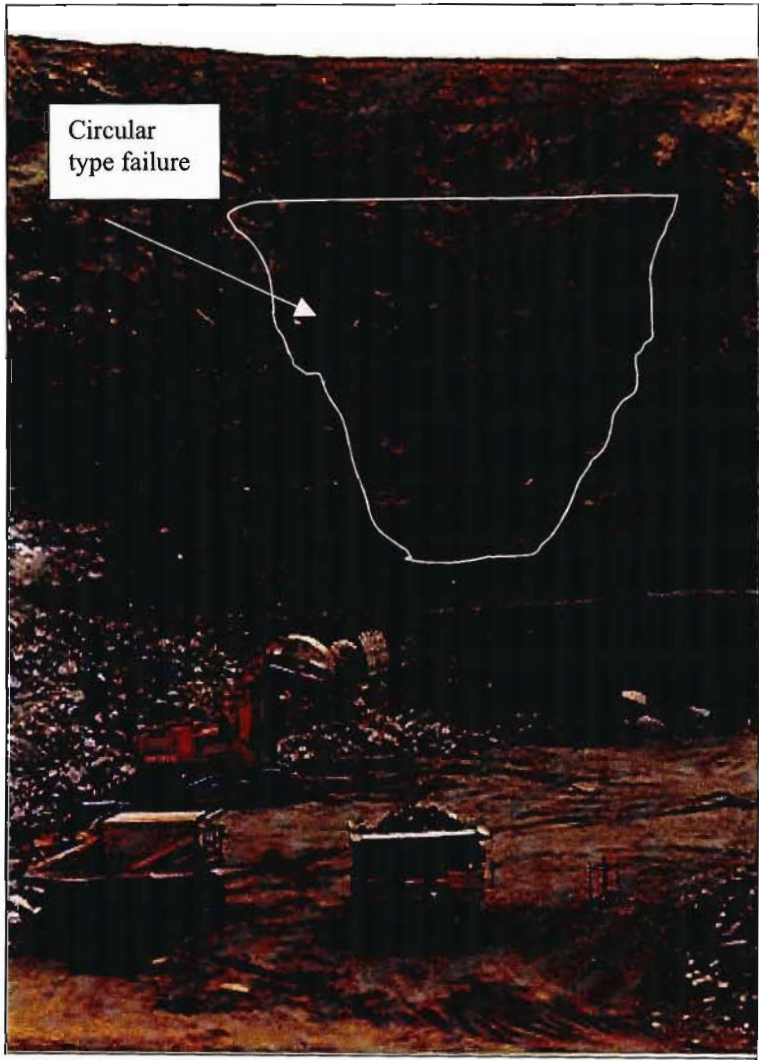


Figure 4.17 Photograph illustrating the Satellite pit eastern highwall.

4.6.4 Zone D (nose zone)

From a geometrical perspective it is logical to assume that concave slopes are far more stable than convex slopes. The nose as illustrated in Figure 4.18 is therefore potentially a problem area as it has a prominent convex geometry. If one considers the lateral constraint provided by the material on either side of a potential failure, it is clear that this restraint will be greater if the slope is concave than it would be if the potential failure is situated in a nose which has freedom to expand laterally (Hoek and Bray, 1981).

The additional stresses the nose is exposed to, due to its geometry and position in terms of blast energy from both the Satellite pit and the South pit, is clearly evident in Figure 4.18. Small-scale planar and wedge failures can be seen around the entire nose area, the extent of the destressing and dilation of joints is also clearly visible.

Figure 4.19 illustrates graphically the influence of slope curvature upon the factor of safety of a slope. It shows the significant increase in the factor of safety that can be achieved by making the slope concave in section.

The nose area consists predominantly of calc-silicate material. This rock type is highly jointed ($RQD = 55\%$), has an UCS of 140 MPa and a MRMR of 42. Thus the geometrical problem is compounded by the fact that the nose consists of a weak rock mass which is continually subjected to blast vibrations.

Although the Satellite pit is now completely back-filled the continued dilation of joints around the area still poses a significant safety hazard; this is compounded by the fact that the nose area is situated above a major haul road. The area therefore requires continual survey monitoring, as well as bench inspections so that any potential failure can be predicted before major damage is incurred.

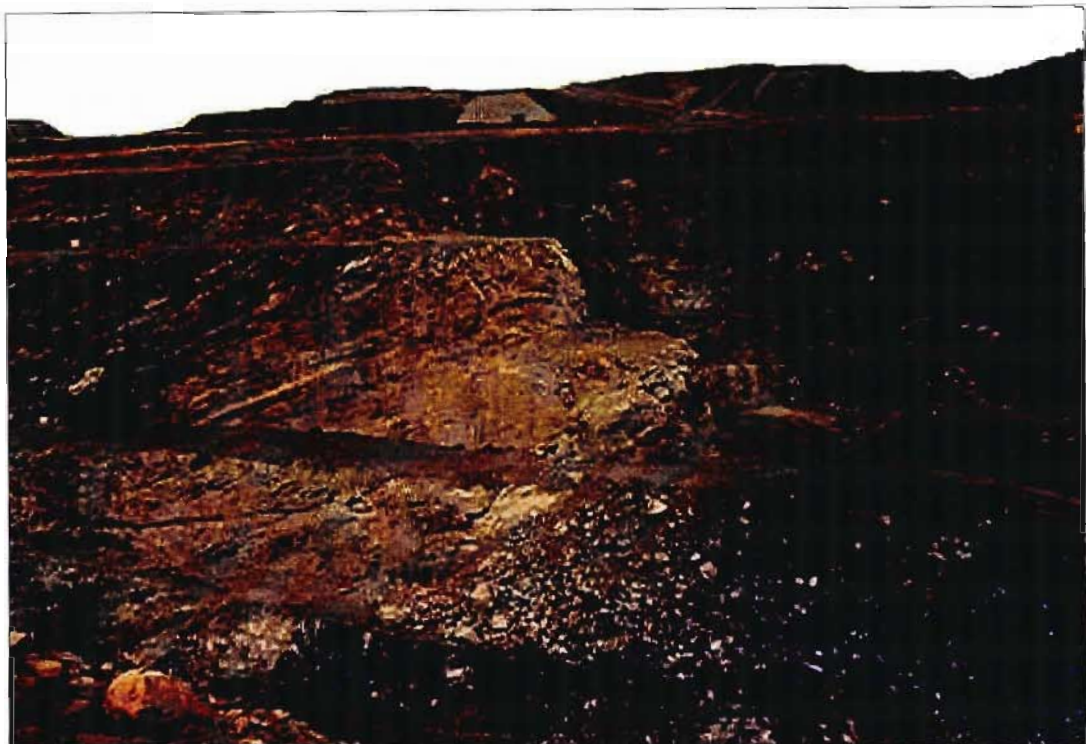


Figure 4.18 Photograph illustrating the problematic nose area.

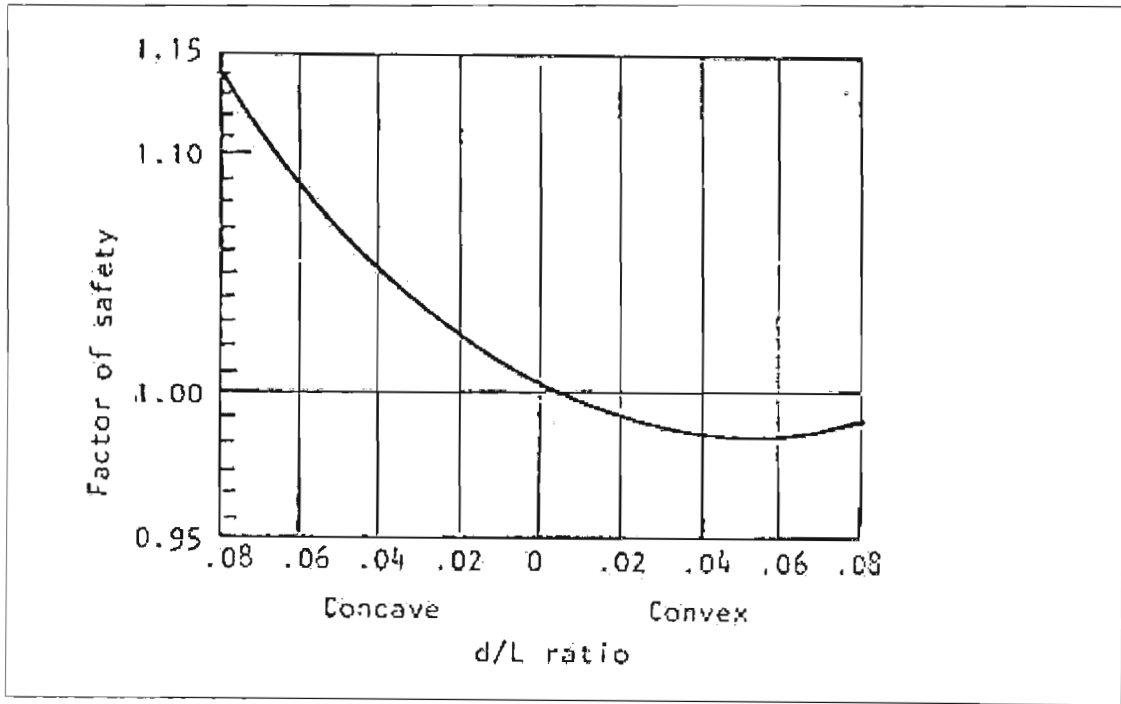


Figure 4.19 Graph illustrating the influence of slope curvature on slope stability (SRK, 1991).

4.6.5 Zone E (planar and toppling failure)

Planar and toppling failures occur in Zone E. As the former failure mechanism and occurrences were discussed in Section 4.5.2, this section focuses on the toppling failure mechanism. Toppling failure involves the rotation or overturning of blocks of rock about some fixed base and is associated with steep slopes and sub-vertical joints dipping back into the slope (Figure 4.20). De Freitas and Watters (1973) provided an excellent description of the toppling failure mechanism.

The regions in the pit where toppling failure has been identified are depicted in Figure 4.12. The joints causing the failures or potential failures are associated with joint set one. Of the number of types or modes of toppling failure discussed by Hoek and Bray (1981), the process of flexural toppling most closely approximates the mechanism identified in Sandsloot open pit. The process describes continuous columns of hard rock separated by well-developed steeply dipping joints, which break in flexure as they bend forward. Although similar, the mechanism witnessed in the pit involves dilation of the joints over time associated with sliding along a shallow dipping joint surface.

Planar and toppling failures are evident along the crests of the footwall and hangingwall in Zone E. The potential failures are destabilised by crest damage from poor presplit blasting and inadequate crest protection measures. Owing to the steep nature of the jointing (70°) and narrow joint spacing, the resultant toppling failures are small in size and are retained by the underlying catchment berm. They therefore do not pose a significant safety hazard.

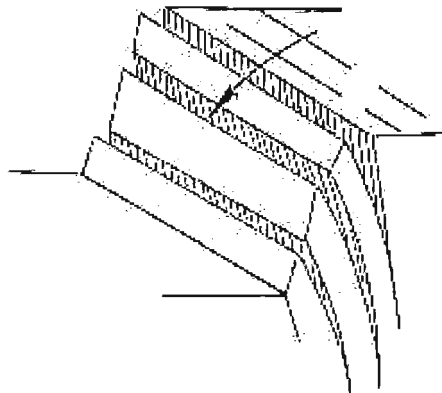


Figure 4.20 Toppling failure mechanism, after Hoek and Bray (1981).

4.6 Summary and Conclusions

Geology and the detailed understanding of its properties are fundamental to the optimal design and successful operation of any mine. The relevant data and sampling methods were introduced in Chapter 4. The interpretation of this data into useful engineering numbers was discussed as well as the methods used to ensure consistent, quality data capture. The extensive field and laboratory testing undertaken, for the definition of each rock types geotechnical properties in the Sandsloot mining area, was described. Kinematic failure analysis data was also presented, as it is used as a basis for slope design.

Table 4.3 summarises all the geotechnical information collected as part of the research project. Extensive fieldwork was conducted to collect geotechnical information, both from exploration boreholes and in-pit mining faces. Over a 5-year period, geotechnical data were collected from 29,213 m of exploration core and 6,873 m of exposed mining faces. This yielded 1,041 data points for the geotechnical design parameters. As discussed in Section 4.2 the collection of rock mass rating information is undertaken by separating the rock mass into visually similar zones and obtaining an average rating for that zone, be it 1 m or 50 m wide. In contrast, geological assay sampling is undertaken on a set 0.5 m basis and thus the total length of geotechnical mapping and logging would have yielded over 72,000 assay samples. It is very important to note this distinction in sampling method and the resultant number of data points for the equivalent sampling area.

Chapter 5 deals with the development of the geotechnical model. An overview of geostatistics and geotechnical engineering is described and this is developed into a specific description of the methods used to construct the Sandsloot 3D geotechnical model.

5 DEVELOPMENT OF THE 3D GEOTECHNICAL MODEL

5.1 Introduction

The relevant data and sampling methods were introduced in Chapter 4 as well as how the application of that data is best facilitated through the use of a 3D model. The interpretation of this data into useful engineering information was discussed as well as the methods used to ensure consistent, good quality data capture. An overview of geostatistics and geotechnical engineering in general is laid out in this chapter. The processes used to develop an ore reserve model are discussed as they form the basis for the development of the geotechnical model. The various construction steps used in the development process are laid out sequentially, culminating in the geostatistical analysis and interpolation method used to generate the final model.

Extensive use is made of computerised planning and production systems at PPL. The computer systems run on various personal computers, workstations and data servers, which are connected via a local area network. Datamine® forms the core of the suite of customised software packages. The functionality of the Datamine® software is presented in the brochure contained in Appendix 8. One of the primary responsibilities of a geology department at a mine is the development and maintenance of an ore reserve model as it forms the basis for all mine planning. The more detailed and accurate information contained in the ore reserve, the lower the risk of the mining venture and therefore better management decisions can be made. To this end, the development of a geotechnical model containing detailed rock mass data can provide valuable information to the mining operation.

The development of a geotechnical model facilitates the provision of geotechnical information well in advance of the mining face. Using the model mining slots can be evaluated not only for grade and tonnage predictions, but also for predictions of rock mass quality. Blast design and explosive requirements can be derived from the rock mass quality predictions. This information can be used for overall mine planning and evaluation, costing, production optimisation and slope design. This allows the full range of mining activities and costs to be inter-connected, thereby lowering costs through the application of the geotechnical model.

5.2 Geostatistics and Geotechnical Engineering

The following discussion has been edited from a review paper undertaken by Rocscience (2003). Geotechnical engineering is constantly evolving and its practitioners are always on the lookout for tools, which improve design and understand the large uncertainties and variations in soil and rock properties. In recent years, several authors have attempted to apply geostatistics to the problems of geotechnical engineering e.g. Lapointe (1990) and Rouhani (1996). To help track the evolution of the interest of geotechnical engineers in this science, Rocscience (2003) conducted a simple survey of geotechnical engineering papers that listed “geostatistics” in their titles, abstracts, descriptions or keywords. The search covered the period from 1970 to 2003 and it only found 64 such publications as illustrated in Figure 5.1.

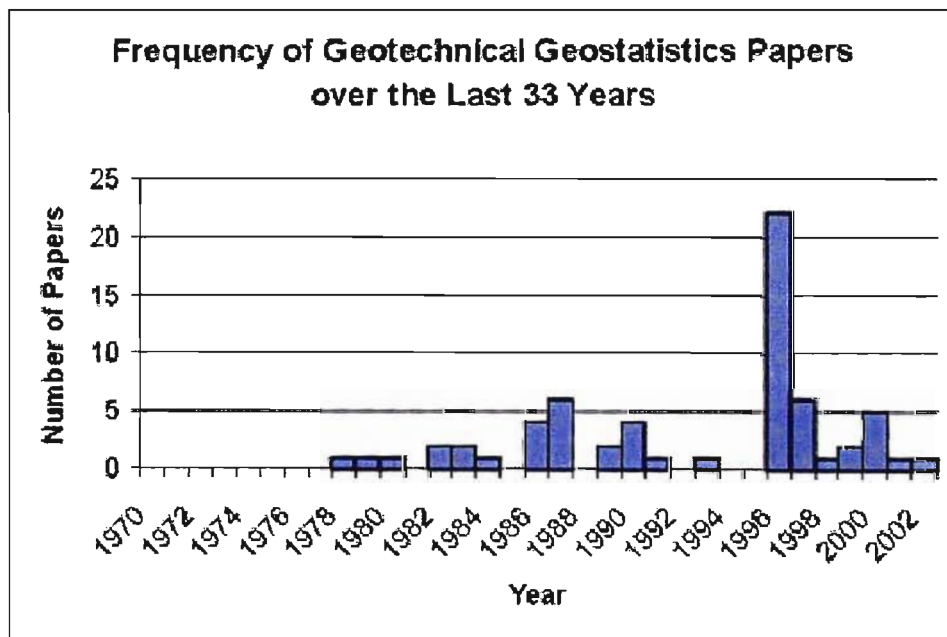


Figure 5.1 A histogram plot of the frequency of geotechnical publications on geostatistics over the last 33 years, after Rocscience (2003).

The histogram indicates that up until 1978, no paper existed that listed its focus as geostatistics and geotechnical engineering. Over the rest of the period, interest seems to peak and fall a few times and current interest appears to be at another low. If the profession is able to fully apply the power of the method and understand its concepts and tools, geotechnical engineering will benefit tremendously.

5.2.1 Geostatistics

Geostatistics deals with spatial data, i.e. data for which each value is associated with a location in space. In such analysis it is assumed that there is some connection between location and data value. From known values at sampled points, geostatistical analysis can be used to predict spatial distributions of properties over large areas or volumes.

To determine geotechnical and geological conditions, such as the stratigraphy of soil or rock layers at a project site, boreholes are drilled at some specified locations. Very often, and as expected, one finds that measurements from boreholes near to each other tend to be more similar than those from widely separated boreholes. This observation forms the basis of the assumption in geostatistics that location has a relationship to measured properties.

Geostatistics differs from conventional statistics in that statistics generally analyses and interprets the uncertainty caused by limited sampling. For example, a conventional statistical analysis of core samples from a site investigation programme might show that measured cohesion values of a material can be described by a normal distribution. This distribution, however, only describes the population of values gathered in the investigation; it does not offer any information on which zones are likely to have high cohesion values and which areas will most likely have low values.

Geostatistical analysis, on the other hand, interprets statistical distributions of data and also examines spatial relationships. For the example given, it is capable of revealing how cohesion values vary over distance and of predicting areas of high and low cohesion values. The discipline provides tools for capturing maximum information on a phenomenon from sparse, often biased and often under-sampled data. Ultimately it produces predictions of the probable distribution of properties in space or a level of confidence of the data located at that point.

The geotechnical engineering profession should give strong consideration to adopting the techniques of geostatistics, as application of the discipline will lead to more ready incorporation of the inherent uncertainty of soil and rock masses into numerical models and the design process.

An appreciation of what geostatistics can do for geotechnical engineering can be obtained by looking at the origins of the discipline and examining its successful application to a variety of fields. The method was originally conceived in the 1960's as a methodology for estimating recoverable reserves in mining deposits. Today it is extensively used in the mining and

petroleum industries and in recent years has been successfully integrated into remote sensing and GIS.

The problem in reserve estimation is that high risk decisions have to be made based on very sparse information. The ratio of the volume of samples recovered from exploration boreholes to the volume of a deposit of interest is often of the order of 1×10^{-9} . Yet on this information recoverable reserves have to be reliably estimated and decisions made on whether to invest large amounts of money into developing the deposit.

Although the financial costs of the average geotechnical project may not be as high as those of exploration projects, geotechnical engineering has similar concerns. In almost every geotechnical project, the volume of samples obtained for characterising soil or rock masses constitutes only a minute fraction of the volume of material. Just like the attributes measured in resource exploration, the engineering properties of soil and rock masses are heterogeneous, with properties varying from location to location. In addition, the financial resources committed to geotechnical field investigations often represent a significant portion of total project costs.

Regularly, either for the sake of simplicity or for lack of information, geotechnical engineers assume that properties are the same throughout a material domain. Nonetheless, they know that the use of averaged parameter values can lead to conclusions that significantly differ from true behaviour. It is also recognized that accurate knowledge of the spatial distribution of soil and rock mass properties promotes safe and economic design. Given the potential improvements to design and the success of geostatistics in resource estimation, it is imperative that the geotechnical engineering discipline seriously considers this tool. Geostatistics facilitates accurate interpretation of ground conditions based on the sparse input information characteristic of geotechnical engineering.

Among its many potential benefits to geotechnical engineering, geostatistical analysis offers the following:

- i. Powerful analytical tools for forming relatively simple, yet accurate, models of inhomogeneous material based on limited sample data
- ii. Approaches for optimising sampling locations so that they maximise the amount of information at minimum cost
- iii. Techniques for estimating engineering properties at different locations with minimum estimation error.

5.2.2 Optimisation of Site Investigation Locations

An additional benefit of applying geostatistics to geotechnical engineering is the optimisation of site investigation sampling locations. A most challenging task in site investigation is to design a cost-effective sampling programme that best captures information on underground conditions. The site investigator is often required to answer the question, “If more ground investigation is to be done, will the additional information acquired justify the extra cost or delay?”

Geostatistics provides spatial modelling tools that can answer these questions. Geostatistical analysis can create maps that show the magnitude and distribution of the values of a parameter over an area or volume. These digital maps provide estimates, which most accurately represent the spatial distributions of sampled properties.

Contour plots of the standard deviations of predicted values at non-sampled locations are a very useful outcome of geostatistical analysis. These contours highlight areas of higher uncertainty (higher standard deviations) and sampling from these locations can substantially improve the accuracy of predictions.

The tools of geostatistics enable the spatial variability of properties to be visualised. They also allow different hypotheses and assumptions on variability to be readily tested. This makes it possible to establish the most likely structure of spatial variability and determine, from a variety of interpretations, the ones most consistent with the available data.

5.2.3 Simulation and Numerical Modelling

Geostatistical simulation can help geotechnical engineers assess uncertainty and risks in design. It produces many, equally likely, digital spatial representations of a parameter that are consistent with values at sampled locations and with *in-situ* variability. The differences between alternative models provide a measure of spatial uncertainty. The spatially distributed realisations of a variable can be entered into numerical models and used to evaluate risks.

Geostatistical simulation has been used to study the hydrology of fractured rock masses. In these studies, different three-dimensional fracture networks are generated and then analysed for flow patterns. Simulation can also be applied to stress analysis problems. In finite element analysis, for example, each element in a model can be assigned its own deformation and strength properties. It is possible to assign different properties to different elements in a manner that realistically reflects the true conditions and heterogeneity of a soil or rock mass using

geostatistics. Studies have shown that the results of such analyses can differ substantially from those obtained from analyses that employ averaged values (Chiles *et al.* 1999).

5.2.4 Successful Application of Geostatistics to the Channel Tunnel Project

Among the many factors that made the success of the Channel Tunnel project possible, geostatistics was deemed to have played a significant role. It enabled the careful assessment of geological risks and was used to optimise the alignment of the tunnel. Engineers were able to improve the originally proposed alignment of the tunnel using geostatistical analysis.

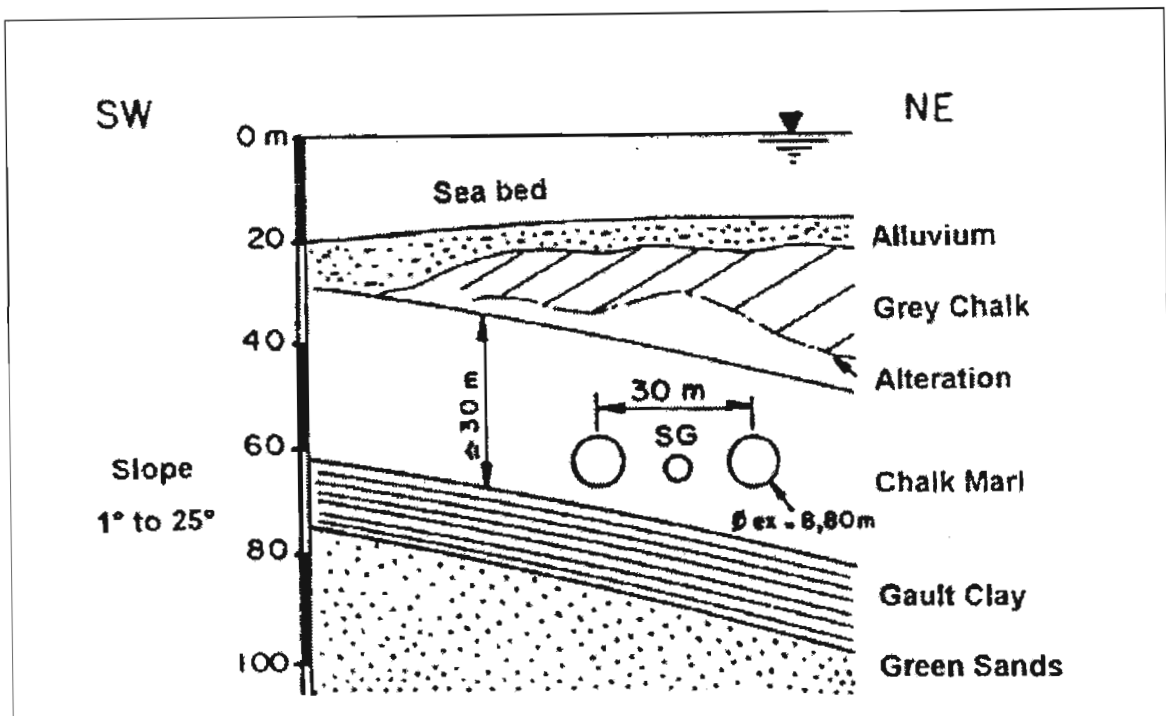


Figure 5.2 Geological cross-section through the seafloor of the Channel Tunnel from Rocscience (2003) and after Chiles *et al.* (1999).

Figure 5.2 shows a typical geological cross-section of the seabed through which the tunnel was excavated. One of the most important criteria in optimising the alignment was to ensure that the tunnel was bored within the Chalk Marl, avoiding the Gault Clay material. Kriging, a geostatistical technique, was used to determine the boundary between the Chalk Marl and the Gault Clay, based on data available before construction. Contours of the standard deviations of predicted depths of this boundary were also generated. As a result of the geostatistical analysis, engineers were able to improve the originally proposed alignment of the tunnel. The standard

deviation contours helped engineers to realise that improved precision was required at certain tunnel sections. As a result of which, they were able to design a complementary geophysical survey of the seafloor. As more data became available from surveys and ongoing construction, geostatistics enabled the tunnel engineers to readily improve the spatial model of the Chalk Marl–Gault Clay interface.

With the help of geostatistical analysis, engineers of the Channel Tunnel were able to maintain the risks of penetrating the Gault Clay at acceptable levels and to achieve their objective of avoiding the Gault Clay formation. Penetration of the Gault Clay occurred only twice and in areas that had already been predicted from the geostatistical model. At the end of the project, when engineers compared actual locations of the Chalk Marl–Gault Clay boundary to the predictions from the geostatistical model, they found the two to be in good agreement.

5.2.5 Integration of Geostatistics

One of the biggest reasons for the limited application of geostatistics in geotechnical engineering could be the widespread unfamiliarity with the concept of geostatistics. Other contributors are the theoretical complexity and the effort required to perform a geostatistical study. Many of the existing geostatistics software tools are not formulated in ways that can be readily integrated into geotechnical analysis. This makes geotechnical engineers unwilling to dedicate the time required to learn and use the method.

Geostatistical analysis tools, appropriately implemented in the company's suite of user-friendly applications, will facilitate powerful and interactive visualisation of the spatial distributions of geotechnical parameters, which in turn will aid in the correct interpretation of data. Such software will also enable and encourage exploration of alternative assumptions and interpretations in the analysis of ground conditions. Through export of the spatial distribution of geotechnical properties, geostatistical software for geotechnical engineers will allow them to realistically incorporate inherent spatial variability into numerical models.

Given the levels of financial, and other, resources devoted to field investigations and data collection, and which already capture the inherent spatial variability of soil and rock masses, geotechnical engineering is well served by adopting geostatistics. The discussion detailed above introduces the potential benefits of geostatistics to geotechnical engineering. The application of these methods for the development of the Sandsloot 3D geotechnical model is discussed in the following sections.

5.3 Ore Reserve Modelling Process

This section details the ore reserve modelling process, which is aimed at illustrating how a geotechnical model can be developed with a similar process (Figure 5.3). The systems used at PPL to develop an ore reserve model are primarily Datamine®, SABLE and AutoCad. Geological data is collected from diamond core exploration boreholes and from the rock chips produced from the drilling of mining blast holes. The ore zones in the core and rock chips are sampled at 1 m and 2.5 m intervals respectively. The blast hole and exploration borehole data are initially dealt with separately and then combined for the modelling process (Figure 5.3).

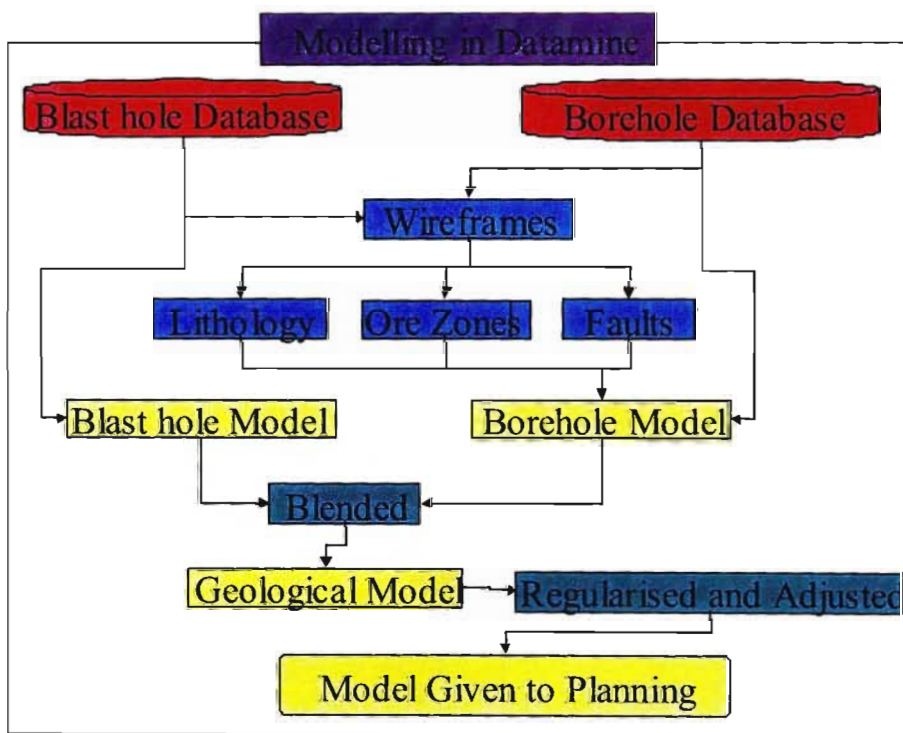


Figure 5.3 Ore reserve data flow diagram, after Reynolds and Millan (1997).

Blast hole data includes collar information, lithology (chip logging) and assay data, which is imported into Datamine®. The information is used to update the blasthole database on a daily basis. The exploration borehole log and assay results are stored in Microsoft Excel spreadsheets. The relevant information (BHID, collar, assay, lithology and RQD) is imported into Datamine®. This information is then used to update the borehole database.

The blast hole and borehole databases are viewed in 3D, using Datamine®, to produce lithology, ore zone and fault wireframes. Face mapping data is also used to update these

wireframes, which then constrain the modelling process. Wireframes are built from strings, which connect all the lithological boundaries, for example between norite and pyroxenite.

Using the two data sets, grades are interpolated within the wireframes to produce two separate models, borehole and blast hole, which are then blended to produce a Geological Ore Reserve Model. The model is a global prediction of the ore reserve tonnages and grades. Figure 5.4 illustrates the geological model of the Sandsloot ore zone, the exploration boreholes and the final pit design.

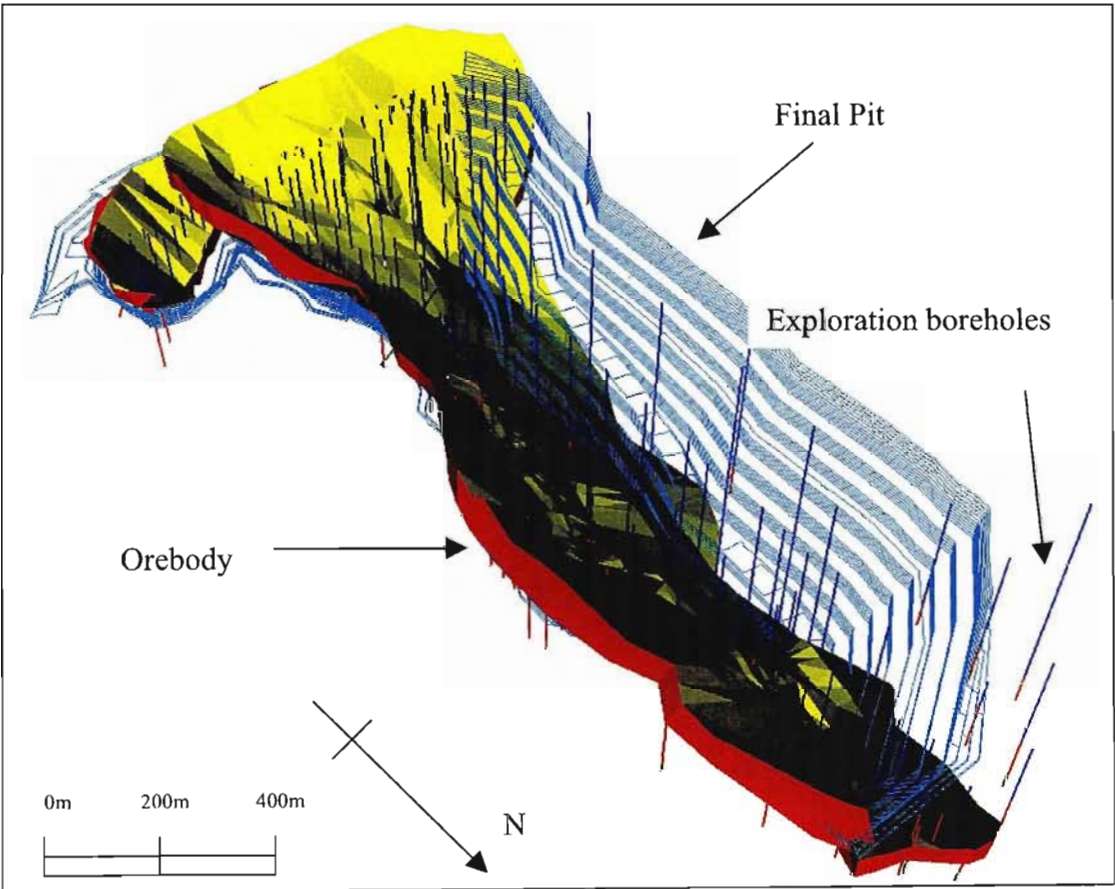


Figure 5.4 Three-dimensional view of Sandsloot open pit, the exploration boreholes and the orebody. The open pit is approximately 2 km in length and 0.5 km wide.

The updated geological model is given to the short-term planning department who can then query it to obtain expected tonnages and grades for a particular blast planned within the pit. This information is used by the short-term planning department as a basis for developing weekly and monthly mining schedules.

The long term planning department uses the ore reserve model to generate an economic mining shell using Datamine® NPV Scheduler. The scheduling software proposes pit outlines and preferred areas of mining based on grade, product prices, mining and processing costs. At Sandsloot, and most other mines, a single mining cost-per-tonne is given for the entire pit, except for consideration of the hauling costs related to pit depth. An optimised pit is then designed around the economic mining shell generated by NPV Scheduler. The mining process is then scheduled and planned over a five-year period and then over the life of the pit in order to optimise profit. The schedule is based on the mining costs versus the grade and tonnage for each ore reserve block. Previously these mining costs at Sandsloot were based on averages and no cognisance was taken of the rock mass conditions and the effect it may have on mining costs and productivity.

Owing to the diverse nature of the geology at Sandsloot, the mining cost-per-tonne varies per geotechnical zone and, in this research, it was therefore generated for each geotechnical zone or model block (15 m³). This information does significantly alter the open pit design and mining schedule, giving a better prediction of costs, ore extraction and therefore profit. The mining costs have subsequently been divided into drilling and blasting costs, based on required powder factors per geotechnical model block. The geotechnical model representing the variability in the rock mass conditions is a valuable planning tool as specific mining costs have been attributed to each geotechnical model block.

5.4 Geotechnical Model Development

A similar data flow process, as described for the ore reserve (Figure 5.3), was used for the development of the geotechnical model. Figure 5.5 details the data flow process of the geotechnical information collected at Sandsloot and used to develop the geotechnical model. The geotechnical field mapping data was captured to AutoCAD and the borehole data was captured to Excel as described in Chapter 4. The data was evaluated within these packages to give rock mass information and sorted so that it can be read directly into the Datamine® geotechnical database.

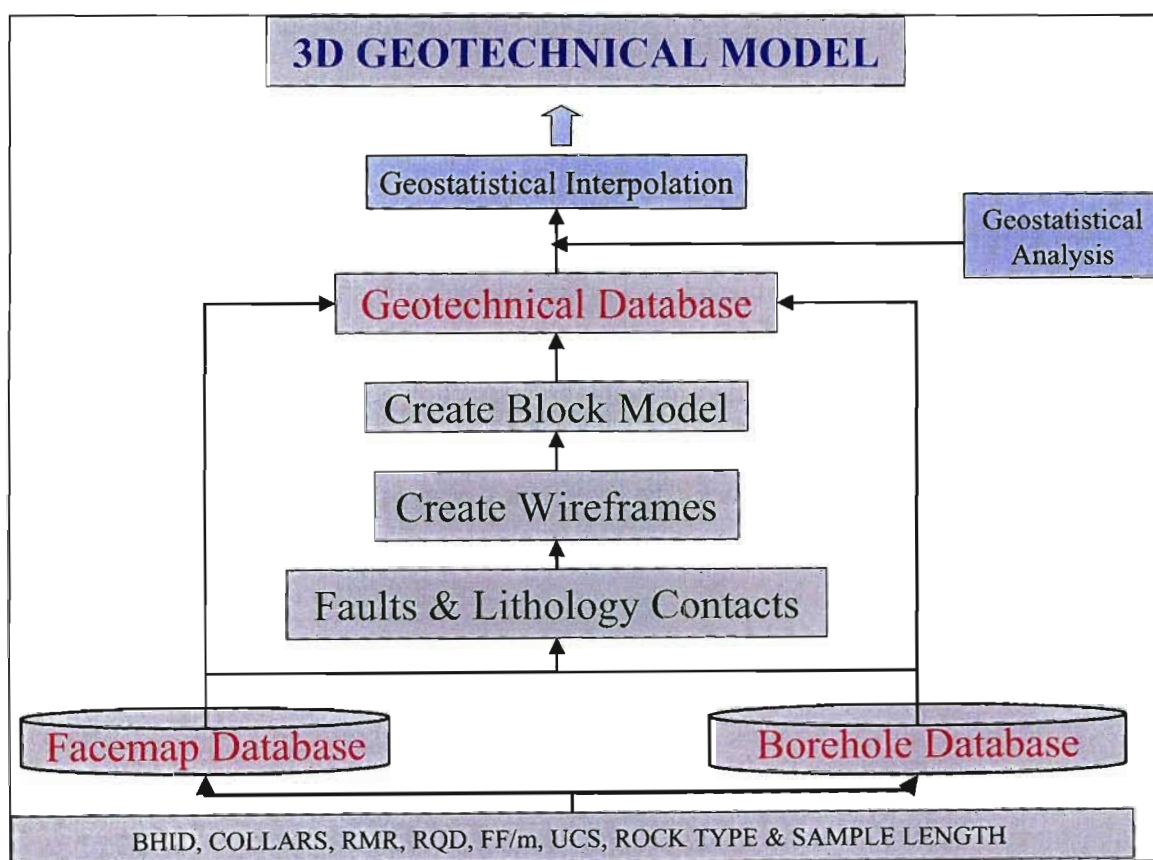


Figure 5.5 The process followed in the development of the geotechnical model.

5.4.1 Data Input

Once the field data is captured to AutoCAD and Excel, as described in Chapter 4, the routines developed within the AutoCAD software allow exporting of relevant geotechnical and structural information in ASCII and CSV (comma separated values) format (CGSS, 1997). This geotechnical information includes the X, Y and Z co-ordinates for each mapped zone as well as

the RMR, UCS, RQD, FF/m, sample length and rock type for that zone. This information is then imported into the Datamine® geotechnical database (Figure 5.5). The geotechnical database is used to store all the geomechanical and geotechnical data collected from field mapping and exploration boreholes.

Geotechnical data, collars and survey files are combined to create orientated geotechnical data samples. Therefore each mapped geotechnical zone has its own X, Y, Z, start and finish co-ordinates, zone length, orientation and geotechnical data. There is thus a facemap and a borehole database containing all the orientated geotechnical information in its correct position in space as illustrated in Figure 5.6. Table 5.1 illustrates an example subset of all the spatial geotechnical data stored in the Datamine® database. The 3D illustration thereof is presented below in Figure 5.6.

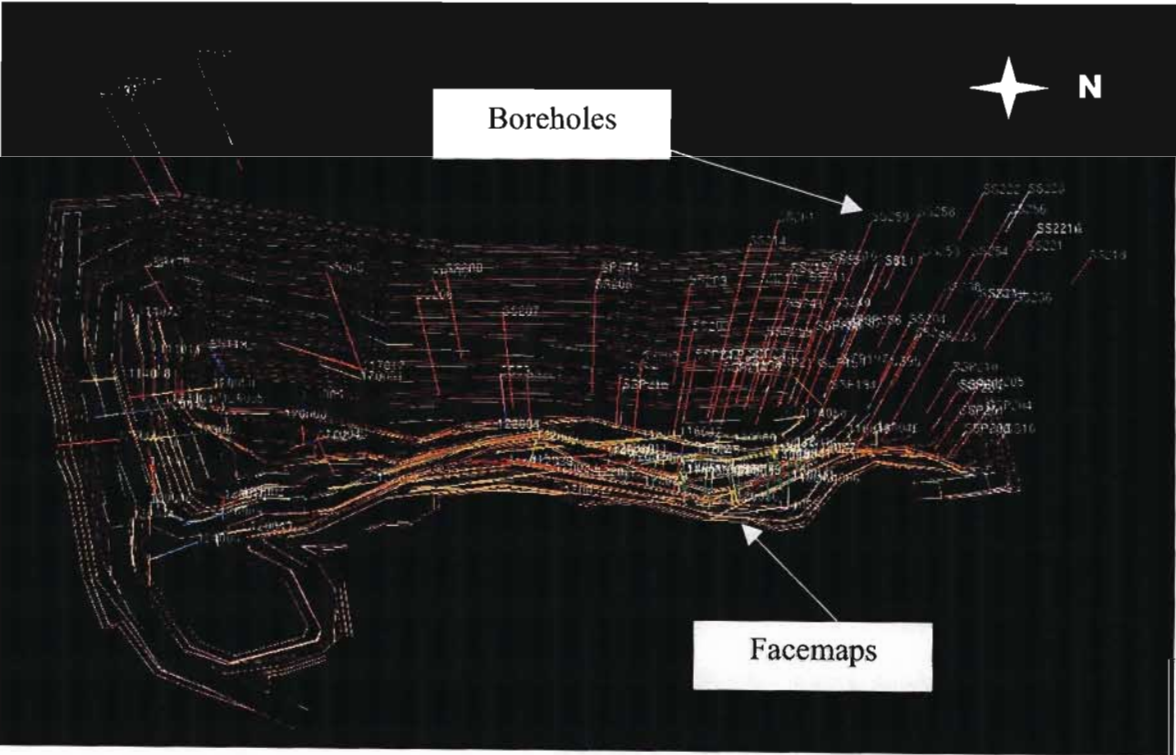


Figure 5.6 Oblique view illustrating the boreholes and facemaps presented in Datamine®.

Table 5.1 Example tabulation, for 4 boreholes, of all the geotechnical data stored in the Datamine® database. (Full table in Appendix 2).

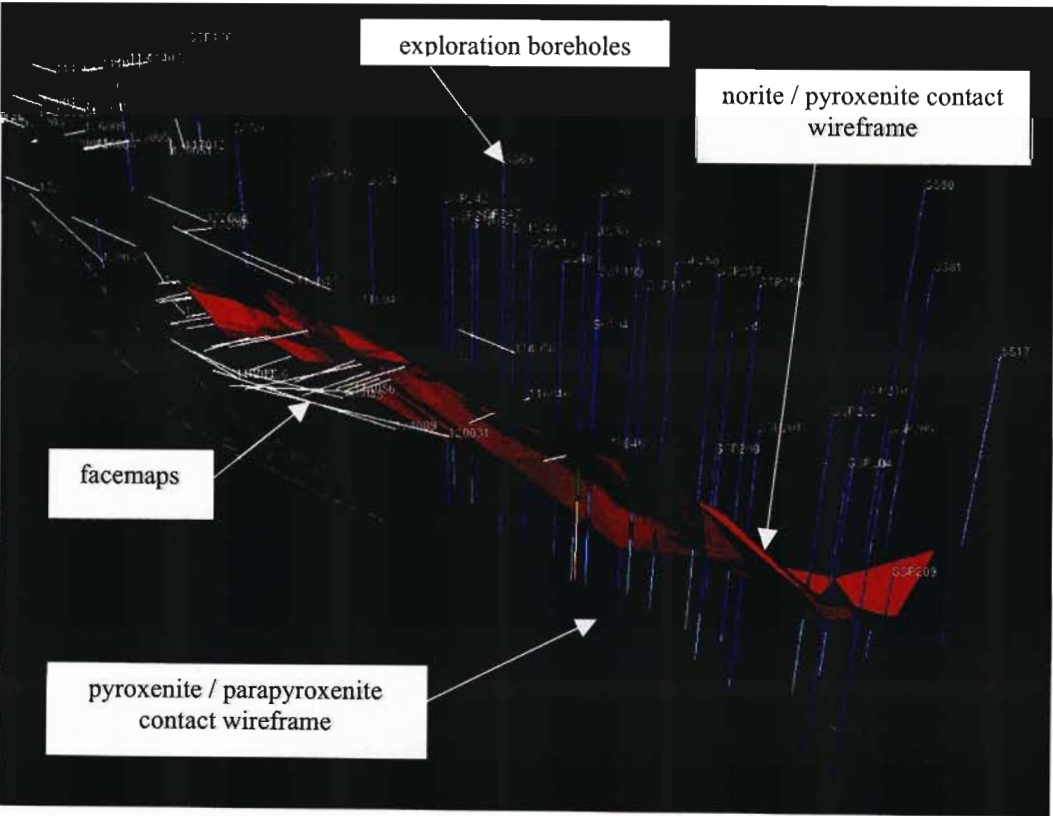
BHID	X	Y	Z	BEARING	DIP	XSTART	YSTART	ZSTART	XEND	YEND	ZEND	FROM	TO	SAMPLE LENGTH	GT ZONE	RQD	UCS	FF/M	MRMR	MRMRQ	MRMRF	AWEATH	AORIENT	ASTRESS	ABLAST	ATOTAL	MRMRF	MRMRQ	ROCK CODE	ROCK DESCRP	ROCK TYPE	
SPST2	-9.217	-66.557	1.086	290	80	-9.217	-66.557	1.086	-9.218	-66.557	1.085	-	2	2	2	1	68	120	88	26	57	51	0.92	0.85	0.94	0.94	0.72	29	26	0	QW	N
SPST2	-9.222	-66.555	1.061	290	80	-9.218	-66.557	1.085	-9.225	-66.554	1.038	2	50	48	2	98	200	98	28	59	60	0.92	0.85	0.94	0.94	0.72	27	28	0	QW	N	
SPST2	-9.227	-66.563	1.027	290	80	-9.225	-66.554	1.038	-9.229	-66.553	1.016	50	72	22	3	88	288	88	26	48	53	1.00	0.85	0.98	0.94	0.78	24	26	0	QW	N	
SPST2	-9.229	-66.553	1.015	290	80	-9.229	-66.553	1.016	-9.229	-66.553	1.014	72	73	2	4	48	200	48	21	43	57	0.86	0.85	0.98	0.94	0.87	15	21	0	QW	N	
SPST2	-9.231	-66.552	1.007	290	80	-9.229	-66.553	1.014	-9.232	-66.552	999	73	89	15	6	90	204	90	25	52	54	0.92	0.85	0.98	0.94	0.72	24	25	0	QW	N	
SPST2	-9.232	-66.552	997	290	80	-9.232	-66.552	999	-9.232	-66.552	996	89	92	4	6	68	200	68	22	47	50	0.86	0.85	0.98	0.94	0.67	20	22	0	QW	N	
SPST2	-9.236	-66.550	977	290	80	-9.232	-66.552	996	-9.239	-66.549	958	92	131	39	7	93	180	93	26	48	53	1.00	0.85	0.98	0.94	0.78	24	25	0	QW	N	
SPST2	-9.239	-66.548	957	290	80	-9.239	-66.548	958	-9.239	-66.549	957	131	132	1	8	74	190	74	35	55	68	0.74	0.85	0.98	0.94	0.72	26	26	0	QW	N	
SPST2	-9.239	-66.549	954	290	80	-9.239	-66.549	957	-9.240	-66.549	950	132	138	5	9	92	200	92	26	55	56	0.92	0.85	0.98	0.94	0.72	26	26	0	QW	N	
SPST2	-9.240	-66.549	950	290	80	-9.240	-66.549	950	-9.240	-66.549	949	138	140	2	10	100	170	100	31	55	66	0.92	0.85	0.98	0.94	0.72	26	26	0	QW	N	
SPST2	-9.242	-66.548	939	290	80	-9.240	-66.549	949	-9.243	-66.547	929	140	160	20	11	96	247	96	24	55	66	0.92	0.85	0.98	0.94	0.72	24	24	0	QW	N	
SPST4	-9.181	-66.201	1.090	250	80	-9.181	-66.200	1.091	-9.181	-66.201	1.088	-	2	2	2	1	68	180	2	32	57	63	0.58	1.00	0.96	0.94	0.52	29	32	0	N	N
SPST4	-9.184	-66.202	1.071	250	80	-9.181	-66.201	1.088	-9.187	-66.203	1.054	2	37	34	2	99	250	1	27	58	55	0.62	0.90	0.96	0.94	0.50	29	27	0	N	N	
SPST4	-9.195	-66.205	1.008	250	80	-9.187	-66.203	1.054	-9.202	-66.208	962	37	131	94	3	89	220	1	25	53	54	0.62	0.85	0.96	0.94	0.48	24	25	0	N	N	
SPST4	-9.203	-66.208	959	250	80	-9.202	-66.208	962	-9.203	-66.209	956	131	137	5	4	91	200	3	25	47	59	0.62	0.80	0.96	0.94	0.45	20	25	0	N	N	
SPST4	-9.204	-66.209	952	250	80	-9.203	-66.209	956	-9.205	-66.209	949	137	144	7	5	98	204	2	23	54	67	0.58	0.80	0.96	0.94	0.42	22	23	0	N	N	
SPST4	-9.205	-66.209	946	250	80	-9.205	-66.209	949	-9.206	-66.209	943	144	150	5	6	76	200	4	22	48	54	0.58	0.80	0.96	0.94	0.42	19	22	0	N	N	
SSP176	-9.325	-67.161	1.073	-	90	-9.325	-67.161	1.085	-9.325	-67.161	1.061	-	24	24	1	100	180	2	55	80	63	1.00	0.95	0.96	0.95	0.87	52	55	0	N	N	
SSP176	-9.325	-67.161	1.056	-	90	-9.325	-67.161	1.061	-9.325	-67.161	1.052	24	33	9	2	96	180	5	53	51	61	1.00	0.95	0.96	0.95	0.87	45	53	0	PEG N	N	
SSP176	-9.325	-67.161	1.039	-	90	-9.325	-67.161	1.052	-9.325	-67.161	1.026	33	59	26	3	99	180	3	59	58	68	1.00	0.95	0.96	0.95	0.87	51	59	0	N	N	
SSP176	-9.325	-67.161	1.009	-	90	-9.325	-67.161	1.026	-9.325	-67.161	993	59	92	34	4	91	180	5	52	51	60	1.00	0.95	0.96	0.95	0.87	45	52	0	MN	N	
SSP176	-9.325	-67.161	970	-	90	-9.325	-67.161	993	-9.325	-67.161	947	92	138	45	5	97	180	3	57	54	66	1.00	0.95	0.96	0.95	0.87	47	57	0	MN	N	
SSP176	-9.325	-67.161	946	-	90	-9.325	-67.161	947	-9.325	-67.161	945	138	140	2	6	90	180	12	51	45	59	1.00	0.95	0.96	0.95	0.87	39	51	4	SR	X	
SSP176	-9.325	-67.161	942	-	90	-9.325	-67.161	945	-9.325	-67.161	939	140	146	6	7	98	180	3	62	60	71	1.00	0.95	0.96	0.95	0.87	52	62	6	QZV	Q	
SSP176	-9.325	-67.161	911	-	90	-9.325	-67.161	939	-9.325	-67.161	884	146	201	65	8	91	260	5	55	55	64	1.00	0.95	0.96	0.95	0.87	48	55	4	SR	X	
SSP194	-8.861	-55.771	1.068	-	90	-8.861	-55.771	1.071	-8.861	-55.771	1.065	-	6	6	1	-	-	-	-	-	-	-	-	-	-	-	-	-	-	-	-	
SSP194	-8.861	-55.771	1.065	-	90	-8.861	-55.771	1.065	-8.861	-55.771	1.064	6	7	1	2	100	180	1	62	71	69	1.00	0.95	0.96	0.95	0.87	60	62	0	QW	N	
SSP194	-8.861	-55.771	1.049	-	90	-8.861	-55.771	1.064	-8.861	-55.771	1.033	7	38	31	3	100	180	0	66	76	74	1.00	0.95	0.96	0.95	0.87	64	86	0	N	N	
SSP194	-8.861	-55.771	1.033	-	90	-8.861	-55.771	1.033	-8.861	-55.771	1.033	38	39	0	4	42	180	11	49	56	54	1.00	0.95	0.96	0.95	0.87	47	49	0	N	N	
SSP194	-8.861	-55.771	1.025	-	90	-8.861	-55.771	1.033	-8.861	-55.771	1.017	39	54	16	5	100	180	1	64	74	71	1.00	0.95	0.96	0.95	0.87	62	64	0	N	N	
SSP194	-8.861	-55.771	1.017	-	90	-8.861	-55.771	1.017	-8.861	-55.771	1.017	54	55	0	6	-	180	19	39	45	51	1.00	0.95	0.96	0.95	0.87	44	39	0	N	N	
SSP194	-8.861	-55.771	993	-	90	-8.861	-55.771	1.017	-8.861	-55.771	969	55	103	46	7	99	180	2	55	63	62	1.00	0.95	0.96	0.95	0.87	54	55	0	N	N	
SSP194	-8.861	-55.771	966	-	90	-8.861	-55.771	969	-8.861	-55.771	963	103	108	6	9	81	180	10	50	57	56	1.00	0.95	0.96	0.95	0.87	48	50	0	N	N	
SSP194	-8.861	-55.771	960	-	90	-8.861	-55.771	963	-8.861	-55.771	957	108	114	6	10	97	180	3	51	59	67	1.00	0.95	0.96	0.95	0.87	49	51	0	N	N	
SSP194	-8.861	-55.771	955	-	90	-8.861	-55.771	957	-8.861	-55.771	952	114	120	6	11	93	180	3	51	59	58	1.00	0.95	0.96	0.95	0.87	50	51	0	N	N	
SSP194	-8.861	-55.771	950	-	90	-8.861	-55.771	952	-8.861	-55.771	947	120	124	4	12	98	150	5	57	66	62	1.00	0.95	0.96	0.95	0.87	53	57	1	B	B	
SSP194	-8.861	-55.771	947	-	90	-8.861	-55.771	947	-8.861	-55.771	948	124	125	1	13	-	150	7	39	45	53	1.00	0.95	0.96	0.95	0.87	46	39	1	B	B	
SSP194	-8.861	-55.771	942	-	90	-8.861	-55.771	946	-8.861	-55.771	938	125	133	8	14	74	170	10	45	52	49	1.00	0.95	0.96	0.95	0.87	43	45	1	B	B	
SSP194	-8.861	-55.771	936	-	90	-8.861	-55.771	938	-8.861	-55.771	933	133	136	5	15	86	200	6	52	60	55	1.00	0.95	0.96	0.95	0.87	48	52	3	A	A	
SSP194	-8.861	-55.771	924	-	90	-8.861	-55.771	933	-8.861	-55.771	916	138	157	18	16	92	210	3	53	61	60	1.00	0.95	0.96	0.95	0.87	52	53	2	R	R	
SSP194	-8.861	-55.771	895	-	90	-8.861	-55.771	916	-8.861	-55.771	875	157	197	40	17	99	210	1	57	66	65	1.00	0.95	0.96	0.95	0.87	56	57	2	R	R	
SSP194	-8.861	-55.771	873	-	90	-8.861	-55.771	875	-8.861	-55.771	870	197	201	4	18	70	170	6	42	49	50	1.00	0.95	0.96	0.95	0.87	43	42	6	Q	Q	
SSP194	-8.861	-55.771	865	-	90	-8.861	-55.771	870	-8.861	-55.771	859	201	212	11	19	43	210	4	45	52	59	1.00	0.95	0.96	0.95	0.87	51	45	2	R	R	
SSP194	-8.861	-55.771	859	-	90	-8.861	-55.771	859	-8.861	-55.771	859	212	212	0	20	-	180	38	37	43	47	1.00	0.95	0.96	0.95	0.87	41	37	2	R	R	
SSP194	-8.861	-55.771	857	-	90	-8.861	-55.771	859	-8.861	-55.771	855	212	217	4	21	87	210	7	47	54	53	1.00	0.95	0.96	0.95	0.87	46	47	2	R	R	
SSP194	-8.861	-55.771	855	-	90	-8.861	-55.771	855	-8.861	-55.771	854	217	217	1	22	25	210	23	37	43	45	1.00	0.95	0.96	0.95	0.87	39	37	2	R	R	
SSP194	-																															

5.4.2 Block Model

The development of the block model is described in the five steps listed below. The process involves the construction of wireframes used to separate the three lithological block models namely, norite, pyroxenite and parapyroxenite. These models are then combined and the geotechnical information is interpolated for them.

Step 1. Wireframes

Wireframes are created using the facemap and borehole lithology information visually represented in the model. Strings or data lines are used to connect the surface contacts of the various rock types as illustrated in Figure 5.7. These wireframes serve to constrain the modelling of the geotechnical data to within the specific rock type associated with that data.



Step 2. Block Model

An empty block model was created for the required model boundaries. Parameters used were as follows:

- X co-ordinates = 9,305 m → 8,500 m
- Y co-ordinates = 56,670 m → 55,400 m
- Depth = 380m (1,100-720 m above mean sea level)
- Length = 1,200 m
- Width = 800 m
- Block size = 15 m³
- Model Volume = 364,000,000 m³

From 1992 to 2000 the majority of the southern half of the Sandsloot pit was mined out. For the remaining life of the mine the mining will focus on the northern half of the final design pit. For these reasons the model was constructed for the northern half of the pit (Figure 5.8). Additionally, a far more significant geotechnical database was available for the northern area, as illustrated in Figure 5.6 and Figure 4.10.

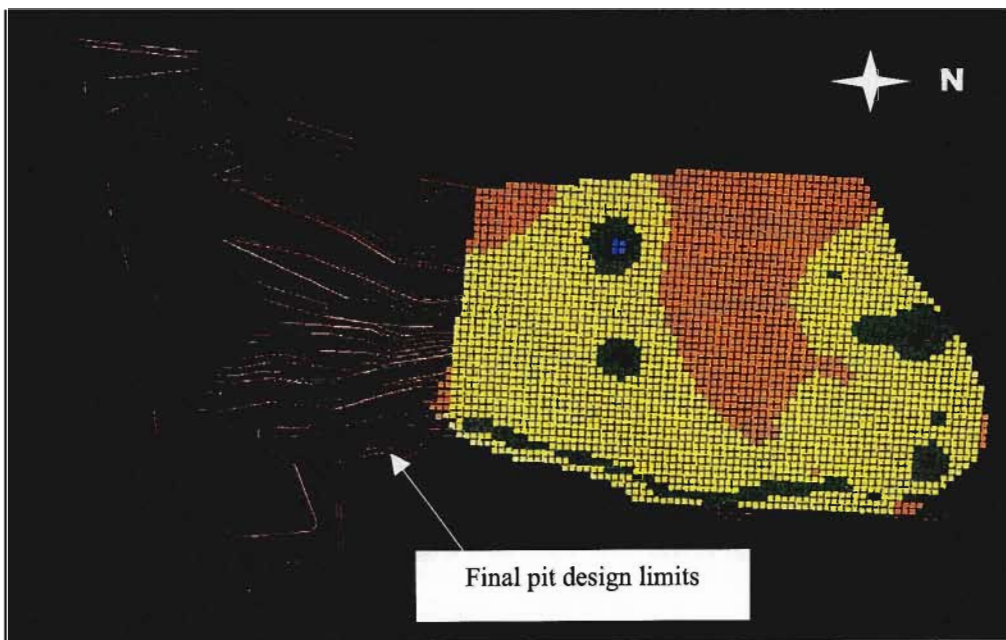


Figure 5.8 Datamine® visualisation illustrating the extents of the block model.

Step 3. Lithology Models

The empty block model was separated into lithology models as constrained by the wireframes constructed from the lithological contacts. Three block models were created representing the dominant rock types occurring in the pit (Figure 5.9). Each lithology model contains the rock type and the rock density as fixed parameters.

- a. Norite model (hangingwall)
- b. Pyroxenite model (reef)
- c. Parapyroxenite model (footwall)

Step 4. Models Combined

Once the three lithology models were defined, they were combined into a single block model representing the entire research area. As can be seen in Figure 5.9, there is a single block model separated into the three dominant rock types.

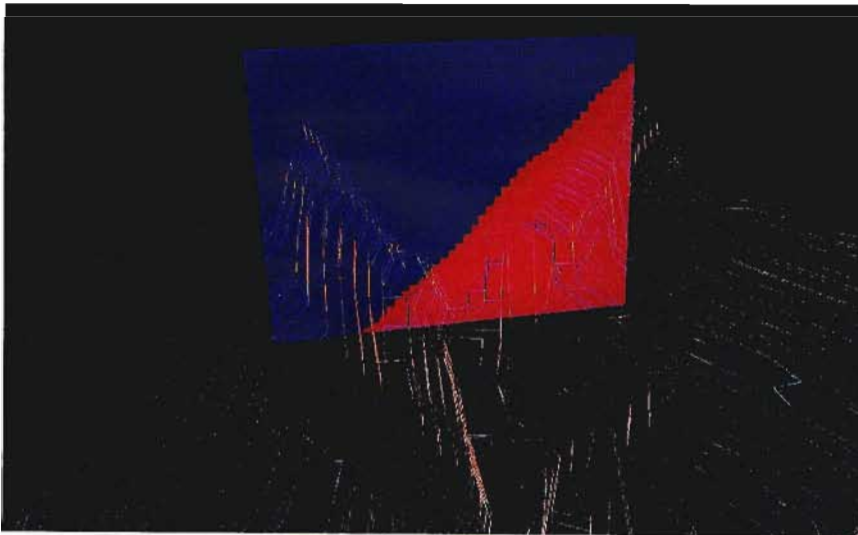


Figure 5.9 Section through the block model illustrating a vertical slice through the three wireframe constrained, lithology models (blue = norite, red = pyroxenite and magenta = parapyroxenite).

Step 5. Interpolation

It is into this block model that the interpolation process populates the model cells with estimated values for the geotechnical data, namely RMR, UCS, RQD and FF/m. It is important to note

that the norite RMR values, for example, are only interpolated from actual boreholes and facemaps containing norite. The model will not interpolate pyroxenite RMR values into the norite block model.

The preceding paragraphs have described the process used to build and define the model extents, as well as how the data is represented in its correct position in space. The wireframes described in step 1 were defined in order to constrain the interpolation process to the correct rock types. These steps are necessary to ensure that the subsequent geostatistical interpolation of values into the block model is undertaken accurately. This process is described in the following sections.

5.4.3 Geostatistical Interpolation

Geostatistics is based on the Theory of Regionalised Variables, which produces the best estimation of the unknown value at some location within an ore deposit (Clarke, 1979). The use of Geostatistics as an estimation technique is best known for its use in interpolating grade within ore reserves. Clarke (1979), however, stresses that estimation techniques can be used wherever a continuous measure is made on a sample at a particular location in space, i.e., where a sample value is expected to be affected by its position and its relationship with its neighbours.

Interpolation Method

Interpolation of estimated values into model blocks can be undertaken by using a variety of methods such as nearest neighbour, inverse power of distance and kriging. Initial interpolation methods involved giving equal weighting to all samples orientated in space. These methods were later evolved to give more weight to the closest samples and less to those farthest from the point of estimation. The obvious way to do this was to make the weight for each sample inversely proportional to its distance from the point estimated (Isaaks and Srivastava, 1989). This can be further developed by using weightings proportional to any power of distance. As the power of distance weighting increases, so the farthest samples become less influential and the closest more so. Traditionally the most common choice for the inverse distance exponent is two.

The Datamine® software package hosts a powerful set of geostatistical interpolation tools principally developed for the definition of ore reserves. The geotechnical data were analysed using histograms (Figure 5.10 – 5.13) to determine the most suitable interpolation method to use

for each modelled parameter, namely RMR, UCS, FF/m and RQD. Due to the bell curve nature of the data sets, the data being evenly spaced and the relatively limited number of data points the inverse power distance (squared) interpolation method was selected. As the database expands, future processing may require more advanced methods such as kriging.

Search Ellipsoid

The Datamine® interpolation search volume is defined by a 3D ellipsoid, which is in turn centred on each subcell of the model and is used to select the samples for interpolating that subcell. The lengths for the three axes may be varied to create an anisotropic volume. Insufficient data was available to justify an anisotropic search volume, thus a spherical search volume was selected. All three axes were set at 350 m, i.e. equal to the radius of the required sphere. Additionally, the search ellipsoid may be orientated by specifying three sets of rotation angles and axes. This was not required for the Sandsloot model. The inverse power of distance method also takes account of the anisotropy and orientation of the search volume when assigning weights to the samples.

Zone Control

The zone control option allows the interpolation process to be controlled by restricting the interpolation to using samples and model blocks that fall within distinct, predefined and homogeneous geotechnical zones or domains. For example, if both the model and sample data files include a numeric rock type field “ROCK”, then specifying the “ROCK” field as the control field for that zone will ensure that model blocks which contain norite will be estimated using samples which are only of the norite rock type.

Using the defined interpolation parameters listed above the geotechnical model was created. The initial models interpolated the MRMR, UCS and RQD parameters. As MRMR is an adjusted parameter it cannot be accurately modelled, as the model will select all data irrespective of the orientation adjustment made for different mining faces. It was therefore decided to model the unadjusted data (RMR) and include the adjustments as a post process option for the modelled RMR values. Specific adjustments can then be made for different face orientations in the pit.

RQD data collected in the field can be heavily biased due to the orientation of the logging or mapping face and therefore the RQD value may not be representative of the rock mass volume where the data was collected. It was therefore decided to use FF/m as a more representative measure of the rock mass condition. This was based on the fact that the boreholes and face mapping covered all the major sampling directions. FF/m is also a distinct measure rather than a percentage, which lends itself to geostatistical analysis and interpolation. This is evident in the histograms illustrated in Figures 5.11 and 5.12, which show the FF/m data generating more consistent bell curves than the RQD data. The reason for the numerous peaks or distributions in the RQD, FF/m and RMR histograms (Figures 5.10 - 5.12) is related to structurally undisturbed rock mass conditions versus rock mass that is sheared or highly faulted. The numerous peaks or distributions in the UCS histogram are related to zones of weathering versus competent unweathered rock conditions.

Over a two-year period the interpolation process evolved through a number of trials with various kriged estimations initially being used. Field verification of the kriged models indicated that the model was predicting a high level of variability not evident in the field. The kriged models also suffered from insufficient data to generate reliable kriging parameters. The inverse distance model gave a better prediction of the rock mass conditions and was verified over an 18-month application of the model, which will be discussed in Chapter 8. In order to assess the reliability of the model a NUMSAM parameter is calculated during the modelling process. This parameter indicates for each model block how many actual data samples were used to interpolate the geotechnical data within the model cell. It therefore gives an indication of the confidence with which that model cell data can be read based on the number of actual samples used to interpolate the block values.

The final geotechnical block model is illustrated in Figure 5.14. Figure 5.15 illustrates the block model, which has been queried, and the report (output window) showing all the data associated with that model block (cell with white cross in it). Each 15 m³ model cells contains a value for RMR, UCS, RQD, FF/m, density, rock type and the number of actual samples used to interpolate into that specific cell.

FREQUENCY PLOT FOR RMR VALUES

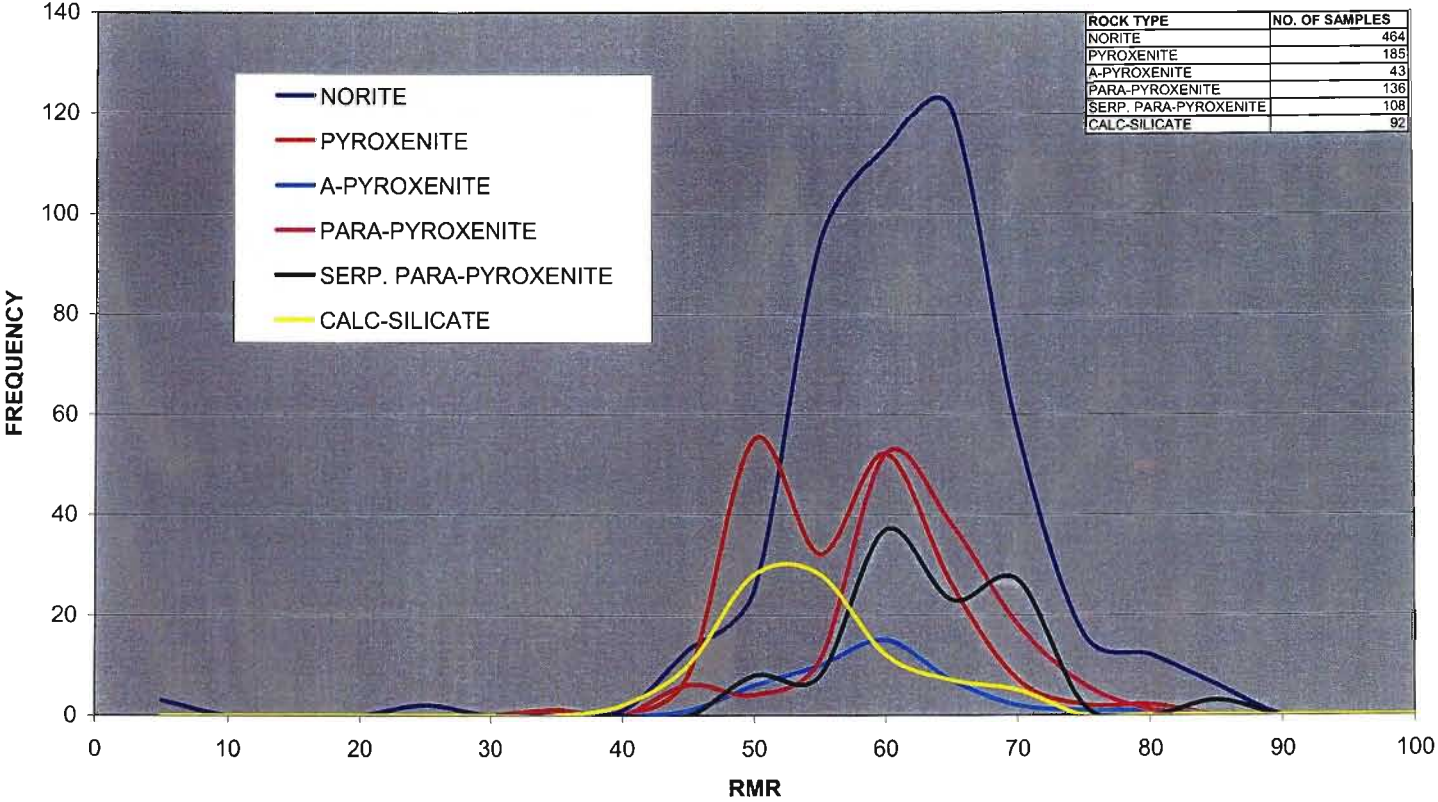


Figure 5.10 RMR histograms for all the rock types occurring in the pit.

FREQUENCY PLOT FOR FF/m VALUES

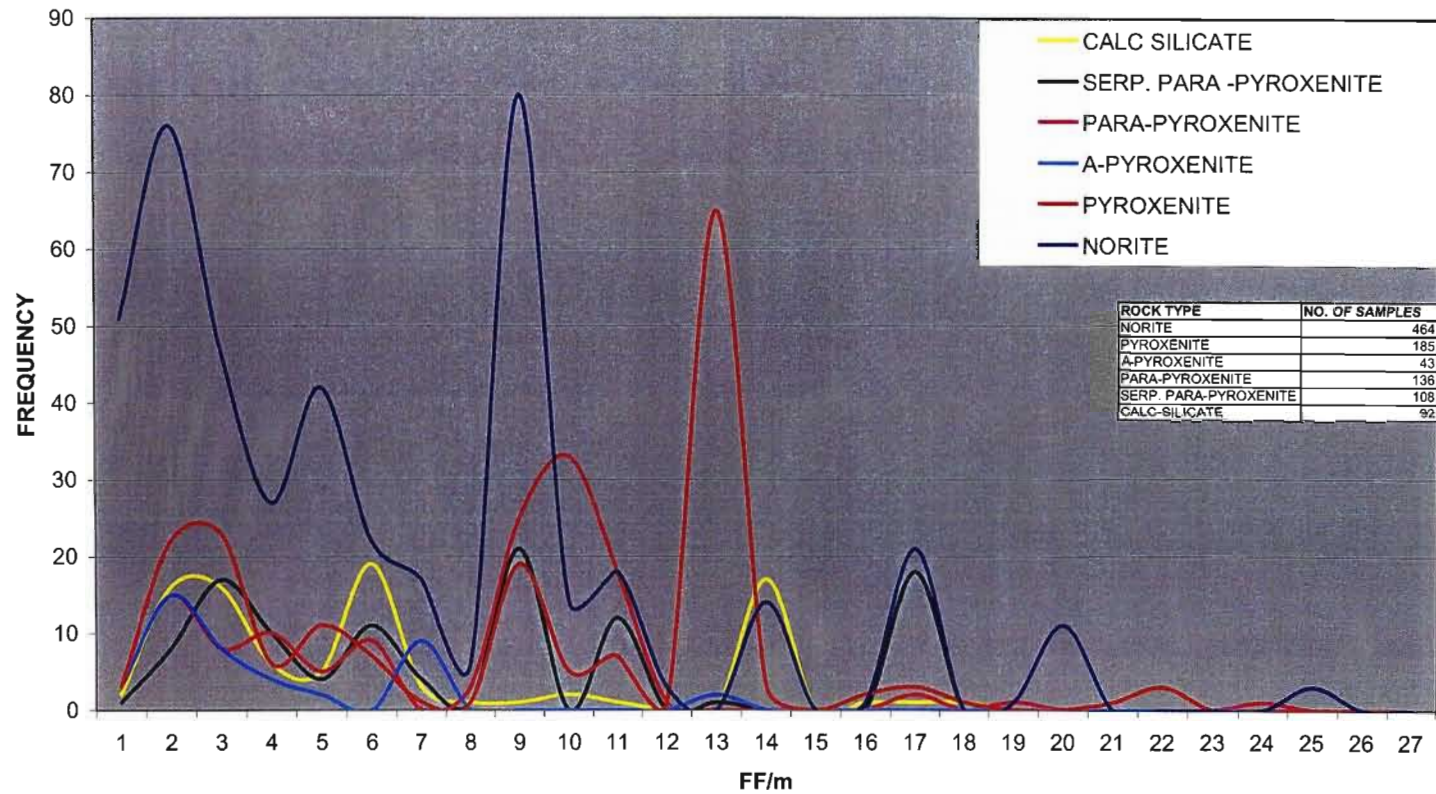


Figure 5.11 FF/m histograms for all the rock types occurring in the pit..

FREQUENCY PLOT FOR RQD VALUES

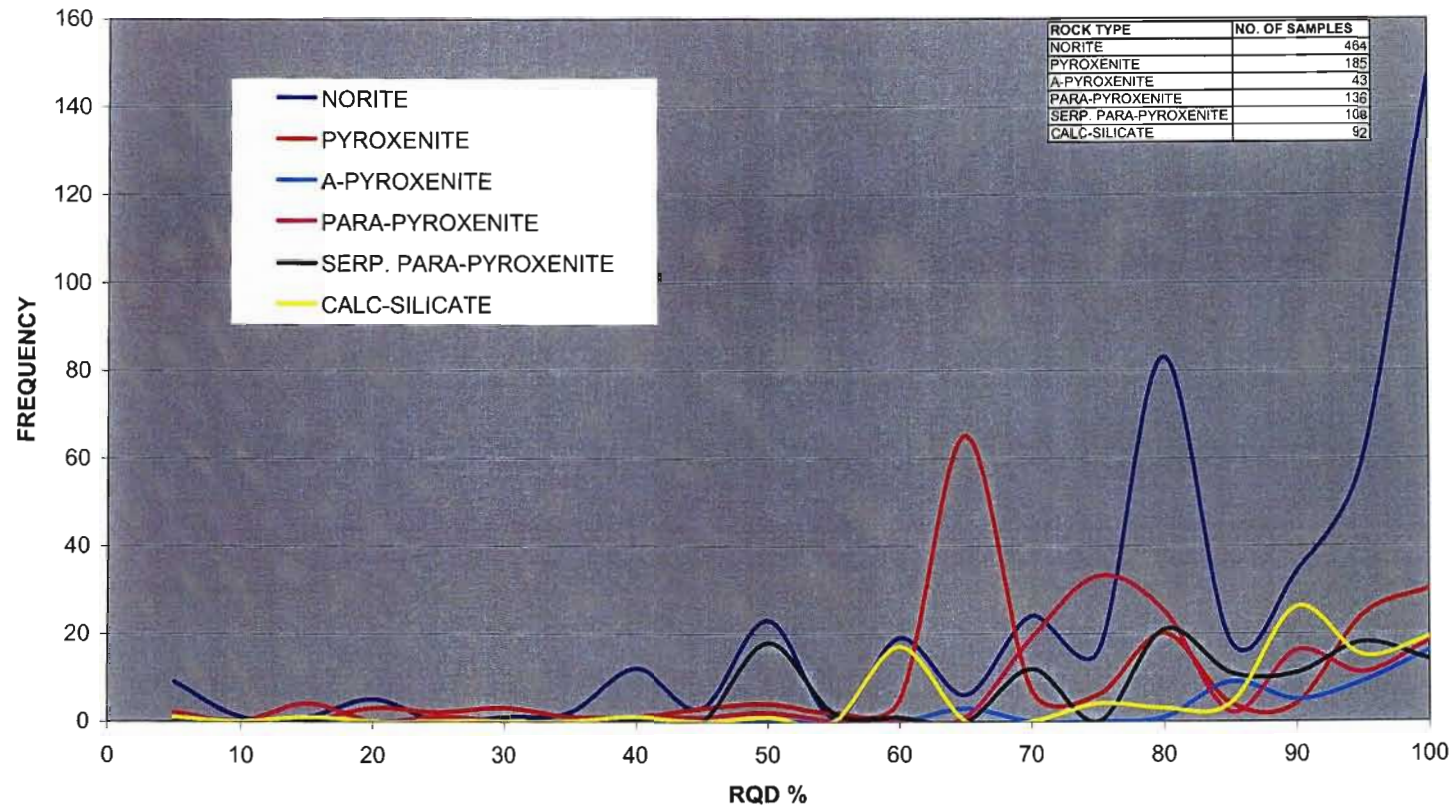


Figure 5.12 RQD histograms for all the rock types occurring in the pit.

FREQUENCY PLOT FOR UCS VALUES

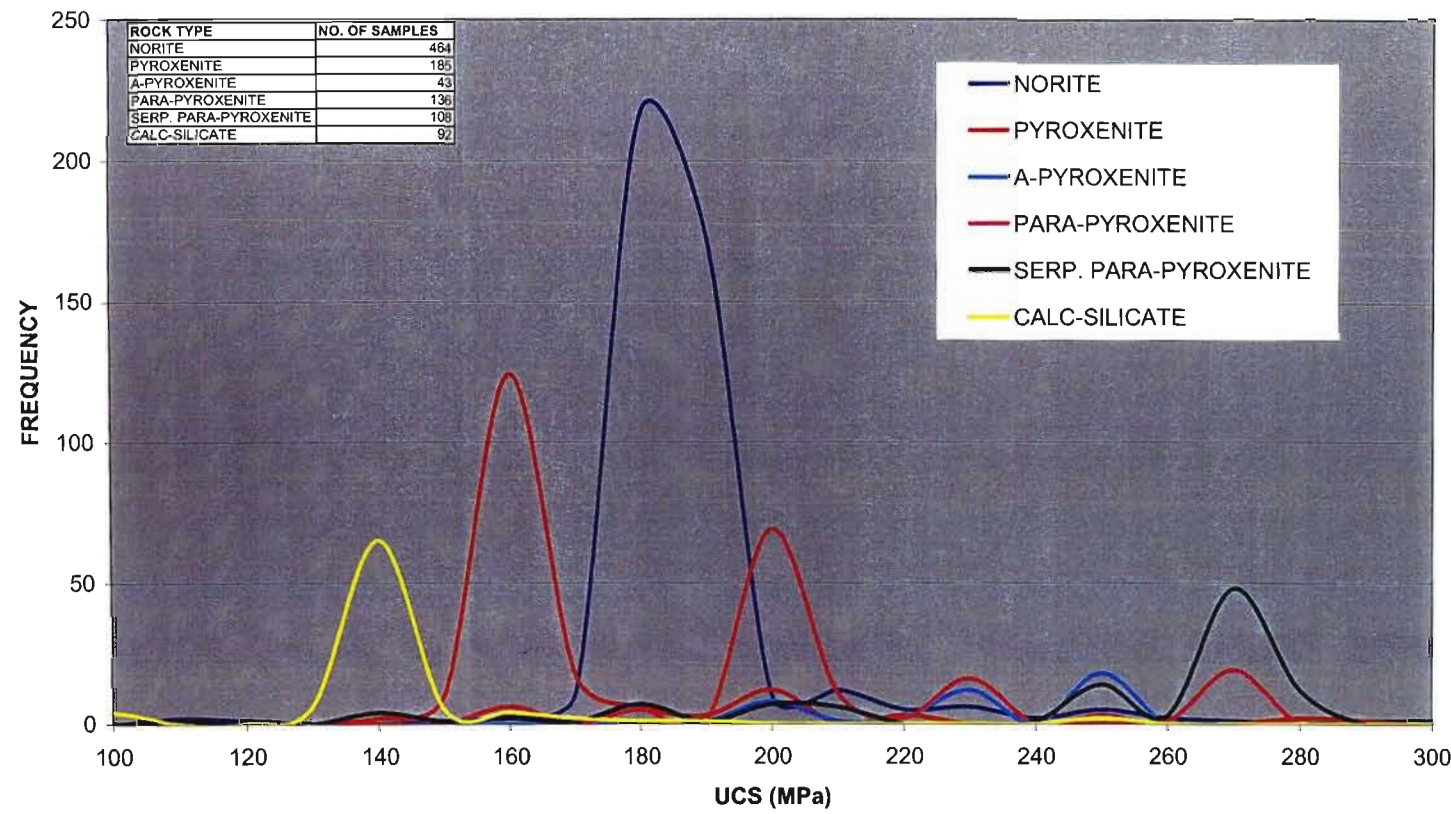


Figure 5.13 UCS histograms for all the rock types occurring in the pit.

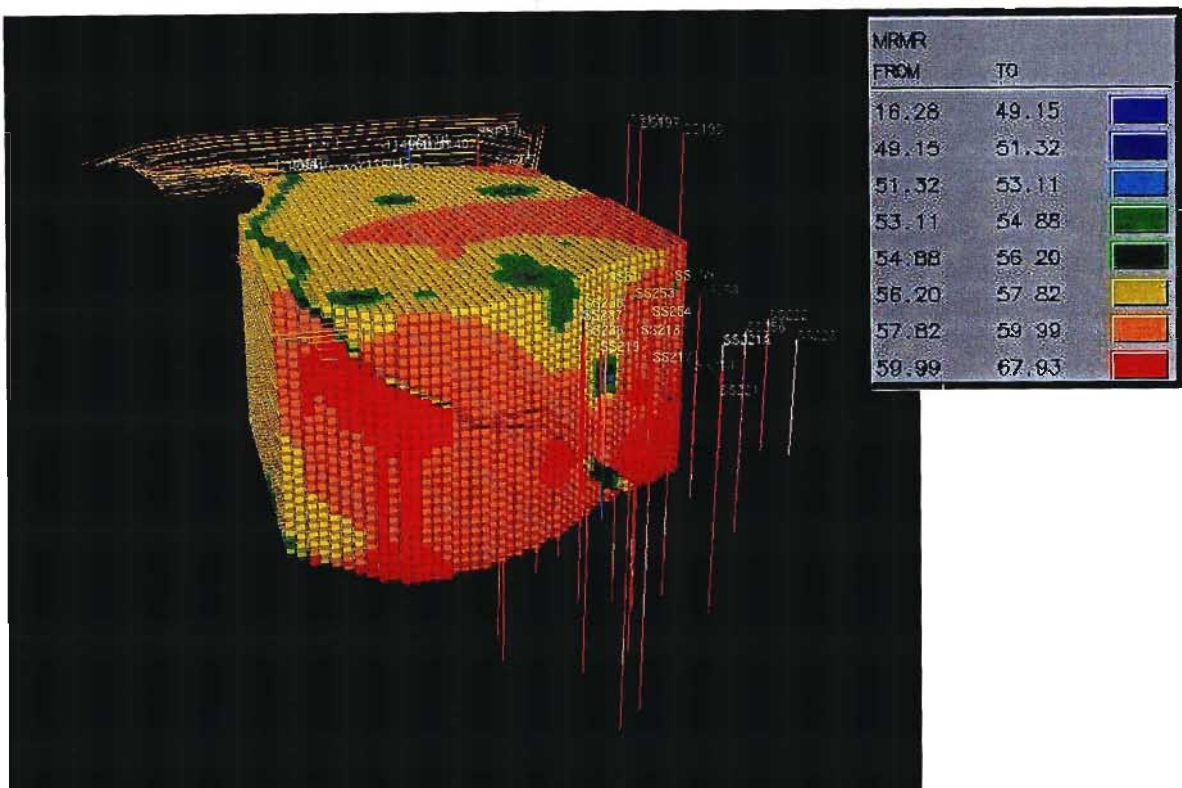


Figure 5.14 Datamine® visualisation of final interpolated block model with boreholes.

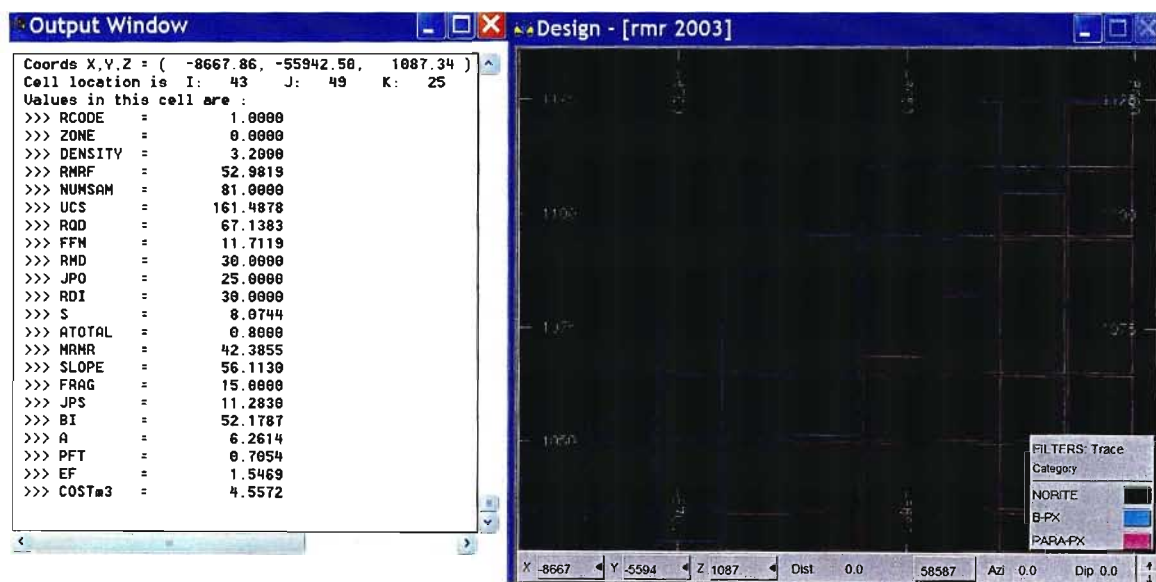


Figure 5.15 Datamine® screen illustrating the resultant model cell data from a query process.

5.5 Summary and Conclusions

Chapter 5 details the development of the 3D geotechnical model. The initial sections discuss the ore reserve modelling processes and their applicability to a geotechnical model. A history of geostatistics and geotechnical engineering is presented as well as examples of the application and potential benefits outside the mining environment.

The model development sequence is discussed and covers the importation of the geotechnical data through to the block model constraints and finally the interpolation process. The interpolation process was preceded by a geostatistical analysis and testing of the model to verify the most appropriate interpolation method.

Geostatistics deals with spatial data, i.e. data for which each value is associated with a location in space. In such analysis it is assumed that there is some connection between location and data value. From known values at sampled points, geostatistical analysis can be used to predict spatial distributions of properties over large areas or volumes.

Due to the bell curve nature of the data sets, the data being evenly spaced and the relatively limited data set, the inverse power distance (squared) interpolation method was used. As the database expands, future processing may require more advanced methods such as kriging.

The geotechnical model provides information well ahead of the mining face, which can then be used for rock quality prediction, production optimisation, slope evaluation and design, as well as planning and costing. Given the levels of financial and other resources devoted to field investigations and data collection, which already capture the inherent spatial variability of soil and rock masses, geotechnical engineering is well served by adopting geostatistics and the development of geotechnical models.

A geotechnical model was developed, representing the rock mass conditions in three dimensions. The majority of the mining process is dependant on the rock mass conditions and design is normally based on an average estimation of the *in-situ* conditions i.e. blast powder factors. There is considerable benefit to be derived by refining these mine designs, based on site-specific rock mass information, available well ahead of the mining face. Before these designs can be refined it is necessary to accurately define the mine design requirements. The next chapter is dedicated to a detailed study on the definition of the blasting departments customer requirements. As blasting is the first step in the mineral beneficiation process or waste

handling it will impact on the subsequent departments or customers. The primary customers defined for this research were the load and haul department and the processing plant, both of which are sensitive to the blast fragmentation delivered.

6 DEFINITION OF CUSTOMER RELATIONSHIPS AND TARGETS

6.1 Introduction

Chapter 5 details the development of the geotechnical model, which provides a complete set of geotechnical parameters contained within an orientated 3D block model. In order to maximise the benefit of this model the optimal design targets for the mine required definition. Chapter 6 examines the relationships between the drill and blast department and the downstream customers, namely the load and haul department and the processing plant. Through analysis of significant data sets, design targets were defined for these customers and subsequently the model was configured to achieve these targets.

An important aspect often neglected in mining operations is the clear definition of the customer relationships within and between the mining and processing operations. Following on the definition of these relationships is the setting of targets that derive the greatest economic benefit for the company as whole rather than isolated cost centres within the departments. Drilling and blasting, however, plays a more important role than just enabling efficient loading. It is the first step in an integrated comminution process leading from solid ore to a marketable product.

The drill and blast department has two primary customers and rather than viewing the department as an isolated cost centre and focussing on minimising drill and blast costs, the study focussed on the fragmentation requirements of the processing plant and the load and haul business areas. It is well understood that chemical energy is the cheapest form of comminution and that major down stream benefits can be derived by increasing drill and blast expenditure (Djordjevic, 1998). In order to evaluate the customers' optimum requirements, two areas of productivity were measured for both waste and ore. These were defined as the instantaneous loading rates and the mean fragmentation (P_{50}) of the blasted muckpile.

Fragmentation

The first measure used to define the customer targets was mean fragment size (P_{50}). The P_{50} value is the sieve size that 50% of the fragmented material will pass through. This is of primary concern to the processing plant whose efficiency is dictated by the fragmentation received by its comminution circuit.

An extensive digital fragmentation study was conducted to define the fragmentation feed from the pit to the plant. Eighteen blasted muckpiles were analysed to determine the fragmentation profiles for both ore and waste. The blasts were analysed over a two-year period and were undertaken over a range of powder factors and hole diameters to ensure the results were representative. Based on the digital fragmentation analysis, a mean fragmentation of 230 mm was set for waste and 150 mm for ore. These fragmentation targets were also equated to the instantaneous loading rates of the shovels. Additionally, the plant design and comminution requirements were assessed during the research, and the fragmentation requirements were evaluated to determine the impact of the mill feed fragmentation on plant performance.

Instantaneous Loading Rate

The second measure used to define the customer requirements was instantaneous loading rate (ILR) and this measure relates to the load and haul customer. Recorded in tonnes per hour, it is a measure of the ease with which a shovel digs the blasted muckpile. This loading rate takes into account only the time the shovels bucket spends in the muckpile and excludes all other operational delays. The Modular Mining Truck/Shovel Dispatch® system is used to continuously measure the instantaneous loading rate.

The ILR study was undertaken in three ways. Firstly, the average monthly loading rate from July 1999 to December 2001 was assessed. Secondly, the average instantaneous loading rate for every mining shift (1,069 shifts) during 2001 was measured and thirdly 238 blasts were analysed to determine the relationship between blast powder factor and the ILR for both waste and ore.

Over the 5 years of research, the process followed in order to define the customers' optimum fragmentation requirements and subsequently design for them based on geotechnical information, was as follows:

- Initially, geotechnical information for the optimisation of blast designs was provided manually, using draughted plans.
- The results of these adjustments were recorded in order to define and benchmark the performance standards, which are recorded in this chapter.
- These performance standards were then defined as the customer targets and subsequently built into the fragmentation model. Chapter 7 describes the development of the

fragmentation model that enabled dynamic blast design and planning well ahead of the mining face, thereby ensuring the customer targets were consistently achieved.

- The application of the fragmentation model to blast design from January 2002 to June 2003 and the resultant improvements are discussed in Chapter 8.

6.2 Processing Plant

The processing plant at Sandsloot concentrates the 4 grams per tonne (g/t) ore received from the open pit to about 100 g/t. The smelting and refining of the platinum is not undertaken on site. The original processing plant commissioned at PPL in 1992 consisted of two 100,000 tonne per month (t/m) mill-float modules. The modules shared a common ore handling, concentrate handling and tailings disposal facility and the process incorporated a sequence of primary, secondary and tertiary milling operations. The process was designed with autogenous primary milling at a capacity of 145 t/hr.

During commissioning at PPL it was determined that the primary crusher product size distribution contained approximately 70% +100 mm material and the percentage of fines was well below the anticipated level. It also became evident during commissioning that the throughput was constrained to approximately 90 t/hr, compared to a target of 145 t/hr, due to the variances in ore mineralogy and fragmentation feed. The primary autogenous mills were originally designed to treat material with a size range of 70% -100 mm and a top size of 200 mm. A significant build-up of pebbles (critical size 25 mm - 125 mm) resulted in a progressive reduction in mill feed rate. This was as a result of unexpected hard ore and a coarser crusher feed. Figure 6.1 illustrates the current ore material flow process from the open pit to the primary mills.

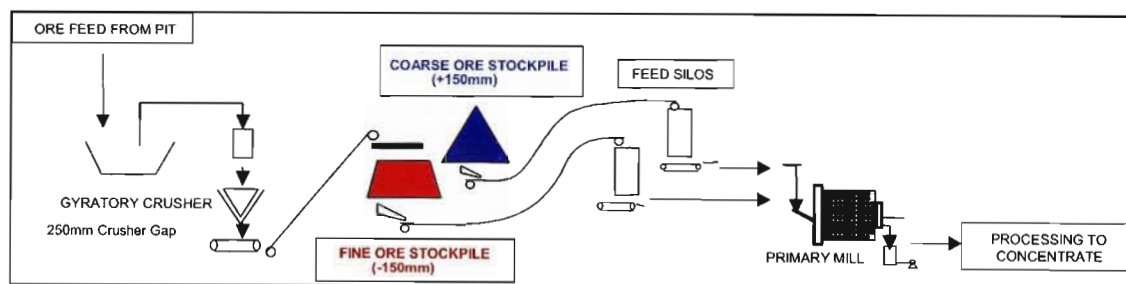


Figure 6.1 Diagram illustrating the ore material low from the pit to the plant.

The original test work conducted on the Sandsloot ore body during the early 1990's indicated its suitability for autogenous milling. The test work, however, was restricted to the pyroxenite ore types, which were perceived to be the primary ore feed. Later, it became apparent that the platinum mineralisation extended beyond the pyroxenite ore types and a significant proportion of the ore feed would come from significantly harder hybrid rock types. The main ore types prevailing in Sandsloot open pit can be summarized as follows:

- **Pyroxenite**

Main minerals: Pyroxene (Mg, Fe) SiO_3 , Feldspar (Ca, Al_2 , Si_3O_8)

Ore Minerals: Sulphides of Cu, Ni, Fe with associated PGMs

- **Hybrid rock types (*Parapyroxenite, Serpentinised Parapyroxenite and Calc-silicate*)**

These hybrid rock types were formed where molten pyroxenite magma had come in contact with the Malmani dolomite footwall and the consequent “flux” of $\text{CaCO}_3 + \text{MgCO}_3 + \text{H}_2\text{O}$ resulted in the main minerals changing to:

Diopside (Ca, Mg) SiO_3 , Garnets $(\text{Ca}_3\text{Al}_2(\text{SiO}_4)_3 / \text{Ca}_3\text{Fe}_2(\text{SiO}_4)_3)$

Serpentine $\text{Mg}_2(\text{Si}_2\text{O}_5)(\text{OH})_4$, Tremolite $\text{Ca}_2\text{Mg}_5\text{Si}_8\text{O}_{22}(\text{OH})_2$

and an ore mineral redistribution to silicate-associated modes.

The two most common alteration minerals that effect mill throughput are diopside and garnet, which are mainly associated with the parapyroxenite, serpentinite and calc-silicate rock types. The analysis of metallurgical plant performance has strongly indicated that changes in the type of ore received from the pit influences the concentrator performance, principally in terms of grindability (mill throughput) and flotation efficiency.

Autogenous mills require a coarse feed (grinding media of +125 mm) and a fine feed (milling media of -25 mm) for optimum performance. The fragmentation content between -125 mm and +25 mm is defined as the critical size, which does not break down in the mill and is discharged as pebbles, which have to be mechanically crushed. Prior to the plant expansion in 1998, the ore feed to the processing plant was via a single stockpile (A-frame), which contained all the post primary crusher material (-250 mm). The plant was therefore entirely dependant on the fragmentation profile delivered from the open pit. Figure 6.2 illustrates the sensitivity of the mill throughput to the fragmentation feed received from the stockpiles.

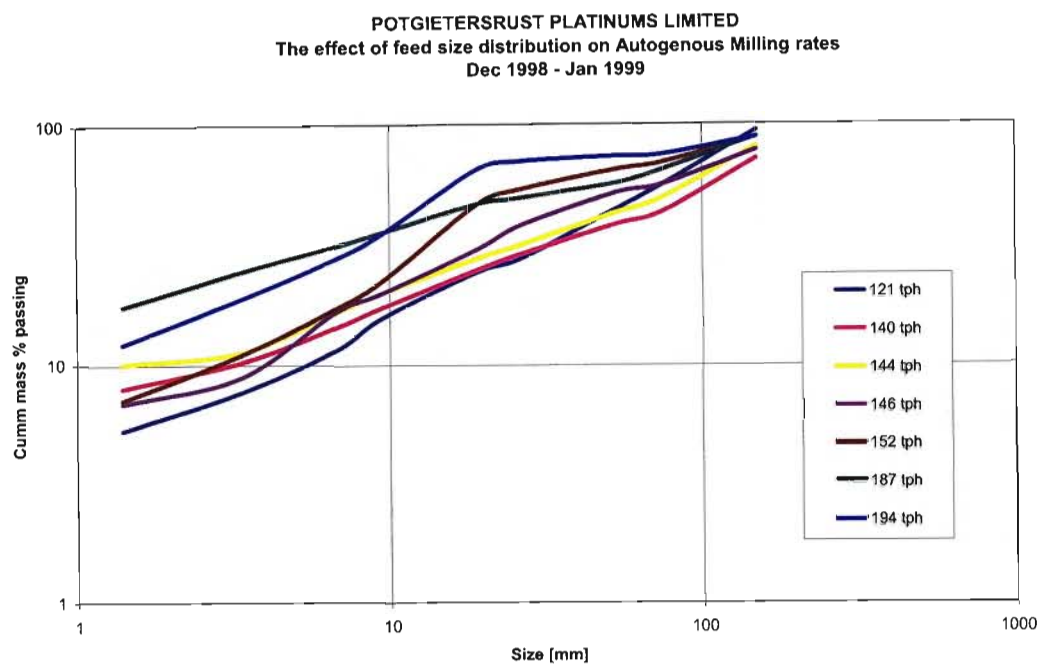


Figure 6.2 The impact the mill feed gradings have on the Autogenous Grind mill production.

Processing Plant Expansion

During 1998, a C-Section (ball mills) was added to increase plant capacity to 425,000 t/m. To achieve and maintain the required throughput, after additions and enhancements, the required autogenous milling rates were calculated to be 194 t/h. The expansion process allowed for all pebbles arising from the primary autogenous mills to be treated in a separate facility. Crushed pebbles would therefore not be returned to the primary milling circuit, allowing the current circuit to continue operating at 270,000 t/m with the balance treated through the additional circuit. This facility was a dedicated milling and flotation section with primary and secondary ball milling. As illustrated in Figure 6.2, a mill feed shift from 78% to 88% -150 mm material would be required in order to increase the milling rates from 146 t/hr to 194 t/hr. The 425,000 t/m plant made provision for a coarse (+ 150 mm) conical stockpile with the finer (-150 mm) fraction diverted to the original A-Frame stockpile (Figure 6.3). A variable blend of “coarse” and “fine” ore could therefore be fed to the primary autogenous mills, in an attempt to provide the optimum size distribution amenable to autogenous milling i.e. maximise throughput. The use of an Expert System for process control also improved stability around the mills and thus increased throughput.

Table 6.1 Adjustments made to ore blast designs during 1997 and 1998.

Date	Powder factor	Burden	Spacing	Hole diameter	Cost / tonne	Kuz-Ram predicted (% -250 mm)
Up to Feb 1997	0.98 kg/m ³	6.5 m	7.5 m	251 mm	R 0.68	69%
Feb 1997	1.15 kg/m ³	6.0 m	6.9 m	251 mm	R 0.80	73%
Oct 1997	1.37 kg/m ³	5.5 m	6.3 m	251 mm	R 0.95	78%
Jan-Feb 1998	1.58 kg/m ³	5.2 m	6.0 m	251 mm	R 1.10	81%
Mar 1998	1.57 kg/m ³	5.0 m	5.8 m	251 mm	R 1.24	86%
Jan 2000 - Dec 2001	1.83 kg/m ³	5.0 m	5.8 m	271 mm	R 1.37	89%

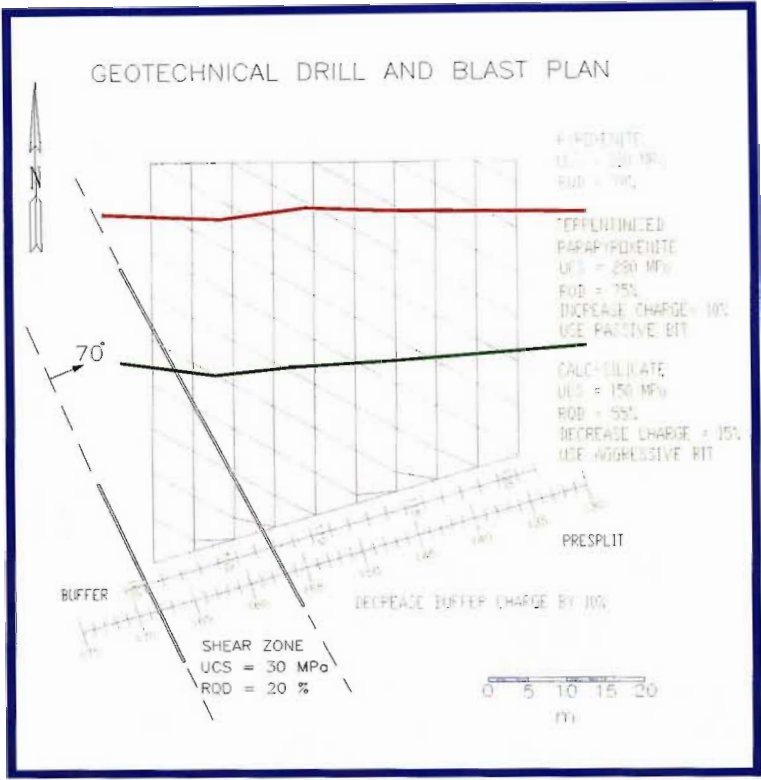


Figure 6.4 An example of a drill and blast plan illustrating the geotechnical information provided manually for the drill and blast department between 1998 and 2001.

The powder factors applied to the ore blasts may seem excessive but this is due to the fragmentation requirements of the autogenous milling system at PPL. Bye (2000) discusses in

detail the substantial financial benefits that have been derived at PPL by harnessing chemical energy in the pit to increase the throughput in the plant.

The adjustment of blast powder factors and later the construction of separate fragmentation stockpiles, which allowed the plant to control the AG mill fragmentation profile, greatly assisted in increasing the milling rates. Figure 6.5 illustrates that an average of 156 t/hr was achieved for the year 2001. It is, however, evident from the graph in Figure 6.5 that there was still a great deal of fluctuation in the AG mill performance and that the plant was still very sensitive to the crusher feed received from the pit.

After the fragmentation feed from the pit had been improved from 1997 to 2001 (Table 6.1), a detailed fragmentation study was undertaken in order to define the actual ore and waste fragmentation profiles delivered to the processing plant and the load and haul fleet. This is discussed in the following section.

The manual method of providing geotechnical information for blast design was both onerous and could not be undertaken well in advance of the mining face. The development of the 3D geotechnical model would therefore easily provide comprehensive information that allows blast designs to be adjusted proactively, thereby ensuring a more consistent mill feed. This is discussed in Chapter 8.

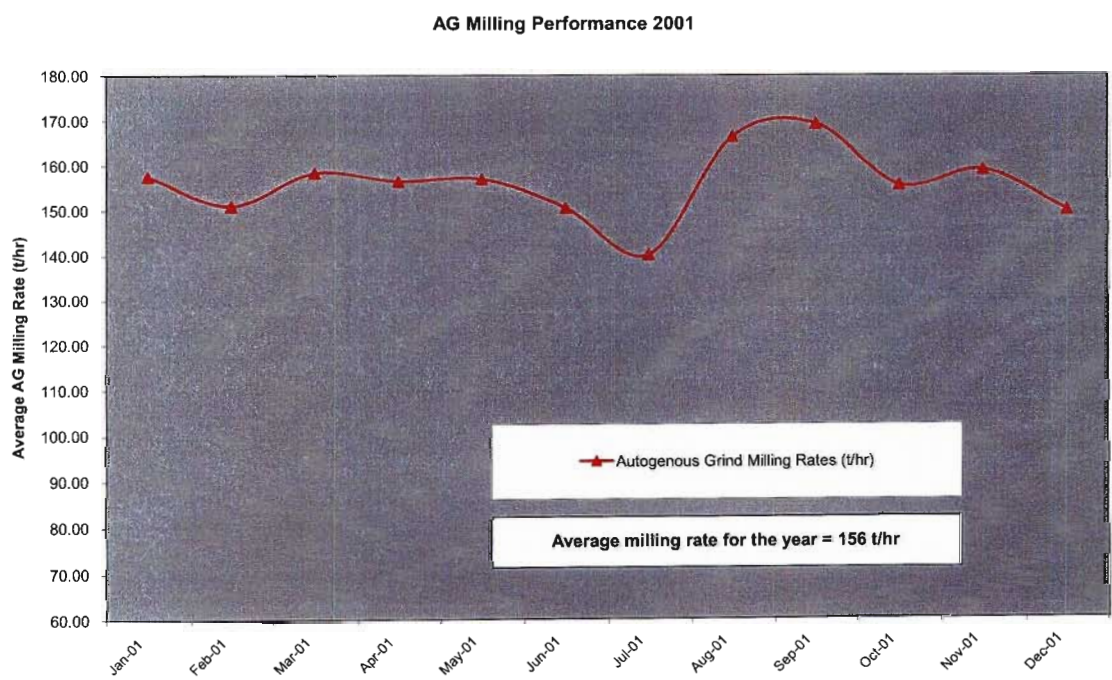


Figure 6.5 Autogenous grind milling performance for 2001.

6.2.1 Digital Fragmentation Analysis

In order to define and benchmark the optimised fragmentation profiles delivered from the pit, digital fragmentation analysis was undertaken during 2001 and 2002. The results were used to define the customer fragmentation targets so that these parameters could be built into the engineering model, thereby providing dynamic blast design and the assurance of consistent fragmentation requirements.

Photoanalysis systems have become practical and useful tools for measuring the performance of explosives in breaking rock, determining the validity of blast models and examining the efficiency of crushers and grinding circuits (Palangio and Maerz, 1999). Optical digital imaging systems are increasingly being used to characterise fragmentation in the mining, comminution and materials handling industries. Larger representative samples can be taken because of the low cost and ease of data capture. Also, the production process need not be interrupted and the turn around time for the information is very short. In the case of large blasted muckpiles (+300,000 t), as is the case at Sandsloot, bulk screening is too prohibitive and optical methods are the only alternative (Maerz and Zhou, 1999). There is some debate about the accuracy of these systems for the determination of 'fines' i.e. -20 mm material (Schleifer *et al.*, 1999). The system was therefore used to assess the top size and characteristic sizes above +100 mm, for which it is regarded as a reliable tool (Kemeny *et al.*, 1999).

Split® Desktop is an image-processing programme designed to calculate the size distribution of rock fragments by analysing digital greyscale images. Digital greyscale images of the blasted muckpiles are acquired manually, in the field, using a digital camera. The Split® software uses algorithms for fragmentation quantification (Split®, 1999).

Digital Fragmentation Analysis Process

The procedure used to collect the digital fragmentation information, as illustrated in Figure 6.6, involved a series of ten to twenty digital photographs taken from various positions on the muckpile, and at various ranges. The photographs were taken perpendicular to the muckpile and in good, even light so that shadows were avoided. It was ensured that loading of the muckpile had begun so that photographs were taken of the inside of the blast so as to get a representative sample of the muckpile. Two 150 mm diameter plastic balls were used as scale objects in all of the photographs.

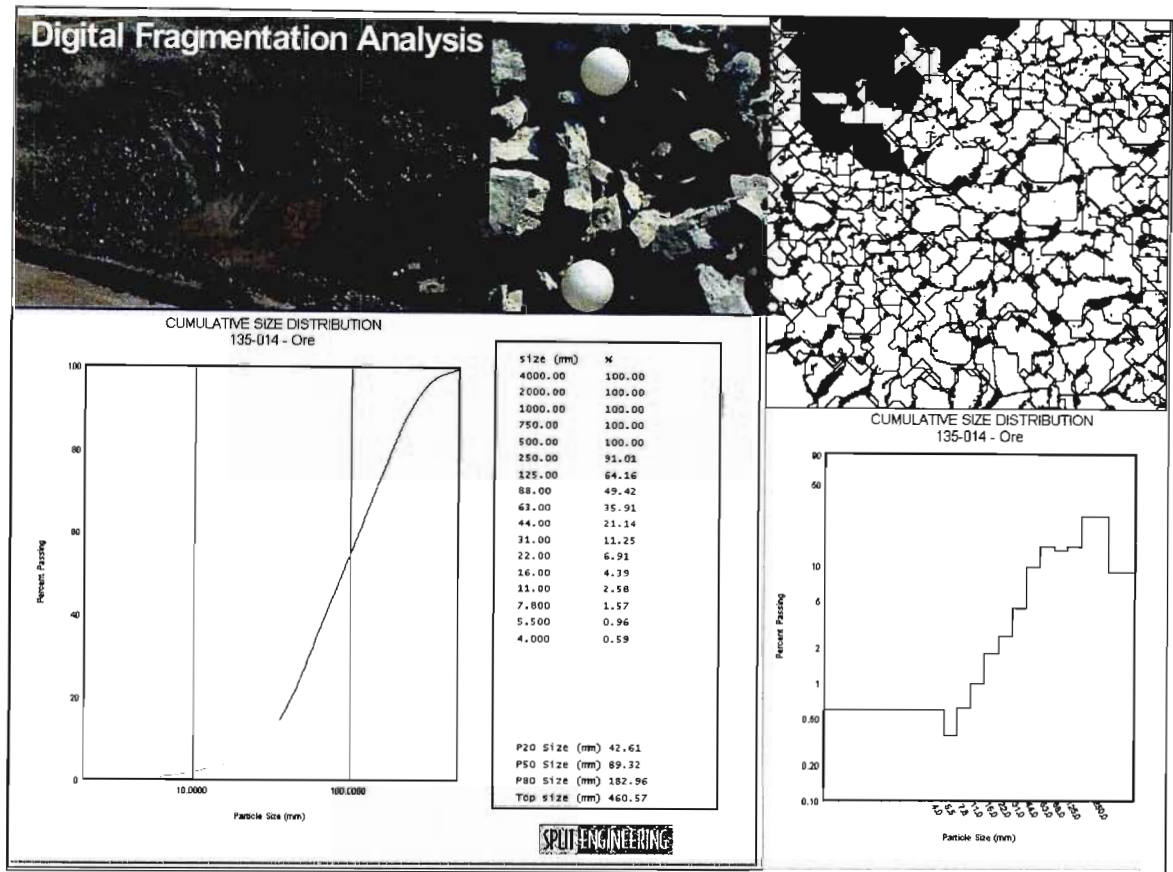


Figure 6.6 Slide illustrating the digital fragmentation analysis process.

The photographs were then imported into the split desktop software as *.JPG or *.TIF files where they were converted to grey scale images. The scale balls were then digitally specified within the photographs for the programme to use as a scaling reference. The Split® algorithm defined the rock fragment boundaries. Some manual editing was required to remove erroneous boundaries and non-rock fragment areas for all the photographs. The final black and white boundary images were then digitally sieved to produce the final fragmentation data, which can be plotted as histograms or cumulative frequency distributions.

Results

Over a four-year period, a mine to mill study was undertaken to determine the potential benefits of blasting a finer ore fragmentation so as to increase the plant throughput, as discussed in the previous section. After optimising the ore blasting, the average fragment size was measured so as to benchmark the results for inclusion into the fragmentation model.

Table 6.2 documents the results of the digital fragmentation analysis study for both ore and waste blasts. Seven waste blasts and eleven ore blasts were analysed from 1998 to 2001. The focus was to assess the broadest range of blasts so as to define an average fragment size, considering various conditions and thereby ensuring the results were representative. The blast powder factor ranged from 1.18 - 2.28 kg/m³ in ore and 0.94 - 1.43 kg/m³ in waste. Ranges of explosive formulations with and without various additives were assessed. Additionally, a range of hole diameters, from 171 mm to 311 mm, were considered. Appendix 5 contains the cumulative frequency distributions of the eighteen analysed blasts.

The focus of the digital analysis was on the 50% passing (P_{50}) and 80% passing (P_{80}) fragment sizes to ensure that the digital method was working in the most reliable ranges. From the fragmentation analysis (Table 6.2) it was determined that the ore blast patterns yielded a mean fragmentation (P_{50}) of 150 mm at a powder factor (Pf) of 1.77 kg/m³. It is important to note that the ore P_{50} of 150 mm also corresponds with the plants stockpile management target of separating +/- 150 mm ore (Figure 6.1). The waste patterns analysed yielded a mean fragmentation (P_{50}) of 230 mm at a Pf of 1.17 kg/m³.

Table 6.2 Summary of the digital fragmentation analysis for ore and waste blasts.

[illegible]

6.3 Load and Haul

Sandsloot open pit is a truck-and-shovel operation, which moves 35 million tonnes of waste and 5 million tonnes of ore per annum. The blasted material is moved with a combination of O&K RH 200 hydraulic shovels and CAT 785 haul trucks (Figure 6.7). Chapter 2 gives a description of the mining conditions at Sandsloot. As with most open pit operations, the productivity of the load and haul equipment is largely dependant on the consistent quality of the muckpile fragmentation.

In order to optimise the complex interactions and allocations of the numerous shovels and trucks, the Modular Mining Dispatch® fleet control system is utilised (Figure 6.8). Dispatch® is a fleet optimisation, reporting and data collection system. The dispatch system uses global positioning satellites (GPS) and field telemetry units on the shovels and trucks to record all position, time and motion interactions continuously.

The primary purpose of drilling and blasting in hard rock mining operations is to fracture solid rock and prepare it for excavation and subsequent transport. The fragmentation must be “fine enough” for the loader, the muckpile must be “loose enough” to facilitate digging, the bottom must not be “too hard” in order to keep the designed level, and there must not be “too many” boulders (Nielsen, 1995).

The success of the blasting can be measured by means of an instantaneous loading rate and this was used to define the requirements of the load and haul customer. Recorded in tonnes per hour, it is a measure of the ease with which a shovel digs the blasted muckpile. This loading rate takes into account only the time the shovels bucket spends in the muckpile and excludes all other operational delays. The Modular Mining Truck/Shovel Dispatch® system is used to continuously measure the instantaneous loading rate.

The ILR study was undertaken in three ways. Firstly, the average monthly loading rate from July 1999 to December 2001 was assessed. Secondly, the average instantaneous loading rate for every mining shift (1,069 shifts) during 2001 was measured and thirdly, 238 blasts were analysed to determine the relationship between blast powder factor and the ILR for both waste and ore (Appendix 6).



Figure 6.7 Photograph illustrating the loading conditions at Sandsloot.

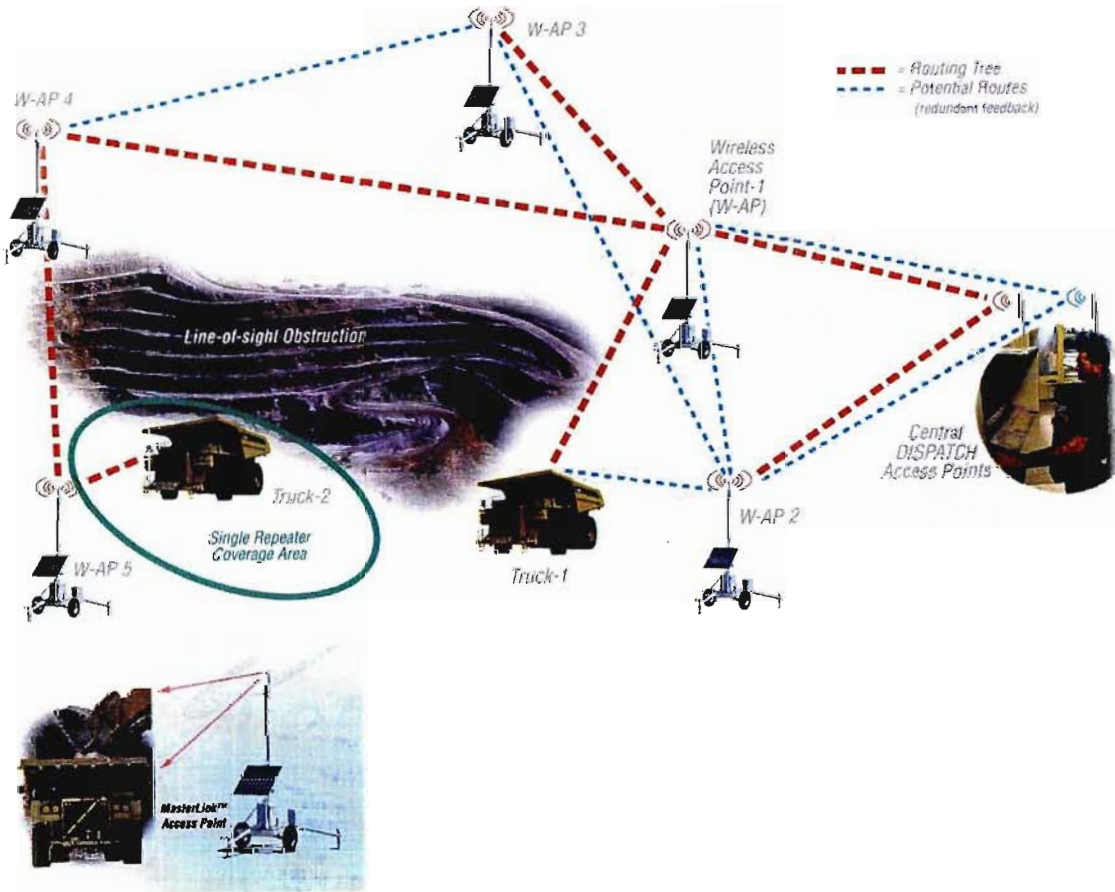


Figure 6.8 Transfer of truck and shovel time and motion information.

6.3.1 Instantaneous Loading Rates

From 1997 to 2001, blast patterns have been adjusted in order to find an economic balance between drill and blast costs and overall mine productivity. Using the Modular Mining Truck Dispatch® System, 238 blasts were assessed as well as 1,069 loading shifts to determine the optimum loading rates for the equipment at Sandsloot. The method used was instantaneous loading rates (ILR), which measures the effective time that the shovel bucket was in the muckpile and is related to tonnes per hour. In other words, it is the ease with which a blasted muckpile can be loaded.

Instantaneous loading rates for Sandsloot can be calculated by measuring the time taken by an O&K RH200 hydraulic shovel to fill a Cat 785B truck (120 t). The time is calculated from the instant that the first bucket of material is dropped into the truck to the time that the truck leaves the shovel and therefore only includes the physical loading time of the shovel. The truck payload is then divided by loading time to give a measure in tonnes per hour (Equation 6.1).

Eq. 6.1
$$\text{ILR} = 3,600 \times \text{Truck payload (120 t)} / \text{Time taken to load the truck (seconds)}$$

Based on a time and motion study of good loading conditions, a RH200 shovel with a bucket containing 40 tonnes will fill an 120 tonne truck in 3 passes, taking 135 seconds. Using Equation 6.1 this equates to a loading rate of 3,200 t/hr ($3,600\text{s} \times 120\text{ t}/135\text{s} = 3,200\text{ t/hr}$). It follows that the finer the fragmentation and the looser the muckpile, the quicker the shovel will fill the truck and the higher the instantaneous loading rate will be.

The trend line in Figure 6.8 illustrates an improvement of 7% in loading rates from 1999 – 2001, which was due to better blast design, based on manually delivered geotechnical information. The average was, however, still below the 3,200 t/hr target and there was great variability in the results. The variability performance is evident from the peaks and troughs illustrated in Figure 6.8. This variability is also evident in Figure 6.9, which illustrates the loading rates per shift achieved over a one-year period. 1,069 loading shifts were assessed and yielded an average loading rate of 3,249 t/hr during 2001.

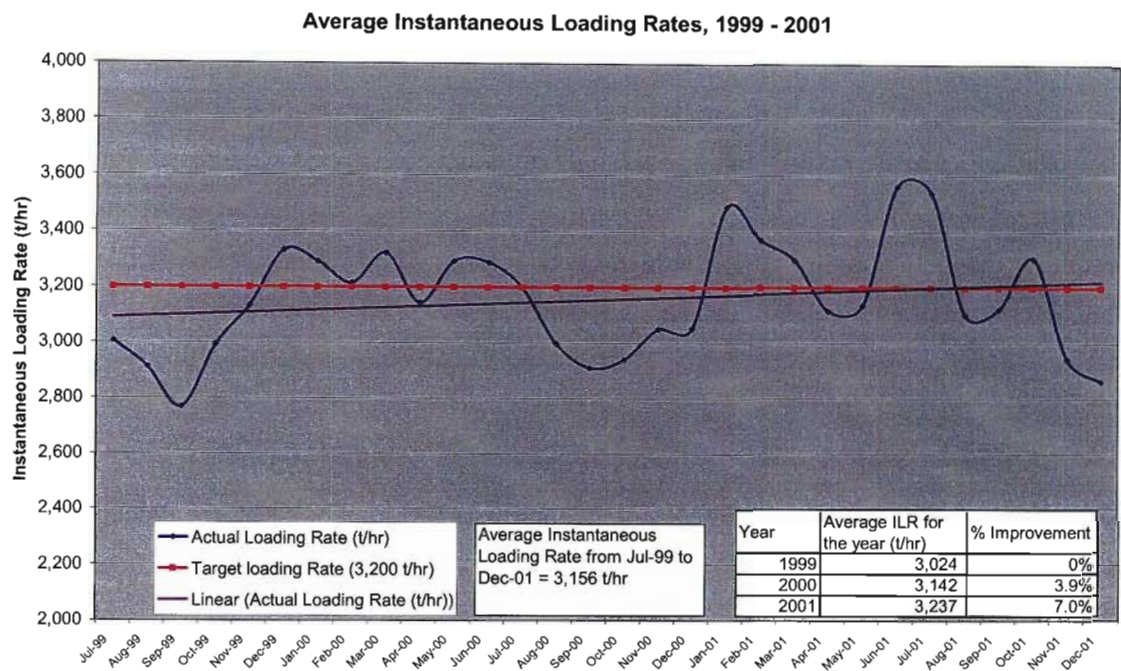


Figure 6.8 Average instantaneous loading rates from 1999 to 2001.

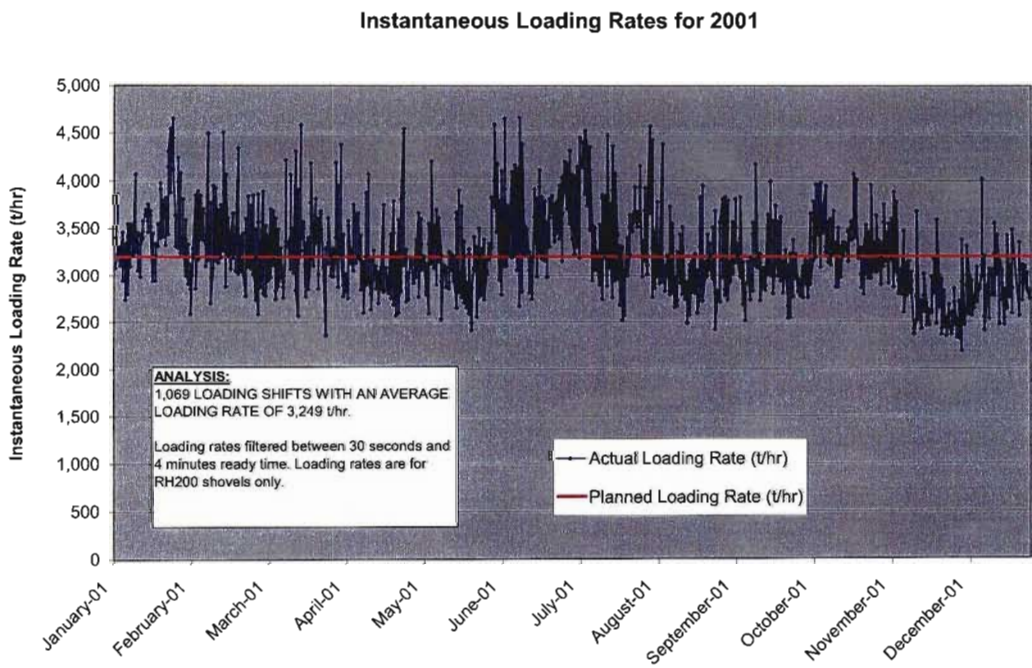


Figure 6.9 Graph of the loading rates per shift achieved over a one year period. 1,069 loading shifts were assessed and yielded an average loading rate of 3,249 t/hr .

Analysis of Individual Blasts

During the period between 1998 and 2001 a blast design optimisation process, based on geotechnical information, had been undertaken. The resultant performance over that period was critical for defining the actual field relationship between blast powder factor and instantaneous loading rates. The resultant data would form the benchmark and design targets for incorporation into the fragmentation model.

Two hundred and thirty eight blasts were analysed in order to define the optimum loading rates for both ore and waste. The summarised results are recorded in Tables 6.3 and 6.4 and the detailed information related to these blasts are recorded in Tables 6.5, 6.6a and 6.6b. For each blast the following information was collected:

- Powder factor (kg/m^3); rock type (ore or waste); explosive formulation; burden (m); spacing (m); bench height (m); drill hole diameter (mm); date first loaded; blast number; average truck loading time (seconds); and instantaneous loading rate (t/hr).

The study revealed that 169 waste blasts at a powder factor of 1.17 kg/m^3 , yielded an average loading rate of 3,182 t/hr. Sixty nine ore blasts yielded an average loading rate of 3,316 t/hr from a powder factor of 1.56 kg/m^3 (Table 6.3).

It was also possible, through the analysis, to determine the most suitable explosive formulation for the rock mass conditions. Table 6.4 illustrates the performance of the various explosive formulations used on the operation. The loading performance was weighted on powder factor i.e. the best loading rates per unit of explosive, then PX03-A achieved the best performance. PX03-A is a bulk emulsion containing 60% ANFO (ammonium nitrate + fuel oil) and 35% emulsion with an additive of 5% Aluminium.

Table 6.3 Comparison of powder factors and loading rates in ore and waste.

Rock Type	Instantaneous Loading Rate (t/hr)	Energy factor (kg/m^3)	No. of Blasts
Waste	3,182	1.17	169
Ore	3,316	1.56	69
			238

Table 6.4 Comparison of explosive formulation performance.

Explosive Formulation *	Instantaneous Loading Rate (t/hr)	Energy factor (kg/m ³)	No. of Blasts	Weighted Performance of Explosive
PX03-A	3,026	1.14	25	1
HEF 206	3,310	1.28	11	2
PX03-T	3,240	1.30	202	3
			238	

* Explosive Formulations	
PX03-A	Bulk emulsion (60% ANFO and 35% Emulsion) + 5% Aluminium
PX03 -T	Bulk emulsion (60% ANFO and 35% Emulsion) + 5% Thermite
HEF 206	Bulk emulsion (60% ANFO and 40% Emulsion)

Nielsen and Kristiansen (1995) suggested that trying to pinpoint an optimal blast design from an economic point of view would be very difficult in actual operations because practical blasting will seldom give consistent results from one blast to the next. This is partially due to varying rock conditions, which always influence results, but more variation is probably caused by implementation of the blast design. Scott (1992) claimed that the most common problem experienced in the field involves the very real differences between blasting operations ‘as designed ‘ and ‘as built’. Implementation variances can be practically corrected, as is the case at Sandsloot, by using common quality assurance methods and techniques as discussed by Nielsen (1993).

The full data set relating to this study is presented in Tables 6.5, 6.6a and 6.6b. It may seem more appropriate to include this information in an appendix, however, the tables are presented in this chapter so that the reader can see the extent of the study required to obtain representative values for design. The tables illustrate the variability in loading rates from one blast to another, which is a function of variable geology and to some extent the operational conditions. The extent of the study therefore takes into account the operational variances as discussed by Scott (1992). Based on this significant data set, which is considered representative of the conditions at Sandsloot, the instantaneous loading rate targets for ore and waste were set at 3,300 t/hr and 3,200 t/hr respectively.

Table 6.5 Data relating to the 69 ore blasts analysed.

Date First Loaded	Blast Number	Number of Loads from Blast	Average Truck Loading Time (Seconds)	Loading Rate (Tonnes/hr)	Powder Factor (kg/m ³)	Rock Type	Explosive Formulation	Burden (m)	Spacing (m)	Bench Height (m)	Drill Hole Diameter (mm)
01-AUG-01 Day Shift	141/029	347	143.57	3,009	1.50	ore	PX03-A	5.5	6.5	15.0	271.0
01-MAY-01 Night Shift	144/007	1,567	125.91	3,431	1.85	ore	PX03-T	5.0	5.8	15.0	271.0
03-APR-01 Night Shift	144/006	1,167	103.28	4,183	1.85	ore	PX03-T	5.0	5.8	15.0	271.0
03-DEC-00 Afternoon Shift	138/038	406	129.42	3,338	1.35	ore	PX03-T	4.0	4.0	15.0	165.0
03-FEB-00 Afternoon Shift	126/065	1,405	122.34	3,531	1.85	ore	PX03-T	5.0	5.8	15.0	271.0
03-JUL-00 Afternoon Shift	135/012	2,265	135.7	3,183	1.85	ore	PX03-T	5.0	5.8	15.0	271.0
03-MAR-00 Day Shift	126/074	18	165.17	2,615	1.35	ore	PX03-T	4.0	4.0	15.0	165.0
04-AUG-00 Night Shift	135/016	628	137.02	3,153	1.85	ore	HEF206	5.0	5.8	15.0	271.0
05-MAY-00 Afternoon Shift	132/022	4,758	128.15	3,371	1.85	ore	PX03-T	5.0	5.8	15.0	271.0
06-APR-00 Afternoon Shift	129/043	1,055	117.78	3,668	1.35	ore	PX03-T	4.0	4.0	15.0	165.0
06-FEB-01 Afternoon Shift	141/028	1,723	115.9	3,727	1.85	ore	PX03-T	5.0	5.8	15.0	271.0
06-JUN-01 Day Shift	138/019	868	133.3	3,241	1.07	ore	PX03-T	4.5	4.5	15.0	165.0
07-DEC-00 Day Shift	138/040	1,974	138.59	3,117	1.85	ore	PX03-T	5.0	5.8	15.0	271.0
08-FEB-00 Afternoon Shift	126/069	969	117.03	3,691	1.85	ore	PX03-T	5.0	5.8	15.0	271.0
08-JUL-01 Afternoon Shift	141/022	1,126	130.54	3,309	0.80	ore	PX03-T	5.5	6.5	15.0	271.0
08-JUN-01 Afternoon Shift	138/023	395	142.74	3,026	1.07	ore	PX03-T	4.5	4.5	15.0	165.0
08-MAY-00 Afternoon Shift	132/024	960	130.13	3,320	1.85	ore	PX03-T	5.0	5.8	15.0	271.0
09-JAN-01 Afternoon Shift	144/014	1,113	131.98	3,273	1.50	ore	PX03-A	5.5	6.5	15.0	271.0
09-JUN-00 Afternoon Shift	132/035	900	124.26	3,477	1.35	ore	PX03-T	4.0	4.0	15.0	165.0
09-MAR-00 Afternoon Shift	129/028	1,515	129.23	3,343	1.85	ore	PX03-T	5.0	5.8	15.0	271.0
10-MAR-00 Afternoon Shift	129/024	2,009	133.75	3,230	1.85	ore	PX03-T	5.0	5.8	15.0	271.0
10-NOV-00 Afternoon Shift	138/016	3,720	138.35	3,123	1.85	ore	PX03-T	5.0	5.8	15.0	271.0
11-MAR-01 Day Shift	144/003	1,155	108.74	3,973	1.85	ore	PX03-T	5.0	5.8	15.0	271.0
11-NOV-00 Day Shift	138/022	1,137	148.74	2,904	1.35	ore	PX03-T	4.0	4.0	15.0	165.0
11-OCT-00 Afternoon Shift	138/039	4,444	148.04	2,918	1.85	ore	PX03-T	5.0	5.8	15.0	271.0
12-DEC-00 Afternoon Shift	141/014	1,394	138.03	3,130	1.35	ore	PX03-T	4.0	4.0	15.0	165.0
12-FEB-01 Day Shift	141/015	210	116.58	3,708	1.85	ore	PX03-T	5.0	5.8	15.0	271.0
12-SEP-00 Day Shift	135/026	946	161.03	2,683	1.35	ore	PX03-T	4.0	4.0	15.0	165.0
12-SEP-01 Afternoon Shift	108/225	1,025	130.33	3,315	1.08	ore	PX03-A	4.0	4.5	10.0	165.0
13-AUG-01 Day Shift	141/030	607	149.32	2,893	1.04	ore	PX03-A	4.0	5.2	15.0	165.0
13-DEC-00 Day Shift	144/001	752	141.88	3,045	1.35	ore	PX03-T	4.0	4.0	15.0	165.0
13-JAN-00 Night Shift	126/050	1,296	135.38	3,191	2.06	ore	PX03-T	3.0	3.5	15.0	165.0
13-JUN-00 Night Shift	132/029	2,952	136.64	3,162	1.35	ore	PX03-T	4.0	4.0	15.0	165.0
13-JUN-00 Night Shift	132/037	2,791	123.22	3,506	1.85	ore	PX03-T	5.0	5.8	15.0	271.0
14-MAR-00 Afternoon Shift	129/033	1,681	114.69	3,767	1.85	ore	PX03-T	5.0	5.8	15.0	271.0
14-MAY-00 Night Shift	129/045	496	138.76	3,113	1.35	ore	PX03-T	4.0	4.0	15.0	165.0
16-JUN-01 Day Shift	141/019	2,068	136.11	3,174	1.85	ore	PX03-T	5.0	5.8	15.0	271.0
16-MAY-01 Day Shift	138/012	1,341	149.47	2,890	1.07	ore	PX03-T	4.5	4.5	15.0	165.0
16-SEP-01 Day Shift	147/003	1,789	126.57	3,413	1.79	ore	PX03-A & HEF206	5.0	6.0	15.0	271.0
17-JUN-00 Night Shift	132/038	1,602	127.38	3,391	1.35	ore	PX03-T	4.0	4.0	15.0	165.0
17-MAY-00 Afternoon Shift	132/026	1,832	132.67	3,256	1.85	ore	PX03-T	5.0	5.8	15.0	271.0
18-JAN-01 Afternoon Shift	141/010	2,362	113.31	3,813	1.85	ore	PX03-T	5.0	5.8	15.0	271.0
19-AUG-00 Night Shift	135/020	1,380	154.87	2,789	1.85	ore	PX03-T	5.0	5.8	15.0	271.0
19-JUL-00 Day Shift	135/014	2,769	126.67	3,410	1.85	ore	PX03-T	5.0	5.8	15.0	271.0
19-MAR-01 Afternoon Shift	144/005	1,645	100.27	4,308	1.85	ore	PX03-T	5.0	5.8	15.0	271.0
20-JUL-00 Afternoon Shift	135/022	957	145.06	2,978	1.35	ore	PX03-T	4.0	4.0	15.0	165.0
21-AUG-00 Night Shift	135/023	1,888	135.27	3,194	1.35	ore	PX03-T	4.0	4.0	15.0	165.0
21-DEC-00 Night Shift	141/009	3,557	128.18	3,370	1.85	ore	HEF206	5.0	5.8	15.0	271.0
21-FEB-01 Afternoon Shift	141/021	834	135.92	3,178	1.35	ore	PX03-T	4.0	4.0	15.0	165.0
21-JUL-01 Afternoon Shift	144/011	965	141.04	3,063	1.50	ore	PX03-T	5.5	6.5	15.0	271.0
22-SEP-00 Afternoon Shift	135/040	702	159.62	2,706	1.35	ore	PX03-T	4.0	4.0	15.0	165.0
23-AUG-01 Day Shift	147/002	1,463	121.57	3,554	1.50	ore	PX03-A	5.5	6.5	15.0	271.0
23-FEB-01 Afternoon Shift	141/016	1,168	114.23	3,782	1.35	ore	PX03-T	4.0	4.0	15.0	165.0
23-MAY-01 Day Shift	138/018	802	144.33	2,993	1.07	ore	PX03-T	4.5	4.5	15.0	165.0
24-MAR-00 Night Shift	129/036	4,221	129.55	3,335	1.85	ore	PX03-T	5.0	5.8	15.0	271.0
24-NOV-00 Afternoon Shift	138/024	1,361	131.05	3,296	1.35	ore	PX03-T	4.0	4.0	15.0	165.0
25-JAN-00 Night Shift	128/062	1,234	124.37	3,474	1.85	ore	PX03-T	5.0	5.8	15.0	271.0
25-JUL-01 Night Shift	106/152	1,830	93.83	4,604	0.96	ore	PX03-T	4.5	4.5	10.0	165.0
25-MAR-00 Afternoon Shift	129/034	1,981	126	3,429	1.35	ore	PX03-T	4.0	4.0	15.0	165.0
26-JUL-01 Afternoon Shift	144/012	1,210	125.02	3,455	1.50	ore	PX03-T	5.5	6.5	15.0	271.0
26-JUN-01 Afternoon Shift	144/009	1,725	116.32	3,714	1.50	ore	HEF206	5.5	6.5	15.0	271.0
26-MAR-01 Afternoon Shift	144/004	1,302	112.3	3,847	1.85	ore	PX03-T	5.0	5.8	15.0	271.0
26-MAY-00 Afternoon Shift	132/027	3,250	127.23	3,395	1.85	ore	PX03-T	5.0	5.8	15.0	271.0
27-MAY-00 Afternoon Shift	132/036	1,004	125.77	3,435	1.35	ore	PX03-T	4.0	4.0	15.0	165.0
27-SEP-00 Afternoon Shift	135/032	1,094	164.71	2,623	1.35	ore	PX03-T	4.0	4.0	15.0	165.0
27-SEP-01 Night Shift	135/005	501	149.4	2,892	1.71	ore	PX03-T	5.0	5.8	15.0	250.0
29-FEB-00 Night Shift	126/073	745	146.35	2,952	1.35	ore	PX03-T	4.0	4.0	15.0	165.0
30-AUG-00 Afternoon Shift	135/024	1,593	155.35	2,781	1.35	ore	PX03-T	4.0	4.0	15.0	165.0
31-JAN-01 Night Shift	141/013	1,218	119.3	3,621	1.85	ore	PX03-T	5.0	5.8	15.0	271.0
AVERAGE				3,310	1.58						

Explosive Formulations

PX03-A	Bulk emulsion (60% ANFO and 40% Emulsion) + 5% Aluminium
PX03 - T	Bulk emulsion (60% ANFO and 40% Emulsion) + 5% Thermit
HEF 206	Bulk Emulsion (60% ANFO & 40% Emulsion)
HEF 100	100% Emulsion

Table 6.6a Data relating to the 169 waste blasts analysed.

Date First Loaded	Blast Number	Number of Loads from Blast	Average Truck Loading Time (Seconds)	Loading Rate (Tonnes/hr)	Powder Factor (kg/m3)	Rock Type	Explosive Formulation	Burden (m)	Spacing (m)	Bench Height (m)	Drill Hole Diameter (mm)
01-APR-01 Afternoon Shift	108/208	1 223	153.64	2.812	1.22	waste	PX03-T	4.0	4.0	10.0	165.0
01-APR-01 Night Shift	108/214	1	121	3.570	1.22	waste	PX03-T	4.0	4.0	10.0	165.0
01-JAN-00 Afternoon Shift	123/046	625	140.43	3.076	1.35	waste	PX03-T	4.0	4.0	15.0	165.0
01-JAN-00 Afternoon Shift	126/056	1 886	129.43	3.338	1.00	waste	PX03-T	6.5	7.5	15.0	271.0
01-MAR-01 Afternoon Shift	141/025	547	131.27	3.291	1.35	waste	PX03-T	4.0	4.0	15.0	165.0
01-SEP-00 Afternoon Shift	135/030	653	134.26	3.218	1.35	waste	PX03-T	4.0	4.0	15.0	165.0
01-SEP-01 Day Shift	144/016	936	135.32	3.192	1.00	waste	PX03-A	6.5	7.5	15.0	271.0
01-SEP-01 Night Shift	110/154	1 324	135.69	3.184	1.08	waste	PX03-A	4.0	4.5	10.0	165.0
02-APR-01 Afternoon Shift	110/155	1 020	150.55	2.869	1.22	waste	PX03-T	4.0	4.0	10.0	165.0
02-APR-01 Day Shift	110/152	974	162.1	2.665	1.22	waste	PX03-T	4.0	4.0	10.0	165.0
02-AUG-00 Afternoon Shift	135/019	679	121.77	3.548	1.35	waste	PX03-T	4.0	4.0	15.0	165.0
02-FEB-01 Day Shift	108/205	643	127.34	3.392	1.22	waste	PX03-T	4.0	4.0	10.0	165.0
02-JUL-00 Night Shift	135/011	2 608	135.05	3.199	0.87	waste	PX03-T	7.0	8.0	15.0	271.0
02-JUL-01 Night Shift	108/212	3 403	137.33	3.146	1.22	waste	PX03-T	4.0	4.0	10.0	165.0
02-MAR-01 Day Shift	108/206	703	130.79	3.303	1.22	waste	PX03-T	4.0	4.0	10.0	165.0
02-NOV-00 Afternoon Shift	106/138	845	162.17	2.664	1.37	waste	PX03-T	3.0	3.0	10.0	127.0
03-AUG-00 Night Shift	110/142	615	119.02	3.630	1.08	waste	PX03-A	4.0	4.5	10.0	165.0
03-DEC-00 Afternoon Shift	106/139	726	160.47	2.692	1.37	waste	PX03-T	3.0	3.0	10.0	127.0
03-JAN-00 Afternoon Shift	126/058	1 190	122.94	3.514	1.35	waste	PX03-T	4.0	4.0	15.0	165.0
03-SEP-01 Afternoon Shift	112/118	1 023	144.13	2.997	1.08	waste	PX03-A	4.0	4.5	10.0	165.0
04-AUG-00 Night Shift	135/015	1 137	146.09	2.957	0.87	waste	HEF206	7.0	8.0	15.0	271.0
04-AUG-01 Day Shift	144/013	598	154.99	2.787	1.04	waste	PX03-A	4.0	5.2	15.0	165.0
04-FEB-01 Day Shift	108/200	1 771	129.27	3.342	1.22	waste	PX03-T	4.0	4.0	10.0	165.0
04-FEB-01 Day Shift	141/024	352	131.93	3.274	1.00	waste	PX03-T	6.5	7.5	15.0	271.0
04-JUL-00 Night Shift	132/041	3 205	142	3.042	0.87	waste	PX03-T	7.0	8.0	15.0	271.0
04-MAR-01 Afternoon Shift	108/207	1 108	143.99	3.000	1.22	waste	PX03-T	4.0	4.0	10.0	165.0
04-MAY-00 Afternoon Shift	129/047	1 938	139.2	3.103	1.35	waste	PX03-T	4.0	4.0	15.0	165.0
04-MAY-01 Night Shift	110/137	795	157.33	2.746	1.22	waste	PX03-T	4.0	4.0	10.0	165.0
04-MAY-01 Night Shift	138/006	615	120.04	3.599	1.35	waste	PX03-T	4.0	4.0	15.0	165.0
04-OCT-00 Afternoon Shift	138/020	2 396	157.27	2.747	1.00	waste	PX03-T	6.5	7.5	15.0	271.0
05-AUG-01 Night Shift	110/141	1 145	133.2	3.243	1.08	waste	PX03-A	4.0	4.5	10.0	165.0
05-JAN-01 Day Shift	106/144	211	166.53	2.594	1.37	waste	PX03-T	3.0	3.0	10.0	127.0
05-JUL-01 Afternoon Shift	106/151	2 626	95.74	4.512	1.22	waste	PX03-T	4.0	4.0	10.0	165.0
05-JUL-01 Afternoon Shift	108/218	1 522	142.66	3.028	1.22	waste	PX03-T	4.0	4.0	10.0	165.0
05-SEP-00 Afternoon Shift	135/033	1 084	127.31	3.393	1.35	waste	PX03-T	4.0	4.0	15.0	165.0
06-AUG-01 Day Shift	108/221	195	174.79	2.472	1.22	waste	PX03-A	4.0	4.0	10.0	165.0
06-JAN-00 Night Shift	126/057	1 854	125.62	3.439	1.00	waste	PX03-T	6.5	7.5	15.0	271.0
06-JUN-01 Day Shift	112/116	1 459	108.22	3.992	1.22	waste	PX03-T	4.0	4.0	10.0	165.0
07-APR-00 Night Shift	129/035	2 029	157.2	2.748	0.87	waste	PX03-T	7.0	8.0	15.0	271.0
07-MAY-00 Night Shift	132/023	2 034	137.59	3.140	0.87	waste	PX03-T	7.0	8.0	15.0	271.0
07-SEP-01 Afternoon Shift	110/156	1 003	142.73	3.027	1.08	waste	PX03-A	4.0	4.5	10.0	165.0
08-APR-01 Night Shift	110/153	663	147.59	2.927	1.22	waste	PX03-T	4.0	4.0	10.0	165.0
08-AUG-00 Afternoon Shift	135/025	967	154.28	2.800	0.87	waste	PX03-T	7.0	8.0	15.0	271.0
08-AUG-01 Afternoon Shift	108/222	586	153.68	2.811	1.22	waste	PX03-A	4.0	4.0	10.0	165.0
08-DEC-00 Day Shift	106/142	820	154.84	2.790	1.37	waste	PX03-T	3.0	3.0	10.0	127.0
08-FEB-00 Afternoon Shift	126/054	807	134.93	3.202	1.35	waste	PX03-T	4.0	4.0	15.0	165.0
08-FEB-00 Afternoon Shift	126/068	1 607	143.35	3.014	1.35	waste	PX03-T	4.0	4.0	15.0	165.0
08-FEB-00 Night Shift	126/070	1 211	130.32	3.315	1.00	waste	PX03-T	6.5	7.5	15.0	271.0
08-FEB-01 Afternoon Shift	108/201	925	137.5	3.133	1.22	waste	PX03-T	4.0	4.0	10.0	165.0
08-JAN-01 Day Shift	106/143	270	153.34	2.817	1.37	waste	PX03-T	3.0	3.0	10.0	127.0
08-JUN-00 Afternoon Shift	132/033	2 135	141.27	3.058	0.87	waste	PX03-T	7.0	8.0	15.0	271.0
08-JUN-01 Night Shift	144/008	2 057	114.71	3.766	1.00	waste	PX03-T	6.5	7.5	15.0	271.0
09-MAY-01 Afternoon Shift	138/010	1 748	145.28	2.974	1.35	waste	PX03-T	4.0	4.0	15.0	165.0
09-SEP-00 Night Shift	135/042	1 108	143.33	3.014	1.35	waste	PX03-T	4.0	4.0	15.0	165.0
09-SEP-01 Day Shift	108/223	617	156.26	2.765	1.08	waste	PX03-A	4.0	4.5	10.0	165.0
09-FEB-00 Night Shift	126/071	431	149.75	2.895	1.35	waste	PX03-T	4.0	4.0	15.0	165.0
09-FEB-01 Day Shift	106/147	1 265	124.32	3.475	1.22	waste	PX03-T	4.0	4.0	10.0	165.0
09-JAN-01 Afternoon Shift	141/011	1 441	131.72	3.280	1.00	waste	PX03-T	6.5	7.5	15.0	271.0
09-MAY-01 Night Shift	141/017	931	120.61	3.582	1.35	waste	PX03-T	4.0	4.0	15.0	165.0
10-APR-01 Afternoon Shift	110/151	911	160.51	2.691	1.22	waste	PX03-T	4.0	4.0	10.0	165.0
10-APR-01 Afternoon Shift	135/037	1 262	117.88	3.665	1.00	waste	PX03-T	6.5	7.5	15.0	271.0
10-AUG-01 Afternoon Shift	110/133	1 068	130.06	3.322	1.08	waste	PX03-A	4.0	4.5	10.0	165.0
10-AUG-01 Day Shift	110/144	83	177.12	2.439	1.06	waste	PX03-A	4.0	4.5	10.0	165.0
10-JAN-01 Afternoon Shift	141/008	1 178	118.22	3.654	1.00	waste	PX03-T	6.5	7.5	15.0	271.0
10-MAR-01 Night Shift	132/046	882	136.03	3.176	1.35	waste	PX03-T	4.0	4.0	15.0	165.0
11-APR-01 Day Shift	110/145	1 161	149.38	2.892	1.22	waste	PX03-T	4.0	4.0	10.0	165.0
11-JUL-00 Night Shift	132/042	1 692	131.84	3.277	0.87	waste	PX03-T	7.0	8.0	15.0	271.0
11-OCT-00 Afternoon Shift	135/044	724	149.43	2.891	1.35	waste	PX03-T	4.0	4.0	15.0	165.0
12-DEC-00 Afternoon Shift	132/043	421	167.82	2.737	2.40	waste	PX03-T	3.0	3.0	15.0	165.0
12-JAN-00 Afternoon Shift	126/060	2 971	120.12	3.596	1.00	waste	PX03-T	7.0	8.0	15.0	271.0
13-APR-00 Afternoon Shift	129/039	2 728	133.97	3.225	0.87	waste	PX03-T	7.0	8.0	15.0	271.0
13-APR-00 Night Shift	129/042	237	112.97	3.824	0.87	waste	PX03-T	7.0	8.0	15.0	271.0
13-FEB-01 Day Shift	106/148	870	136.98	3.154	1.22	waste	PX03-T	4.0	4.0	10.0	165.0
13-FEB-01 Night Shift	108/202	1 129	127.76	3.381	1.22	waste	PX03-T	4.0	4.0	10.0	165.0
13-JAN-00 Afternoon Shift	123/045	599	125.55	3.441	1.35	waste	PX03-T	4.0	4.0	15.0	165.0
13-JAN-00 Afternoon Shift	126/059	1 661	146.38	2.951	1.00	waste	PX03-T	6.5	7.5	15.0	271.0
13-JUL-01 Day Shift	112/112	2 963	119.46	3.616	1.08	waste	PX03-T	4.0	4.5	10.0	165.0
13-JUL-01 Day Shift	141/027	788	130.84	3.302	1.00	waste	PX03-T	6.5	7.5	15.0	271.0
13-MAR-01 Afternoon Shift	132/045	1 036	137.52	3.141	1.35	waste	PX03-T	4.0	4.0	15.0	165.0
13-SEP-01 Day Shift	112/121	2 453	138.66	3.093	1.08	waste	HEF206	4.0	4.5	10.0	165.0
14-APR-00 Night Shift	129/041	1 742	130.33	3.315	0.87	waste	PX03-T	7.0	8.0	15.0	271.0

Table 6.6b Data relating to the 169 waste blasts analysed.

Date First Loaded	Blast Number	Number of Loads from Blast	Average Truck Loading Time (Seconds)	Loading Rate (Tonnes/hr)	Powder Factor (kg/m ³)	Rock Type	Explosive Formulation	Burden (m)	Spacing (m)	Bench Height (m)	Drill Hole Diameter (mm)
14-AUG-00 Afternoon Shift	135/041	1,019	154.49	2,796	1.35	waste	PX03-T	4.0	4.0	15.0	165.0
14-JUN-01 Day Shift	141/020	1,562	148.5	2,969	1.00	waste	PX03-T	6.5	7.5	15.0	271.0
14-MAR-00 Night Shift	129/031	2,564	126.66	3,411	0.87	waste	PX03-T	7.0	8.0	15.0	271.0
14-SEP-00 Afternoon Shift	135/043	1,572	153.88	2,807	1.00	waste	PX03-T	6.5	7.5	15.0	271.0
15-FEB-01 Afternoon Shift	144/002	1,119	121.92	3,543	1.85	waste	PX03-T	5.0	5.8	15.0	271.0
16-JAN-01 Night Shift	106/146	1,431	109.17	3,957	1.37	waste	HEF100	3.0	3.0	10.0	127.0
16-JUN-01 Day Shift	112/115	639	137.17	3,149	1.22	waste	PX03-T	4.0	4.0	10.0	165.0
16-MAY-00 Afternoon Shift	132/025	2,219	125.41	3,445	0.87	waste	PX03-T	7.0	8.0	15.0	271.0
16-JAN-01 Day Shift	138/011	1,110	122.47	3,527	1.00	waste	PX03-T	6.5	7.5	15.0	271.0
17-APR-00 Night Shift	129/044	891	124.86	3,460	0.87	waste	PX03-T	7.0	8.0	15.0	271.0
17-AUG-01 Day Shift	141/031	75	155.39	2,780	1.04	waste	PX03-A	4.0	5.2	15.0	165.0
17-FEB-01 Night Shift	106/149	1,146	148.94	2,900	1.22	waste	PX03-T	4.0	4.0	10.0	165.0
17-MAY-01 Afternoon Shift	112/111	2,048	136.1	3,174	1.22	waste	PX03-T	4.0	4.0	10.0	165.0
17-NOV-00 Day Shift	106/140	1,410	148.85	2,902	1.37	waste	PX03-T	3.0	3.0	10.0	127.0
18-AUG-01 Day Shift	110/143	1,061	161.8	2,846	1.08	waste	PX03-A	4.0	4.5	10.0	165.0
18-AUG-01 Day Shift	114/160	746	147.34	2,932	1.08	waste	PX03-A	4.0	4.5	10.0	165.0
18-AUG-01 Day Shift	144/015	791	141.23	3,059	1.20	waste	PX03-A	4.0	4.5	15.0	165.0
18-FEB-00 Night Shift	126/072	801	137.72	3,137	1.35	waste	PX03-T	4.0	4.0	15.0	165.0
18-FEB-00 Night Shift	126/076	1,195	140.55	3,074	1.35	waste	PX03-T	4.0	4.0	15.0	165.0
18-FEB-00 Night Shift	129/027	2,487	128.3	3,367	0.87	waste	PX03-T	7.0	8.0	15.0	271.0
18-JAN-00 Night Shift	126/053	451	103.24	4,184	1.00	waste	PX03-T	6.5	7.5	15.0	271.0
18-JAN-01 Night Shift	106/145	1,159	142.59	3,030	1.37	waste	HEF100	3.0	3.0	10.0	127.0
18-MAR-01 Night Shift	132/047	750	160.26	2,696	1.35	waste	PX03-T	4.0	4.0	15.0	165.0
18-MAY-00 Night Shift	132/032	412	132.86	3,252	0.87	waste	PX03-T	7.0	8.0	15.0	271.0
18-MAY-00 Night Shift	132/034	1,327	134.8	3,205	1.35	waste	PX03-T	4.0	4.0	15.0	165.0
19-APR-01 Afternoon Shift	110/138	687	142.5	3,032	1.22	waste	PX03-T	4.0	4.0	10.0	165.0
19-APR-01 Afternoon Shift	135/038	963	121.99	3,541	1.35	waste	PX03-T	4.0	4.0	15.0	165.0
19-JAN-01 Night Shift	106/150	268	120.14	3,596	1.37	waste	PX03-T	3.0	3.0	10.0	127.0
19-JUL-00 Night Shift	135/013	1,762	139.51	3,097	0.87	waste	PX03-T	7.0	8.0	15.0	271.0
19-JUN-01 Afternoon Shift	110/139	2,738	103.3	4,182	1.22	waste	PX03-T	4.0	4.0	10.0	165.0
19-SEP-00 Night Shift	141/001	2,062	158.52	2,725	1.35	waste	PX03-T	4.0	4.0	15.0	165.0
20-JUN-01 Afternoon Shift	110/140	1,058	107.15	4,032	1.22	waste	PX03-T	4.0	4.0	10.0	165.0
20-MAR-00 Afternoon Shift	138/001	920	149.38	2,892	1.98	waste	PX03-T	5.0	5.0	15.0	250.0
20-OCT-00 Night Shift	138/031	2,150	125.92	3,431	1.00	waste	PX03-T	6.5	7.5	15.0	271.0
20-SEP-01 Afternoon Shift	112/119	1,545	138.19	3,126	1.08	waste	PX03-A & HEF206	4.0	4.5	10.0	165.0
21-FEB-00 Night Shift	129/001	1,430	150.96	2,862	1.35	waste	PX03-T	4.0	4.0	15.0	165.0
21-JAN-00 Night Shift	126/061	700	153.2	2,820	1.35	waste	PX03-T	4.0	4.0	15.0	165.0
21-JUL-00 Afternoon Shift	132/044	1,007	138.6	3,117	1.35	waste	PX03-T	4.0	4.0	15.0	165.0
21-MAR-01 Night Shift	108/215	453	156.78	2,755	1.22	waste	PX03-T	4.0	4.0	10.0	165.0
21-MAY-01 Afternoon Shift	108/210	3	126.33	3,420	1.22	waste	PX03-T	4.0	4.0	10.0	165.0
21-SEP-01 Night Shift	112/120	380	141.97	3,043	1.08	waste	HEF206	4.0	4.5	10.0	165.0
22-DEC-00 Day Shift	138/035	1,350	140.88	3,086	1.35	waste	PX03-T	4.0	4.0	15.0	165.0
22-JAN-01 Night Shift	141/012	1,316	104.74	4,124	1.85	waste	PX03-T	5.0	5.8	15.0	271.0
22-JUN-00 Night Shift	132/031	1,225	161.78	2,846	1.35	waste	PX03-T	4.0	4.0	15.0	165.0
23-AUG-01 Day Shift	110/146	1,121	141.25	3,058	1.08	waste	PX03-A	4.0	4.5	10.0	165.0
23-AUG-01 Day Shift	114/161	762	155.73	2,774	1.08	waste	PX03-A	4.0	4.5	10.0	165.0
23-MAY-01 Afternoon Shift	138/014	856	134.97	3,201	1.00	waste	PX03-T	6.5	7.5	15.0	271.0
24-FEB-01 Afternoon Shift	108/203	999	125.71	3,436	1.22	waste	PX03-T	4.0	4.0	10.0	165.0
24-JAN-00 Night Shift	126/075	146	169.05	2,555	1.00	waste	PX03-T	6.5	7.5	15.0	271.0
24-MAR-01 Afternoon Shift	108/209	1,332	147.71	2,925	1.22	waste	PX03-T	4.0	4.0	10.0	165.0
24-NOV-00 Day Shift	106/141	871	139.34	3,100	1.37	waste	PX03-T	3.0	3.0	10.0	127.0
25-APR-01 Day Shift	138/017	600	123.75	3,491	1.00	waste	PX03-T	6.5	7.5	15.0	271.0
25-AUG-00 Night Shift	135/034	1,571	144.37	2,992	1.00	waste	PX03-T	6.5	7.5	15.0	271.0
25-MAY-00 Night Shift	132/039	1,989	133.89	3,227	1.35	waste	PX03-T	4.0	4.0	15.0	165.0
25-MAY-01 Afternoon Shift	112/114	2,410	124.54	3,469	1.22	waste	PX03-T	4.0	4.0	10.0	165.0
26-APR-01 Afternoon Shift	108/216	2,298	135.77	3,182	1.22	waste	PX03-T	4.0	4.0	10.0	165.0
26-APR-01 Afternoon Shift	108/217	1,955	152.28	2,837	1.22	waste	PX03-T	4.0	4.0	10.0	165.0
26-APR-01 Day Shift	110/149	26	166	2,602	1.22	waste	PX03-T	4.0	4.0	10.0	165.0
26-FEB-00 Afternoon Shift	126/077	1,100	134.06	3,222	1.35	waste	PX03-T	4.0	4.0	15.0	165.0
26-JAN-00 Afternoon Shift	126/052	238	143.38	3,013	1.35	waste	PX03-T	4.0	4.0	15.0	165.0
26-JAN-01 Night Shift	141/023	2,334	126.88	3,405	1.00	waste	PX03-T	6.5	7.5	15.0	271.0
26-JUN-01 Afternoon Shift	141/026	873	143.33	3,014	1.07	waste	HEF206	4.5	4.5	15.0	165.0
26-JUN-01 Afternoon Shift	144/010	1,264	106.07	4,073	1.00	waste	HEF206	6.5	7.5	15.0	271.0
26-OCT-00 Day Shift	138/015	2,309	139.7	3,092	1.00	waste	PX03-T	6.5	7.5	15.0	271.0
27-JAN-00 Night Shift	126/063	1,910	132.75	3,254	1.00	waste	PX03-T	6.5	7.5	15.0	271.0
27-JAN-00 Night Shift	126/066	3,030	143.79	3,004	1.35	waste	PX03-T	4.0	4.0	15.0	165.0
27-JUL-00 Afternoon Shift	135/018	1,199	133.32	3,240	1.35	waste	PX03-T	4.0	4.0	15.0	165.0
27-NOV-00 Afternoon Shift	138/013	1,322	132.53	3,260	1.00	waste	PX03-T	6.5	7.5	15.0	271.0
27-SEP-01 Afternoon Shift	108/226	446	132.28	3,266	1.08	waste	PX03-A & HEF206	4.0	4.5	10.0	165.0
27-SEP-01 Day Shift	112/122	663	143.68	3,007	1.08	waste	HEF206	4.0	4.5	10.0	165.0
28-APR-00 Night Shift	129/046	1,644	136.36	3,168	1.35	waste	PX03-T	4.0	4.0	15.0	165.0
28-AUG-01 Afternoon Shift	110/148	572	146.02	2,968	1.08	waste	PX03-A	4.0	4.5	10.0	165.0
28-FEB-00 Night Shift	129/026	535	124.22	3,478	0.87	waste	PX03-T	7.0	8.0	15.0	271.0
28-FEB-01 Afternoon Shift	108/204	369	136.42	3,167	1.22	waste	PX03-T	4.0	4.0	10.0	165.0
28-JUL-01 Night Shift	108/219	1,424	155.91	2,771	1.22	waste	PX03-T	4.0	4.0	10.0	165.0
28-NOV-00 Day Shift	138/041	877	116.99	3,631	1.35	waste	PX03-T	4.0	4.0	15.0	165.0
29-FEB-00 Night Shift	129/025	2,648	133.87	3,227	0.87	waste	PX03-T	7.0	8.0	15.0	271.0
29-FEB-00 Night Shift	129/029	1,952	133.08	3,245	1.35	waste	PX03-T	4.0	4.0	15.0	165.0
29-JUL-00 Night Shift	135/021	3,180	140.78	3,069	0.87	waste	PX03-T	7.0	8.0	15.0	271.0
29-JUN-00 Night Shift	132/040	1,082	118.55	3,644	1.35	waste	PX03-T	4.0	4.0	15.0	165.0
29-MAY-01 Afternoon Shift	138/021	1,662	142.67	3,028	1.07	waste	PX03-T	4.5	4.5	15.0	165.0
29-MAY-01 Afternoon Shift	141/018	2,107	111.86	3,862	1.00	waste	PX03-T	6.5	7.5	15.0	271.0
30-APR-00 Afternoon Shift	132/021	1,421	123.73	3,491	0.87	waste	PX03-T	7.0	8.0	15.0	271.0
30-AUG-01 Night Shift	112/117	115	129.57	3,334	1.08	waste	PX03-A	4.0	4.5	10.0	165.0
30-DEC-00 Afternoon Shift	138/036	851	133.5	3,236	1.35	waste	PX03-T	4.0	4.0	15.0	165.0
30-JUL-01 Afternoon Shift	108/220	1,294	109.67	3,939	1.22	waste	PX03-T	4.0	4.0	10.0	165.0
30-MAR-00 Night Shift	129/038	2,566	148.31	2,913	0.87	waste	PX03-T	7.0	8.0	15.0	271.0
30-MAY-00 Afternoon Shift	132/028	982	130.95	3,299	0.87	waste	PX03-T	7.0	8.0	15.0	271.0
31-JAN-01 Night Shift	108/199	653	158.34	2,728	1.22	waste	PX03-T	4.0	4.0	10.0	165.0
AVERAGE				3,142	1.17						

6.4 **Summary and Conclusions**

Chapter 6 gives an overview of the mining and processing operations and the sensitivity of their performance to the geotechnical conditions at Sandsloot. The drill and blast designs were optimised from 1997 to 2001 (Table 6.1) and a detailed fragmentation study was then undertaken in order to define the actual ore and waste fragmentation profiles delivered to the processing plant and the load and haul fleet.

The plant design and comminution requirements were assessed during the research, and the fragmentation requirements were evaluated to determine the impact of the mill feed fragmentation on plant performance. Based on the digital fragmentation analysis a mean fragmentation of 230 mm was set for waste and 150 mm for ore.

The instantaneous loading rate study was undertaken in three ways. Firstly, the average monthly loading rate from July 1999 to December 2001 was assessed. Secondly, the average instantaneous loading rate for every mining shift (1,069 shifts) during 2001 was measured and thirdly 238 blasts were analysed to determine the relationship between blast powder factor and the ILR for both waste and ore.

Based on the analysis, a target loading rate was set at 3,200 t/hr for waste and 3,300 t/hr for ore. The study was undertaken over a range of energy factors and hole diameters to ensure the results were representative. Table 6.7 relates the fragmentation targets to the instantaneous loading rates of the shovels. Table 6.8 defines the final design targets for the drill and blast customers and for inclusion into the fragmentation model.

Table 6.7 Summary of the base data used to define the customer targets.

	Fragmentation Study		Instantaneous Loading Rate Study		
	Pf (kg/m ³)	P ₅₀ (mm)	Pf (kg/m ³)	ILR (t/hr)	Average ILR (shift analysis)
Ore	1.77	150.1	1.56	3,316	3,249 t/hr
Waste	1.18	228.1	1.17	3,182	

Table 6.8 Benchmark design information for the drill and blast department’s customers.

Customer	Material	Instantaneous Loading Rate	Fragmentation Size @ P ₅₀
Load and Haul	Waste	3,200 t/hr	50% passing @ 230 mm
Processing Plant	Ore	3,300 t/hr	50% passing @ 150 mm

Initially, geotechnical information for the optimisation of blast designs was provided manually, using draughted plans. The results of these adjustments were recorded in order to define and benchmark the performance standards, which were recorded in this chapter. These performance standards were then defined as the customer targets and subsequently built into the fragmentation model. Chapter 7 describes the development of the fragmentation model that enabled dynamic blast design and planning well ahead of the mining face, thereby ensuring the customer targets were consistently achieved. The application of the fragmentation model to blast design from January 2002 to June 2003 and the resultant improvements are discussed in Chapter 8.

Chapter 6 clearly defines the customer relationships within and between the mining and processing operations. Following on the definition of these relationships, the targets that derive the greatest economic benefit for the company as whole, were described (Table 6.8).

7 FRAGMENTATION MODEL

7.1 Introduction

Drilling and blasting is the first step in the physical mining process and therefore plays a major role in the performance of downstream functions. The inherent rock mass properties are one of the biggest unknown factors in blast design and play a major role in blasting costs and the productivity of the downstream functions. The 3D geotechnical model provides detailed rock mass information and was therefore applied to the blast designs in order to improve the efficiency of blasting.

Chapter 5 describes the development of the geotechnical model, which contains detailed geotechnical information within a 3D block model, for the proposed pit mining area. Chapter 6 details the process through which the optimum design targets were obtained for the drill and blast customers. A mean fragmentation size of 230 mm in waste and 150 mm in ore were defined as the targets for inclusion into the fragmentation model. The development of the 3D geotechnical model provides information for the proactive adjustment of blast designs, thereby ensuring a more consistent fragmentation feed. This consistent achievement of the design customer targets and the resultant benefits are discussed in Chapter 8.

A number of steps were followed in order to utilise the 3D geotechnical information for drill and blast optimisation, budgeting and planning. Figure 7.1 illustrates, through a flow diagram, the process followed to apply the geotechnical model information to blast design and fragmentation optimisation. The process is described as follows:

- A detailed study was undertaken to define the fragmentation requirements for the drill and blast customers (Chapter 6).
- The geotechnical information in the model was first converted into a Blastability Index (BI), (Lilly, 1986).
- A fragmentation model was then developed using the BI and the Kuz-Ram equation (Cunningham, 1986) to calculate the required energy factor (quantities of explosives) to achieve the defined fragmentation requirements. The fragmentation model takes into account the varying rock mass conditions by querying the geotechnical information contained in the model.

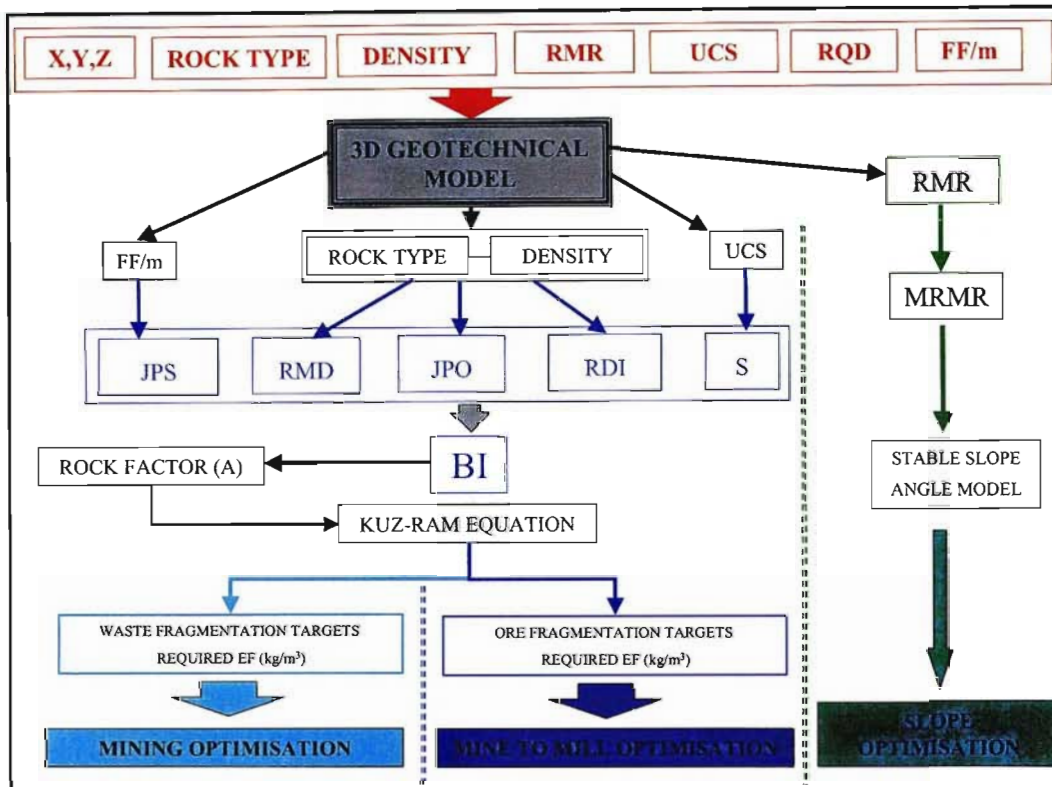


Figure 7.1 Flow diagram illustrating how the geotechnical model is used to calculate the Blastability Index, required energy factor and subsequent optimisations.

The fragmentation model was based on a re-worked Kuz-Ram equation, which gave the required energy factor for a set fragmentation target. The Kuz-Ram equation contains a rock factor, which accounts for the influence of the rock mass' geotechnical properties. The rock factor was derived from the BI, which in turn was derived from the geotechnical information contained in the model. The drill and blast costs were calculated from the required energy factor and empirical charts were developed, based on the information contained in the model, to allow quick reference for blast design.

For more dynamic use, all the information was incorporated and automated into a fragmentation model using the Datamine® software package. The user-interface/functionality is provided via a simple front-end query screen. The drill and blast engineer will overlay the outline of the planned blast area and run a query on the model. The query function interrogates the model and provides a summary table of all the relevant mining information i.e. rock type, geotechnical properties, BI, design fragmentation target, blast tonnage, required energy factor and the expected drill and blast costs associated with that mining area. For longer term planning and

budgeting, the mining slots are queried in series to provide the required drill and blast information.

The fragmentation model has optimised the blast design and planning process by firstly reducing the level of uncertainty associated with rock mass information; secondly by defining precisely the customer requirements and thirdly by combining the entire process into a 3D model that can be queried for any planned mining slot.

7.2 Blastability Index

In order to deal with the complex interaction of rock mass variables in engineering design empirical equations were developed by Bieniawski (1973, 1976) [RMR], Barton *et al.* (1974) [Q-system] and Laubscher (1990) [MRMR] amongst others. The rock mass ratings derived from these systems allow semi-quantitative estimates for engineering design. This concept has been extended by Lilly (1986) to include rock mass blastability.

The Blastability Index (BI) was developed by Lilly (1986, 1992) and reviewed by Widzyk-Capehart and Lilly in 2001. The purpose of the BI was to develop a tool for characterising a rock mass in terms of the ease of breakage by means of blasting. Site-specific correlations can then be established between blast energy factor and the BI. Bickers *et al.* (2001) has extended this process by applying the BI to the design of wall control blasts.

The BI incorporates easily recognisable rock mass parameters, which are significant in affecting blast performance and muck pile diggability. Diggability refers to the ease with which an excavator can load a blasted muck pile. The information relating to the BI can be collected from exploration holes and exposed rock faces and therefore can be used for both operational mines and feasibility studies.

The calculation of the BI is detailed in equation 7.1 and the various BI parameters are calculated from the tables and equations listed below. Lilly (1986) notes that the index is heavily weighted towards the nature and orientation of the planes of weakness in the rock mass, as these planes generally control the post blast block size. A more detailed study of pre and post blast block sizes has been undertaken by Widzyk-Capehart *et al.* (2001).

Eq. 7.1 **BI** = **0.5 x (JPS+RMD+JPO+RDI+S)**

- BI = Blastability Index
- JPS = Joint Plane Spacing
- RMD = Rock Mass Description
- JPO = Joint Plane Orientation
- RDI = Rock Density Influence
- S = Rock Strength

7.2.1 Joint Plane Spacing (JPS)

The joint plane spacing parameter refers to all discontinuities in the rock mass and includes mining induced fractures. The inherent rock mass block sizes, which are bounded by discontinuities, give the engineer a good indication of the post blast fragmentation size. Table 7.1 details the weighting placed on the degree of jointing when calculating the BI.

Table 7.1 Joint Plane Spacing (JPS)

	Description	Rating
1	Close (<0.1 m)	10
2	Intermediate (0.1 to 1 m)	20
3	Wide (>1m)	50

7.2.2 Rock Mass Description (RMD)

The rock mass description is the parameter used to give a general description of the global rock mass conditions (Table 7.2). This assessment of the global rock mass is extremely important as the fragment size distribution of a totally massive rock will be dependant on the generation of blast induced fractures whereas the fragmentation of a friable rock mass will be dictated by the inherent jointing.

Table 7.2 Rock Mass Description (RMD)

	Description	Rating
1	Powdery/Friable	10
2	Blocky	20
3	Totally Massive	50

7.2.3 Joint Plane Orientation (JPO)

The orientation of the dominant joint sets in relation to the free blast face plays a major role in blast performance. Planes dipping in the direction of the free face can result in blocky fragmentation and rough floors while horizontal bedding poses few blasting problems. Joint orientation information can be rapidly collected by scanline mapping. From the scanline mapping, joint sets are derived and an open pit can be zoned according to the dominant joint orientations, as discussed in Chapter 4.6. Table 7.3 describes the BI rating for various joint plane orientations in relation to the free face of the blast.

Table 7.3 Joint Plane Orientation (JPO)

	Description	Rating
1	Horizontal	10
2	Dip out of face	20
3	Strike normal to face	30
4	Dip into face	40

7.2.4 Rock Density Influence (RDI)

RDI expresses the influence the density of the rock has on the BI as evident in Equation 7.2.. A heavier rock mass requires more explosive energy to move the rock so that it can be efficiently loaded. This parameter has a less significant weighting in the BI equation when compared to the influence of jointing.

Eq. 7.2 $RDI = (Density\ (g/cm^3) \times 25) - 50$

7.2.5 Rock Hardness (S)

It follows that the harder the inherent properties of the rock, the greater the explosive energy required to generate the design fragmentation. The uni-axial compressive strength (UCS) values are obtained from laboratory testing, as well as field equipment such as a point load apparatus or a Schmidt hammer. Equation 7.3 documents the formula used to calculate the rock hardness rating for the BI.

Eq. 7.3 $S = (\text{UCS (in MPa)} \times 0.05)$

The five BI parameters described above are then added together and multiplied by 0.5 to derive the BI (Eq. 7.1). As with other rock mass rating systems, the BI has gained widespread acceptance as a useful blasting tool since it was published in 1986. The BI provides the quantitative link between the *in-situ* rock mass conditions and blast design parameters. Site-specific charts can then be developed to relate the BI to these blast design parameters, such as energy factor (Lilly, 1992).

The blast powder factor can be defined as the quantity of explosives used, per unit volume of rock, measured in kg/m^3 . There are a number of different explosive formulations available in the market and depending on which one is used the energy delivered by the powder factor will vary. For this reason the relative weight strength (RWS) of the explosive is obtained. The RWS is the strength of the explosive, as a percentage, in comparison to ammonium nitrate fuel oil (ANFO) explosives. ANFO is widely used in the mining industry and is therefore used as a standard for comparison of explosive energies. In order to ensure consistency, for comparison of blast powder factors, the energy factor is used. The energy factor is determined by multiplying the powder factor by the RWS of the explosive.

7.3 Calculation of the Blastability Index from the Geotechnical Model

The Blastability Index was used to relate the information stored in the geotechnical model to blast design. Figure 7.1 illustrates schematically the process followed in order to convert the geotechnical information into the BI and then into blast design information. In order to develop the geotechnical model, sample co-ordinates, sample length, rock type, UCS, RQD, FF/m and RMR were collected for each sample zone mapped within the pit and in exploration boreholes (Figure 6.1). This geotechnical information was then modelled in 3D to generate the geotechnical model. Each model cell (15m x 15m x 15m) contains all the base geotechnical information listed above. The BI values were then calculated from this base information.

With reference to Figure 7.1 the following text describes in detail how the geotechnical information collected from boreholes and face maps was converted into the Blastability Index and subsequently into blast design information.

Joint Plane Spacing (JPS)

Lilly's (1986) JPS rating table (Table 7.1) has three broad categories, namely close, intermediate and wide spacing. These categories can be directly related to FF/m as shown in Table 7.4. For the development of the geotechnical model, FF/m data was collected from field mapping and exploration boreholes. The FF/m values were then interpolated into the model blocks to provide an indication of the degree of jointing in the Sandsloot rock mass.

A correlation was developed for FF/m and JPS as listed in Table 7.4. The data in the table was then plotted in Figure 7.2 so that a correlation equation could be defined for JPS and FF/m. Figure 7.2 illustrates the non-linear relationship between FF/m and JPS, which is due to the heavy weighting the BI gives JPS in highly fractured rock. Two separate graphs and correlation equations were therefore developed for more accurate estimation of the JPS values. The data was separated into FF/m values greater than and smaller than one. Figure 7.3 and equation 7.5 represent the correlation for FF/m values greater than one. Figure 7.4 and Equation 7.6 represent the correlation for FF/m values less than one.

$$\text{Eq. 7.5} \quad \text{JPS} = (-0.5964 \times \text{FF/m}) + 18.268 \quad (\text{FF/m} > 1)$$

Eq. 7.6 $JPS = (-42.449 \times FF/m) + 60.969$ **(FF/m<1)**

JPS = Joint plan spacing parameter used in the Blastability Index.

FF/m = fracture frequency per metre

Table 7.4 Table relating FF/m to JPS - developed to apply more accurate JPS ratings to the detailed jointing information available in the geotechnical model.

FF/m	JOINT SPACING (m)	JPS	BI DESCRIPTION
0.25	4.00	50.00	WIDE SPACING
0.50	2.00	40.00	WIDE SPACING
0.75	1.33	30.00	WIDE SPACING
0.90	1.11	22.00	WIDE SPACING
1.00	1.00	20.00	INTERMEDIATE SPACING
2.00	0.50	19.00	INTERMEDIATE SPACING
3.00	0.33	18.00	INTERMEDIATE SPACING
4.00	0.25	17.00	INTERMEDIATE SPACING
5.00	0.20	16.00	INTERMEDIATE SPACING
6.00	0.17	15.00	INTERMEDIATE SPACING
7.00	0.14	14.00	INTERMEDIATE SPACING
8.00	0.13	13.00	INTERMEDIATE SPACING
9.00	0.11	12.00	INTERMEDIATE SPACING
10.00	0.10	11.00	INTERMEDIATE SPACING
11.00	0.09	10.00	CLOSE SPACING
12.00	0.08	9.55	CLOSE SPACING
13.00	0.08	9.10	CLOSE SPACING
14.00	0.07	8.65	CLOSE SPACING
15.00	0.07	8.20	CLOSE SPACING
16.00	0.06	7.75	CLOSE SPACING
17.00	0.06	7.30	CLOSE SPACING
18.00	0.06	6.85	CLOSE SPACING
19.00	0.05	6.40	CLOSE SPACING
20.00	0.05	5.95	CLOSE SPACING
21.00	0.05	5.50	CLOSE SPACING
22.00	0.05	5.05	CLOSE SPACING
23.00	0.04	4.60	CLOSE SPACING
24.00	0.04	4.15	CLOSE SPACING
25.00	0.04	3.70	CLOSE SPACING
26.00	0.04	3.25	CLOSE SPACING
27.00	0.04	2.80	CLOSE SPACING
28.00	0.04	2.35	CLOSE SPACING
29.00	0.03	1.90	CLOSE SPACING
30.00	0.03	1.45	CLOSE SPACING
31.00	0.03	1.00	CLOSE SPACING

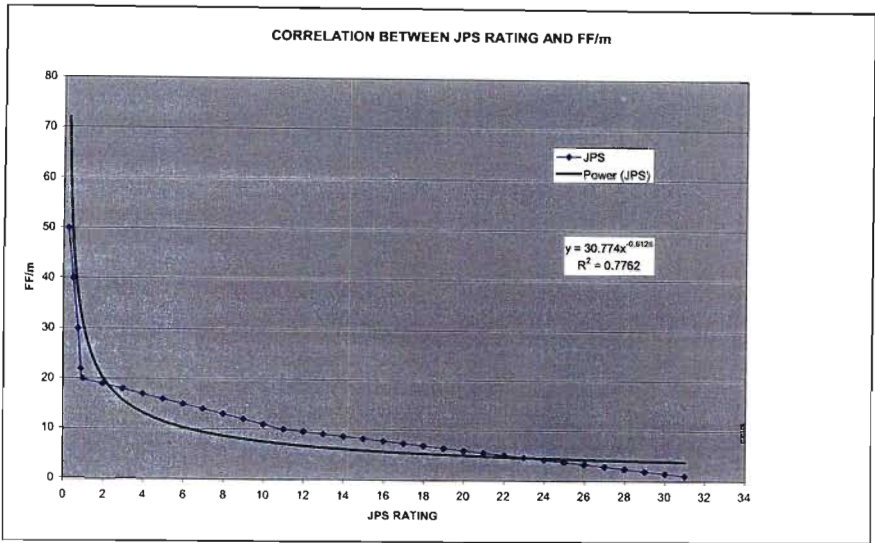


Figure 7.2 Graph depicting a poor correlation of JPS to FF/m for a single equation.

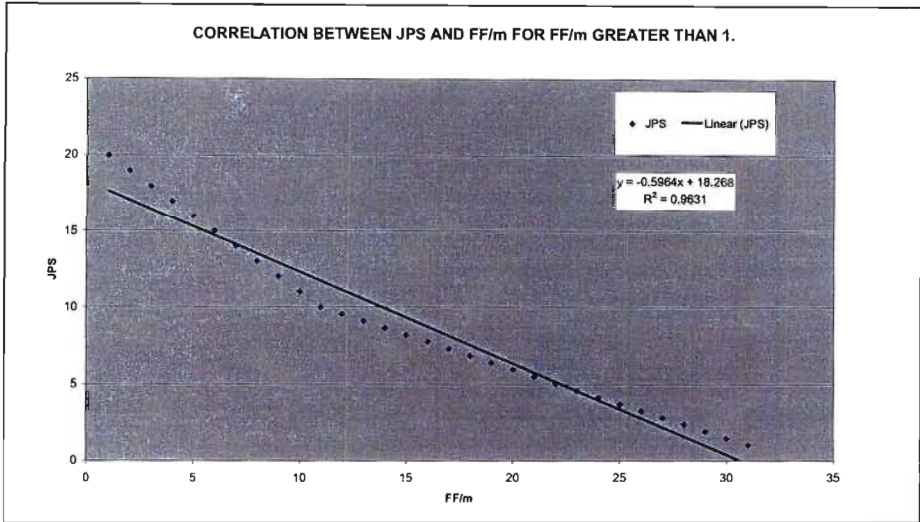


Figure 7.3 Graph illustrating the correlation for JPS and FF/m greater than one.

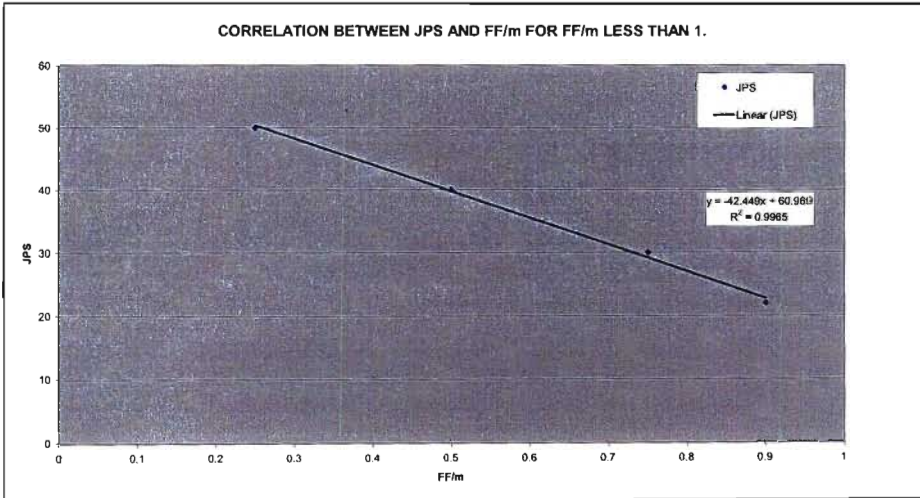


Figure 7.4 Graph depicting a better correlation for JPS and FF/m less than one.

Rock Mass Description (RMD) and Joint Plane Orientation (JPO)

Based on extensive field mapping and scanline surveys, the average RMD and JPO values were generated for all the major rock types occurring in the pit. These values are listed below in Table 7.5.

Table 7.5 Information relating rock type information in the model to density, JPO and RMD.

Ore / Waste	Rock Type	RMD	JPO	Density (tonnes/m³)
Waste	Norite	35	25	2.9
Ore	Pyroxenite	30	25	3.2
Ore	Parapyroxenite	40	35	3.2
Ore	A-pyroxenite	35	40	3.2
Ore	Serpentinised parapyroxenite	40	35	3.2
Waste	Calc-silicate	15	15	2.9
Waste	Quartz/feldspar vein	40	40	2.9

Rock Density Influence and Rock Strength

These are simple calculations (Eq. 7.2 and Eq. 7.3) embedded in the model whereby the density and UCS values in the model blocks are used directly to derive the RDI and Rock Strength parameter values respectively.

The previous sections describe the correlations or direct calculations, which were developed from the geotechnical information contained in the model to the Blastability Index parameters. All the parameters were then automatically calculated in the model to generate a BI value for each model block, as per equation 7.1. In addition to the geotechnical information, the 3D model now contained the BI parameters and final BI value for each 15 m³ model block.

7.4 Fragmentation Model

Cunningham (1986) developed a fragmentation equation (Kuz-Ram equation), based on the Kuztenov equation and the Rosin-Ramler distribution, which estimated the mean fragmentation that would result from a known energy factor used in specific rock mass conditions. By inputting the known rock mass conditions the equation allows the blasting engineer to assess the impact a change in energy factor will have on mean fragmentation size. In order to derive the mean fragmentation of a blasted muckpile the Kuz-Ram equation required the following inputs:

- Mass of explosive per blasthole (Q), rock yield volume per blast hole (V), relative weight strength of the explosive (RWS) and a Rock Factor (A).

Based on the detailed study discussed in Chapter 6, a mean fragmentation target of 150 mm was set for delivery to the crushing circuit and a mean fragmentation of 230 mm was set for waste loading from the pit. In order to incorporate this information into the geotechnical model, Cunningham's (1986) fragmentation equations were utilised.

The Kuz-Ram equation (Eq. 7.7) gives a prediction of the mean fragmentation based on the explosive energy and rock properties. At Sandsloot, however, there was a detailed geotechnical model and known fragmentation targets. The Kuz-Ram equation was therefore reworked in order to produce a required energy factor equation (Eq. 7.8) based on the known rock properties and fragmentation targets.

$$\text{Eq. 7.7} \quad X = A \times \left(\frac{V}{Q} \right)^{0.8} \times Q^{0.167} \times \left(\frac{RWS}{115} \right)^{-0.633}$$

X = Predicted mean fragmentation diameter (cm)

A = Rock Factor (A = 0.12 x BI)

Q = Mass of explosive per blast hole (kg)

V = rock volume or yield (m³)

RWS = Relative weight strength of explosive (ANFO = 100)

Equation 7.7 can be reworked, if all the other variables are known, to provide a required energy factor (Eq 7.8).

Eq. 7.8 $Ef = [X / ((A \times Q^{0.167}) \times ((RWS / 115)^{-0.633}))]^{-1.25}$

Ef = Required energy factor (kg/m³)

X = Customer required mean fragment diameter (cm)

Rock Factor (A)

The Rock Factor (A) value in the Kuz-Ram equation is used to take into account variations in rock mass conditions. The Blastability Index was first derived from the geotechnical information contained in the model. This BI value was then used to calculate the Rock Factor (A) for input into the required energy factor equation (Eq. 7.8). Work by Cunningham (1986) has related the Rock Factor to the Blastability Index through the use of equation 7.9.

Eq. 7.9 A = BI x 0.12

BI = Blastability Index (Lilly, 1986)

A = Rock Factor value used in the Kuz-Ram equation to represent rock mass variation

The reworking the Kuz-Ram equation to provide a required energy factor, effectively harnesses all the geotechnical information contained in the 3D model with the customer design targets, thereby providing a fragmentation model and dynamic blast design tool.

7.5 Drill and Blast Costing Model

Section 7.4 describes the equations used to define the required energy factor needed to generate the customer fragmentation targets. This energy factor takes into account the variable geotechnical conditions represented in the model through the use of a Blastability Index. In order to achieve the defined fragmentation targets, the volumes of explosives consumed will vary based on the required energy factor (kg/m^3). This simple relationship between required energy factor and costs was therefore defined and included in the fragmentation model so that costs related to each blast design could be automatically generated.

The consumption of explosives in mining is a variable cost and has a linear relationship between blasted rock volume (kg/m^3) and expenditure (R/m^3), which is illustrated in Figure 7.5. Based on the known drill and blast costs used at Sandsloot, a correlation was developed between the required energy factor and cost per cubic metre (Eq. 7.10). These costs included drilling, explosives, labour and drill maintenance. A detailed breakdown of the costs related to various blast patterns is presented in Table 7.6.

Eq. 7.10. $\text{Cost per m}^3 = E_f \times 2.946$

E_f = Required energy factor (kg/m^3) obtained from Eq. 7.8.

The equations and relationships defined in the previous sections are illustrated graphically in Figure 7.6, which represents the impact of the Blastability Index on the required energy factor and the associated drill and blasts costs. The fragmentation model design chart (Figure 7.6) is essentially a 2D representation of the 3D calculations and relationships, which are included in the fragmentation model.

The fragmentation chart (Figure 7.6) is a powerful design tool and the impact of the distinctly harder hybrid ore types can be clearly seen, as well as the different fragmentation targets for ore and waste. For example the range in BI for waste is 41 to 57 while in ore it is from 50 to 61. The associated energy factors required to achieve the ore and waste targets are as low as 0.7 kg/m^3 in waste but don't drop below 1.4 kg/m^3 in the ore. The substantially higher costs associated with the different energy factors in ore and waste are evident with the ore blasting costing as much as $\text{R } 5.60 \text{ m}^3$ while the waste peaks at $\text{R } 3.00 \text{ m}^3$.

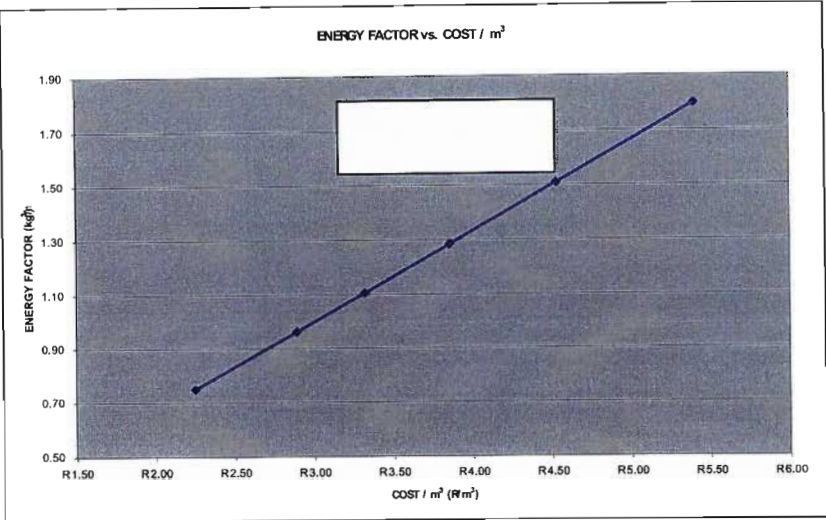


Figure 7.5 Relationship between energy factor and cost per m³, for Sandsloot open pit.

Table 7.6 Information used to calculate the relationship between cost and energy factor.

PATTERN SIZE (Burden x Spacing)	5.0m x 6.0m	5.5m x 6.5m	6.0m x 7.0m	6.5m x 7.5m	7.0m x 8.0m	8.0m x 9.0m
EXPLOSIVE						
Explosive Type	HEF 206	HEF 206	HEF 206	HEF 206	HEF 206	HEF 206
Charge Mass/Metre (kg/m)	71.75	71.75	71.75	71.75	71.75	71.75
Explosive Mass Per Hole (kg)	825.15	825.15	825.15	825.15	825.15	825.15
Effective Charge Diameter (mm)	270.00	270.00	270.00	270.00	270.00	270.00
Average In-hole Density (g/cm³)	1.25	1.25	1.25	1.25	1.25	1.25
Stemming Volume (m³)	0.34	0.34	0.34	0.34	0.34	0.34
BLAST GEOMETRY						
Stemming Length (m)	6.00	6.00	6.00	6.00	6.00	6.00
Column Length (m)	11.50	11.50	11.50	11.50	11.50	11.50
Hole Depth (m)	17.50	17.50	17.50	17.50	17.50	17.50
Bench Height (m)	15.00	15.00	15.00	15.00	15.00	15.00
Sub-Drill (m)	2.50	2.50	2.50	2.50	2.50	2.50
Hole Diameter (mm)	270.00	270.00	270.00	270.00	270.00	270.00
PATTERN						
Burden (m)	5.00	5.50	6.00	6.50	7.00	8.00
Spacing (m)	6.00	6.50	7.00	7.50	8.00	9.00
Scaled Burden	0.59	0.65	0.71	0.77	0.83	0.94
ENERGY						
Powder Factor (kg/m³)	1.83	1.54	1.31	1.13	0.98	0.76
Energy Factor (kg/m³)	1.80	1.51	1.28	1.11	0.96	0.75
RWS	98.00	98.00	98.00	98.00	98.00	98.00
ASV	3.72	3.72	3.72	3.72	3.72	3.72
RBS	153.13	153.13	153.13	153.13	153.13	153.13
PRODUCTION						
Drilling: Cubic metres per metre	30.00	35.75	42.00	48.75	56.00	72.00
Drilling: Metres per cubic metre	0.03	0.03	0.02	0.02	0.02	0.01
Yield Per Hole (m³)	450.00	536.25	630.00	731.25	840.00	1080.00
Rock Tonnes per hole	1305.00	1555.13	1827.00	2120.63	2436.00	3132.00
FRAGMENTATION						
Expected Mean Fragment Size (cm)	16.22	18.66	21.23	23.92	26.73	32.68
Uniformity Index	0.83	0.82	0.80	0.79	0.78	0.75
Characteristic Size (cm)	25.22	29.24	33.53	38.06	42.86	53.24
DRILL & BLAST COSTS						
Drilling Cost/Hole	R 787.50	R 787.50	R 787.50	R 787.50	R 787.50	R 787.50
Explosive Cost/Hole	R 1,567.78	R 1,567.78	R 1,567.78	R 1,567.78	R 1,567.78	R 1,567.78
Initiation Cost/Hole	R 57.00	R 57.00	R 57.00	R 57.00	R 57.00	R 57.00
Other Costs/Hole (Gas Bags)	R 18.50	R 18.50	R 18.50	R 18.50	R 18.50	R 18.50
Total Cost/Hole	R 2,430.78	R 2,430.78	R 2,430.78	R 2,430.78	R 2,430.78	R 2,430.78
Drilling Cost/m³	R 1.75	R 1.47	R 1.25	R 1.08	R 0.94	R 0.73
Explosive Cost/m³	R 3.48	R 2.92	R 2.49	R 2.14	R 1.87	R 1.45
Initiation Cost/m³	R 0.13	R 0.11	R 0.09	R 0.08	R 0.07	R 0.05
Other Costs/m³	R 0.04	R 0.03	R 0.03	R 0.03	R 0.02	R 0.02
Total Cost/m³	R 5.40	R 4.53	R 3.86	R 3.32	R 2.89	R 2.25
Total Cost/tonne	R 1.86	R 1.56	R 1.33	R 1.15	R 1.00	R 0.78

Effect of Blastability Index on Cost/m³ & Ef (kg/m³) for Set Fragmentation Targets

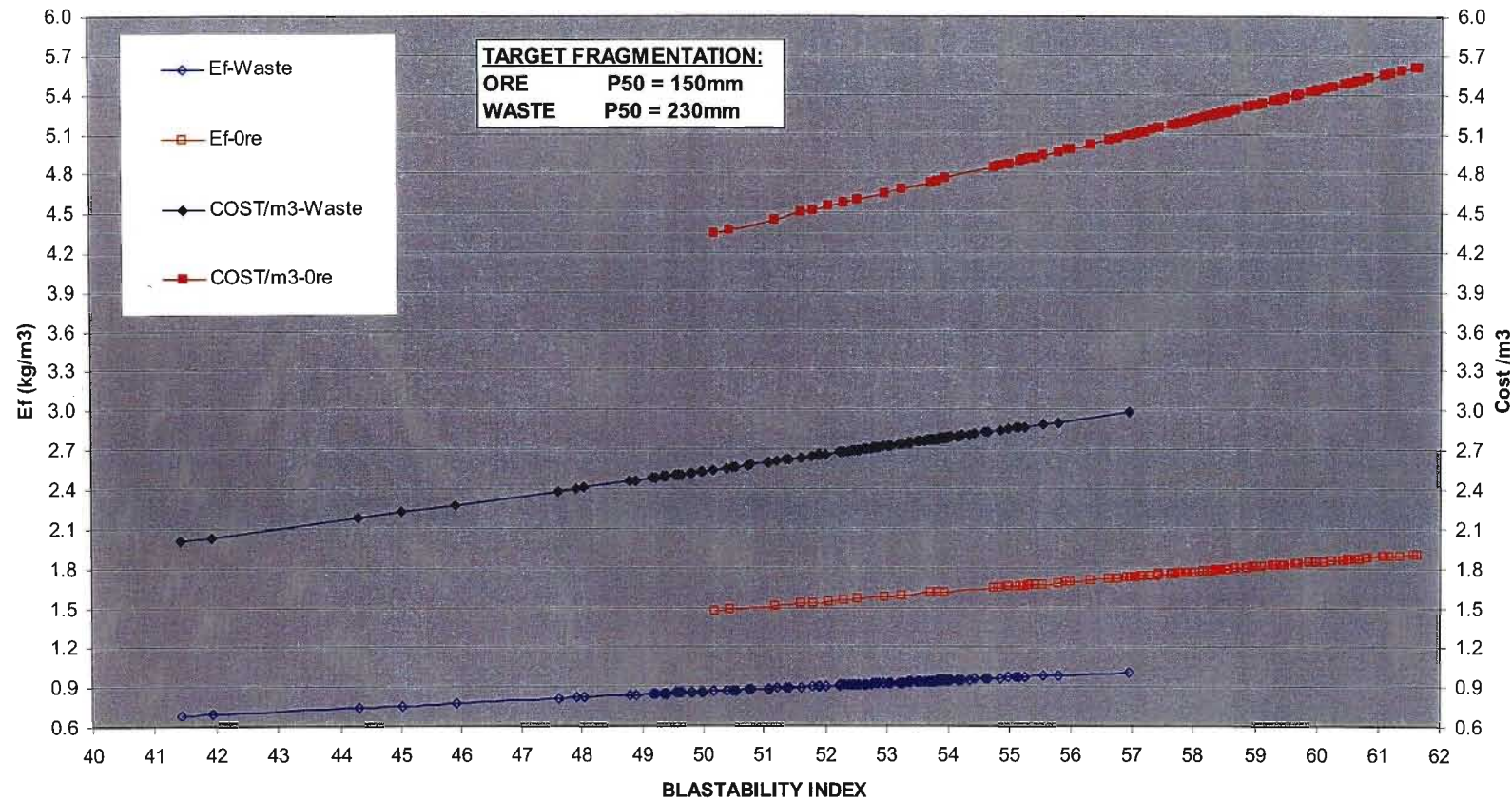


Figure 7.6 Illustrates graphically the effect of Blastability Index on the required energy factor and the associated drill and blasts costs for set fragmentation targets.

7.6 Model Query and Planning Functionality

The previous sections describe all the calculations used in the 3D geotechnical model to generate the fragmentation model within Datamine®. In order to utilise this information for planning, a model query function was developed (Figure 7.7). This involves taking the blast design boundary in its orientated position and then querying the fragmentation model for all the information contained within the blast design area (Figure 7.8).

The Datamine® software uses a series of commands to undertake the model calculations described in the previous sections. For someone unfamiliar with the Datamine® functions it would be an onerous task to generate useful information from the model. In order to create a user-friendly environment from which any unskilled Datamine® user can run the fragmentation model a visual basic front-end was created. The front-end is illustrated in Figure 7.7 and is essentially a series of buttons, which automatically run the required equations or functions needed to interrogate the model. Mr. Lance Reynolds is gratefully acknowledged for his guidance and assistance in developing the front end. The front end in Figure 7.7 is divided into the following four sections:

- ***Data Files***

This section opens the required model files and runs all the fragmentation calculations (“process button”). Additionally, it allows the user to open “Mining Blocks” which are the blast design boundaries to be queried and a results file for the information derived from the mining block query.

- ***Colour and Categorise Block Model***

This section allows the user to filter the block model on the listed parameter buttons such as MRMR, RQD, Rock Type etc. The process allows the visualisation of the model based on the various listed parameters and enables the user to see rock mass variations at any point within the block model or proposed mining area.

- ***Evaluate Mining Blocks Against Block Model***


This section opens the blast design boundary and queries the fragmentation model for all information contained within the boundary. The process also creates a results file with the average model information for each rock type. An example mining block and results table is presented in Figure 7.8 and Table 7.7 respectively. It is this results file that is used for the actual design blast parameters used in the field. Figure 7.9 illustrates a series of planned mining blocks, which are evaluated sequentially to generate blast design and cost information well ahead of the mining face.

- ***Export Model Slice for AutoCAD***

This section allows the user to export any of the listed model parameters to an AutoCAD *.dxf file. The user specifies the export parameter i.e. MRMR and bench elevation and a colour filtered *.dxf drawing is generated. This functionality was created so that the draughting department could overlay the geotechnical information onto the mines official blast design plans, which are created in AutoCAD. The blaster in the field will therefore have a plan indicating the rock mass variability.

The simple user front-end has enabled the fragmentation model to be utilised by non-Datamine® experts thereby ensuring that the design tool is user-friendly and functional. The fragmentation model was used on a day-to-day basis for all blast design. In the longer term, it is used for blast planning and budgeting. The significant benefits related to this dynamic blast design process are discussed in Chapter 8.

3D GEOTECH MODEL - Mining Application



Data Files

In Model:

Out Model:

Mining Blocks:

Results File:

Colour & Categorise Block Model

MRMR

EF

Energy Factor (kg/m³)

RQD

SLOPE

Slope Angle (Degrees)

RTYPE

CM3

Cost (R/m³)

UCS

BI

Blastability Index

FFM

Button

Evaluate Mining Blocks against Block Model

Near Distance: m

Far Distance: m

Evaluate All Blocks:

Export Model Slice for ACAD

Bench Height:

Bench: (1 - 75)

Crest Elev:

Export Value:

◀

▶

Script

Design

Standard

Advanced

Figure 7.7 Computer front-end developed for interfacing with the 3D geotechnical model.

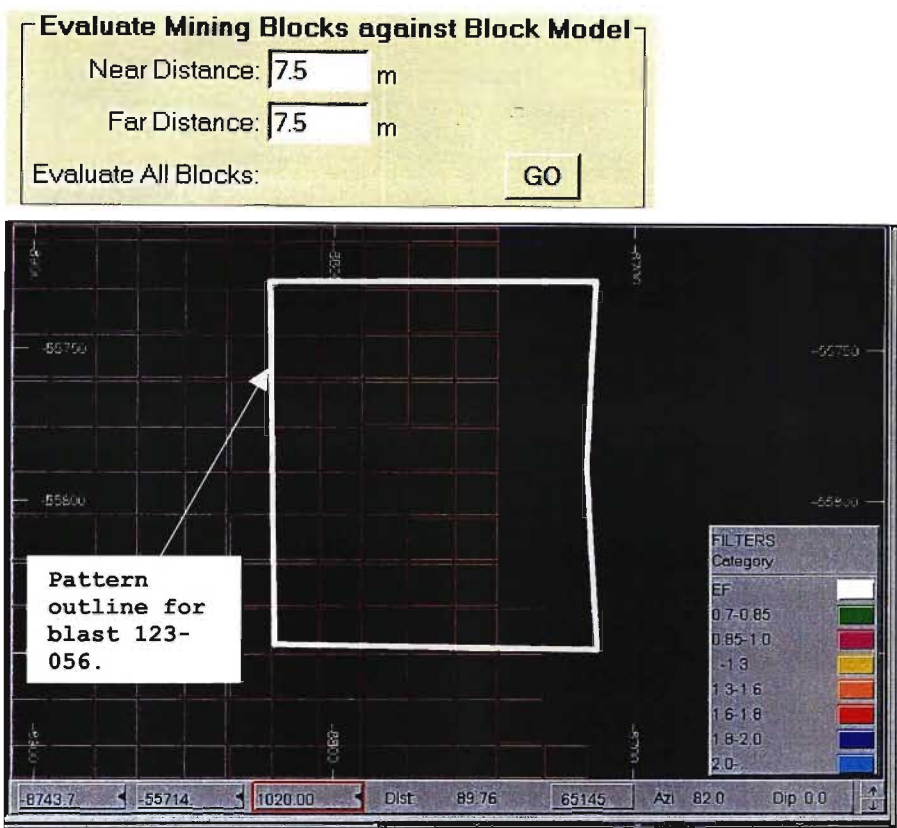


Figure 7.8 Screen view of the model query for blast outline 123 – 056, filtered on energy factor (Ef). Note: 123-056 ≡ (1= pit one (Sandsloot); 23 = bench 23; 056 = the 56th blast on bench 23).

Table 7.7 Summary table of information derived from the geotechnical model query function, “evaluate mining blocks”, for blast 123-056.

Code	Description	Units	Model Data		
RTYPE	Rock Type		Norite	Pyroxenite	Parapyroxenite
RCODE	Model Rock Code		0	1	2
MRMR	Mining Rock Mass Rating		54	49	48
UCS	Uniaxial Compressive Strength	MPa	197	160	183
RQD	Rock Quality Designation	%	80	77	77
RDI	Rock Density Influence		23	30	30
S	Rock Hardness		10	8	9
RMD	Rock Mass Description		35	30	40
JPO	Joint Plane Orientation		25	25	35
FFM	Fracture Frequency per Metre		8	9	9
JPS	Joint Plane Spacing		13	13	13
BI	Blastability Index		52.83	52.95	63.49
FRAG	Defined Fragmentation Target	mm	230	150	150
A	Rock Factor		6.34	6.35	7.62
EF	Required Energy Factor	kg/m³	0.92	1.58	1.98
COST / m ³	Drill & Blast Cost	R/m ³	2.71	4.64	5.82
VOLUME	In-situ Rock Volume to be Blasted	m ³	64,976	58,689	67,860
TONNES	In-situ Rock Tonnage to be Blasted	Metric Tonnes	188,430	187,806	217,153

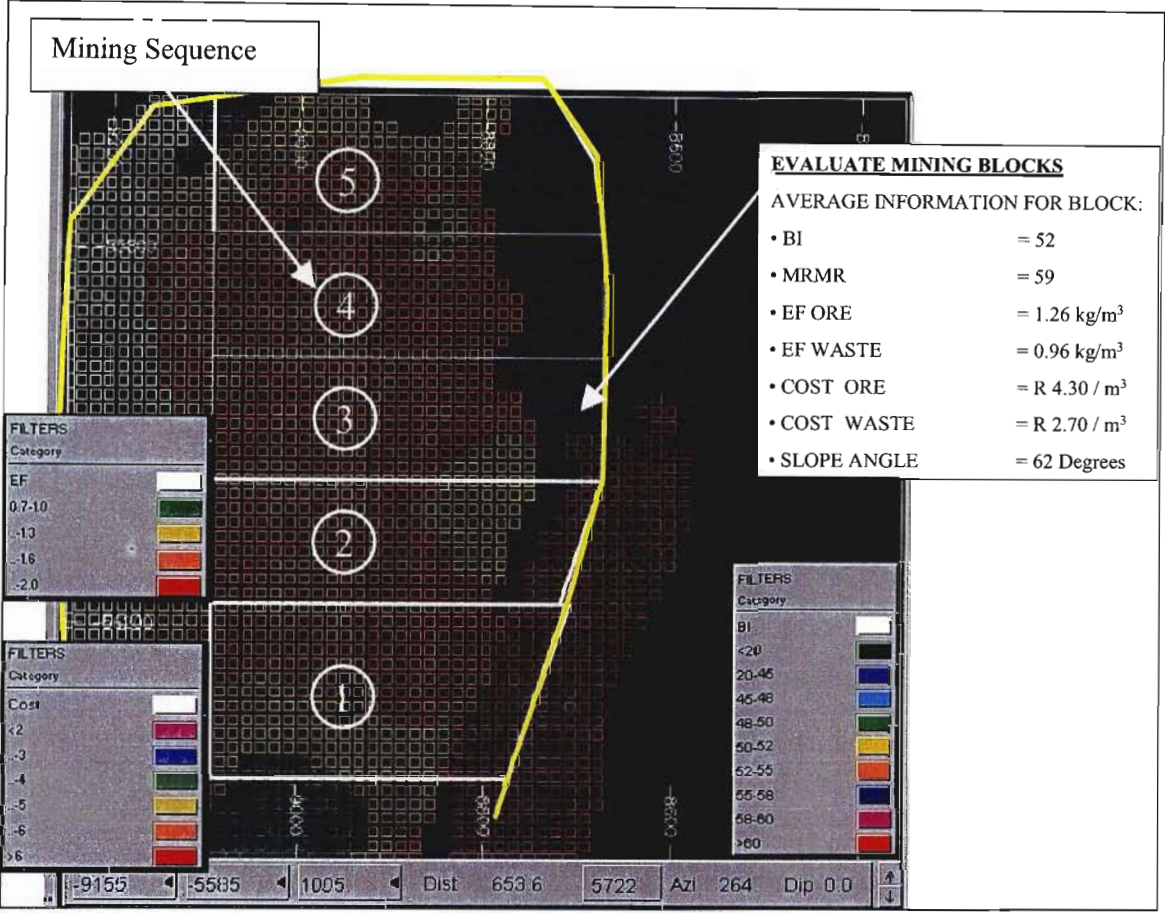


Figure 7.9 Plan view of slice through the fragmentation model on elevation 1,005 m, including future mining blocks to be queried for blast design. The filters illustrate the information associated with each colour-coded block.

7.6 Summary and Conclusions

Drilling and blasting is the first step in the physical mining process and therefore plays a major role in the performance of downstream functions. The inherent rock mass properties are one of the biggest unknown factors in blast design and play a major role in blasting costs and the productivity of the downstream functions. The 3D geotechnical model provides detailed rock mass information and was therefore applied to the blast design in order to improve the efficiency of blasting.

The Blastability Index provides the quantitative link between the *in-situ* rock mass conditions and blast design parameters. As with other rock mass rating systems the BI has gained widespread acceptance as a useful blasting tool since it was published in 1986. In addition to the geotechnical information the 3D model now contained the BI parameters and a BI value for each 15 m³ model cell.

The Kuz-Ram equation gives a prediction of the mean fragmentation resulting from the interaction of explosive energy and rock properties. At Sandsloot there was a detailed geotechnical model and known fragmentation targets, the Kuz-Ram equation was therefore reworked in order to produce a required energy factor equation, based on the known rock properties and fragmentation targets. The reworking of the Kuz-Ram equation to provide a required energy factor, effectively harnesses all the geotechnical information contained in the 3D model with the customer design targets, thereby providing a fragmentation model and dynamic blast design tool.

The consumption of explosives in mining is a variable cost and has a linear relationship between volume (kg/m³) and expenditure (R/m³). Based on the known drill and blast costs used at Sandsloot a correlation was developed between the required energy factor and cost per cubic metre. The model will therefore generate a required energy factor and an associated cost. This information is represented graphically in a design chart. The design chart is essentially a 2D representation of the 3D calculations and relationships, which are represented in the fragmentation model.

The fragmentation chart is a powerful design tool and the impact of the distinctly harder hybrid ore types is evident. The substantially higher costs associated with the different energy factors in ore and waste are also evident. The chart illustrates graphically the effect of the Blastability

Index on the required energy factor and the associated drill and blasts costs for set fragmentation targets.

The simple user front-end has enabled the fragmentation model to be used by personnel not skilled in Datamine® software thereby ensuring that the design tool is user friendly and functional. The fragmentation model was used on a day-to-day basis for all blast design and in the longer term it was used for blast planning and budgeting.

Chapter 7 has described the calculations used to convert the 3D geotechnical information into useful mining parameters. The 3D geotechnical model provides information well ahead of the mining face. The fragmentation model has optimised the blast design and planning process by firstly reducing the level of uncertainty associated with rock mass information; secondly by defining precisely the customer requirements and thirdly by combining the entire process into a 3D model that can be queried for any planned mining slot. The fragmentation model is a dynamic tool to ensure that the customer requirements described in Chapter 6 are consistently achieved. The significant benefits related to this dynamic blast design process are discussed in Chapter 8.

8 APPLICATION OF THE FRAGMENTATION MODEL

8.1 Introduction

Open pit mining involves a process of controlled destruction of the rock mass so that the waste may be stripped and the ore extracted. The blasting engineer is faced with the conflicting requirements of providing large quantities of well-fragmented rock for the processing plant, keeping drill and blast costs to a minimum and minimizing the amount of damage inflicted upon the rock slopes left behind. A reasonable compromise between the conflicting demands can only be achieved if the blasting engineer has a very sound understanding of the factors which control rock fragmentation, damage and slope stability (Hoek and Bray, 1981). This understanding was significantly enhanced through the use of a 3D geotechnical model, as discussed in Bye *et al.* (2002) and Bye (2002).

Chapter 3 has described the rock mass conditions present at Sandsloot and Chapter 4 the systems used to define the *in-situ* properties. Chapter 5 detailed the development of the interpolated 3D geotechnical model and Chapter 6 the definition of the optimum customer fragmentation targets. Chapter 7 discussed the development of the fragmentation model and the dynamic blast design tool used to ensure the consistent achievement of the customer targets by taking into consideration the variation in rock mass conditions. Chapter 8 will demonstrate the considerable productivity and financial benefits realised at Sandsloot during the eighteen-month model application period.

Blasting plays a more important role than just fragmenting the rock. It is the first step of an integrated comminution process leading from solid ore to a marketable product. According to Nielsen *et al.* (1995) blasting operations in the mining industry should be designed and optimised in order to obtain the lowest overall product costs. It is important to ascertain how primary drilling and blasting influences the costs of the subsequent steps in the production process and how far down the flow sheet blasting will have a significant influence on the economic results. These are questions posed by Nielsen *et al.* (1995) and Chapter 8 will illustrate how the fragmentation model is used to ensure the optimal fragmentation is consistently delivered for the benefit of the total mining operation.

According to Nielsen *et al.* (1995), the potential gains that can be realised by total blast optimisation from solid rock to a marketable product, is most often overlooked. The reason is

simply the way most mineral operations are organised. The drill and blast, excavation, transport and primary crushing of the ore is the responsibility of the mining department, whereas the responsibility for the secondary/tertiary crushing, grinding and further processing lies with the processing department. The two departments will try to make their own operations as cost-effective as possible, a practice which may easily lead to sub-optimisation when looking at the whole production process. Sandsloot has the same organisational structure as described above, however, it is not so much the structure of the organisation as the business focus that will define the companies efficiency. This research illustrates the improvement in business efficiencies that has been realised at Sandsloot, not from a restructuring but by assessing the companies total business process and defining a customer focus from the drill and blast department. This customer focus was facilitated by the use of a fragmentation model. Figure 8.1 illustrates a section through the block model with a list of the information associated with the queried cell.

This chapter deals initially with the processing plant and the mine to mill initiatives used to improve the plant's autogenous milling performance. The subsequent section deals with the productivity of the load and haul customer, through analysis of instantaneous loading rates. Historical performance will be compared to the results obtained over the eighteen-month period that the fragmentation model was applied, which was from January 2002 to June 2003. Appendix 7 contains a Microsoft PowerPoint presentation of the 3D geotechnical model as well as the Datamine® visualisation software for rotating and viewing the model file.

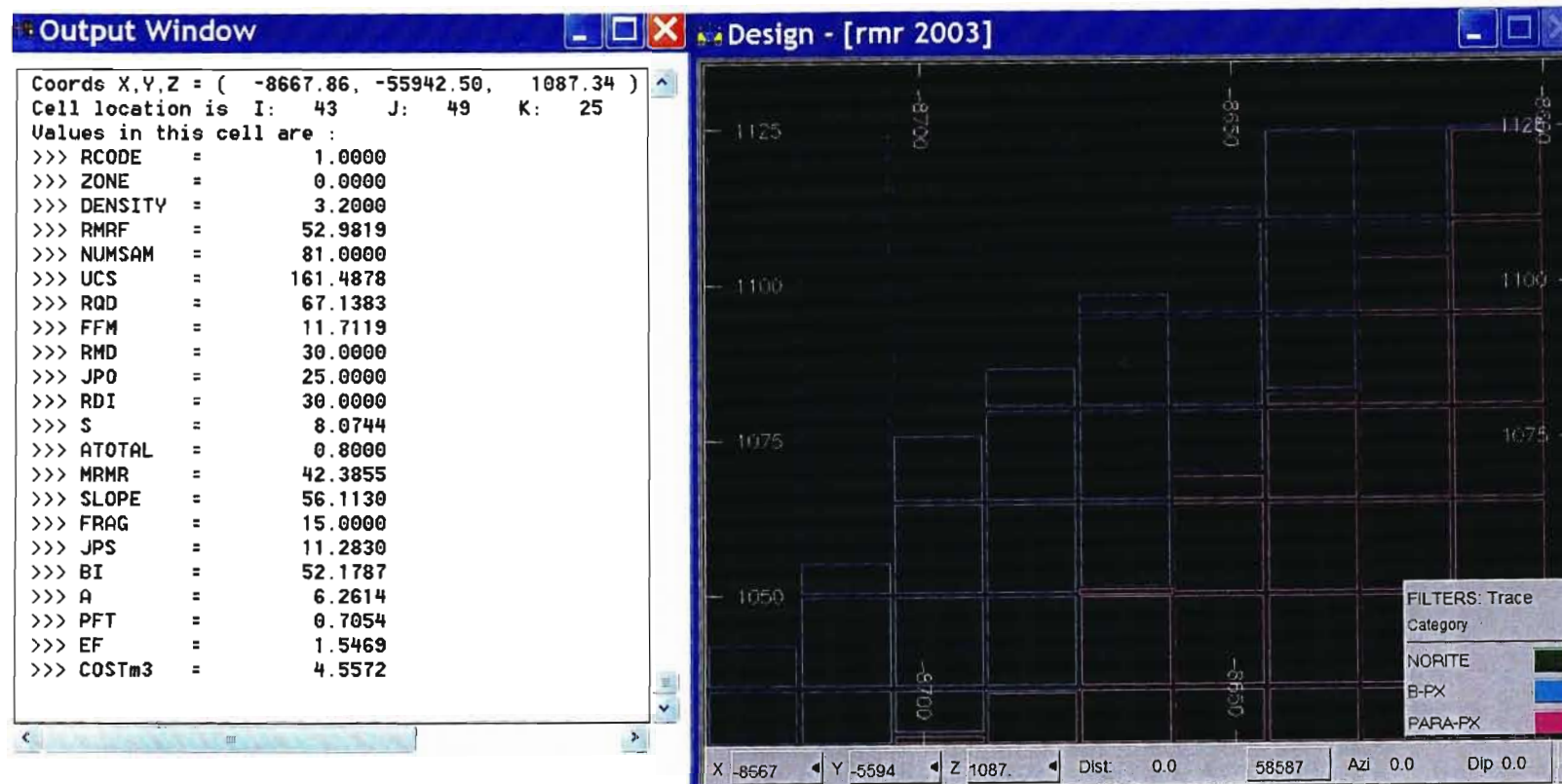


Figure 8.1 Section through the model illustrating the information available in each model cell. The information listed on the left is related to the cell with the white cross.

8.2 Mine to Mill Optimisation

Djordjevic (1998) defined good blast fragmentation as that which will be most instrumental for increased profitability of the entire mining process. Blast fragmentation not only has an effect on loading and hauling but most significantly on the efficiency of crushing and milling operations. The mill performance at PPL is strongly influenced by the size distribution and mechanical properties of the ore from the pit, especially as autogenous milling is utilised.

Minimisation of the costs for making a marketable product is the most likely criterion for deciding on the optimum blast design. However, this design may also lead to an increased capacity for the rest of the comminution system following after primary blasting. If any additional production can be sold, which is often possible, the increased revenues and operating profits may prove substantial. This may in turn shift the optimum blast design towards even higher energy levels.

Loading, crushing and milling rates are a function of blast fragmentation. By optimising blast design per geotechnical zone, rather than applying one uniform design, these productivity rates have been improved. Essentially, improved blast fragmentation can be achieved due to a better understanding of the interaction of blast energies with geological structures and the geotechnical characteristics of the rock mass.

In order to improve the autogenous grind (AG) mill performance, geotechnical information was originally provided from field mapping and based on this the blast design powder factors were increased substantially. The blast powder factors were increased in those blast patterns identified by field mapping to contain harder hybrid rock types. From 1997 to 2001 geotechnical information was provided manually to improve the blast design and thereby the fragmentation feed to the processing plant (Bye *et al.* 1988 and Bye 1988). Over this four-year period a mine to mill study was undertaken to determine the potential benefits of blasting a finer ore fragmentation so as to increase the plant throughput (Bye and Bell, 2001).

The manual method of providing geotechnical information for blast design was both onerous and could not be undertaken well in advance of the mining face. The development of the 3D geotechnical model therefore provided information so that blast designs could be adjusted proactively and thereby ensuring a more consistent mill feed.

The adjustment of blast powder factors and later the construction of separate fragmentation stockpiles, which allowed the plant to control the AG mill fragmentation profile, greatly assisted in increasing the milling rates. An average of 156 t/hr was achieved for the year 2001 up from 120t/hr prior to the plant expansion. It was, however, evident that there was still a great deal of fluctuation in the AG mill performance and that the plant was still very sensitive to the crusher feed received from the pit.

From the fragmentation analysis discussed in Chapter 6, it was determined that the ore blast patterns yielded a mean fragmentation of 150 mm at a powder factor of 1.77 kg/m^3 . The mean ore fragmentation target of 150 mm also corresponds with the plants stockpile management target of separating +/- 150 mm ore.

Analysis of the 2001 and 2002 AG Milling Performance

Figure 8.2 illustrates the required mill feed size to generate 146 t/hr and 194 t/hr of mill throughput respectively. It can be seen that the higher the percentage of -150 mm material, the greater the resultant mill production. Using a baseline production of 121 t/hr the additional monthly revenue associated with increased production has been plotted on the right hand axis. In summary, each additional tonne of mill production per month will generate an additional R299,856 of revenue for the company. The revenue value is obtained by calculating the number of platinum ounces liberated per tonne of ore, based on operational recoveries, and then multiplying these ounces by the market value. It must be noted that the revenue value was based on conservative recoveries and market prices.

The fragmentation model was applied from January 2002, whereby each ore blast was queried in the model to give the required blast design parameters, based on the customer requirement of a mean fragmentation of 150 mm. The resultant improvement in AG mill performance is illustrated in Figure 8.3. During 2001 the average milling rates were 156 t/hr while this improved to 163 t/hr during 2002. This 4.3% increase in productivity can be equated to a R 2,098,996 per month or R25,187,952 over the year.

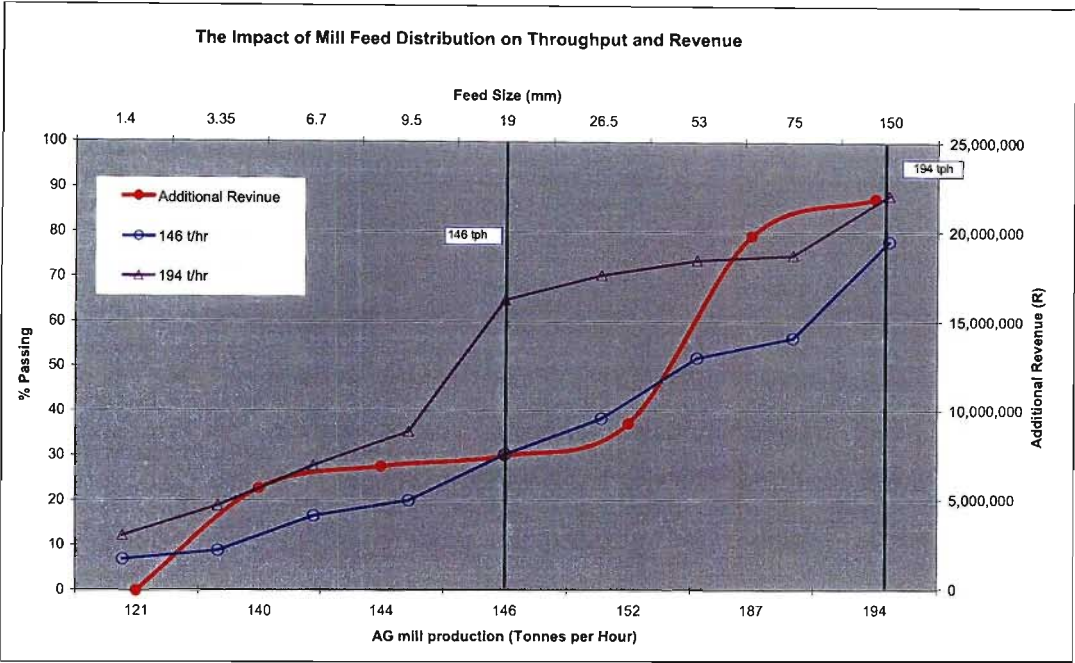


Figure 8.2 Graph illustrating the impact feed size has on mill throughput and revenue.

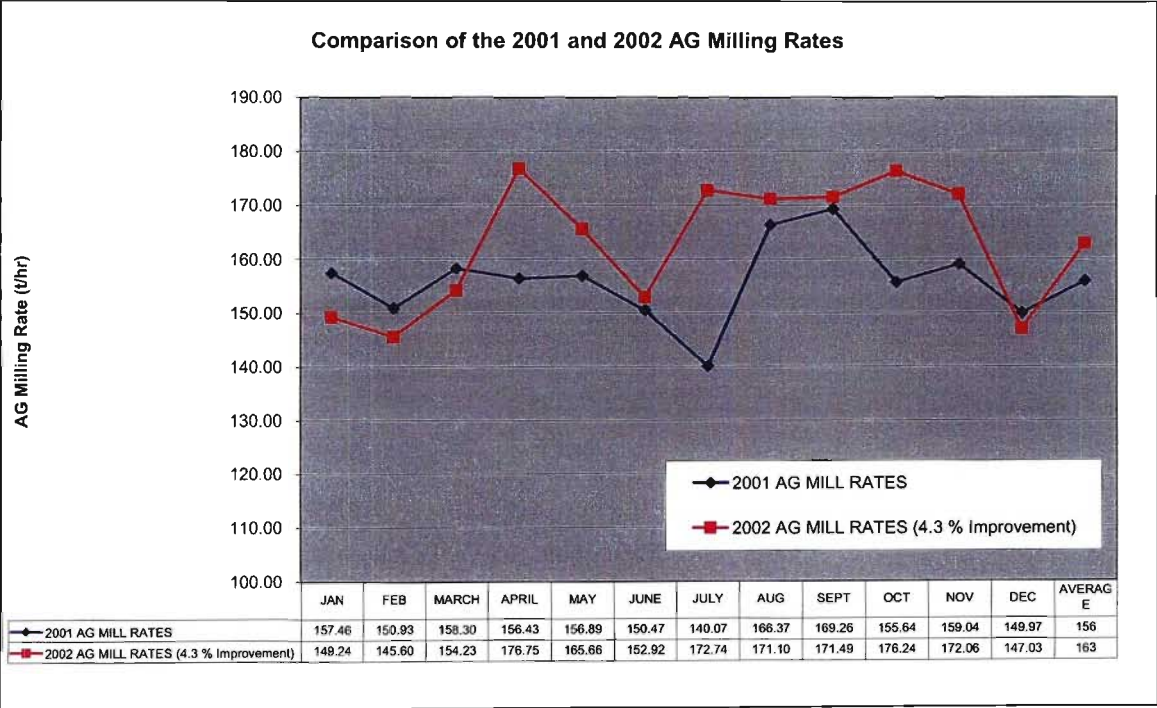


Figure 8.3 Actual AG milling rate comparison for 2001 and 2002.

Analysis of the 2003 AG Milling Performance

During January and February 2003 the fragmentation model was not used for blast design, due to changes in operational staff. During these months the milling rates dropped from 163 tph during 2002 to 143 t/hr, as illustrated in Figure 8.4. A standard blast design was used during early 2003 rather than the blast design parameters predicted by the model. The average powder factor used in ore during 2002 was 1.77 kg/m^3 , during January to February 2003 this was reduced to 1.3 kg/m^3 . Once the fragmentation model was applied from March to June 2003 the model prescribed a much higher blast powder factor between $1.74 - 1.89 \text{ kg/m}^3$. The impact of this change in blasting design is clearly evident in Figure 8.4 and Figure 8.5.

Figure 8.5 illustrates the impact the higher powder factors used from April to June 2003 had on the mill feed fragmentation profile. On the 14th of March and 29th of May two belt cut samples were taken from the conveyor belt exiting the primary crusher. The dashed blue line illustrates the ideal plant fragmentation profile and the solid purple and blue line the actual fragmentation. There is a clear shift of the fragmentation curve towards the ideal from March to May 2003.

The AG mills are very sensitive to the fragmentation received from the open pit and this has a major impact on the productivity of the processing plant. After application of the fragmentation model to blast design, the milling rates improved from 143 t/hr to 173 t/hr, representing a 16% improvement. If the 173 t/hr milling rates can be sustained for the remainder of 2003 the increased productivity from 2002 will equate to an additional monthly revenue of R 2,908,610.

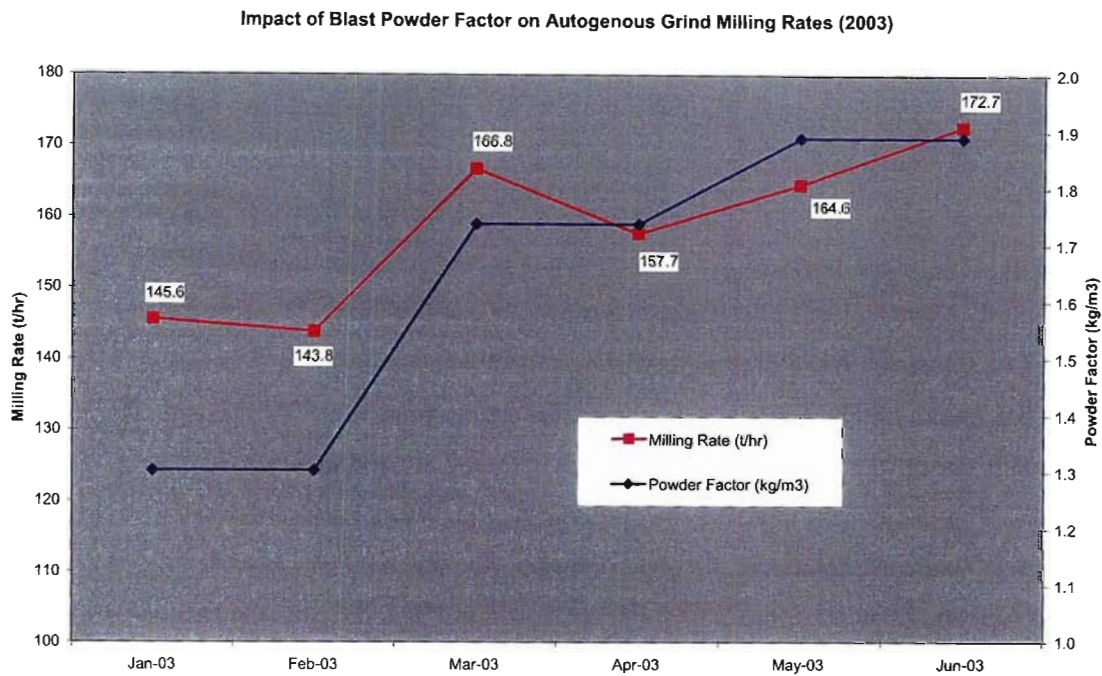


Figure 8.4 Blast design powder factors and AG mill performance for 2003.

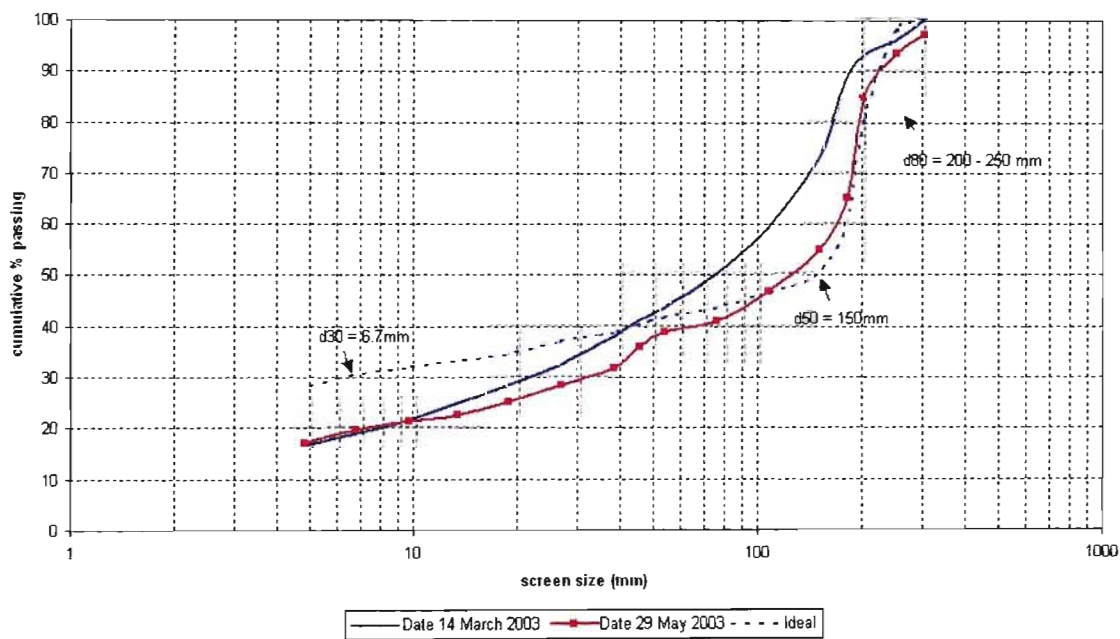


Figure 8.5 Mill feed fragmentation profiles obtained from belt cut samples for March and May 2003.

Primary Crushing Performance Analysis (2003)

In conjunction with the AG mill performance study undertaken during 2003, an analysis of the impact of blast fragmentation on primary crushing performance was also investigated. According to Nielsen (1995) the elastic strain energy generated by blasting will, together with the gas energy, lead to the primary fragmentation of the rock, while a portion of the strain energy will generate micro-cracks. Revniztev (1988) claimed that the micro-cracks generated by explosives may have a total surface which is one to two times larger than the total surface of the primary fragmentation itself. These cracks will influence and enhance the later crushing and grinding of the rock material.

The impact of the model prescribed higher blast powder factors is presented in Figure 8.4 and Figure 8.5, which compare the autogenous milling rates, primary crushing costs and the blast powder factor for the first six months of 2003. There is a clear correlation between the higher blasting powder factor and the crushing and milling performance.

Bond's Third Law of Comminution

Bond's Working Index (BWI) measured in kWh/tonne is a measure of how much energy is required by a comminution circuit to reduce one tonne of rock to the desired fragment size. Bond's Third Law of Comminution (Bond, 1961) describes the association between the Bond Working Index of the primary crusher feed and the energy consumption required to reduce that feed size to the desired post-crushed product size. Alternatively this can be described as the crushing energy required to convert the pit production fragmentation to the post-crusher fragmentation size. The power draw of a crusher is dependant upon the ore feed size and the size reduction through the machine. This relationship is defined in equation 8.1.

Eq. 8.1
$$W = [(10 \times Wi) / (P_{80})^{0.8}] - [(10 \times Wi) / (F_{80})^{0.5}]$$

W = Energy consumption, kWh/tonne

Wi = Bond's Working Index, kWh/tonne

P80 = Product size, 80 per cent passing, micron

F80 = Feed size, 80 per cent passing, micron

Optimised blasting should aim at balancing the use of chemical and electrical energy throughout the whole production process in order to give the lowest cost for making a marketable product. Table 8.1 shows the impact of the primary crusher feed size on energy consumption and crushing costs using Bond's Third Law of Comminution. During 2003 the blasting costs were increased from R 1.31 per tonne to R 1.89 per tonne. It is clear from the table that a small additional expenditure on blasting results in significant crushing savings.

Figure 8.6 illustrates how the increase in blast powder factor during 2003 reduced the crusher feed size from 390 mm to 260 mm and how this reduction impacted on the cost per tonne crushed. The crusher feed size was calculated from the Kuz-Ram equation (Cunningham, 1986) and the energy consumption and crushing costs from Bond (1961), using equation 8.1.

Table 8.1 shows the reduction in crushing costs from R 0.72 to R 0.31 during this same period. This purely relates to a saving in energy consumption or power draw on the crusher. As the mine crushes 400,000 tonnes per month, the reduction in the costs due to finer fragmentation and a lower power draw on the crusher was R 168,877 per month.

The additional drill and blast costs incurred in order to deliver the finer fragmentation were R 0.58 per tonne and R 231,538 per month. This additional cost is virtually recovered on the energy savings from the primary crusher alone. The significant financial benefits achieved in the AG milling process have been discussed and the loading efficiency improvements will be detailed in the subsequent section. There is clearly a significant business advantage to be obtained by developing a fragmentation model and thereby ensuring the drill and blast customers receive their design feed, by taking into account variations in the rock mass conditions

Table 8.1 Impact of primary crusher feed size on energy consumption and crushing costs.

DATE	Bond's Working Index (Wi)	Feed size (F ₈₀)	Product Size (P ₈₀)	Energy Consumption (W)	D&B Costs (R/t)	Crushing cost (R/t)
Jan-03	24	390	200	4.82	R 1.31	R 0.72
Feb-03	24	390	200	4.82	R 1.31	R 0.72
Mar-03	24	300	200	3.11	R 1.74	R 0.47
Apr-03	24	300	200	3.11	R 1.74	R 0.47
May-03	24	260	200	2.09	R 1.89	R 0.31
Jun-03	24	260	200	2.09	R 1.89	R 0.31

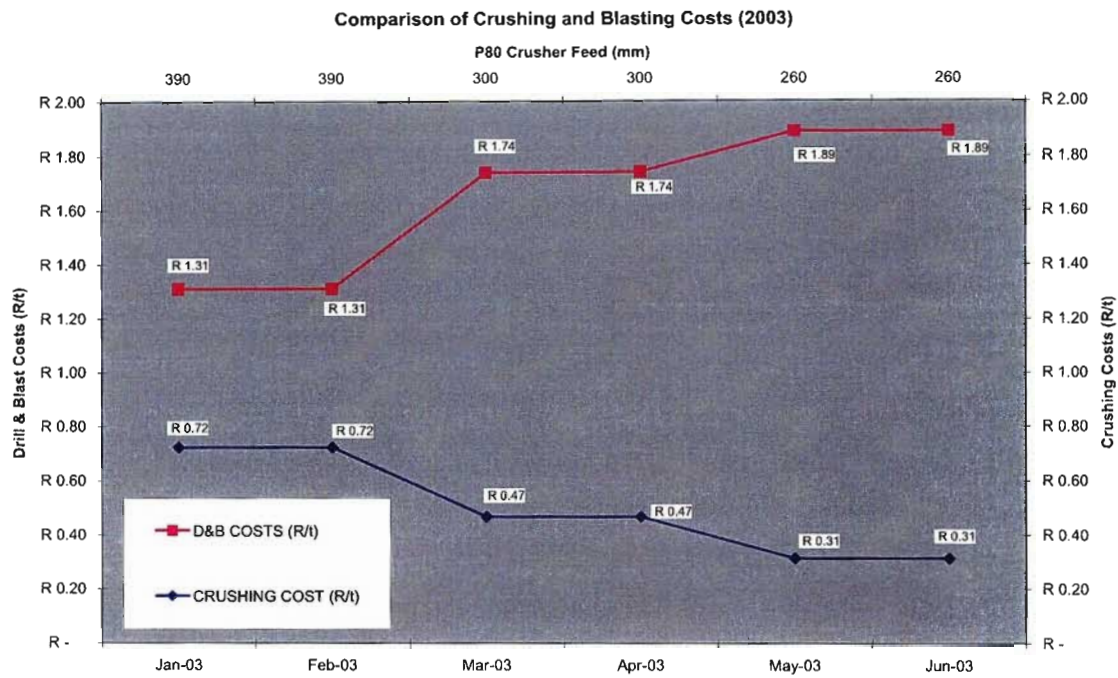


Figure 8.6 Comparison of blast powder factor and primary crushing costs for 2003.

8.3 Production Loading Optimisation

Blasting performance can be measured by means of an instantaneous loading rate and this was used to assess the performance of the load and haul customer. Recorded in tonnes per hour, it is a measure of the ease with which a shovel digs the blasted muckpile. This loading rate takes into account only the time the shovels bucket spends in the muckpile and excludes all other operational delays. The Modular Mining Truck / Shovel Dispatch® system is used to continuously measure the instantaneous loading rate.

Based on a time and motion study of good loading conditions, an RH200 shovel with a bucket containing 40 tonnes will fill an 120 tonne truck in 3 passes, taking 135 seconds, which equates to a loading rate of 3,200 t/hr. It follows that the finer the fragmentation and the looser the muckpile the quicker the shovel will fill the truck and the higher the instantaneous loading rate will be.

From January 2002 through to June 2003 the fragmentation model was used for blast design so as to deliver the correct blast fragmentation to the load and haul department. Table 8.2 shows the improvement in instantaneous loading rates over the 18-month model application period. From 2001 to 2002 the loading rates increased by 5.5% and the 2002 benchmark was sustained during 2003. Figure 8.7 illustrates the average loading rates from 1999 to 2003. There is a clear distinction in performance before and after the fragmentation model was applied. The variability in loading rates are clearly evident prior to 2002 and this is due to the blast designs not taking into account the variations in rock mass conditions. After 2002 the loading rate is above the design target every month.

Figure 8.8 and 8.9 illustrate graphically the loading performance for 2001 and 2002. In excess of 1,000 shifts were measured in order to compare the actual performance. It is clear from Figure 8.8 that the loading rates during 2002 show less variability and are consistently above the 3,200t/hr target. This can be directly attributed to the consistent quality of the fragmented muckpiles delivered during 2002.

Table 8.2 Analysis of the instantaneous loading rates from 2001 to 2003.

Year	Average Instantaneous Loading Rate (t/hr)	% Average Improvement
2001	3,249	-
2002	3,437	5.5%
2003	3,469	0.1%

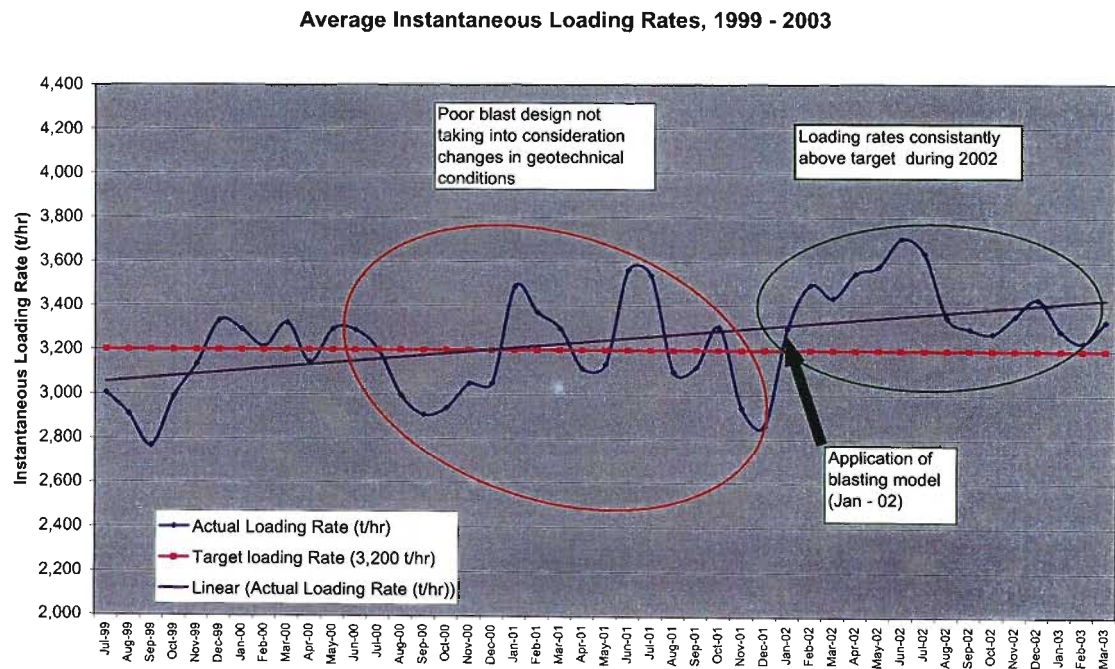


Figure 8.7 Loading rates showing the impact of the fragmentation model for blast design.

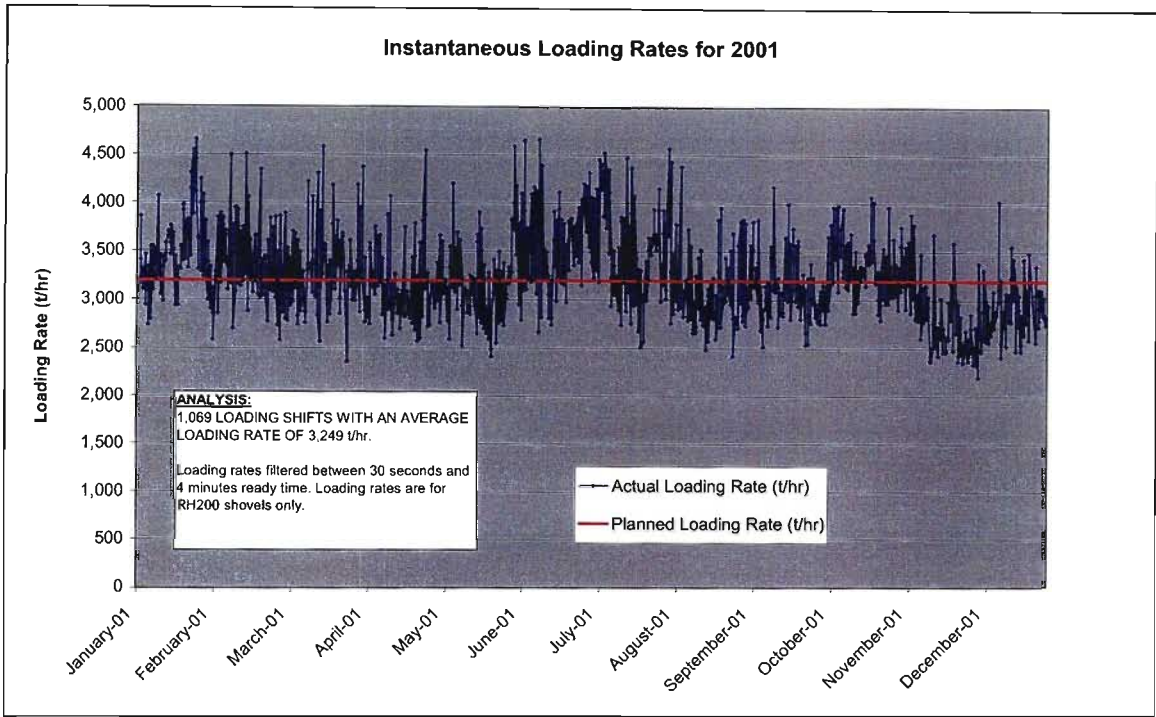


Figure 8.8 Instantaneous loading rates recorded by shift for 2001.

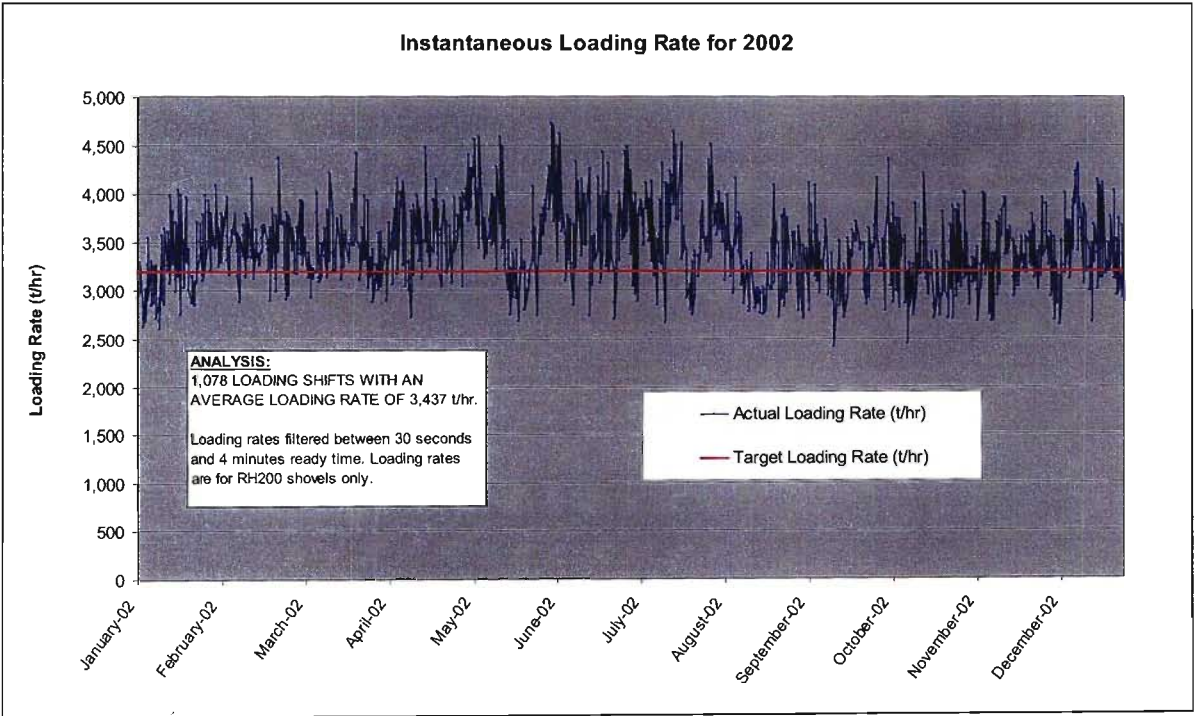


Figure 8.9 Instantaneous loading rates recorded by shift for 2002.

A detailed analysis of the performance of the drill and blast department was undertaken during 2002. Figure 8.10 illustrates a comparison of blast powder factor, loading rate and drill and blast costs for each month of the year. The graph only refers to the blasts designed in waste as these blasts accounted for 80 % of the blast tonnage during 2002. As can be seen the blast powder factor was reduced during the course of the year to take into account the changes in rock mass conditions where mining was being undertaken. The result was a reduction in the drill and blast costs from R 1.30 to R 1.07 per tonne. The loading rates during this period are also presented and show a correlation with the adjustments in blast powder factor. It is important to note that throughout the powder factor adjustments the loading rates remained above the design target and this illustrates clearly the power of the fragmentation model as a dynamic blast design tool.

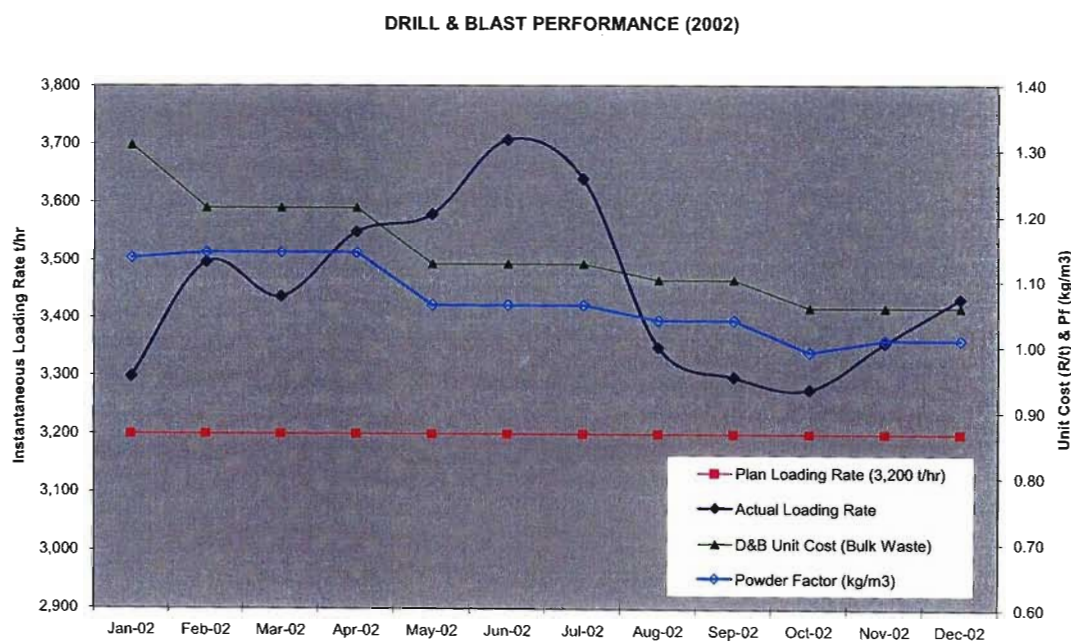


Figure 8.10 Graph illustrating the performance of the drill and blast department in terms of costs and instantaneous loading rates, related to powder factor.

8.4 Summary and Conclusions

The application of the fragmentation model to blast design and the resultant improvements in the processing and load and haul departments has been clearly demonstrated. Figure 8.11 illustrates the 8.5% and 8.8% improvement in loading and milling rates, respectively from 2001 to 2003. It must be stressed that these are actual production figures measured over a two and a half year period and therefore represent a significant record of performance.

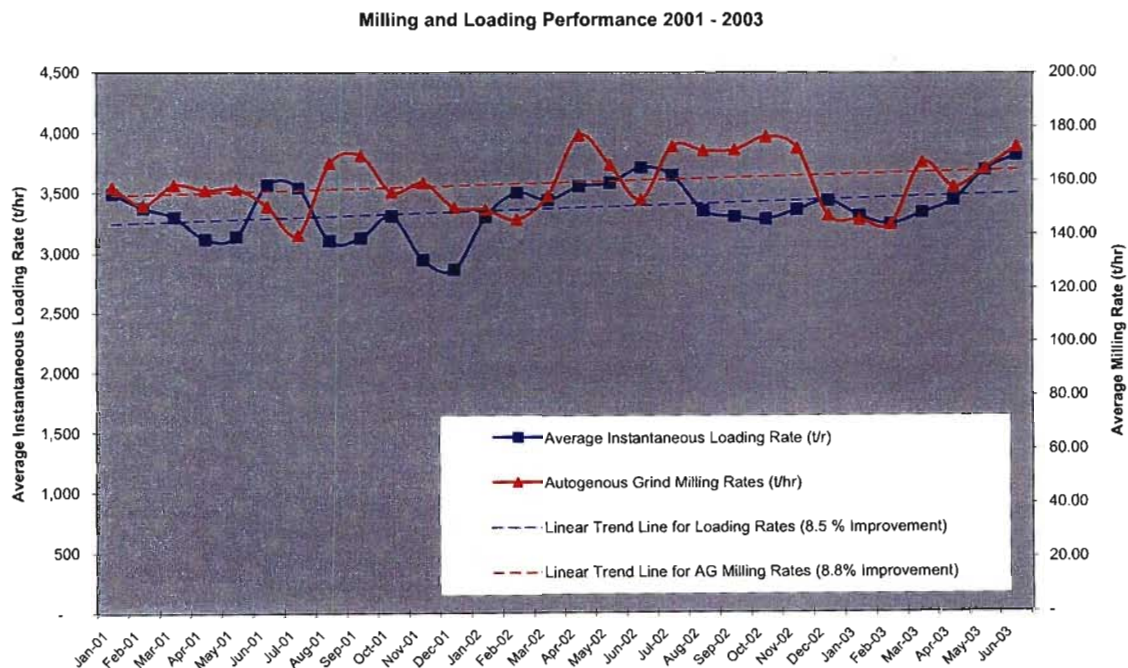


Figure 8.11 Loading and milling performance from 2001 to 2003.

Figure 8.12 analyses all the customer performance measures for the period from January to June 2003. There is a clear improvement across all the performance indicators, which include the following:

- Average plant milling rate (AG and Ball mills) 18% improvement
- Average AG milling rate 16% improvement
- Average instantaneous loading rate (Ore and Waste) 13% improvement
- Average instantaneous loading rate (Ore) 11% improvement

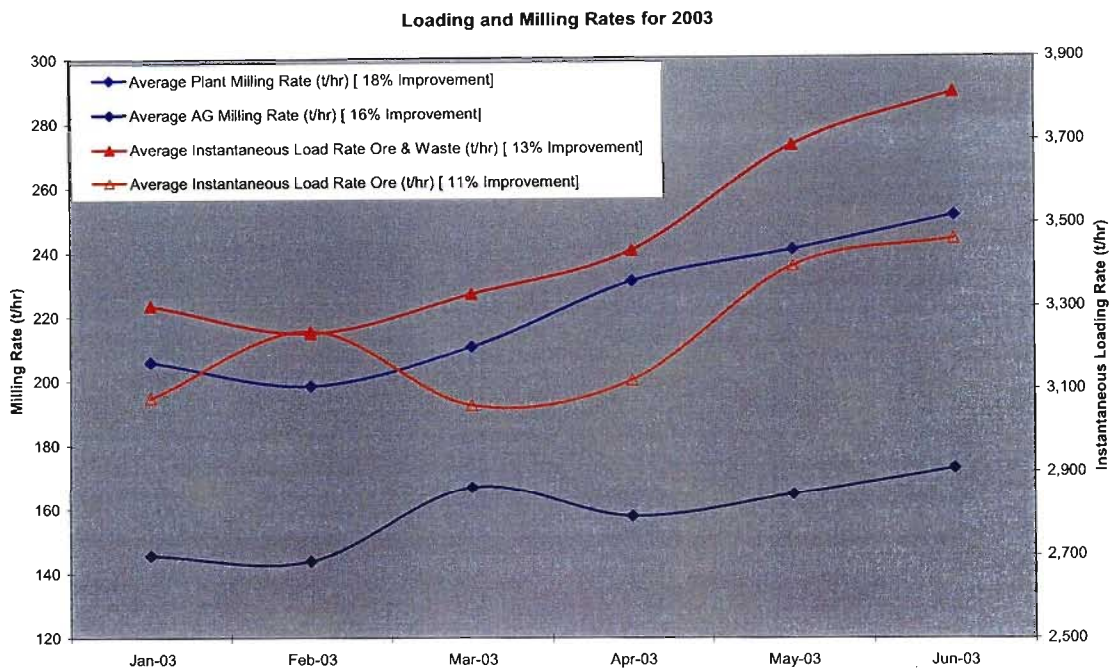


Figure 8.12 Graph illustrating the performance of the drill and blast department's two customers during 2003. The loading rates include ore and waste and the milling rates include both the AG and ball mills.

These performance improvements represent a substantial value add to the overall business and the associated financial benefits are significant in terms of millions of Rand per month. Just the improvement in the AG milling rates during 2002 accounted for R 2,1 million per month in additional revenue.

Chapter 8 has demonstrated the benefits gained through the application of a fragmentation model, which derives rock mass information from the 3D geotechnical model. A further application of the 3D geotechnical model is discussed in Chapter 9. This chapter describes the development of a slope stability model from the geotechnical parameters contained in the 3D geotechnical model. The resultant optimisation of the Sandsloot final pit design, based on this model is also presented.

9 SLOPE DESIGN MODEL

9.1 Introduction

Chapter 8 has demonstrated the opportunities for business optimisation that a 3D geotechnical model offers. This is primarily due to the enhanced understanding of the rock mass properties, and their variability across the mining area, which the geotechnical model offers. A further and most obvious application of the 3D geotechnical model was for the design of the Sandsloot pit slopes. Figure 9.1 illustrates the slope optimisation processes, based on the 3D geotechnical model.

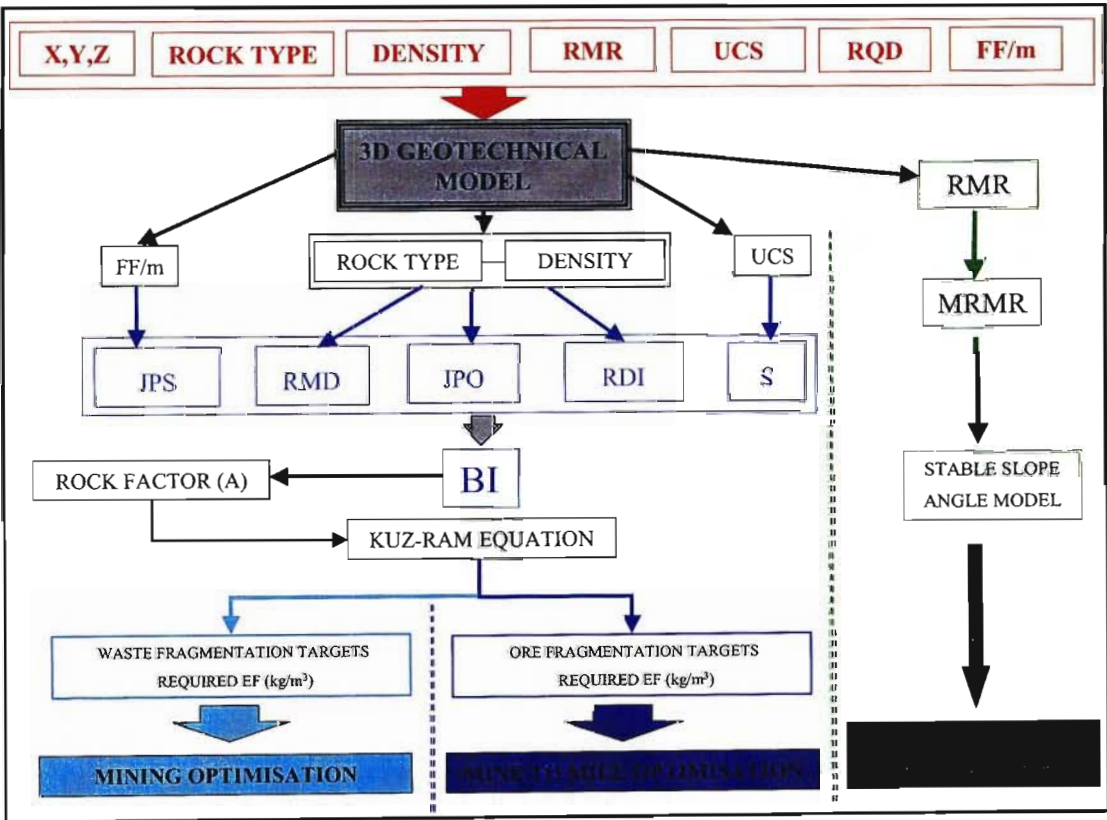


Figure 9.1 Flow diagram illustrating the process used for slope optimisation.

The delineation of similar geotechnical domains or zones is an accepted practice in geotechnical engineering and slope design parameters are then defined for each of these domains. The definition of these domains is generally broad-based and restricted to dominant rock types or major structural features. Initial slope design at Sandsloot was based on limit equilibrium methods and applied to the pit slopes based on the dominant rock types, as is the case with many open pit operations. The stable slope angles were based on rock mass rating values and an

average slope angle was applied to the average rock mass conditions present in that particular domain. Additionally, the slope design was based on the information represented in 2D cross sections. This method was later enhanced by the development of slope design charts for each rock type, which enabled more detailed slope design. A major shortcoming of these methods is that the data collected is only representative of a visual mining face or isolated borehole and does not take into account the 3D rock mass conditions. The rock mass information used for design is therefore limited and often results in overly conservative or high-risk slope profiles, as the 3D rock mass conditions are not accounted for.

The 3D geotechnical model at Sandsloot offered the opportunity to undertake slope design based on a significant set of geotechnical parameters for every 15 m³ model cell covering the entire mining area. The model would therefore aid the engineer in defining an optimum slope configuration based on the 3D rock mass conditions represented in the model. The development of a slope design model based on interpolated geotechnical information represents a novel design tool not previously utilised in the mining industry.

The development of the slope design model provided the opportunity to move away from one design process for the entire pit and customisation of slope designs and configurations were then developed to cater for local variations in the rock mass condition. The availability of the geotechnical information in 3D and the improved level of confidence of that data resulted in a slope optimisation of the final pit slopes. By undertaking numerical modelling based on the enhanced geotechnical database the final walls were optimised by three degrees, resulting in revenue increase for the mine in excess of R 900 million. The slope optimisation was linked to a risk-reward design approach, which was made possible by the confidence in the geotechnical information used for the design options.

9.2 Development and Application of the Slope Design Model

Figure 9.1 illustrates the third phase of the mining optimisation process involving the geotechnical model. The flow diagram illustrates how the modelled RMR values are converted to mining rock mass rating (MRMR) values, which can then be used in recognised design charts. The modelled RMR data contained in each model cell is converted into a stable slope design angle for the rock mass conditions present in that cell.

Prior to the development of the 3D model, empirical design charts were created for stable slope height versus slope angle for the dominant rock types occurring in the pit. The graph was developed from the Haines and Terbrugge (1991) chart, which allows estimation of a stable slope angle from MRMR data (Figure 9.2). Instead of applying one design to the whole pit, a unique stack configuration and optimised slope angle were developed per geotechnical zone, taking into account practical constraints. This can be seen in Figure 9.3, which illustrates the stable slope height, with a factor of safety (FOS) of 1.2, for the different rock types present at Sandsloot. The chart also illustrates the stability envelope of the norite hanging wall, developed from the numerical modelling, as discussed in Section 9.3. Apart from slope optimisation the charts were used to provide an estimate during pit design, of the stable stack angles that are possible for the various rock types occurring in the pit. During daily operation the chart was useful for providing a rapid means of estimating stable slope heights for each rock type or zone within the pit.

Geotechnical field mapping or core logging using the MRMR system will yield a rock mass rating value for that specific area mapped. The stable slope angle for any slope height can then be derived by using the Haines and Terbrugge (1991) design charts. This can be a time consuming process and provides a point value on a 2D cross section. An addition to the geotechnical model functionality was the automatic calculation of the stable stack angle, which could be viewed in 3D. The resultant slope design model has a stable slope angle for each model cell and therefore slope design could be undertaken more accurately rather than applying an average design angle to an entire highwall.

The functionality was built into the model by calculating a stable inter-ramp angle for a 100 m stack. The stable angle is calculated from the MRMR values within the model and a design factor of safety of 1.2 is applied. The equation (Eq. 9.1) for deriving a stable slope angle was developed from the Haines and Terbrugge (1991) design chart using the graph in Figure 9.4.

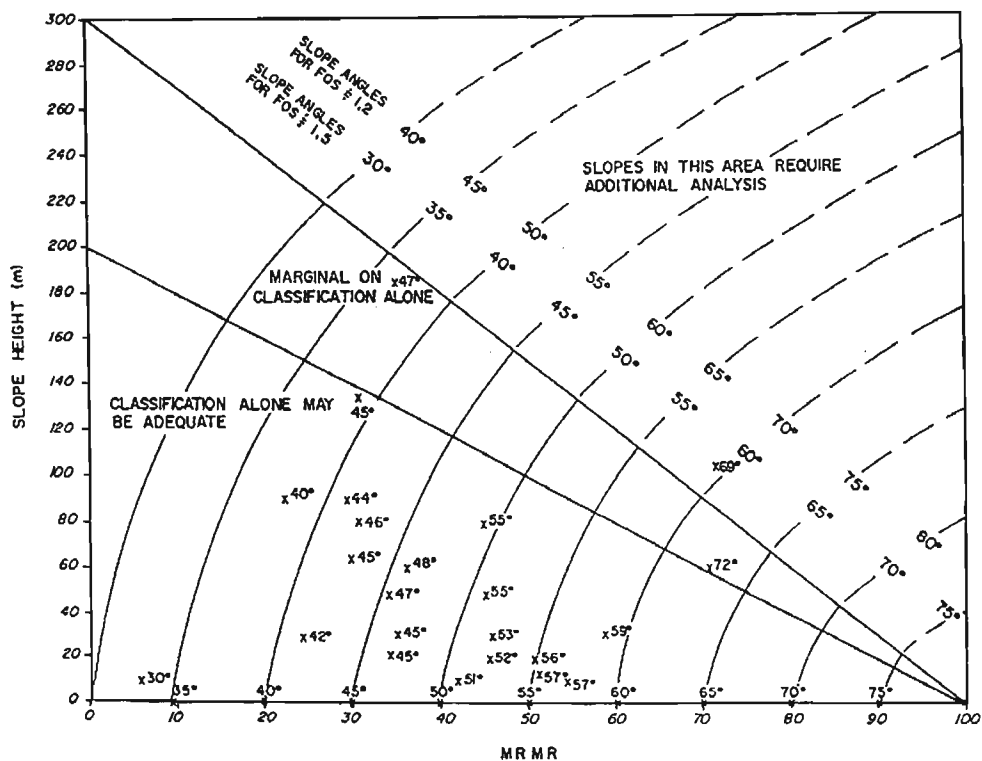


Figure 9.2 Design chart for the determination of stable slope angles from MRMR classification data, after Haines and Terbrugge (1991).

Eq. 9.1 Slope = $(0.4456 \times \text{MRMR}) + 37.226$

 Slope = Stable slope angle for a 100 m slope at FOS of 1.2

 MRMR = Mining rock mass rating value (Laubscher, 1990)

A mining adjustment was formulated for each rock type occurring within the pit. The weathering, stress and blasting adjustments were selected specifically for each rock type, while the joint orientation adjustment was taken into account by determining the typical direction of the mining face and the dominant jointing for each rock type. These adjustments are incorporated into the geotechnical model calculations and for each modelled RMR value the relevant mining adjustment is applied and the stable slope angle calculated from equation 9.1. The total adjustments are listed in Table 9.1. For example, a RMR value of 60 contained in the block model is adjusted down to a MRMR value of 52.2. Using equation 9.1 a stable slope angle of 60.5° is calculated from the MRMR value of 52.2 contained in that particular model block. These calculations are run automatically for each model block within the 3D slope design model.

Table 9.1 Mining adjustments, for the slope design model applied to the rock types present at Sandsloot.

Rock Type	Mining Adjustment
Norite	0.87
Pyroxenite	0.80
Parapyroxenite	0.90
Serpentinised parapyroxenite	0.95
Calc-silicate	0.75
Feldspathic pyroxenite	0.95
Quartz-feldspar vein	0.87

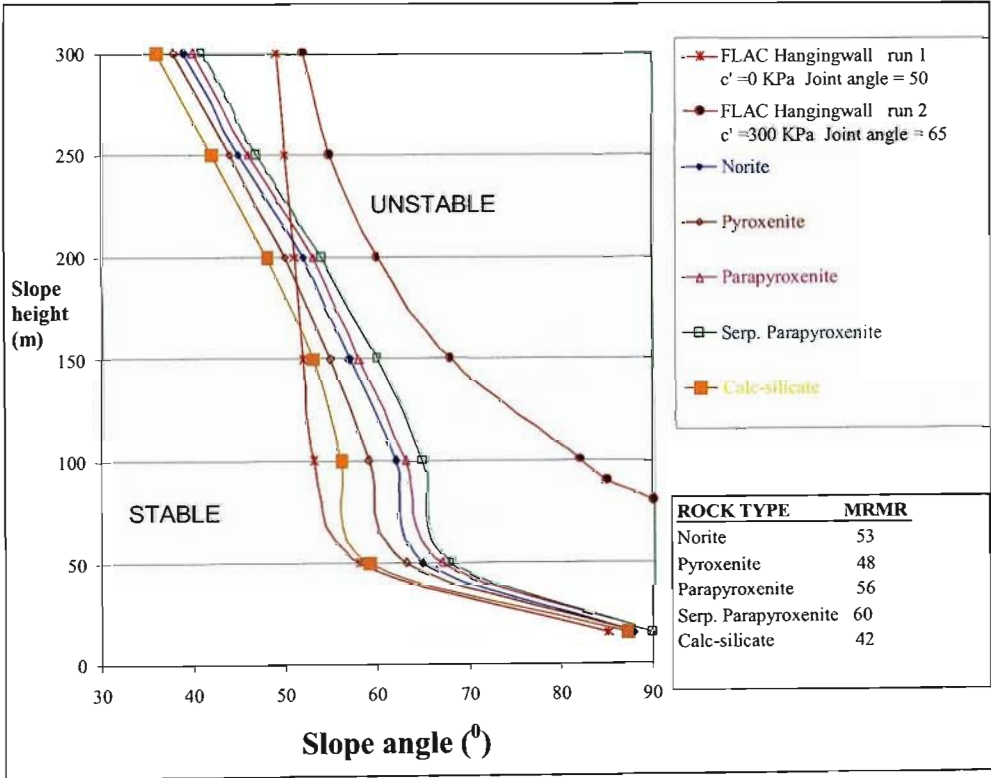


Figure 9.3 Slope design charts for Sandsloot rock types based on MRMR and FLAC modelling.

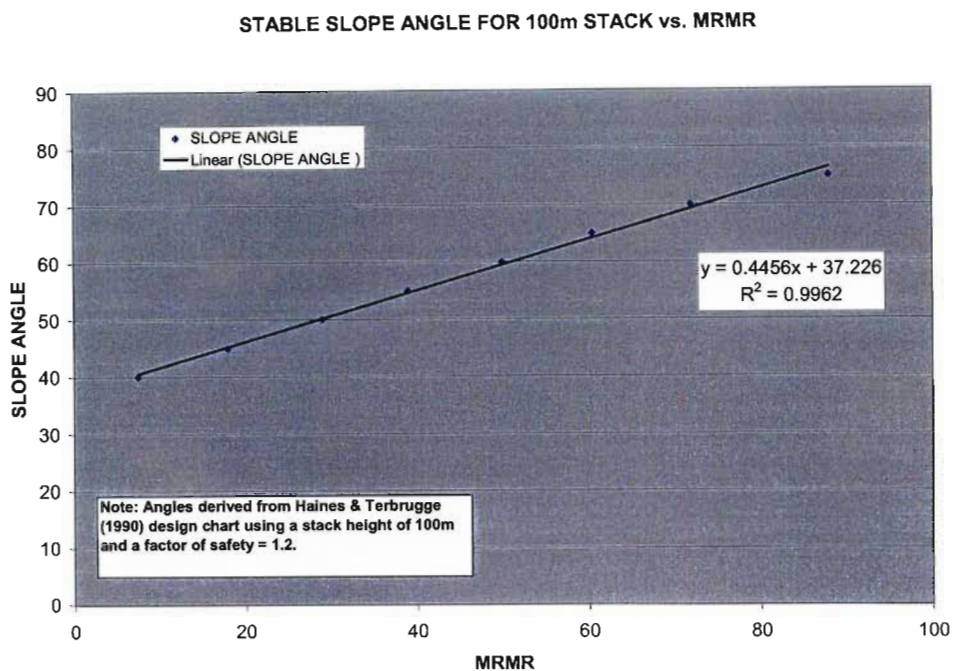


Figure 9.4 Stable slope design chart for 100m stacks, incorporated in the 3D geotechnical model.

Figure 9.5 illustrates a section through the slope stability model, which is filtered on the stable stack angle. The cooler colours (blues) represent poor quality rock mass conditions and flatter slope angles while the hotter colours (reds) propose steeper stack angles. Figure 9.6 illustrates an oblique view of the final design pit with a colour-coded wireframe, of the slope stability model, draped onto the design slopes. Datamine® allows a wireframe to be generated where the block model intersects the pit design limits. The model blocks are evident on the wireframe and are filtered based on the stack angle value. For example, in the northwest corner of the design pit, light green cells are evident indicating poorer rock mass conditions and a stable stack angle of 55 degrees. The Datamine® functionality enabling the creation of model intersection wireframes provides a powerful design tool whereby any area or interim design slope within the open pit can be visualised and the design adjusted accordingly. Future work will enable this adjustment of the slope design to be done automatically by the pit design software, based on the geotechnical properties contained within the 3D geotechnical model.

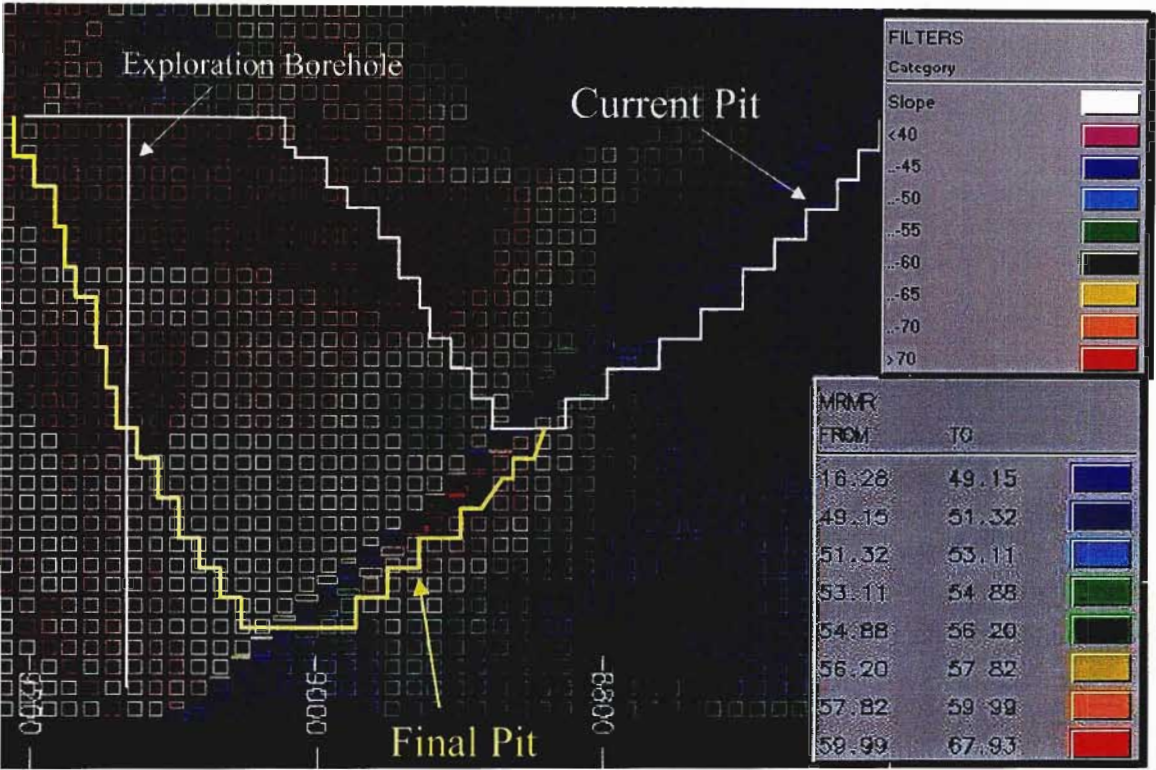


Figure 9.5 Section through the slope design model, colour filtered on the 100m stable slope angle.



Figure 9.6 Wireframe sliced through the 3D slope stability model illustrating the appropriate stack design angle for the various areas of the pit.

9.3 Numerical Modelling and Design of Final Slopes

In newly developed open pits initial slope designs are generally based on sparse information due to lack of geological exposure and tight development budgets. As the pit develops, design configurations can be adjusted to accommodate identified failure mechanisms and thereby design slopes are more stable and an optimised pit design is developed. At Sandsloot there has been an evolution of slope configurations due to improved geotechnical information and evolved mining processes. Bye *et al.* (1999) discusses the benefits associated with optimising slope designs and limit blasting programmes. The paper details the economic benefits that can be derived from the implementation of a successful limit blasting programme in terms of slope stability and stripping ratios.

After analysis of the line survey, face mapping, shear testing and borehole rock mass classification data collected from the geotechnical programme, it was observed that the norite hangingwall was composed of consistently good quality rock. This coupled with the relatively homogeneous nature of the norite rock type would enable the hangingwall to support potentially steeper angles than the current design. Subsequent Fast Lagrangian Analysis of Continua (FLAC) modelling of the pit slopes was undertaken based on the information derived from the geotechnical programme.

In conjunction with SRK (1998) a rigorous analysis was carried out on the hangingwall of the Sandsloot Pit in order to re-evaluate aspects of stability on bench, stack and overall slope angles with the enhanced database. Analysis was carried out with the aid of computer simulation models utilising FLAC Version 3.30 (Itasca Inc.). FLAC is numerical modelling software that uses an explicit finite difference code that facilitates simulation of the behaviour of structures constructed from soils, rock and other material, which may undergo plastic deformation when the yield limit is exceeded. In the FLAC model, materials are represented by zones, which form a grid, fitting the shape of the excavation to be modelled with each element of the grid following a linear or non-linear stress-strain law in response to the applied forces and boundary restraints.

FLAC solves the equations of motion at each grid point in a time stepping manner, thus enabling the development of yield or plastic flow to be examined. It should be noted that the time steps used in FLAC code are not in real time, except in the case of seepage flow modelling,

which was not used in this investigation (SRK, 1998). Two different constitutive material models were used to assess the behaviour of the hangingwall norite slope:

- i). The Mohr-Coulomb plasticity model where the plasticity formulation assumes an elastic, perfectly plastic solid, in plane strain, which conforms to a Mohr-Coulomb yield condition and non-associated flow rule. The model has been used for various failure simulations using rock mass parameters based on the MRMR rating system and laboratory testing values.
- ii). The ubiquitous joint model, which is an isotropic plasticity model, assumes a series of weak planes, embedded in a Mohr-Coulomb solid. This was done to represent the continuous nature of joint set one present in the hangingwall. The data input into the FLAC ubiquitous joint model is presented in Table 9.2. Yield may occur in the solid or along a slip plane, or both, depending on the material properties of the solid and plane, the stress state, and the angle of the slip plane. The model was used for various failure simulations using intact and natural joint rock parameters.

The stability criteria applied to the model are based on three general behaviour models:

- A progressive behaviour model (failure)
- Creeping (steady state)
- A regressive behaviour model (stable)

In the case of a progressive behaviour model (failure), slope displacements or velocities continue to accelerate to a point of final collapse. In the case of creep, slope displacements or velocities remain constant with time, while in the case of regressive behaviour the slope displacements or velocities decelerate and finally stabilise.

Using the FLAC program a sensitivity analysis was undertaken by using a number of ubiquitous joint model runs to take into account the effect of the critical joints on slope stability. Model runs with variations in joint cohesion and critical joint angle were undertaken in order to determine parameter sensitivity and a stability envelope for the norite hangingwall. A critical joint dip variation of 50° - 65° was modelled as well as a cohesion variation from 0kPa - 300 kPa. Figure 9.7 illustrates the stability envelope, of the norite hanging wall, developed from the series of FLAC analyses.

The results of the FLAC modelling proved that the overall slope angle for a 300 m slope could be increased by three degrees, from 51° to 54° (Bye and Bell, 2001). The optimised slope design

has extended the life of mine by two full benches thereby allowing the mine to accrue over R900 million in additional revenue. The slope optimisation process would not have been possible without the detailed geotechnical information that was collected and later used to build the 3D geotechnical model.

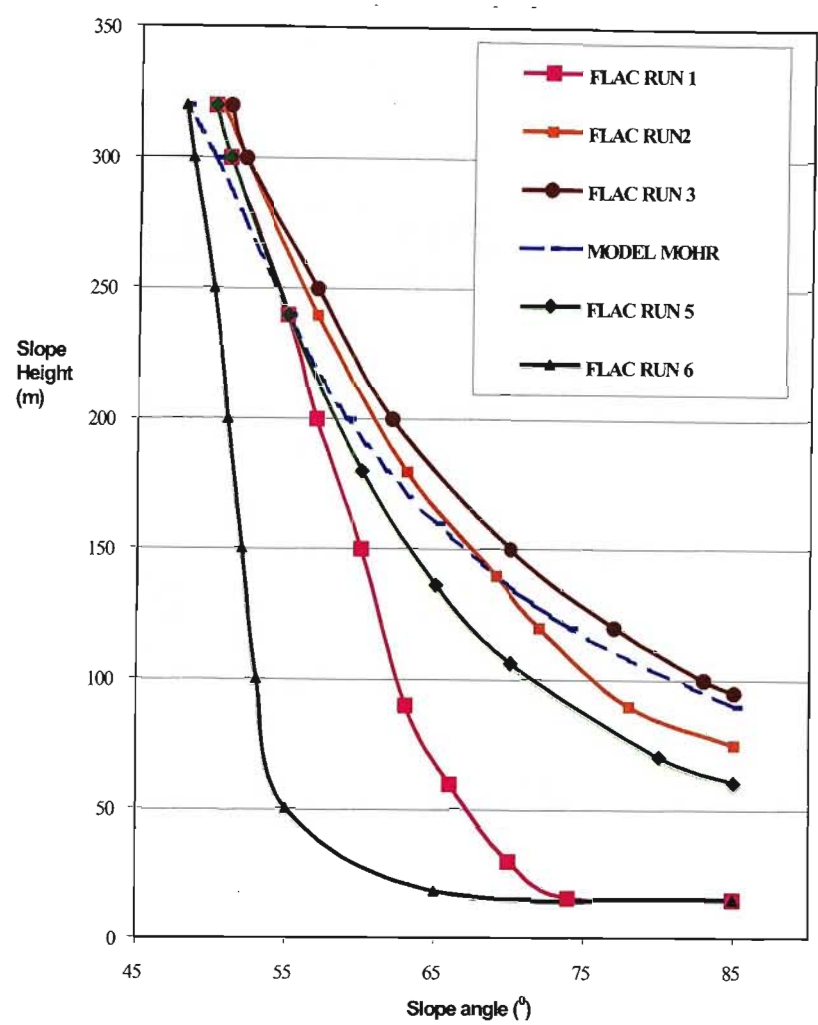


Figure 9.7 Stability envelope of the norite hangingwall developed from the series of FLAC analyses.

Table 9.2 Rock mass input parameters for the FLAC ubiquitous joint model.

Young’s modulus	10 GPa	Poisson’s ratio	0.2
Friction angle	35°	Cohesion (c)	30 kPa
Joint friction angle	43°	Joint cohesion (c)	0-300 kPa
Unit weight	2,700 kg/m ³	Ubiquitous joint dip	50° and 65°
FLAC Model Run No.	c (kPa)	Joint angle (°)	Joint tension (kPa)
1	0	65	0
2	100	65	10
3	300	65	30
4	MODEL MOHR	-	-
5	50	65	5
6	0	50	0

9.4 Risk and Reward Design Application

The development of the slope design model provided the opportunity to move away from one design process for the entire pit and customisation of slope designs and configurations were then developed to allow for local variations in the rock mass conditions. This slope optimisation was linked to a risk-reward design approach, which was made possible by the confidence in the geotechnical information used for the design options.

The risk-reward analysis was undertaken by obtaining a number of optimum pit shells, restricted to final slope angles of between 51° and 62° . The Datamine® NPV software was used to obtain the economic shells, which are estimated by using the Lerchs-Grossmann algorithm. Analysis of each economic shell provided financial and design information as summarised in Table 9.3. For example, the slope optimisation of 3 degrees from 51° to 54° resulted in an additional 2,5 million tonnes of ore and increased revenue of R 902,317 million. Figure 9.8 illustrates the increase in revenue as the pit slope is optimised.

The reason for the increase in revenue is as follows. The stripping ratio of ore to waste will decrease as the pit slope angle increases, which results in a decrease in the cost per tonne of ore mined. The Sandsloot orebody extends at 45° to significant depths (+1,600 m) and therefore the decrease in the cost per tonne of ore mined means that the pit depth can be increased until the break even stripping ratio is achieved. This will result in an increase in the gross revenue. Table 9.3 illustrates this point with the stripping ratio at Sandsloot reducing from 6.22 to 6.06 as the pit deepens and the gross revenue generated increases. Figure 9.8 illustrates the revenue associated with steepening the pit slopes from 51° to 62° degrees and the associated deepening of the pit from 290 m to 350 m.

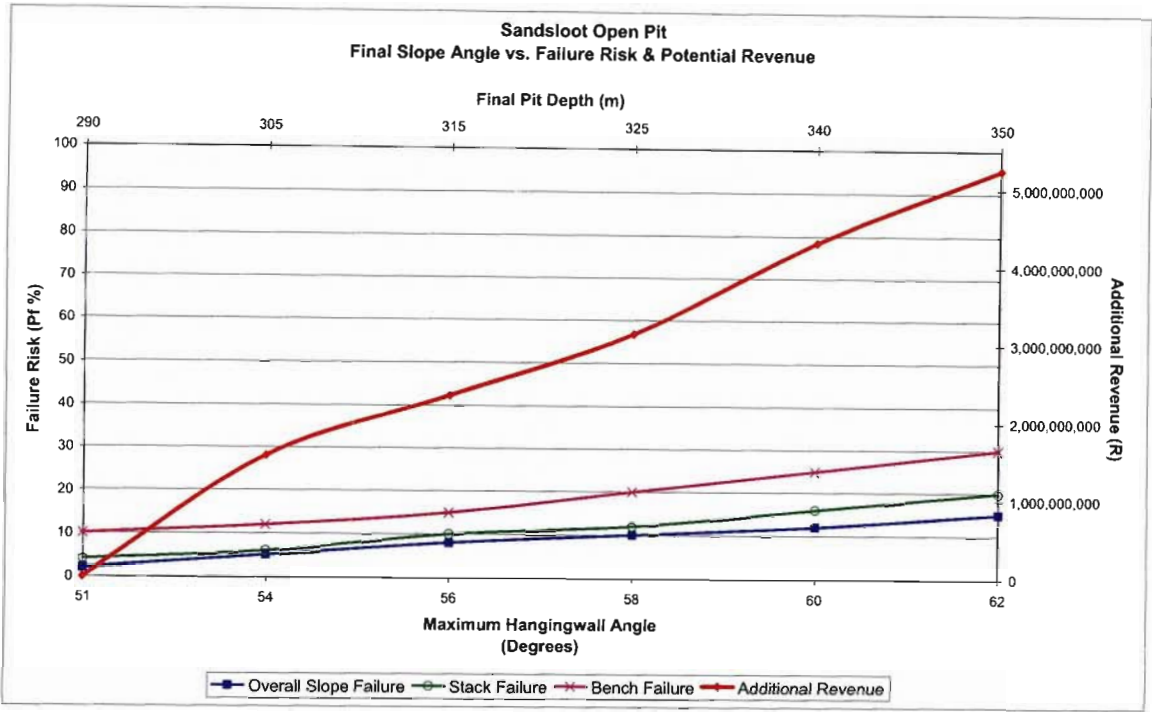


Figure 9.8 Risk-reward slope design chart developed for Sandsloot open pit

Table 9.3 Summary of risk-reward design information plotted in Figure 9.8.

Slope Design		Mining				Slope Failure Risks		
Slope Angle	Maximum Depth (m)	Stripping Ratio	Additional Waste Tonnes (000's)	Additional Ore Tonnes (000's)	Additional Revenue R (000's)	Overall Slope Failure Pf %	Stack Failure Pf %	Bench Failure Pf %
51	290	6.22	0.00	0.00	0.00	2	4	10
54	305	6.18	13,731.47	2,536.41	902,317.19	5	6	12
56	315	6.21	21,933.23	3,601.69	1,360,113.19	8	10	15
58	325	6.12	25,270.05	4,876.68	1,825,108.34	10	12	20
60	340	6.07	35,226.06	6,924.54	2,518,880.33	12	16	25
62	350	6.06	43,661.58	8,334.93	3,063,530.54	15	20	30

The reward portion of this method of design has been explained, however there are additional risks associated with optimised pit slopes. For each pit slope design the probabilities of failure for bench, stack and overall slopes were estimated. As illustrated in Figure 9.8 the probability of slope failure increases as the slopes are steepened. For Sandsloot the probability of overall slope failure increases from 2 % to 15 % with a move from 51° to a 62° slope angle.

The risk-reward design process and slope optimisation was verified with numerical modelling as discussed in section 9.3 The final pit walls were increased from 51° to 54° , resulting in an increased probability of stack failure from 4 % to 6 %. Using the risk-reward process, management was able to make business decisions based on reliable information. The increased revenue and associated higher risk was leveraged by instituting higher levels of slope management. The costs of this risk management are comfortably covered by the gains in revenue. The availability of the geotechnical information in 3D and the improved level of confidence of that data resulted in the successful application of the risk-reward slope optimisation.

9.5 Summary and Conclusions

The slope design process at Sandsloot has evolved through a number of processes, initially being based on limit equilibrium designs using the MRMR system. Subsequently, numerical modelling of the final pit slope was undertaken. The 3D slope design model was then developed using the MRMR design charts. All this information was used for the risk-reward design, based on probability of failure and additional revenue. The net result being an optimised final slope angle and an increase in revenue of approximately R 900 million.

This evolution is evidence of the increased geotechnical knowledge, which has enabled higher levels of design and confidence in the slope parameters. As initially discussed in the introduction of this thesis, lack of geotechnical knowledge represents the greatest risk in a mining venture and overly conservative or unsafe designs are often the result. The significant financial benefits that were derived from obtaining comprehensive geotechnical information at Sandsloot have been clearly described. The application of the slope stability model has resulted in optimised slope configurations, increased revenue and an extension of the life of the mine. The development of a 3D geotechnical model offers mining operations a distinct business and safety advantage.

10 CONCLUSIONS

The research documented in this thesis records the procedures and developments undertaken to compile a comprehensive geotechnical database, and the application of the geotechnical data to open pit mining, beneficiation and planning. The utilisation of the geotechnical information was enhanced through the development and application of a novel computerised, 3D geotechnical model.

The objective of the research, as defined in the introduction, was to develop an engineering solution, based on a significant geotechnical database, which was automated, sustainable and aligned with the company's business objectives. This was achieved in the following manner:

- i). A significant database of geotechnical information was collected from exploration boreholes, in-pit face mapping and rock strength testing.
- ii). An interpolated 3D geotechnical model was developed from the data.
- iii). The model was tested and adjusted until the model predictions were representative of the field conditions.
- iv). The customer relationships and design targets which derive the largest economic benefit for the company as a whole were defined.
- v). The 3D geotechnical model was used as a platform to develop engineering design tools for mine optimisation. These tools were developed as fragmentation and slope design models.
- vi). A simple user-interface (front-end) to the model was designed, which enabled mine planners and engineers to use the model.
- vii). The model was applied over an eighteen-month period and the efficiency and financial benefits were recorded.

The following sections summarise the results and conclusions of the various research phases undertaken during this study. The thesis is concluded with a discussion of future research suggestions.

10.1 Geotechnical Information

Chapter two to four laid the foundation for understanding how important quality, geotechnical information is for an integrated approach to mine design. The interpretation of this data into useful engineering numbers was discussed as well as the methods used to ensure consistent, quality data capture.

The interaction of the Platreef pyroxenitic unit at Sandsloot with different sedimentary sequences has resulted in a complex and unique suite of rock types. The research illustrates how geology and the detailed understanding of its properties are fundamental to the optimal design and successful operation of any mine. Extensive fieldwork was conducted to collect geotechnical information, both from exploration boreholes and in-pit mining faces. Over a five year period, geotechnical data were collected from 29,213 m of exploration core and 6,873 m of exposed mining faces. Extensive field and laboratory testing was undertaken in order to define the complete set of geotechnical properties for each rock type in the Sandsloot mining area. A significant set of geotechnical properties were recorded ranging from RMR, FF/m and elastic properties to a slake durability index.

10.2 Model Development

Chapter 5 detailed the development of the 3D geotechnical model. The initial sections discuss the ore reserve modelling processes and their applicability to a geotechnical model. A history of geostatistics and geotechnical engineering was presented as well as examples of the application and potential benefits outside the mining environment.

Geostatistics deals with spatial data, i.e. data for which each value is associated with a location in space. In such analysis it is statistically proven that there is a connection between location and data values. From known values at sampled points, geostatistical analysis can be used to predict spatial distributions of properties over large areas or volumes. An overview of geostatistics and geotechnical engineering and the processes used to develop an ore reserve model were discussed as they formed the basis for the development of the geotechnical model. The various construction steps used in the development process were laid out sequentially, culminating in the geostatistical analysis and interpolation method used to generate the final model. Various interpolation processes were used to develop the model and subsequently tested to verify that the inverse distance method was most appropriate for the Sandsloot geotechnical model.

The application of geostatistical analysis tools, has facilitated powerful and interactive visualisation of the spatial distributions of geotechnical parameters, thereby aiding the correct interpretation of data. The model has enabled and encouraged exploration of alternative assumptions and interpretations in the analysis of ground conditions. Through an understanding of the spatial distribution of geotechnical properties, contained in the 3D model, incorporation of the inherent spatial variability into numerical and blast design models was facilitated. The aim of the subsequent research was to derive benefit by refining mine designs based on the 3D rock mass information. The model made this possible well ahead of the mining face.

10.3 Customer Requirements

An important aspect often neglected in mining operations is the clear definition of the customer relationships within and between the mining and processing operations. Following on the definition of these relationships is the setting of targets that derive the greatest economic benefit for the company as whole rather than isolated cost centres within the mining or processing departments.

In order to maximise the benefit of the 3D geotechnical model, the optimal design targets for the mine were defined. Chapter 6 examined the relationships between the drill and blast department and the downstream customers, namely the load and haul department and the processing plant. Through analysis of significant data sets, design targets were defined for these customers and subsequently the fragmentation model was configured to achieve these targets.

Rather than viewing the department as an isolated cost centre and focussing on minimising drill and blast costs, the study focussed on the fragmentation requirements of the processing plant and load and haul business areas. In order to evaluate the customers' optimum requirements, two areas of productivity were measured for both waste and ore. These were defined as the instantaneous loading rates and the mean fragmentation (P_{50}) of the blasted muckpile.

Over the five years of research a defined process was followed in order to verify the customers' optimum fragmentation requirements. Initially, geotechnical information for the optimisation of blast designs was provided manually, using draughted plans. The results of these adjustments were recorded in order to define and benchmark the performance standards. These performance standards were then set as the customer targets and subsequently built into the fragmentation model.

The plant design and comminution requirements were assessed during the research, and the fragmentation requirements were evaluated to determine the impact of the mill feed fragmentation on plant performance. Based on the digital fragmentation analysis a mean fragmentation of 230 mm was set for waste and 150 mm for ore. Additionally, the target loading rate was set at 3,200 t/hr for waste and 3,300 t/hr for ore. The study was undertaken over a range of energy factors and blast hole diameters to ensure the results were representative. Chapter 6 clearly defined the customer relationships within and between the mining and processing operations and the targets that derived the greatest economic benefit for the company as whole.

10.4 Fragmentation Model

In a large open pit environment the cost of rock fragmentation associated with blasting (drilling, blasting, digging and hauling) represents just 10 % - 15 % of the comminution costs that occur within the crushing plant. Clearly, even a significant increase in blasting costs associated with delivering an optimal feed to the crushing plant was easily justified by only a modest increase in the productivity of the crushing circuit. This investigation highlights the importance of fragment size distribution on mill performance, the critical economic balance between blasting, crushing and milling in the overall comminution process and the need for quantitative geological information in blast design. Ineffective fragmentation and poor mill performance is largely influenced by the lack of technical communication between the engineering geologist, blasting engineer and the metallurgist responsible for the crushing and milling.

Drilling and blasting is the first step in the physical mining process and therefore plays a major role in the performance of downstream functions. The inherent rock mass properties are one of the biggest unknown factors in blast design and play a major role in blasting costs and the productivity of the downstream functions. The 3D geotechnical model provides detailed rock mass information and was therefore applied to the blast design in order to improve the efficiency of blasting.

A number of steps were followed in order to utilise the 3D geotechnical information for drill and blast optimisation, budgeting and planning. Initially the geotechnical information in the model was converted into a Blastability Index (Lilly, 1986). A fragmentation model was then developed using the BI and the Kuz-Ram equation to calculate the required energy factor (quantities of explosives) needed to achieve the defined fragmentation requirements. The fragmentation model takes into account the varying rock mass conditions by querying the geotechnical information contained in the model.

Chapter 7 describes the calculations used to convert the 3D geotechnical information into useful mining parameters. The fragmentation model has optimised the blast design and planning process by firstly reducing the level of uncertainty associated with rock mass information; secondly by defining precisely the customer requirements and thirdly by combining the entire process into a 3D model that can be queried for any planned mining slot. The fragmentation model was developed as a dynamic tool to ensure that the customers design requirements were consistently achieved.

10.5 Customer Performance

Open pit mining involves a process of controlled destruction of the rock mass so that the waste may be stripped and the ore extracted. The blasting engineer is faced with the conflicting requirements of providing large quantities of well-fragmented rock for the processing plant, reducing drill and blast costs and minimising the amount of damage inflicted upon the rock slopes left behind. A reasonable compromise between the conflicting demands can only be achieved if the blasting engineer has a very sound understanding of the factors which control rock fragmentation, highwall damage and slope stability (Hoek and Bray, 1981). This understanding was significantly enhanced through the use of a 3D geotechnical model.

Manual information systems used for design require significant dedication and time commitments and can be onerous to continually update. They often rely on the commitment of a single individual and are therefore not sustainable. The 3D geotechnical model is a user-friendly and sustainable tool, which can be readily updated and therefore does not suffer from the limitations of a manual system.

The application of the fragmentation model to blast design resulted in an 8.5% and 8.8% improvement in loading and milling rates, respectively from 2001 to 2003. It must be stressed that these are actual production figures measured over a two-and-a-half year period and therefore represent a significant record of performance. A more detailed analysis of all the customer performance measures was undertaken for the period from January to June 2003. There is a clear improvement across all the performance indicators, which include the following:

- | | |
|--|-----------------|
| • Average plant milling rate (AG and Ball mills) | 18% improvement |
| • Average AG milling rate | 16% improvement |
| • Average instantaneous loading rate (Ore and Waste) | 13% improvement |
| • Average instantaneous loading rate (Ore) | 11% improvement |

These performance improvements represent a substantial value add to the overall business and the associated financial benefits are significant in terms of millions of Rand per month. The improvement in the autogenous grind milling performance for the 18-month model application

10.7 Suggestions for Further Research

A 3D geotechnical model has application to any major civil or mining venture that requires a detailed understanding of the variability in rock mass conditions. A geotechnical model does not propose to generate solutions by creating information from a limited data set. It does, however, give the engineer a tool whereby he can assess the spatial variability of the rock mass information and thereby identify data-deficient or high risk areas. There are numerous case histories detailing the failure or significant over-expenditure of civil, tunnelling and mining projects caused by a lack of knowledge of the variability of the *in-situ* rock mass. The application of one's mind in terms of future research related to 3D geotechnical models will generate a myriad of relevant projects and research theses.

At Sandsloot, work is continuing to include mineralogical properties into the block model and thereby develop a mineralogy model. Mineralogy is closely linked to rock type and alteration and therefore has a spatial distribution. Plant recovery is directly affected by the mineralogy of the processing material and therefore an expected recovery could be included in the model cell. Additionally, a correlation between rock hardness and expected milling rates can be obtained by using a Bond Work Index model. The Bond Work Index is related to rock type and mineralogy and therefore a milling rate model could be developed.

10.7.1 Geostatistics

The geotechnical model at Sandsloot was developed using an inverse distance interpolation method, after initial trials using kriging were unsuccessful due to a statistically limited data set. Kriging is a more powerful interpolation process and as the model database grows the application of kriging to the modelling process will be investigated. The kriged model gives an indication of a kriged variance or confidence value in each model cell for each parameter. This confidence value will highlight data-deficient areas, which pose a high risk due to the limited information in that area.

for the entire pit, except for consideration of the hauling costs related to pit depth. A practical pit is then designed around the economic mining shell, generated by the scheduling software, using an average stable slope angle. The schedule is based on the mining costs versus the grade and tonnage for each ore reserve block.

A further application of the geotechnical model, described in this thesis, would be to use the scheduling software to generate economic mining shells based on the comprehensive geotechnical and mining information contained in the geotechnical model. As the geotechnical model has a stable slope angle contained in each cell, it is feasible that the scheduling software could generate far more accurate economic shells, based on this information, rather than a single slope angle for the entire pit highwall.

10.7.3 Feasibility Projects

Feasibility studies for new projects require an expected budget expenditure estimate to within 5% of actual costs. This level of accuracy is expected by mining companies and investors but cannot be achieved without a sound knowledge of the rock mass variability. By developing a 3D geotechnical model as part of the feasibility study and using the same geological model exploration boreholes, a significantly better understanding of the rock mass conditions can be obtained. This rock mass information can be used for equipment selection, economic pit layouts, processing plant design, underground mining layouts and support requirements, to name but a few design parameters which are dependant on rock mass conditions. There is the potential for the application of geotechnical models to be equally successful in underground operations, as well as considerable scope for the implementation of these methods as a tool for mine evaluation and feasibility assessments of new ore deposits.

The ore reserve model has gained widespread acceptance as an invaluable tool for a mining operation. Certainly most financial organizations will not invest in a mining project that does not have an ore reserve model. There is the potential for geotechnical models to be accepted as vital tools to the mining process, as is the case with ore reserve models. The development of a geotechnical model facilitates the provision of geotechnical information well in advance of the mining face. Using the model, mining areas were evaluated not only for grade and tonnage predictions but also for predictions of rock mass quality. Blast design and explosive requirements were derived from the rock mass quality predictions. This information was used for overall mine planning and evaluation, costing, production optimisation and slope design. This allows the full range of mining activities and costs to be inter-connected, thereby lowering costs and improving

efficiencies through the application of the geotechnical model. The cumulative benefit delivered to the PPL operation by the development of the 3D geotechnical model was significant. The direct, quantified financial benefits were in the short term, in excess of R 29 million and in the long term over R 900 million. Other mining operations would be well served through the development of a similar geotechnically driven, business initiative.

11 REFERENCES

- Allen, S.W. 1996. *General geology and history of the Potgietersrust prospect*. Unpublished Technical Report for Amplats, Johannesburg.
- Ainsworth, C.S. 1994. *The role of the production geologist at Potgietersrust Platinums Limited*. Unpublished Technical Report. Geologists Technical Meeting, Johannesburg Consolidated Investments, **9**, 32-44.
- Ainsworth, C.S. 1998. *How many magma injections did it take to bring PGE enrichment to the Platreef in the Sandsloot area?* 8th International Platinum Symposium, South African Institute of Mining and Metallurgy, Symposium series **18**, 3-5.
- Anon. 1970. The logging of cores for engineering purposes. Working Party Report Engineering Geology Group. *Quarterly Journal Engineering Geology*, **3**, 1-24.
- Armitage, P.E.B., McDonald, I., Edwards, S.J. and Manby, G.M. 2002. PGE mineralisation in the Platreef and Calc-silicate footwall at Sandsloot, Potgietersrus District, South Africa. *Transactions of the Institute of Mining and Metallurgy*, **111**, January-April 2002.
- Barton, N., Lien, R. and Lunde, J. 1974. Engineering classification of rock masses for the design of rock support. *Rock Mechanics*, **6**, 189-236.
- Barton, N. 1978. Suggested methods for the quantitative description of discontinuities in rock masses. ISRM Commission on Standardisation of Laboratory and Field Tests. *International Journal Rock Mechanics, Mineral Science and Geomechanical Abstracts*, **15**, 319-368.
- Bell, F.G. 1992. *Engineering in Rock Masses*. Butterworth-Heinemann, Oxford. 580 pp.
- Bickers C.F., Dunbar C.T., Le Juge G.E., and Walker P.A. 2001. *Wall control blasting practices at BHP Billiton iron ore Mt Whaleback*. EXPLO 2001. Hunter Valley, NSW, October 2001, 93-102.
- Bieniawski, Z.T. 1973. Engineering classification of jointed rock masses. *Transcripts South African Institution Civil Engineers*, **15**, 335-344.

- Bieniawski, Z.T. 1976. Rock mass classification in rock engineering. *Exploration for rock engineering*. A.A. Balkema, Cape Town. **1**, 97-106
- Bond, F.C. 1961. Crushing and grinding calculations Part I and Part II. *Brochure of Chemical Engineering*. **6**, 378-385 and 543-548.
- Brown, E.T. 1981. *Rock Characterization, Testing and Monitoring*, Pergamon, Oxford.
- Buchanan, D.L. 1988. Platinum group element exploration. *Developments in Economic Geology*, **26**. Elsevier, Amsterdam, 185 pp.
- Button, A. 1976. Stratigraphy and relations of the Bushveld floor in the Eastern Transvaal. *Transactions of the Geological Society of South Africa*, **79**, 3-12.
- Bye, A.R. 1996. *Detailed geotechnical and structural mapping of Sandsloot open pit*. Unpublished Honours Thesis, University of Natal, Durban.
- Bye, A. R. 1998. Using geotechnical methods as production and planning tools. *Abstracts, 8th International Platinum Symposium, Rustenburg*. SAIMM, **S18**, 51-54.
- Bye, A. R., Jermy, C. A. and Bell, F. G. 1998. Using geotechnical methods as production and planning tools. *Proc. 8th Int. Congress IAEG. Vancouver*. Balkema: Rotterdam, **5**, 2995-3003.
- Bye, A.R., Jermy, C.A. and Bell, F.G. 1999. *Slope optimisation and review of the geotechnical conditions at Sandsloot open pit*. Proceedings of the 9th ISRM Conference, Paris. Balkema: Rotterdam, **1**, 77-82.
- Bye, A. R. and Bell, F. G. 2001. Stability assessment and slope design at Sandsloot open pit, South Africa. *International Journal of Rock Mechanics and Mining Sciences*. Pergamon, **38**; 449-466.
- Bye, A. R. and Bell, F. G. 2001. Geotechnical applications in open pit mining. *Geotechnical and geological engineering*. Kluwer, **19**, 97-117.

- Bye, A. R., Jermy, C. A. and Bell, F. G. 2002. The development and application of a 3D geotechnical model at Sandsloot open pit, South Africa. *Engineering Geology for Developing Countries - Proceedings of 9th Congress of the International Association for Engineering Geology and the Environment*. Durban, South Africa, 16 - 20 September 2002. [Ed. J. L. van Rooy and C. A. Jermy], 1770-1779.
- Bye, A. R. 2002. Mining the Platreef. Mineral deposits studies group (MDSG) annual meeting. Southampton. *Transactions of the Institute of Mining and Metallurgy*. Section B, Applied Earth Science. Sep-Dec 2001. **110**, B209-B210.
- Bye, A. R. 2002. A 3D geotechnical model for mining optimisation. *FRAGBLAST 7. 7th International Symposium on Rock Fragmentation by Blasting*. Beijing, China, 245-251. Metallurgical Industry Press, Beijing. [Ed. Prof. Wang Xuguang]. 819 pp.
- Campbell, G. and Heidstra, P.T. 1994. *How to find a water wellfield: Geophysical mapping and borehole pump testing for the PPL Mine water supply*. Technical Report to Potgietersrust Platinums Ltd. Johannesburg Consolidated Investment Company, Johannesburg.
- Cawthorn, R.G., Barton, J.M., and Viljoen, M.J. 1995. Interaction of floor rocks with Platreef on Overysel, Potgietersrus, Northern Transvaal. *Economic Geology*, **80**, 988-1006.
- Cawthorn, R.G. 1996. *Layered Intrusions*. Elsevier Science, London.
- CGSS. 1998. AutoCAD software customisation consultants. 9 Devereux Rd. Windsor, Berkshire, UK.
- Chiles, J-P. and Delfiner, P. 1999. *Geostatistics: Modelling Spatial Uncertainty*, John Wiley and Sons, Toronto.
- Clarke, I. 1979. *Practical Geostatistics*. Elsevier Applied Science, London and New York.
- Cunningham, C.V.B. 1986. *The Kuz-Ram model for prediction of fragmentation from blasting*. Proceedings of the 1st International Symposium on rock fragmentation by blasting, Lulea, Sweden. 439-452.

- Deere, D.V. and Miller, R.P. 1966. *Engineering classification and index properties for intact rock*. Technical Report No. AFNL-TR-65-116. Air Force Weapons Laboratory, Kirtland, New Mexico, USA.
- De Freitas, M.H. and Watters, R.J. 1973. Some field examples of toppling failure. *Geotechnique*, **23**, 495-514.
- Dempers, G.D. 1996. *Optimal usage of exploration core for geotechnical purposes*. Unpublished Report. Steffen, Robertson and Kirsten, Consulting Engineers. Johannesburg.
- Djordjevic, N. 1998. Optimal blast fragmentation. *Mining Magazine*, **2**, 121-125.
- Dunnicliff, J. 1988. *Geotechnical Instrumentation for Monitoring Field Performance*. Wiley-Interscience, New York.
- Etheridge, M. 2001. *Review of the structural geology input into geotechnical risk management*. Steffen, Robertson and Kirsten Consulting (Australasia). Unpublished Internal Report.
- Friese, A.E.W. 2002. *Structural geology of the Overysel-Zwartfontein North prospect area*. Unpublished Internal Report.
- Friese, A.E.W. 2002. *The tectono-sedimentary evolution of the southern Free State Goldfield within the Witwatersrand Basin, with implications for the development of the Kaapvaal Craton, South Africa*. Unpublished PhD Thesis, University of the Witwatersrand, Johannesburg, South Africa.
- Good, N. 1999. *Structural and thermal control on basinal fluid flow and mineralisation beneath the Bushveld Complex and along the adjacent Thabazimbi-Murchison lineament; Kaapvaal Craton, South Africa*. Unpublished PhD Thesis, University of Cape Town, South Africa.
- Haines, A. and Terbrugge P.J. 1991. *Preliminary estimation of rock slope stability using rock mass classification systems*. Proceedings of the 7th International Congress. International Society of Rock Mechanics. Aachen. Balkema, Rotterdam, **2**, 887-892.

- Harris, C. and Chaumba, J.B. 2001. Crustal contamination and fluid-rock interaction during the formation of the Platreef, northern limb of the Bushveld Complex, South Africa. *Journal of Petrology*, **42**, no. 7, 1321-1347.
- Hoek, E. and Bray, J. 1981. *Rock Slope Engineering*. Revised 3rd edition. Institution of Mining and Metallurgy. London. 358 pp.
- Hucka, V.A. 1965. A rapid method for determining the strength of rock *in-situ*. *International Journal of Rock Mechanics, Mining and Sciences*. Pergamon, **2**, 127-134.
- Itasca Consulting Group Inc. 1995. *Fast Lagrangian Analysis of Continua, basics manual*. Version 3.30. Minneapolis, Minnesota.
- Isaaks, E.H. and Srivastava, R.M. 1989. *An Introduction to Applied Geostatistics*, Oxford University Press, Toronto.
- ISRM commission on standardisation of laboratory and field tests. 1979. Suggested methods for determining the uniaxial compressive strength and deformability of rock materials. *International Journal of Rock Mechanics, Mining, Science & Geomechanics Abstracts*, **16**, 135-140.
- ISRM commission on standardisation of laboratory and field tests. 1983. Suggested methods for determining the strength of rock materials in triaxial compression: Revised version. *International Journal of Rock Mechanics, Mining, Science and Geomechanics Abstracts*, **20**, 283-290.
- ISRM commission on standardisation of laboratory and field tests. 1974. *Suggested methods for determining shear strength*. Final Draft.
- ISRM commission on standardisation of laboratory and field tests. 1979. Suggested methods for determining water content, porosity, density, absorption and related properties and swelling and slake-durability index properties. *International Journal of Rock Mechanics, Mining, Science & Geomechanics Abstracts*. **16**, 141-156.

- Kemeny, J., Girdner, K., Bobo, T. and Norton, B. 1999. *Improvements for fragmentation measurement by digital imaging: Accurate estimation of fines. FRAGBLAST 1999*. South African Institute of Mining and Metallurgy. Johannesburg, 103-109.
- Kinloch, E.D. and Peyerl, W. 1990. Platinum-group minerals in various rocks types of the Merensky Reef: genetic implications. *Economic Geology*, **85**, 537-555.
- La Pointe, P.R. 1990. *Analysis of the spatial variation in rock mass properties through geostatistics*. In: *Proceedings of the 21st Symposium on Rock Mechanics: A State of the Art*, University of Missouri, Rolla, May 28 – 30, 1980, 570-580.
- Laubscher, D.H. 1990. A geomechanics classification system for the rating of rock mass in mine design. *Journal of South African Institute of Mining and Metallurgy*, **90**, 257-273.
- Lilly, P. A. 1986. An empirical method of assessing rock mass blastability. *The Australian IMM. Large Open-pit Mining Conference*. Newman Combine Group. October, 1986, 89-92.
- Lilly, P. A. 1992. The use of the Blastability Index in the design of blasts for open pit mines, in *Proceedings Western Australian Conference on Mining Geomechanics*, (Eds. T. Szwedzicki, G. R. Baird and T. N. Little. Western Australian School of Mines, Curtin University of Technology: Kalgoorlie). 421-426.
- Maerz, N.H. and Zhou, W. 1999. *Calibration of optical digital fragmentation measuring systems. FRAGBLAST 6*. South African Institute of Mining and Metallurgy. Johannesburg, 125-130.
- Nickson, S., Ecobichon, D., Leclerc, M., and Cote, E. 1996. A methodology for rock mechanics feasibility studies. *CIM Bulletin*, **89**, 120-125.
- Nielsen, K. 1993. Safety versus production? Quality assurance in blasting. *Proceedings FRAGBLAST 4, Rock fragmentation by blasting*, [Ed. P. Rossmanith]. Balkema, Rotterdam.
- Nielsen, K. and Kristiansen, J. 1995. *Blasting and grinding – An integrated comminution system*. EXPLO 1995 Conference. Brisbane, September, 1995, 113-117.

- Norbury, D. R. 1986. The point load test. In *Site Investigation Practice: Assessing BS 5930, Engineering Geology Special Publication*, No. 2, [Ed. A.B. Hawkins], Geological Society, London, 326-329.
- Özçelik Y. 1998. Effect of discontinuities on fragment size distribution in open-pit blasting-a case study. *Transactions of the Institute of Mining and Metallurgy* (Section A: Mining Industry), **107**, A146-A151.
- Palangio, T.C. and Maerz, N.H. 1999. *Case studies using WhipFrag image analysis system. FRAGBLAST 6*. South African Institute of Mining and Metallurgy. Johannesburg. 117-120.
- Reynolds, L.R. and Millan, P. 1997. *The evolution of geology and mine planning systems at Potgietersrust Platinums Limited using Datamine as the core package*. Unpublished Proceedings, Datamine User Conference, Johannesburg.
- Revnivstev, V.I. 1988. *We really need revolution in comminution*. Proceedings XVI International Mineral Processing Congress, 93-114.
- Rorke, A.J. 1995. *Presplitting and highwall control techniques*. Technical Report to Potgietersrust Platinums Limited. Blastinfo Africa, Johannesburg.
- Rocscience Inc. 2000. *Geomechanics software and research*. 31 Balsam Ave., Toronto, Ontario, Canada, M4E 3B5.
- Rocscience. 2003. *Geostatistics in Geotechnical Engineering: A fad or an empowering approach?* Article prepared for RocNews 2003. www.rocscience.com.
- Rouhani, S., Srivastava, R.M., Desbarats, A.J., Cromer, M.V. and Johnson A.I. 1996. *Geostatistics for Environmental and Geotechnical Applications*, ASTM STP 1283.
- Sandy, D.A. 1991. *Open pit wall control at Rossing Uranium Mine*. RTZ Mining Conference, Salt Lake City.

- Schleifer J., Tessier, B. and Srhiar, T. 1999. *What type of difficulties are to be expected in order to 'benchmark' fragmentation assessment systems. FRAGBLAST 6*. South African Institute of Mining and Metallurgy. Johannesburg, 121-124.
- Scott, A. 1992. A technical and operational approach to the optimisation of blasting operations. *Proceedings MASSMIN*. SAIMM: Johannesburg, South Africa, **92**, 247-252.
- Sen, Z. and Kazi, A. 1984. Discontinuity Spacing and RQD Estimates from Finite Length Scanlines. *International Journal of Rock Mechanics, Mining, Science & Geomechanics Abstracts*, **21**, 203-212.
- Sharpe, J.C. 1989. *Monitoring of major excavated slopes in stable and unstable rock masses*. Proceedings of the Conference of Geotechnical Instrumentation in Civil Engineering Projects, Institution of Civil Engineers, University of Nottingham.
- Sharpe, M.R., Bahat, D. and von Gruenewaldt, G. 1981. The concentric elliptical structure of feeder sites to the Bushveld Complex and possible economic implications. *Transactions of the Geological Society of South Africa*, **84**, 239-244.
- Split Engineering LLC. *Digital fragmentation analysis software*. P.O. Box 41766. Tucson, AZ85716, USA. www.spliteng.com.
- Steffen, Robertson and Kirsten Inc. 1980. *Overysel, Potgietersrus project report on the geotechnical evaluation*. Technical Report to Potgietersrust Platinums Ltd. No.182414, Johannesburg.
- Steffen, Robertson and Kirsten Inc. 1991. *Mining geotechnical evaluation of the Overysel, Zwartfontein and Sandsloot open pits*. Technical Report to Potgietersrust Platinums Ltd. No. 186322, Johannesburg.
- Steffen, Robertson and Kirsten Inc. 1991. *Sandsloot pit dewatering and groundwater management*. Technical Report to Potgietersrust Platinums Ltd. No. 187846/2, Johannesburg.
- Steffen, Robertson and Kirsten Inc. 1998. *Quarterly Report*. Technical Report to Potgietersrust Platinums Ltd. No. 186332, Johannesburg.

- Stewart, R.M. and Kennedy, B.A. 1971. *The role of slope stability in the economics, design and operation of open pit mines*. Proceedings of the 1st Symposium on Stability in Open Pit Mining, Vancouver. A.I.M.E., New York, pp. 5-21.
- Syrjänen, P. and Lovén, P. 1998. Geostatistics and block modelling in rock mechanics. 9th *International Congress on Rock Mechanics. International Society for Rock Mechanics*. Paris, France. [Ed. Vouille G. and Berest P.] A.A Balkema. Rotterdam, **1**, 503-506.
- Thompson, P.W. 1989. *Slope stability at Finsch mine*. Proceedings of the Symposium on Rock Slope Stability, SANGORM. Johannesburg.
- Van der Merwe, M.J. 1976. The layered sequences of the Potgietersrus Limb of the Bushveld Complex. *Economic Geology*, **71**, 1337-1351.
- Vermaak, C.F. 1976. The Merensky Reef - thoughts on its environment and genesis. *Economic Geology*, **71**, 1270-1298.
- Vogler, U.V. and Kovari, K. 1978. Suggested methods for determining the strength of rock materials in triaxial compression. ISRM Commission on Standardisation of Laboratory and Field Tests. *International Journal of Rock Mechanics, Mining Science and Geomechanics Abstracts*, **15**, 47-51.
- Wagner P.A. 1929. *The platinum mines and deposits of South Africa*. Oliver and Boyd, Edinburgh, 326 pp.
- Walraven, F., Armstrong, R.A. and Kruger, F.J. 1990. A chronostratigraphic framework for the north-central Kaapvaal Craton, the Bushveld Complex and Vredefort structure. *Tectonophysics*, **171**, 23-48.
- White, J.A. 1992. *The Potgietersrus prospect, geology and exploration history*. Unpublished Technical Report for Johannesburg Consolidated Investments, Johannesburg.
- Widzyk-Capehart, E. and Lilly, P. 2001. *A review of general considerations for assessing rock mass blastability and fragmentation*. EXPLO 2001. Hunter Valley, NSW, October 2001, 93-102.

